UNIVERSITY OF LIVERPOOL

Exploring the role of nuclear phosphatases and their associated proteins in cell growth and development

Thesis submitted in accordance with the requirements of the University of Liverpool for the degree of Doctor in Philosophy by

Louise Rebecca Duncalf

December 2014

Declaration

This thesis is the result of my own work unless otherwise stated and is based upon results from experimental and theoretical work performed as a PhD student between October 2010 and July 2014 within the Institute of Integrative Biology at the University of Liverpool.

Neither this thesis nor any part of it has been submitted in support of an application for another degree at this or any other University or Institute of Learning.

Louise Rebecca Duncalf

December 2014

Contents

List of figures and tables

Chapter 1:

Chapter 2:

Chapter 3:

Supplementary figures and tables for paper:

Chapter 4:

Abbreviations

3-AT	3-aminotriazol
AD	activation domain
ATP	Adenosine Triphosphate
Bam	bag of marbles
BDGP	Berkeley *Drosophila* Genome Project
bp	base pair
CDK	Cyclin-dependent kinase
CDS	Coding Sequence
ChIP	chromatin immunoprecipitation
co-IP	co-immunoprecipitation
CSLM	confocal laser scanning microscope
CTD	C-Terminal Domain
CyO	Curly Oster
da	daughterless
DamID	DNA adenine methyltransferase identification
DAPI	4', 6-diamidino-2-phenylindole
DARPP-32	dopamine and cAMP-regulated phosphoprotein M_r 32000
DBD	DNA binding domain
DGRC	*Drosophila* genomics resource centre
DSPs	dual specificity phosphatases
ECFP	Enhanced Cyan Fluorescent Protein
em	emission
ERR	Estrogen Related Receptor
e*y*	eyeless
EYFP	Enhanced Yellow Fluorescent Protein
Flp	flippase
FRET	Fluoresence Resonance Energy Transfer
FRT	flippase recognition target
$GAL80^{ts}$	temperature sensitive GAL80
GFP	Green Fluorescent Protein
H3	Histone H3
H3K4	Histone H3 Lysine 4
H3K27	Histone H3 lysine 27
H3S10/28	Histone H3 serine 10 or 28
HMG	High Mobility Group
hnRNP	heterogeneous nuclear ribonucleoprotein
I-1	Inhibitor-1
I-2	Inhibitor-2
IC	Individualisation complex
JaCOP	just another colocalisation plot
kb	kilobase
kDa	kiloDaltons
LCP1	Langerhans Cell Protein 1
Nig-Fly	Fly Stocks of National Institute of Genetics
NIPP1	Nuclear Inhibitor of PP1
NLS	nuclear localisation signal
ORF	open reading frame

PABP	poly(A) binding protein
PcG	Polycomb Group
PCR	polymerase Chain Reaction
PEV	position effect variegation
PI3K	Phosphoinositide 3-Kinase
PIC	Protease Inhibitor Cocktail
PIP2	Phosphatidylinositol-4,5-bisphosphate
PIP3	Phosphatidylinositol-4,5-triphosphate
PIPs	PP1 interacting proteins
PMSF	Phenylmethylsulphonyl Fluoride
PNUTS	PP1 Nuclear Targeting Subunit
PP1c	PP1 catalytic subunit
PP1	Protein Phosphatase 1
PP2A	Protein Phosphatase 2A
PPP	Phosphoprotein phosphatase
PRC	polycomb repressive complex
PSTPs	protein serine/threonine phosphatases
PTPs	protein tyrosine phosphatases
Rb	retinoblastoma
RFP	Red Fluorescent Protein
RNAi	RNA interference
RNAPII	RNA Polymerase II
ROI	region of interest
RT-PCR	reverse transcription – polymerase chain reaction
S2/Ser2	Serine 2
S2R+	S2 receptor +
S5/Ser5	Serine 5
S7/Ser7	Serine 7
Tft	Tufted
TRiP	transgenic RNAi project
Trx	trithorax
TSS	Transcription Start Site
UAS	Upstream activating sequence
UTR	Untranslated region
wt	wild type
Y2H	yeast two-hybrid

Acknowledgements

I would like to thank my supervisor, Daimark Bennett for his guidance and support throughout my PhD and for instilling confidence in me when I doubted my ability. I would also like to thank other members of the Bennett lab, past and present; Neville Cobbe, Vincent Jonchere, Lauren Dodgson, Nick Lansdale, Mirel Lucaci, Nada Alqadri and in particular Anita Lucaci for all the help and support during the first two years and Christopher Lofthouse and Nick Jones for your advice and friendship.

I also wish to extend my gratitude to other colleagues within the Institute of Integrative Biology especially Marco Marcello for his help with confocal microscopy, James Wilson and Andrew Marriott for their help with cell culture and Jean Wood for technical support in the lab.

Most importantly I thank my husband, parents, grandparents, parents in-law and sister for their unwavering support throughout the years, in particular my mother Colette and husband Matthew for their patience and ability to calm me down during times of stress.

Abstract

Reversible protein phosphorylation is a key regulatory mechanism for controlling various cellular processes that determine cell fate. Phosphorylation status is controlled by kinases and phosphatases, which phosphorylate and dephosphorylate specific residues in target proteins respectively. Protein Phosphatase 1 (PP1) is a major serine/threonine phosphatase that is highly conserved in eukaryotes. Its catalytic subunit (PP1c) associates with numerous subunits that target and regulate its activity to specific subcellular localisations and substrates to define its role in various processes. PP1 Nuclear Targeting Subunit (PNUTS) is one of the most abundant regulatory subunits of PP1 in the nucleus. The aim of this work was to characterise a *Drosophila* orthologue of PNUTS and identify interacting proteins to further understand the role of PNUTS-PP1 in nuclear processes using various genetic and biochemical approaches. Mutational analysis revealed *dPNUTS* is essential for cell growth and survival as mutant animals die as 1st instar larvae and mutant cells are eliminated from developing tissues. PNUTS-PP1 co-localise on *Drosophila* polytene chromosomes, with many sites also marked by RNA Polymerase II (RNAPII). Biochemical analysis revealed Serine 5 of the C-terminal domain of RNAPII (CTD-Ser5) is a possible substrate of PP1-dPNUTS. Various RNAPII-dependent genes are misregulated in *dPNUTS* mutant animals, including genes involved in metabolic processes, most likely as a consequence of deregulated CTD-Ser5 phosphorylation. Another possible mechanism could be through regulation of histone modifications that determine gene expression patterns since clonal analysis revealed various histone marks are upregulated in dPNUTS and PP1 mutant cells. Methodologies to screen for regulatory enzymes affecting histone phosphorylation were also assessed.

To further understand the role of dPNUTS in cell growth and development, a yeast two-hybrid approach together with biochemical analysis was used to identify dPNUTS

interacting proteins. The top hit was dTOX4, the *Drosophila* homologue of LCP1/TOX4, which binds to PNUTS in humans. Mutational analysis revealed *dTOX4* is essential for fertility in female and male adult flies. Homozygous mutant females displayed defects in nurse cell chromosome dispersal and abnormal dorsal-ventral patterning in the oocyte. Homozygous mutant males failed to complete spermatogenesis and exhibited a range of abnormal phenotypes in the testes, including defective cytokinesis, small nuclei, decondensed chromatin and Stellate crystal formation. Novel dPNUTS-interactors were also identified, which could offer further mechanistic insight into dPNUTS-PP1 function.

1. Introduction

A major mechanism employed by cells to regulate intracellular signalling pathways that determine cell fate is reversible protein phosphorylation. Phosphorylation is a post-translational modification that acts to regulate protein activity by either activating or deactivating the target and can also affect protein localisation, stability and the ability to interact with other proteins. Phosphorylation state is finely balanced through the action of kinases and phosphatases, which phosphorylate and dephosphorylate proteins respectively. Protein kinases are responsible for catalysing the transfer of a phosphate group (PO_3^{2-}) from adenosine triphosphate (ATP) to a specific residue in a protein target and protein phosphatases antagonise this reaction by removing the phosphate group (Figure 1.1). The importance of phosphorylation in the cell is highlighted by the fact that approximately one third of cellular proteins are regulated by phosphorylation and protein kinases are one of the largest families of proteins in eukaryotes with 518 members in humans, contributing 2% of the genome (Cohen, 2002b; Ubersax and Ferrell, 2007; Sacco *et al*., 2012).

Protein phosphatases comprise approximately 200 members in humans and have been largely under-studied and under-appreciated in comparison to kinases because they were thought to have a non-specific role in regulating phosphorylation from *in vitro* studies (Sacco *et al*., 2012; Virshup and Shenolikar, 2009). However *in vivo* studies have revealed phosphatases are essential for maintaining appropriate levels of protein phosphorylation and play a key role in rapidly controlling various cellular activities in response to internal and external stimuli (Sacco *et al*., 2012; Virshup and Shenolikar, 2009).

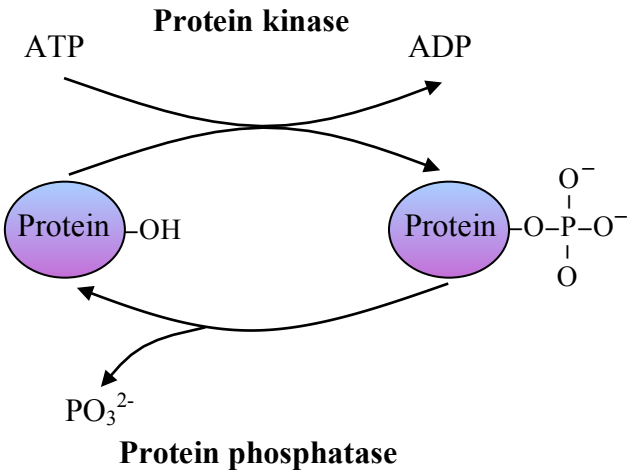

Figure 1.1. Reversible protein phosphorylation by kinases and phosphatases. Protein kinases transfer a phosphate group from ATP to the hydroxyl group of amino acids. Protein phosphatases catalyse the removal of the phosphate group.

1.1. Discovery of protein phosphorylation

Edmond Fischer and Edwin Krebs first uncovered the concept of phosphorylation in the 1950's during studies on glycogen metabolism. They described how the conversion of inactive glycogen phosphorylase '*b*' to active phosphorylase '*a*' required ATP and was a result of the transfer of a phosphate group onto '*a*' by phosphorylase kinase (Fischer and Krebs, 1955). Work on glycogen phosphorylase and its two forms had originated in the 1930's when Carl and Gerty Cori described the requirement of adenylic acid (AMP) for phosphorylase '*b*' activity, but not phosphorylase '*a*', however, they did not know how the two forms were different (Fischer, 2010). The work done by Edmond Fischer and his colleagues revealed AMP was not needed for the activation of phosphorylase '*b*' as originally thought (Fischer, 2010).

It was not realised at the time, how fundamental their finding was and since then phosphorylation has been shown to regulate not just glycogen metabolism but a large number of diverse cellular processes that determine cell fate including cell growth and proliferation, the cell cycle, apoptosis as well as numerous signal transduction pathways (reviewed in Bononi *et al*., 2011). This has led to protein phosphorylation being referred to as a major 'molecular switch' to control such physiological processes in response to various cues (Bononi *et al*., 2011).

1.2. Classification of protein phosphatases

In eukaryotes, the amino acids serine (ser), threonine (thr) and tyrosine (tyr) are predominantly targeted by phosphorylation, each accounting for 86.4, 11.8 and 1.8% of phosphorylated residues in humans respectively (Shi, 2009; Olsen *et al*., 2006). These form the basis of classification as phosphatases are grouped into families according to their substrate specificity. There are four major protein phosphatase families: 1) phosphoprotein phosphatases (PPPs); 2) metal-dependent protein phosphatases (PPMs); 3) aspartate based phosphatases (FCPs); and, 4) protein tyrosine phosphatases (PTPs) (Shi, 2009). The PPP, PPM and FCP families dephosphorylate serine and threonine residues and include the well-studied PPP, Protein Phosphatase 1 (PP1), the main subject of this work (Shi, 2009). The PTP family targets tyrosine for dephosphorylation and is divided into various classes, one being the dual-specificity protein phosphatases (DSPs), which dephosphorylate both phosphoserine/threonine and phosphotyrosine (Jeong *et al*., 2014; Mustelin, 2007).

1.3. Protein Serine/Threonine phosphatases (PSTPs)

PSTPs are classified into the three distinct families based upon their biochemical properties and amino acid sequence homology (McConnell and Wadzinski, 2009). PPPs make up the largest family and are further classified into the following subfamilies: PP1, PP2A, PP2B (calcineurin), PP4, PP5, PP6 and PP7 (Shi, 2009; Bollen and Beullens, 2002). The PPM family is derived from phosphatases that depend on magnesium/manganese (Mg^{2+}/Mn^{2+}) ions and comprises PP2C, PP2C 'like' phosphatases and pyruvate dehydrogenase phosphatase (McConnell and Wadzinski, 2009). The FCP family is the smallest and most recently identified family and includes FCP1 and SCP1, which dephosphorylate Ser5 on the C-terminal domain of the largest RNA polymerase II (RNAPII) subunit (Yeo *et al*., 2003).

1.3.1. The PPP family

PP1 and PP2A have been extensively studied and are the two most abundant serine/threonine phosphatases, accounting for 90% of phosphatase activity in eukaryotes (Aggen *et al*., 2000; Virshup and Shenolikar, 2009; Moorhead *et al*., 2007). Initial characterisation depended on their sensitivity to two inhibitors termed Inhibitor-1 (I-1) and Inhibitor-2 (I-2) and their ability to dephosphorylate either the α or the β subunit of phosphorylase kinase (Cohen, 1989). Type 1, now known as PP1, targeted the β subunit and was sensitive to both inhibitors whereas Type 2, now known as PP2, targeted the α subunit and was insensitive to both inhibitors (Cohen, 1989). Type 2 phosphatases were further characterised into the three distinct enzymes we know today by their dependence on divalent cations, with PP2A not requiring them at all and PP2B and PP2C (a PPM, see 1.3.7) requiring calcium (Ca^{2+}) and magnesium (Mg^{2+}) respectively, for activity (Cohen, 1989).

All members of the PPP family have a structurally similar catalytic subunit, which consists of a β-sheet between two α-helices and therefore display a similar mechanism of action, which was used to identify the newer members of the family (Shi, 2009). Their activity is distinguished by the proteins they interact with and this is determined by their exposed loops, which specify the shape and charge of the surface of the protein and their affinity for different ligands (Bollen *et al*., 2010; Heroes *et al*., 2013). There are less than 40 serine/threonine phosphatases in the human genome, which counteract approximately 300 serine/threonine kinases and a similarly high ratio is seen in *Drosophila* (Cohen, 2002b). This has led to the questions: how is such versatility achieved with such a small number of catalytic subunits and how can they regulate the phosphorylation status of so many proteins individually? (Bollen *et al*., 2010). We now know this is possible due to the association of PPP catalytic subunits with numerous regulatory subunits that form distinct holoenzymes. These target PPPs to particular tissues and subcellular localisations and determine their substrate specificity and phosphatase activity by enhancing or suppressing their catalytic activity towards particular substrates (Virshup and Shenolikar, 2009).

1.3.2. PP1c

Protein Phosphatase 1 (PP1) is a major protein serine/threonine phosphatase that is highly conserved in all eukaryotes (Shi, 2009; Ceulemans, 2004). Its catalytic subunit (PP1c) is responsible for dephosphorylating and regulating thousands of independent protein targets *in vivo*, which is possible due to its broad specificity (Cohen, 2002b). In mammals, three PP1 catalytic subunit (PP1c) genes exist, namely PP1α, PP1β/δ and PP1γ, from which two splice variants ($PP1\gamma_1$ and $PP1\gamma_2$) are

generated; all are ubiquitously expressed apart from PP1γ_2, which is enriched in the testes (Ceulemans, 2004). *Drosophila* encodes four PP1c genes, which are named according to their cytological locations: *PP1α87B*, *PP1α96A*, *PP1α13C*, which are related to mammalian PP1α/PP1γ, and *PP1β9C*, which is related to PP1β/δ (Bennett and Alphey, 2007; Cohen, 2002b; Dombrádi *et al*., 1993). The level of conservation between each PP1c isoform is very high (>85%) and their enzymatic activities are very similar, which has made it difficult to study their specificity using biochemical analysis (Bennett and Alphey, 2007; Kirchner *et al*., 2008). For this reason, a lot of work has been done to identify PP1c regulatory subunits that target PP1 to different subcellular localisations and regulate its activity towards specific substrates involved in a diverse array of cellular and developmental processes including the cell cycle, transcription, apoptosis, RNA processing and intracellular signalling (Cohen, 2002b; Trinkle-Mulcahy *et al*., 2003; Jerebtsova *et al*., 2011).

Various strategies have been used to identify PP1-interacting proteins (PIPs) including classical biochemical approaches, yeast two-hybrid screens, *in silico* methods, affinity chromatography and antibody arrays (Bollen *et al*., 2010). To date, PP1 is known to interact with approximately 200 proteins in humans, creating numerous stable PP1 holoenzymes that target separate and distinct substrates (Heroes *et al*., 2013). With so many regulatory subunits already discovered, it is clear how PP1 can be involved in many independent processes and it highlights the importance of PP1 and phosphorylation in the cell. It also raises the question, how can so many unrelated and structurally distinct proteins interact with PP1. This has been partly answered through the discovery of a short canonical sequence K/R/H/N/S-(x)-V/I/L-x-F/W/Y (where x is any amino acid) generally referred to as the RVxF motif in PIPs

(Zhao and Lee, 1997). This motif is present in approximately 70% of PIPs and interacts with a hydrophobic channel in PP1c that is distant from the catalytic site of the enzyme, therefore binding of RVxF proteins does not have a major effect on the activity of the phosphatase (Egloff *et al*., 1997; Bollen, 2001; Bollen *et al*., 2010). Instead, it is believed the motif functions as an anchor for PP1 to allow other contacts to be made with various regulatory subunits that determine its activity and substrate specificity (Bollen, 2001). Other PP1 docking motifs exist in PIPs, including the SILK-motif, which contains the consensus sequence G/SILR/K and the MyPhoNE (Myosin Phosphatase N-terminal Element) motif which interacts with the consensus sequence RxxQVI/LK/RxY/W (where x is any amino acid) (Hendrickx *et al*., 2009).

1.3.3. *Drosophila* PP1c

PP1α87B is the major PP1c isoform in *Drosophila*, accounting for approximately 80% of the total PP1 activity in *Drosophila* larvae (Dombrádi *et al*., 1990). Mutational and inhibitory analysis of *PP1α87B* in *Drosophila* has revealed it is essential for survival as mutants die as larvae and is necessary for proper chromosome segregation, condensation and spindle organisation during mitosis (Axton *et al*., 1990; Wang *et al*., 2008). Certain homozygous mutant alleles of *PP1α87B* also suppress position-effect variegation (PEV), a phenomenon whereby genes become silenced upon translocation to a heterochromatic region by chromosomal rearrangements (reviewed in Schotta *et al*., 2003). *PP1β9C* and *PP1α96A* each contribute approximately 10% of the total PP1 activity (Bennett and Alphey, 2007). *PP1β9C* corresponds to the *flapwing* (*flw*) gene, with weak mutant alleles exhibiting crumpled or blistered wings and defects in the indirect flight

muscles, which render them flightless and stronger mutant alleles displaying semi lethality and degeneration of the indirect flight muscles (Raghavan *et al*., 2000).

Mutational analysis of *PP1α96A* revealed it is not an essential gene and unlike *PP1α87B*, it does not suppress PEV (Kirchner *et al*., 2007). It genetically interacts with *PP1β9C* as *PP1α96A* mutants enhance a weak *PP1β9C* mutant allele and has a role in regulating non-muscle myosin (Kirchner *et al*., 2007). Complementation analysis revealed that a certain level of redundancy exists between the different PP1 isoforms. *PP1α96A* and *PP1β9C* are redundant with *PP1α87B*, as the lethal phenotype of *PP1α87B* transheterozygous mutants can be rescued by overexpressing *PP1α96A* and *PP1β9C*, suggesting lethality is a consequence of a reduction in total PP1 activity (Kirchner *et al*., 2007). However, ectopic *PP1β9C* cannot rescue *PP1α87B, PP1α96A* double mutants and a *PP1β9C* mutant cannot be rescued by overexpression of *PP1α87B* or *PP1α96A*, suggesting non-overlapping functions do exist between the different isoforms (Kirchner *et al*., 2007). *PP1α13C* is the most recently identified member of the PP1 family and exhibits low levels of expression and is not essential for viability (Dombrádi *et al*., 1993; Clyne *et al*., 1999; Bennett *et al*., 2006).

1.3.4. PP1c regulatory subunits

Given PP1 is the main phosphatase in eukaryotes, a lot of work has been done to identify PP1 regulatory subunits to understand its role and regulation in various cellular processes. Some PIPs serve to regulate PP1 activity towards different substrates and are sometimes themselves targets of PP1 dephosphorylation. Other

PIPs act more to target PP1 and other interacting proteins to various substrates but have no role in regulating PP1 activity and others serve as both regulatory and targeting subunits. Many of the regulatory subunits that do not serve to target PP1 are inhibitor proteins, some of which are only present in particular tissues and subcellular localisations. Inhibitor proteins that interact with PP1 in humans include I-1 (*PPP1R1A*)/DARPP-32 (dopamine and cAMP-regulated phosphoprotein M_r 32000), which is mainly present in the brain but also the kidney (Hemmings *et al*., 1984; Cohen, 2002b) and I-2 (*PPP1R2*), which also interacts with PP1 in *Drosophila* and is widely distributed (Bennett *et al*., 2006; Wang *et al*., 2008).

The concept that PP1 associates with targeting/regulatory subunits came from studies on glycogen metabolism (Strålfors *et al*., 1985). These revealed PP1 has an important role in the metabolic response to insulin signals and at least four regulatory subunits associate with PP1 that target it to glycogen; G_M (R3, *PPP1R3A*), G_L (R4, *PPP1R3B*), R5 (PTG, *PPP1R3C*) and R6 (*PPP1R3D*) (Cohen, 2002b). These subunits have distinct spatial expression patterns and act as molecular scaffolds for PP1 and its metabolic substrates. Substrates that are targeted and regulated by PP1 in glycogen metabolism include glycogen phosphorylase, which becomes deactivated upon dephosphorylation by PP1 as well as glycogen synthase and phosphorylase kinase (Dent *et al*., 1990; Newgard *et al*., 2000). Other regulatory subunits have been identified that implicate PP1 in smooth muscle relaxation by associating with M_{110} (Myosin phosphatase targeting subunit) to dephosphorylate the myosin P-light chains at Ser19 (Cohen, 2002b) and apoptosis by interacting with and dephosphorylating Bcl-2 proteins that control the permeability of the outer mitochondrial membrane (Garcia *et al*., 2003; Cohen, 2002b).

1.3.5. Nuclear PP1c targeting/regulatory subunits

The role of PP1 in glycogen metabolism and myosin targeting has been well studied but such roles only represent cytosolic forms of PP1. PPPs, including PP1, are known to be enriched in the nucleus with PPPs in general showing a 2-10 fold higher concentration compared to the cytoplasm, yet they don't have a canonical nuclear localisation signal (Bollen and Beullens, 2002). They are targeted to the nucleus via association with regulatory subunits that specify their role in various nuclear processes including transcription, mRNA processing, mitosis and chromosome decondensation (Landsverk *et al*., 2005). Major regulatory/targeting subunits identified to date include Nuclear Inhibitor of PP1 (NIPP1) (Van Eynde *et al*., 1995) and the PP1 Nuclear Targeting Subunit (PNUTS, p99) (Allen *et al*., 1998), both of which are conserved and bind to PP1 in *Drosophila* (Bennett *et al*., 2006). The PNUTS-PP1 holoenzyme is the main focus of this thesis and a discussion of its structure and function can be found in Chapter 3. NIPP1 is an RNA binding protein (Jagiello *et al*., 1997) and a nuclear inhibitor of PP1c (Van Eynde *et al*., 1995). It is distributed in the nucleus as nuclear speckles, where it largely co-localises with factors involved in pre-mRNA splicing including small nuclear ribonucleic proteins (snRNPs) and targets PP1 to dephosphorylate and activate proteins required for the first catalytic step of splicing (Trinkle-Mulcahy *et al*., 1999).

As previously mentioned, some regulatory subunits of PP1 do not target it to a specific location but to specific substrates and in some cases the interacting protein is the substrate itself. The well known tumour suppressor Retinoblastoma (Rb) is an example of this and is a major regulator of the eukaryotic cell cycle and cell proliferation, implicating PP1 as an important phosphatase in regulating cell growth

and development (Berndt and Ludlow, 2004; van den Heuvel and Dyson, 2008). Rb activity is controlled by its phosphorylation status at several serine/threonine residues, which are targeted by PP1. Rb becomes activated upon dephosphorylation, allowing it to repress expression of cell cycle genes by sequestering the E2F1-3 transcription factors that control gene expression of cell cycle related genes such as cyclin E and cyclin A (Kolupaeva and Janssens, 2012). However, recent evidence suggests other PP1 regulatory subunits may be responsible for targeting PP1 to Rb and regulating its phosphorylation status in response to various cues such as oxidative stress and hypoxia, including the myosin targeting subunit M_{110} and PNUTS (Udho *et al*., 2002) (see Kolupaeva and Janssens, 2012, for a review). Finally the Trithorax group (TrxG) of epigenetic regulators have been shown to bind PP1c on polytene chromsomes in *Drosophila* (Rudenko *et al*., 2003). TrxG proteins are required for the normal expression of genes including homeotic genes and PP1 is believed to regulate Trx dependent transcriptional control but whether it is a substrate of PP1 itself remains to be determined (Rudenko *et al*., 2003).

1.3.6. Regulatory subunits of other PPP's

Like PP1, PP2A is known to be involved in a diverse array of physiological processes including mitosis, signal transduction, transcription and translation, metabolism, cell proliferation, DNA replication and apoptosis (Rivers, 1996; Seshacharyulu *et al*., 2013). PP2A is a heterotrimeric holoenzyme consisting of a structural A subunit, a variable regulatory B subunit that determines substrate specificity, localisation and phosphatase activity and a catalytic C subunit, which can be regulated by post-translational modifications to control association with various B-type subunits (Sents *et al*., 2013). In humans, there are at least four families of B

subunits, namely PR55 (B), PR61 (B'), PR72 (B") and PR93/PR110 (B'") each encoded by several genes that have tissue and subcellular specific expression patterns (Janssens and Goris, 2001; Janssens *et al*., 2008; Lambrecht *et al*., 2013). For example PR55 is encoded by four genes; *PR55α*, *PR55β*, *PR55γ* and *PR55δ* with PR55α showing a wide-spread tissue distribution and PR55β being enriched in the brain (Janssens and Goris, 2001). These B-type regulatory subunits target the PP2A holoenzyme to different substrates such as Rb, which is targeted by PR70/B" (a member of the PR72 family) and mitogen-activated protein kinase (MAPK), which is targeted by PR61/B' (Kolupaeva and Janssens, 2012; Janssens *et al*., 2008). PP2A holoenzymes are also critical regulators of the Bcl-2 and PI3K-Akt signalling pathways (Garcia *et al*., 2003).

1.3.7. The PPM Family

Protein phosphatases belonging to the PPM family are present in both eukaryotes and prokaryotes and were not only characterised by their requirement for exogenous bivalent metal ions but also their insensitivity to inhibitors of the PPP family, including the broad-spectrum inhibitor okadaic acid (Barford, 2010; Lammers and Lavi, 2007). The defining member is PP2C, which shares no sequence similarity with members of the PPP family but comparison of the crystal structures revealed PP2C has a similar tertiary structure and catalytic domain architecture, which is formed by two anti-parallel β-sheets flanked by two antiparallel α-helices (Barford, 2010). So far, at least 16 PP2C genes have been identified in humans with several of them shown to be involved in cell growth and cell cycle progression by regulating cyclin-dependent kinase (CDK) activity (Cheng *et al*., 2000) and cellular stress pathways such as the MAPK stress activated signalling pathway (Hanada *et al*., 1998) (for a

review see Lammers and Lavi, 2007). Unlike PPPs they do not associate with regulatory subunits for controlling activity and instead are likely to be regulated by spatially specific expression, post-translational modifications and degradation (Lammers and Lavi, 2007)

1.3.8. The FCP Family

FCP1 is the major member of the FCP family and is highly conserved throughout eukaryotes. It is an essential gene required for the recycling of hyperphosphorylated RNA polymerase II (RNAPII) and directly targets the C-terminal domain (CTD) of RNAPII for dephosphorylation (Kamenski *et al*., 2004; Yeo *et al*., 2003). SCP1 is the newest member of the family and also targets the CTD of RNAPII for dephosphorylation at Serine 5, with a preference for RNAPII that has been phosphorylated by TFIIH (Yeo *et al*., 2003).

1.4. Protein Tyrosine Phosphatases (PTPs)

PTP's are only present in eukaryotes and were originally thought to have a housekeeping role in signal transduction pathways (Tonks and Neel, 2001). Instead, it is now known they are a large superfamily of related proteins and are involved in numerous signalling pathways that regulate gene transcription, mRNA processing, cell growth and differentiation (Alonso *et al*., 2004; Tonks and Neel, 2001). They are defined by the catalytic sequence motif H-C-X-X-G-X-X-R in their active site and can be subdivided into classical PTPs (those that target only tyrosine) and dual specificity phosphatases (DSPs) that target tyrosine and serine/threonine (Tonks and Neel, 2001). Classical PTPs can be subdivided into transmembrane receptor-like (includes CD45 and PTPα/β/γ/μ/ε) and non-transmembrane (includes PTP1B and

SHP1/2) (Tonks and Neel, 2001). DSPs are also subdivided into VHR-like and Cdc25 and also include the well-known tumour suppressor PTEN, which can dephosphorylate both proteins and lipids. DSPs are able to dephosphorylate tyrosine and serine/threonine due to the formation of a shallow catalytic site. This allows the shorter side chains of serine and threonine to reach the cysteine residue that sits in the active site whereas classical PTPs have a deep active site which only allows the longer side chain of tyrosine to reach the cysteine residue (Böhmer *et al*., 2012).

1.5. RNA polymerase II phosphorylation

Studies on PP1 have often focused on its role in transcriptional regulation and in 2002, Washington *et al.,* described the carboxy-terminal domain (CTD) of RNA polymerase II (RNAPII) as a target of PP1 (Washington *et al*., 2002). RNAPII is one of three eukaryotic, highly conserved nuclear DNA-dependent RNA polymerases and is responsible for the synthesis of various classes of RNA including all mRNA and many noncoding RNAs (Hahn, 2004; Hsin and Manley, 2012). The CTD of its largest subunit, Rbp1 (possesses the enzyme's catalytic activity), is well characterised and comprises a consensus heptapeptide repeat, $Y_1S_2P_3T_4S_5P_6S_7$, which is subject to phosphorylation on its five hydroxylated amino acids (Tyr-1, Ser-2, Thr-4, Ser-5 and Ser-7 but principally Ser-2 and Ser-5) (Phatnani and Greenleaf, 2006). The number of heptapeptide repeats varies between species from 26 in yeast to 45 in *Drosophila* and 52 in mammals (Hirose and Manley, 2000; Egloff and Murphy, 2008). Regulation of CTD phosphorylation by various CTD kinases and phosphatases (see Hsin and Manley, 2012 for review) is essential throughout the different stages of transcription and for coordinating events required for RNA synthesis and processing for maturation of the transcript (Hsin and Manley, 2012). It

is required for the recruitment of various histone modifiers, chromatin modifying complexes to influence transcription and various enzymes and complexes that are necessary for processing mRNA to mature RNA for export from the nucleus (Hsin and Manley, 2012). Phosphorylation at different residues alters the structure of RNAPII and its ability to interact with the various different factors (Rosado-Lugo and Hampsey, 2014; Egloff and Murphy, 2008; Hintermair *et al*., 2012).

Before transcription initiation, the CTD is unphosphorylated (designated RNAPIIA) when it is recruited to the promoter and forms part of the preinitiation complex but upon initiation the CTD becomes hyperphosphorylated (designated RNAPIIO) and a pattern of phosphorylation begins, marking the different stages of transcription (Hsin and Manley, 2012). Ser-5 phosphorylation occurs concomitantly with transcription initiation and peaks around the transcription start site (TSS) (Hsin and Manley, 2012). It is essential for coupling transcription to the first mRNA processing event, 5' capping, by associating with the capping enzyme (guanylytransferases) (Schroeder *et al*., 2000; Komarnitsky *et al*., 2000). As the nascent RNA emerges from RNAPII shortly after initiation, when it reaches 20-30 nucleotides in length, the capping enzyme adds a methylguanosine cap to the 5' end to stabilise and regulate the nascent mRNA (Egloff and Murphy, 2008; Schroeder *et al*., 2000).

As RNAPII clears the promoter and enters the elongation phase, dynamic changes in phosphorylation occur as Ser-5 becomes gradually dephosphorylated and Ser-2 becomes phosphorylated until the end of genes (as RNAPII nears termination) when both are dephosphorylated and RNAPII is recycled for another round of transcription (Hsin and Manley, 2012; Buratowski, 2009). It is thought phosphorylation of Ser-2 is

required for RNAPII to enter the elongation phase (Egloff and Murphy, 2008). There is much evidence to suggest elongating RNAPII is responsible for coupling transcription to splicing, the next stage of RNA processing. Most mRNAs contain introns, which are removed by a large macromolecular complex termed the splicesome during splicing to produce functional RNAs. Various splicing factors have been shown to associate with phosphorylated RNAPII and specifically the elongating form including mammalian CA150 and U2AF65, to activate and enhance splicing and thus couple this RNA processing event to transcription (David *et al*., 2011; Hsin and Manley, 2012; Hirose and Manley, 2000; Egloff and Murphy, 2008).

The final stage of RNA processing, polyadenylation is also coupled to transcription through the CTD phosphorylated at Ser-2. Polyadenylation is a two-step process marked by the polyadenylation signal at the 3'end of protein coding genes, where ChIP analysis suggests most of the Ser-5 phosphorylation has been lost (Egloff and Murphy, 2008; Komarnitsky *et al*., 2000). The first stage is endonucleolytic cleavage followed by Poly(A) tail synthesis by a very complex set of proteins, to stabilise the RNA for export from the nucleus and to aid translation (Shi *et al*., 2009; Hsin and Manley, 2012). Several 3' end processing factors are known to interact with the CTD including the polyadenylation cleavage factor (Pcf)11, which directly binds to CTD repeats phosphorylated at Ser-2 (Egloff and Murphy, 2008; Meinhart and Cramer, 2004; Hsin and Manley, 2012). Both the Poly(A) signal in RNA and Ser-2 phosphorylation are thought to contribute to the recruitment and assembly of the polyadenylation complex (for review see Hsin and Manley, 2012). There is also evidence to suggest the interaction between the CTD and polyadenylation factors

contribute to transcription termination, for example Pcf11 has been linked to termination (Buratowski, 2009).

Other residues of the heptapeptide repeat are also phosphorylated but their exact roles are poorly understood. Ser-7 has been shown to somewhat overlap with Ser-5 phosphorylation at the start of transcribed genes but has also been shown to peak at the 3' end of genes (Egloff and Murphy, 2008; Egloff *et al*., 2012). It has been demonstrated to be required for the recruitment of the integrator complex, which is involved in 3' end processing of snRNA genes (Egloff *et al*., 2012). Thr-4 phosphorylation overlaps with Ser-2 phosphorylation towards the 3' end of transcribed genes and it appears to be dependent on Ser-2 phosphorylation (Hsin and Manley, 2012; Hintermair *et al*., 2012; Egloff and Murphy, 2008; Svejstrup, 2012). This phospho site has been implicated in transcription elongation and may therefore be essential for linking transcription to splicing (Hintermair *et al*., 2012). No clear function has been linked to Try-1 phosphorylation.

1.6. Protein phosphorylation and disease

Aberrant phosphorylation has been linked to many pathological conditions including cancer, Alzheimer's, diabetes and autoimmune disease (He *et al*., 2014; Stebbing *et al*., 2014; Ma *et al*., 2013). As kinases and phosphatases are the enzymes that control the phosphorylation state of proteins, they have been the targets of therapeutic compounds to treat these diseases using inhibitors. Together they make up 26% of the druggable genome, which is predicted based on what makes a good drug (e.g. degree of potency) and what makes a good drug target (e.g. the number of ligand binding domains, implicated in human disease) (Hopkins and Groom, 2002; Pandey

and Nichols, 2011). As kinases contribute the larger portion of that percentage, with 22%, they have been the main focus for the development of therapeutic compounds to treat diseases characterised by abnormal phosphorylation patterns (Hopkins and Groom, 2002). Their popularity as drug targets is demonstrated by the fact that approximately 30% of drug discovery programs in the pharmaceutical industry are targeting kinases (Cohen, 2002a). One of the better-known examples of the successful use of a kinase inhibitor to treat disease is Rapamycin. This inhibits the protein kinase mammalian Target of Rapamycin (mTOR), which is involved in cell growth, proliferation and survival through the PI3K signalling pathway and T-cell proliferation (Cohen, 2002a; Ballou and Lin, 2008). It has successfully been used for the treatment of cancer and as an immunosuppressant for patients undergoing organ transplants (Ballou and Lin, 2008). Another famous example is Imatinib (otherwise known as Gleevec), a tyrosine kinase inhibitor, to treat chronic myeloid leukemia as well as other malignancies that involve expression of a tyrosine kinase (Dulucq and Krajinovic, 2010).

It is only in recent years that efforts have been made to study the clinical potential of phosphatases and discover therapeutic compounds that target them, but their successful use in treatment is made difficult by their broad specificity (Figueiredo *et al*., 2014). Most phosphatases are involved in numerous signalling pathways and cellular processes and manipulation of their activity could be detrimental without a deep understanding of how they achieve selectivity in these processes (Figueiredo *et al*., 2014). The only phosphatase inhibitor that is approved for clinical use is Cyclosporin A, which targets the serine/threonine phosphatase PP2B/calcineurin and is used as an immunosuppressant for organ transplants (McConnell and Wadzinski,

2009). As we now know, specificity is achieved through temporal and spatial association with protein complexes and regulatory subunits that target phosphatases to specific substrates (Faux and Scott, 1996). Therefore identification and characterisation of these complexes and subunits will aid in the development of therapeutic compounds that can selectively target a broad phosphatase in a particular pathway or process. Small molecules are already being developed to target regulatory subunits in phosphatase complexes specific to a physiological process. Guanabenz binds to the PP1 regulatory subunit GADD34 to prevent dephosphorylation of the transcription initiation factor eIF2α in stress conditions (Tsaytler *et al*., 2011). Under stress conditions, dephosphorylation of eIF2α leads to the accumulation of misfolded proteins, which can be lethal, therefore the use of Guanabenz could be relevant for the treatment of conditions characterised by the accumulation of misfolded proteins (Tsaytler *et al*., 2011).

PP2A is a well-established tumour suppressor showing reduced expression in various human cancers as well as other diseases such as Alzheimer's and other neurodegenerative disorders. Pre-clinical studies are already underway to identify pharmacological compounds that can restore PP2A in such diseases and even inhibitors of PP2A that lead to cancer cell death (Lambrecht *et al*., 2013).

1.7. *Drosophila* as a model organism

Drosophila melanogaster has been used as a model organism for over a century due to its rapid generation time, easy manipulation, genetic tractability and the wealth of sophisticated genetic tools and resources available for functional genomic studies. It has become a predominant model for the study of numerous aspects of biology,

which has become more significant with the discovery that genes necessary for development in *Drosophila* also play a role in mammalian development (Jennings, 2011). It is the origin of many significant discoveries in the history of science, including the finding by Thomas Hunt Morgan, who won the Nobel Prize in Physiology and Medicine in 1933, for his work in *Drosophila* showing chromosomes are the carriers of genetic traits (Rubin and Lewis, 2000; Pandey and Nichols, 2011). Morgan was also responsible for the isolation of the first *Drosophila* mutant as a way to characterise gene function, which was followed by Muller in 1927, who discovered gene mutations could be generated by exposure to x-rays (Muller, 1927). Since then a large collection of *Drosophila* mutations have been generated using ionising radiation and other classical chemical mutagenesis approaches such as the alkylating agent ethyl methanesulphonate (EMS) and are widely available to researchers.

Muller was also responsible for the development of balancer chromosomes, to allow stocks of homozygous lethal mutations to be maintained as balanced heterozygotes (Muller, 1918; Hentges and Justice, 2004). Balancer chromosomes have multiple inversions to suppress recombination and a dominant phenotypic marker such as curly wings (*CyO*) to enable tracking of chromosomes across generations (Hentges and Justice, 2004). They are also recessive lethal so the balancer chromosome cannot exist in the homozygous state and the experimental chromosome cannot be lost (Hentges and Justice, 2004). Since the development of balancer chromosomes in *Drosophila* other model systems have adopted this tool in functional genomic studies including the mouse and *Caenorhabditis elegans* (*C.elegans*) (Boles *et al*., 2009; Kile *et al*., 2003).

The available resources for functional genomic studies was further increased after the *Drosophila* genome was successfully sequenced and annotated in March 2000, becoming the first major complex organism to have its genome sequenced (Adams *et al*., 2000; Jennings, 2011). This greatly enhanced already existing online tools such as FlyBase, a database of *Drosophila* genes and a resource for *Drosophila* related data and information (Pierre *et al*., 2014). The significance of sequencing the fly genome was highlighted a few years later after sequencing of the human genome was completed. It became apparent a significant degree of homology exists between the two genomes, which supports the use of *Drosophila* as a model organism to study various aspects of human biology and disease. A staggering 77% of disease causing genes in humans have a *Drosophila* orthologue and this data has been consolidated into an online database called Homophila, which links the two genomes to aid *Drosophila* studies addressing human disease (Reiter *et al*., 2001; Chien *et al*., 2002). This is further supported by FlyAtlas, a database of gene expression data from 9 adult tissues (brain, head, testis, ovaries, crop, midgut, male accessory glands, hindgut and Malpighian tubules), based on micro-array data (Chintapalli *et al*., 2007). This helps to identify the best tissues in which to study genes of interest and is particularly relevant as human disease genes often show a similar tissue expression pattern to their homologues in *Drosophila* (Chintapalli *et al*., 2007).

1.7.1. *Drosophila* transposable elements

Many of the tools used for studying gene function in *Drosophila* have been revolutionised by *P*-element mediated transgenesis (Ejsmont and Hassan, 2014). *P*-elements are transposable (mobile) genetic DNA elements (transposons) that naturally occur in wild *Drosophila* strains. They are present in many organisms and

can integrate into genomes with the catalytic help of the enzyme transposase for germ line transmission when injected into G0 *Drosophila* embryos (Venken and Bellen, 2007). The source of transposase can either be genetically encoded in the *P*-element (autonomous) or external, for example in an engineered construct (non-autonomous) (Ryder and Russell, 2003). They are an efficient method for introducing foreign DNA into the *Drosophila* genome for various approaches to study gene function including genetic rescue (Rubin and Spradling, 1982), generating mutants by their insertion or excision (Cooley *et al*., 1990; Cooley *et al*., 1988) and gene cloning (Searles *et al*., 1982).

The use of non-directed *P*-elements for generating transgenic strains does have limitations. Integration into the genome is random and to identify the desired site specific transgenic insertion event requires extensive genetic screening. Random integration means position effects can complicate analysis as regulation of the transgene is influenced by the surrounding chromatin environment, with insertion into a heterochromatic region resulting in repression of the transgene (Venken and Bellen, 2007). For integration of genomic rescue constructs it is necessary to control the site in which it is integrated to avoid position effects. Furthermore large DNA fragments (>40kb) cannot be integrated as they are unstable in high copy number plasmids in bacteria, which hampers the study of large genes (Venken *et al*., 2006). These limitations have been overcome using the irreversible bacteriophage ΦC31 (phiC31) integrase for site specific transgenesis (Groth *et al*., 2004). This allows site-specific integration into the genome by catalysing recombination between two engineered docking sites in the *Drosophila* genome, the phage attachment (*attP*) and the bacterial attachment (*attB*) to create *attL* and *attR* sites (Venken *et al*., 2006). It

also enables integration of large DNA fragments (>100kb) into the *Drosophila* genome using low-copy number plasmids such as BAC (Bacterial Artificial Chromosome), which have been modified by including an inducible *oriV* origin of replication to amplify plasmid copy number (Venken *et al*., 2006; Venken and Bellen, 2007).

1.7.2. The *Drosophila* Gene Disruption Project

The *Drosophila* Gene Disruption Project (GDP) was established in 1991 and exploited the properties of transposons to disrupt gene function using insertional mutagenesis, to generate a genome wide collection of mutants for analysing gene function (Bellen, 2004; Spradling *et al*., 1999). This project generated a public collection of mutant strains, with genes disrupted through the insertion of a *P*-transposable element at the 5' end of individual genes (Bellen *et al*., 2011). Annotation of the genome enabled more strains to be generated and by 2004 approximately 40% of *Drosophila* genes had at least one strain carrying a *P*-element, which are available from the Bloomington Stock Centre (Bellen, 2004). To increase genome coverage and generate stronger loss-of-function alleles other transposable elements have been used including *piggyBac* (Thibault *et al*., 2004; Handler and Harrell, 1999), *mariner* (Garza *et al*., 1991) and *minos* (Metaxakis, 2005; Loukeris *et al*., 1995; Ryder and Russell, 2003; Venken and Bellen, 2007), which has likely increased gene coverage closer to 65% (Venken and Bellen, 2005). Transposable elements have different target site specificities with *P*-elements showing bias for the 5' end of genes, as well as distinctive 'hotspots' (sites that attract insertion of transposable elements at a high frequency) and 'coldspots', as well as different gene targets, with *piggyBac* targeting genes encoding transcription and chromatin factors

and genes involved in growth and behaviour (Bellen *et al*., 2011). In most strains gene function is directly affected but the transposable elements are also useful tools for generating additional mutations through imprecise excision (see Chapter 5) and for determining chromatin structure by utilising the position effects seen upon random integration (Bellen *et al*., 2011).

1.7.3. The GAL4/UAS binary system in *Drosophila*

P-element transgenesis has provided the *Drosophila* community with a range of other tools that can be used to study gene function. Probably the most revolutionary example described by Brand and Perrimon in 1993, is the use of the yeast GAL4/UAS binary expression system to ectopically express genes or transgenes in a cell or tissue specific manner and to fine-tune expression patterns both temporally and spatially in *Drosophila* (Brand and Perrimon, 1993). GAL4 is a transcription factor identified in the yeast *Saccharomyces cerevisiae*, which binds to the Upstream Activating Sequence (UAS) to activate transcription. A *P*-element carrying a UAS is inserted near the 5' end of an experimental gene in one parental strain and is crossed to another parental strain carrying a GAL4 driver, which expresses GAL4 in a spatially specific pattern (Figure 1.2). In the progeny, the experimental gene is expressed in a pattern that reflects the driver used to mediate GAL4 expression. A range of GAL4 drivers are publicly available to target gene expression to various tissues including the ovaries, testis, imaginal discs and brain as well as specific cells such as the border cells in the ovary. Expression of GAL4 can be further refined using the GAL80 repressor, which binds to the carboxy-terminal of GAL4 and prevents it from activating transcription. This is the basis of the TARGET (temporal and regional gene expression targeting) system, which uses a temperature sensitive

variant of GAL80 ($GAL80^{ts}$) under the control of the tubulin promoter ($tubGAL80^{ts}$) to temporally control gene expression (McGuire *et al*., 2003). When raised at 18/22°C, GAL80 remains bound to GAL4 and represses GAL4-mediated expression of UAS (Figure 1.2b). Upon shifting to 25/29°C, GAL80 repression is relieved to enable expression of UAS by GAL4 (Figure 1.2c). This approach is particularly useful when studying developmentally lethal gene mutations as it allows expression of these mutant transgenes to be induced after the lethal phase.

The GAL4/UAS system can also be combined with heritable RNA interference (RNAi) technology to target knockdown of experimental genes to specific tissues or cells (Dietzl *et al*., 2007). Heritable RNAi is discussed in Chapter 6 but briefly gene knockdown can be achieved by expressing double stranded 'hairpin' RNA by cloning an experimental gene fragment as an inverted repeat (Kennerdell and Carthew, 2000). Expression of the gene specific inverted repeat can be under the control of the GAL4/UAS system to ectopically achieve gene knockdown in different tissues at any stage of development. Various resources are available that supply strains containing inverted repeat constructs downstream of UAS to allow users to cross to the desired GAL4 driver (Dietzl *et al*., 2007). The Transgenic RNAi Project (TRiP) is one of those resources, which used ΦC31 mediated integration to incorporate these constructs into the *Drosophila* genomes (Ni *et al*., 2009; Dietzl *et al*., 2007).

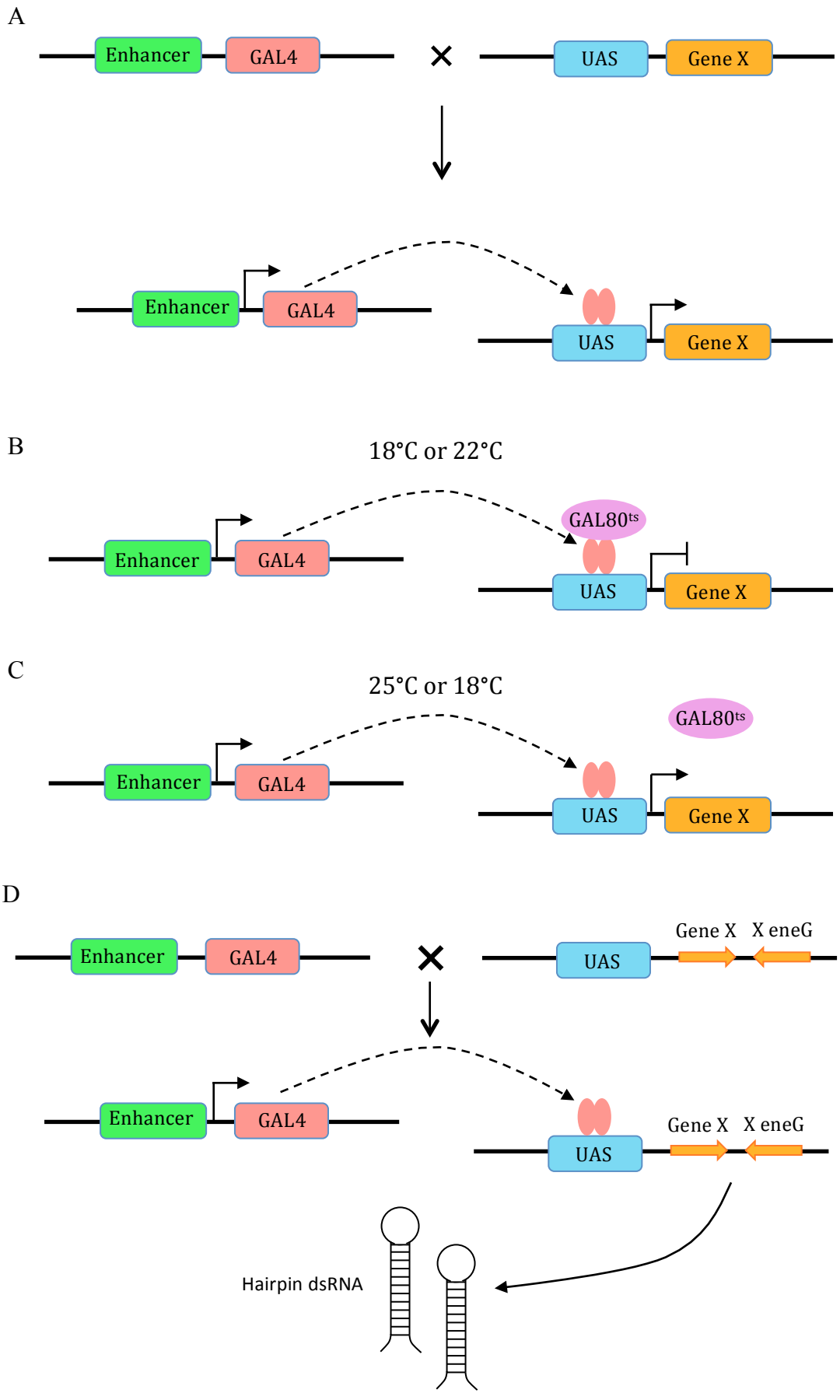
A
Enhancer
GAL4
UAS
Gene X
B
18°C or 22°C
GAL80ts
C
25°C or 18°C
D
Gene X X eneG
Hairpin dsRNA

Figure 1.2 (previous page). The GAL4/UAS binary and TARGET systems in *Drosophila*. a) The yeast transcriptional activator GAL4 is expressed in a spatially restricted pattern specifically defined by an enhancer/driver. The GAL4 protein binds to UAS sites in the *Drosophila* genome and activates transcription of the experimental gene (gene X), which lies downstream of the UAS. b,c) $GAL80^{ts}$ is a temperature sensitive inhibitor of GAL4 mediated expression. At the restrictive temperature (18 or 22°C) GAL80 binds to the carboxy-terminal of GAL4 and represses its activity. At the permissive temperature (25 or 29°C) GAL80 repression is relieved, allowing GAL4 to activate transcription of the experimental gene. d) The GAL4/ UAS system can also be used to target knockdown of experimental genes to specific tissues/cells. An inverted repeat for the experimental Gene X is positioned downstream of UAS. Upon transcription activation by GAL4 under the control of a tissue/cell specific enhancer/driver a dsRNA hairpin structure is produced.

1.7.4. The Flp/FRT system

The Flp/FRT system is another tool that has benefited from *P*-element transgenesis (Golic and Lindquist, 1989). This system can be used to generate mosaic tissues composed of cells with different genotypes to study genes involved in developmental processes (Theodosiou and Xu, 1998). It utilises an enzyme derived from yeast called flippase (Flp) to induce mitotic recombination between Flippase Recognition Target (FRT) sites that have been inserted on homologous chromosomes at specific cytological locations close to the centromere (Golic and Lindquist, 1989). Flp and FRTs are usually integrated using site-specific *P*-element mediated transgenesis. In a heterozygous parent, one chromosome carries a wild type allele of the gene of interest and the other carries a mutant allele, on the same chromosome arm as the

FRT site. The wild type allele is usually marked by green fluorescent protein (GFP) under the control of a ubiquitous promoter and presence of the mutant allele is negatively marked by absence of GFP. Upon recombination between the FRT sites, tissues have a mix of GFP positive homozygous wild type cells (often referred to as a 'twin spot') and GFP negative homozygous mutant cells allowing the behaviour of mutant cells to be directly compared to that of wild type in the same tissue (Figure 1.3). Although FRT-mediated recombination has a much higher recombination rate compared to other methods used to induce recombination such as irradiation, it is not 100% efficient and some cells will remain in the heterozygous state (Blair, 2003). Expression of Flp is usually under the control of an inducible promoter, most commonly a heat shock promoter, to allow temporal control over the induction of mitotic recombination. This is necessary when studying genes involved in cell growth and cell survival, allowing control over the size of the clonal patch, with clones induced early during development producing large patches and clones induced late producing smaller but more numerous clonal patches (Blair, 2003). Stocks are available with FRTs inserted at various locations on each of the chromosome arms as well as various strains that express Flp under the control of the heat shock inducible promoter.

In some experiments it is an advantage to generate large patches of mutant cells. This can be achieved by giving them a growth advantage in developing tissues using dominant mutations at *Minute* (*M*) loci (Morata and Ripoll, 1975). *Minutes* are a class of mutants that carry mutations in genes encoding various ribosomal proteins (e.g. RpL27a) resulting in death in homozygous animals due to cell lethality (Amoyel and Bach, 2014). Heterozygous animals are viable but exhibit delayed

development due to a reduction in cell division rates (Amoyel and Bach, 2014; Marygold *et al*., 2007). In a homotypic environment heterozygous animals eventually produce a normal organism but when induced in a wild type background they are eliminated due to cell competition (Amoyel and Bach, 2014). In the context of the Flp/FRT system, *M* alleles can be recombined onto wild type chromosome arms bearing an FRT site so that wild type cells exhibit delayed growth in comparison to their mutant counterpart. This is particularly useful when studying genes involved in cell growth and development.

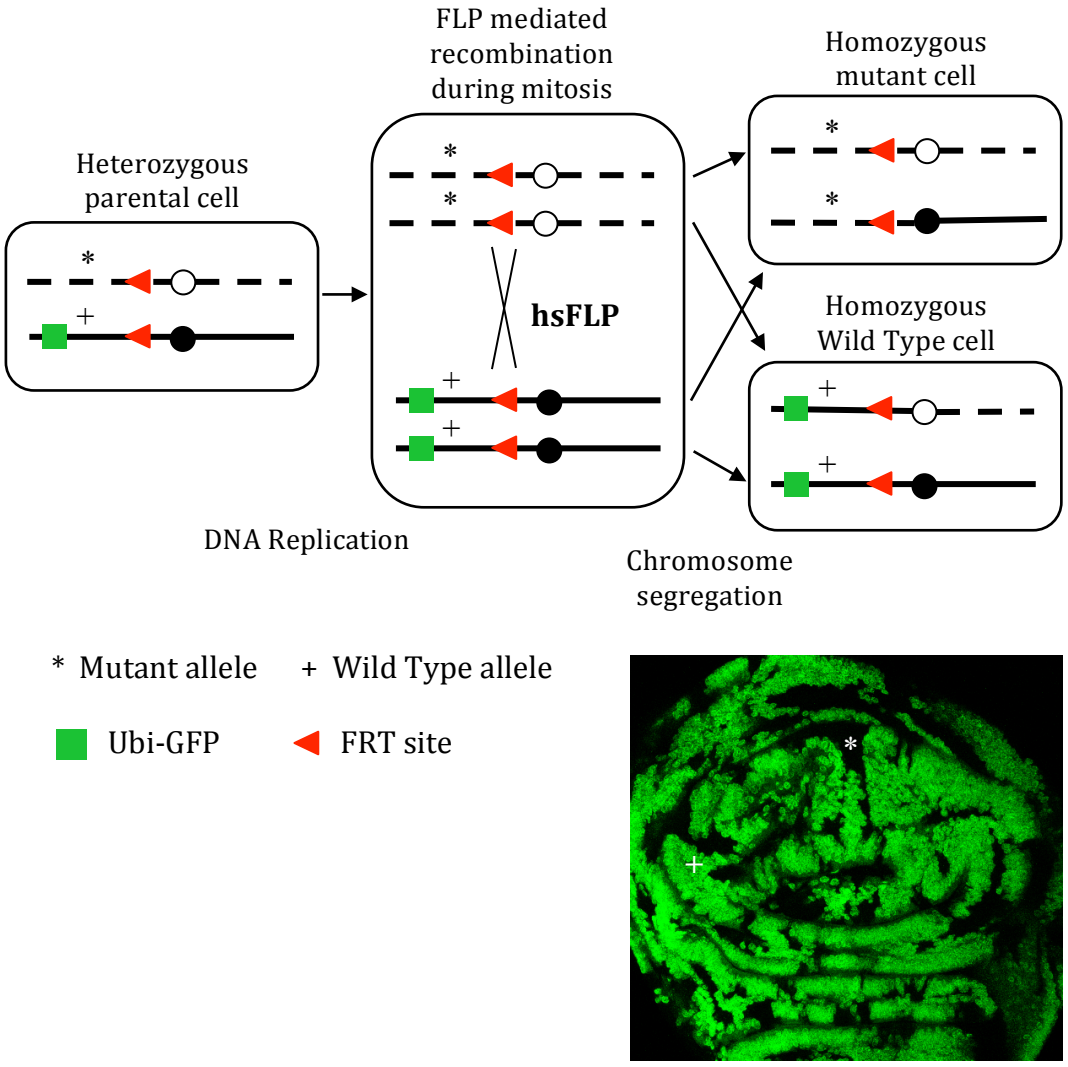

Figure 1.3. The Flp/FRT system for generating mosaic tissues. Upon heat shock, expression of the enzyme flippase (FLP) induces recombination between FRT sites on homologous chromosome arms. A ubiquitous GFP marker is also present on the same chromosome arm as the experimental wild type allele. During mitosis recombinant chromosomes are segregated producing two daughter cells with one carrying two copies of the mutant allele (negatively marked by absence of GFP) and one carrying two copies of the wild type allele (positively marked by presence of GFP). An example of a *Drosophila* wing imaginal disc with mosaic clones is shown below with negatively marked homozygous mutant patches (white star) and

positively marked homozygous wild type patches (white plus sign). Heterozygous cells are also GFP positive as they carry one copy of the wild type allele.

1.8. Research Aims

The aim of this research was to explore the *in vivo* role of the PP1 regulatory subunit PNUTS in *Drosophila* and to identify and characterise PNUTS interacting proteins to provide further insight into the complex regulation and targeting of PP1 and PNUTS in the nucleus. The identification of new substrates of the PNUTS-PP1 holoenzyme in the nucleus was also explored to understand its role in various nuclear processes.

2. Materials and methods

2.1. Commonly used media and solutions

LB (Luria-Bertani) Broth (BDH laboratory supplies)

Required for growth of bacterial strains: 1.0% (w/v) Tryptone, 0.5% (w/v) Bacto-yeast extract and 1.0% (w/v) NaCl dissolved in pure deionised water (pH 7.0) and autoclaved before use.

LB Agar (BDH laboratory supplies)

Required for growth of bacterial strains on solid plates: 1.0% (w/v) Tryptone, 0.5% (w/v) Bacto-yeast extract, 1.0% (w/v) NaCl and 1.6% (w/v) agar dissolved in pure deionised water (pH 7.0). Autoclaved and cooled to 55°C before adding the appropriate antibiotic, pouring into plates and allowing to set. Stored at 4°C.

Apple juice agar

For egg laying experiments: 15g agar powder dissolved in 335ml pure deionised water by gentle heating. 8g sucrose dissolved in 165ml Apple Juice plus 2ml 10% (v/v) Nipagen. Apple juice/sucrose/nipagen solution then added to agar once slightly cooled and poured into 35mm plates and allowed to set. Stored at 4°C.

SOC (Super Optimal Broth) medium (Life Technologies)

A nutrient-rich bacterial growth medium, which enables higher transformation efficiencies of plasmids: 2.0% (w/v) Tryptone, 0.5% (w/v) Yeast Extract, 10mM NaCl, 2.5mM KCl, 10mM $MgCl_2$, 10mM $MgSO_4$ and 20mM glucose.

Complete Schneider's Insect Medium

Schneider's Insect Medium (with L-glutamine and sodium bicarbonate, Sigma) substituted with 10% (v/v) heat inactivated Foetal Calf Serum (FCS, Gibco) and Penicillin-Streptomycin (Invitrogen) to a final concentration of 50 units Penicillin G and 50μg/ml Streptomycin sulphate.

Tris-EDTA (TE) Buffer (Sigma)

For resuspension of DNA: 10mM Tris-Cl pH 7.5 and 1mM EDTA (Ethylenediaminetetraacetic acid).

ChromoTek lysis buffer

Optimised by the manufacturer for GFP-trap immunoprecipitation and enables efficient cell lysis a protein solubilisation while avoiding protein degradation and interference with the proteins immunoreactivity and biological activity: 10mM Tris-Cl pH 7.5, 150mM NaCl, 0.5mM EDTA and 0.5% (v/v) NP-40.

2× SDS sample buffer

Laemmli sample buffer (Sigma) was used for protein extraction and loading of protein samples onto SDS-polyacrylamide gels for SDS-PAGE and Western Blotting: 4% SDS, 20% glycerol, 10% (v/v) 2-mercaptoethanol, 0.004% (w/v) bromophenol blue and 0.125M Tris-HCl, pH 6.8.

1× SDS-PAGE Running Buffer

For protein separation during SDS-polyacrylamide gel electrophoresis: 25mM Tris (Anachem), 250mM Glycine (Anachem) pH8.3 and 0.1% (v/v) SDS dissolved in pure deionised water.

Tris-glycine Transfer Buffer

For protein transfer from SDS-PAGE gels to nitrocellulose membrane: 25mM Tris, 193mM glycine and 20% (v/v) methanol in pure deionised water.

Tris-buffered saline with Tween (TBST)

For washing nitrocellulose membranes for during western blotting: 150mM NaCl, 10mM Tris-HCl and either 0.1% or 0.05% (v/v) Tween-20 (SIGMA) diluted in pure deionised water.

3.7%/ 10% (w/v) Paraformaldehyde (Sigma)

3.7% for fixing *Drosophila* tissue and 10% for fixing S2R+ cells. An approximately 37% stock was made by dissolving 0.185g in 500µL (+7µL 1M NaOH to aid solubilisation) 1 x PBS at 95°C for 5 minutes. Absolute concentration was determined after incubation and diluted accordingly for the each experiment.

Blocking solution (Drosophila tissues)

1 x PBS, 5% (w/v) Fetal Bovine Serum, 0.1% (v/v) Triton X-100.

Blocking buffer (Western Blots)

5% (w/v) Marvel skimmed milk powder or 5% (w/v) Bovine Serum Albumin (BSA, Sigma Aldrich) in 0.05% TBST

PBS (Purchased as 10× stock solution from Roche)

1 × solution: 137mM NaCl, 2.7mM KCl, 8mM Na_2HPO_4, 2mM KH_2PO_4

PBST (Drosophila tissues)

1 × PBS, 0.1% (v/v) Triton X-100

1 × TAE buffer

0.04M Tris-acetate, 1mM EDTA in pure deionised water.

Testis buffer

183mM KCl, 47mM NaCl, 10mM Tris-HCl, pH 6.8 in pure deionised water.

2.2. Chromatin Immunoprecipitation (ChIP) buffers/reagents

10 x buffer A stock (store at room temperature)

600mM KCl, 150mM NaCl, 150mM Hepes-KOH, pH 7.6, 10mM EDTA, 1mM EGTA, 100mM Sodium Butyrate, autoclaved pure deionised water.

1 x complete buffer A stock (make on day of assay)

10 x buffer A stock, 0.15mM spermine, 0.5mM spermidine, 0.5mM DTT, autoclaved pure deionised water.

Buffer A+ (make on day of assay)

1 x complete buffer A, 12mM EDTA, 0.5% (v/v) NP-40, 1 x Protease Inhibitor Cocktail (PIC, Roche cOmplete ULTRA mini EDTA-free tablets), 1mM Phenylmethylsulphonyl Fluoride (PMSF, SIGMA).

Buffer AS (make on day of assay)

1 x complete buffer A, 10% (w/v) sucrose.

Buffer A+NP-40 (make on day of assay)

10 x buffer A stock, 0.1% (v/v) NP-40, autoclaved pure deionised water.

37% (w/v) Paraformaldehyde (Sigma), stock solution for crosslinking

An approximately 37% stock was made by dissolving 0.185g in 500µL (+7µL 1M NaOH to aid solubilisation) 1 x PBS at 95°C for 5 minutes. Absolute concentration was determined after incubation and diluted accordingly for the each sample to a final concentration of 1.8%.

Nuclei Lysis Buffer (store stock at room temperature)

1% (v/v) SDS, 50mM Tris-HCl pH 8.0, 10mM EDTA, 10mM Sodium Butyrate.

TE Buffer (store stock at room temperature)

10mM Tris-HCl pH 8.0, 1mM EDTA.

Chromatin IP buffer

25mM Tris-HCl pH 8.0, 137mM NaCl, 2.7mM KCl, 1% (v/v) Triton X-100, 1mM EDTA, 10mM Sodium Butyrate.

RIPA Buffer

140mM NaCl, 10mM Tris-HCl pH 8.0, 1mM EDTA, 1% Triton X-100, 0.1% (w/v) Sodium Deoxicolate, 0.1% (v/v) SDS. Add 1mM PMSF (SIGMA) immediately before use.

Lithium Chloride (LiCl) Buffer

250mM LiCl, 10mM Tris-HCl pH 8.0, 1mM EDTA, 1% Triton X-100, 0.1% (w/v) Sodium Deoxicolate, 0.5% (v/v) NP-40.

2.3. Bacterial lines and vectors used

One Shot® Top 10 chemically competent *E.coli* (Life Technologies)

F- *mcrA* Δ(*mrr-hsd*RMS-*mcr*BC) Φ80*lac*ZΔM15 Δ *lac*X74 *rec*A1 *ara*D139 Δ(*araleu*)7697 *gal*U *gal*K *rps*L (StrR) *end*A1 *nup*G

***dam*⁻/*dcm*⁻ Competent *E.coli* (New England Biolabs)**

ara-14 leuB6 fhuA31 lacY1 tsx78 glnV44 galK2 galT22 mcrA dcm-6 hisG4 rfbD1 R(zgb210::Tn10) Tet^S *endA1 rspL136* (Str^R) *dam13::Tn9* (Cam^R) *xylA-5 mtl-1 thi-1 mcrB1 hsdR2*

Table 2.1. Vector details

Vector	Type	Source/stock #	Main Features	Resistance
pCasPeR3	Destination	DGRC/1064	Gateway cassette, CaSpeR backbone, GAL4-SV40	Amp
pAGW	Epitope tagged, destination	DGRC/1071	act5c promoter, Gateway cassette, N-terminal EGFP tag	Amp, Chlor
pAFMW	Epitope tagged, destination	DGRC/1120	act5c promoter, Gateway cassette, N-terminal 3xFLAG- 6xMYC tag	Amp, Chlor
pAW	Destination	DGRC/1127	act5c promoter, Gateway cassette	Amp Chlor
pPGW	Epitope tagged, destination	DGRC/1077	UASp promoter, Gateway cassette, N-terminal EGFP tag	Amp, Chlor
pDEX	Destination	Donated by T. Maehama (Maehama *et al*., 2004)	act5C promoter subcloned into pTRE	Amp

Amp = ampicillin, chlor = chloramphenicol

Ampicillin, kanamycin and chloramphenicol were prepared as 100mg/ml, 50mg/ml and 35mg/ml filter-sterilised stock solutions respectively and stored at -20°C. Ampicillin was used at a concentration of 100μg/ml, kanamycin at 50μg/ml and chloramphenicol at 12.5μg/ml.

2.4. Cell lines used

Drosophila Schneider Receptor + (S2R+) cells

A highly adherent cell line derived from *Drosophila* Schneider (S2) cells, originally isolated from early stage (20-24 hours old) *Drosophila* embryos, which possesses the wingless receptors Dfrizzled-1 and Dfrizzled-2 (Schneider, 1972; Yanagawa *et al*., 1998).

2.4.1. Initiating cultures from frozen stocks

Cells were quickly thawed at room temperature and resuspended in 5ml complete Schneider's medium (see section 2.1) in a 15ml centrifuge tube. The cells were centrifuged at 1500 x g for 5 minutes and the supernatant discarded to remove DMSO present in the storage medium. The cells were resuspended in 10ml fresh complete Schneider's medium and split into two $25cm^2$ tissue culture flasks (5ml each). The cells were incubated at 28°C for 3-4 days until they reached a density of 6-20 $x10^6$ cells/ml.

2.4.2. Passaging S2R+ cells

Upon reaching optimum confluency, the most adherent cells were selected for by gently tapping the flask to remove the least adhered cells. The excess medium was

discarded and adhered cells were resuspended in 10ml fresh complete medium by washing the surface of the flask. The cells were split 1:3 (5ml resuspended cells in 10ml fresh complete Schneider's medium) in 75cm^2 flasks.

2.5. Growth and maintenance of *Drosophila*

Fly stocks were kept at 18°C, 22°C or 25°C on standard yeast/dextrose medium (1% (w/v) agar, 7.3% (w/v) dextrose, 5% (w/v) yeast, 6.7% (w/v) organic wholemeal flour, 0.25% (v/v) nipagin, 0.3% (v/v) propionic acid) in 30/50ml vials or 250ml bottles as appropriate. Flies were anaesthetised with CO_2 and examined using Nikon SMZ-645 or Nikon SMZ-800 microscopes and Photonics 200 light sources using standard fly-pushing techniques (Greenspan, 2004). Fly stocks were ordered from the Vienna *Drosophila* RNAi Centre (VDRC, Austria), The National Institute of Genetics (NIG-FLY, Japan) and The Bloomington Stock Centre (Indiana, USA). Crosses were kept at 25°C and transferred to fresh vials every 2-3 days.

2.6. *Drosophila* genotypes used

2.6.1. For induction of PNUTS^{13B} and wild type clones (For crossing schemes see Appendix 1)

hsFLP^{122}; Ubi-GFP^{nls}, FRT40A/Cyo (made by Daimark Bennett in house)

(Made using Bloomington stock 5629 and hsFLP^{122}; en-GAL4, UAS-GFP/Cyo; TM2/TM6B as a source of Flippase. Expresses the enzyme Flippase under the control of the Hsp70 promoter, ubiquitously expresses GFP in the nucleus)

w; dPNUTS^{13B}, FRT40A/Cyo (made in house by Daimark Bennett)

(dPNUTS null allele)

w; M(2)24F, Ubi-GFP^{nls}, FRT40A/Gla, Bc (gift from Daniela Grifoni)

(M(2)24F is a dominant *minute* allele of ribosomal protein RpL27A, ubiquitously expresses GFP in the nucleus)

hsFLP^{122}; dPNUTS^{13B}, FRT40A/Cyo (made in house by Daimark Bennett)

(Expresses Flippase enzyme under control of Hsp70 promoter, dPNUTS null allele)

hsFLP^{122}/hsFLP^{122}; en-GAL4, UAS-GFP/Cyo; TM2/TM6B (gift from Laura Johnston)

(Source of hsFLP^{122} – expresses Flippase enzyme under control of Hsp70 promoter, ignore en-GAL4, UAS-GFP – this was not needed)

w; P[w+]30C, FRT40A (Bloomington stock # 1646)

(A strain carrying a P transposon that carries a wild type *white* gene to generate wild type clones in the wing disc. This strain was used to make genotype below)

hsFLP^{122}/hsFLP^{122}; P[w+]30C, FRT40A/Cyo (made by author)

(To generate wild type clones in the wing disc, expresses the enzyme Flippase under the control of the Hsp70 promoter, carries a P transposon that carries a wild type *white* gene)

Final genotypes analysed:

hsFLP^{122}; dPNUTS^{13B}, FRT40A/ Ubi-GFP^{nls}, FRT40A

hsFLP^{122}; dPNUTS^{13B}, FRT40A/ m(2)24F, Ubi-GFP^{nls}, FRT40A

hsFLP^{122}; FRT40A, P[w+]30C/m(2)24F, Ubi-GFP^{nls}, FRT40A

2.6.2. For induction of PP1 mutant clones in salivary gland (For crossing scheme see Appendix 2)

hsFLP^{122}; +/Cyo; Ubi-GFP^{nls}, FRT82B/TM6B (made in house by Daimark Bennett)

(Expresses the enzyme Flippase under the control of the Hsp70 promoter, ubiquitously expresses GFP in the nucleus)

w;;FRT82B, PP187B$^{Su(var)3-6[1]}$/TM6B (gift from Luke Alphey)

(Hypomorphic allele of PP187B – Flybase ID: FBal0013933)

Final genotype analysed:

hsFLP^{122}; ;FRT82B, PP187B$^{Su(var)3-6[1]}$/ Ubi-GFP^{nls}, FRT82B

2.6.3. For figure S6B – RNAPII phosphor marks in L1 larvae

w^{1118}; dPNUTS^{exKG}/dPNUTS^{exKG} (made in house by Daimark Bennett)

(dPNUTS allele with P-element precisely excised)

w^{1118}; dPNUTS^{9B}/dPNUTS^{9B} (made in house by Daimark Bennett)

(dPNUTS mutant allele)

2.6.4. For ChIP from L3 larvae

w^{1118} (Bloomington # 6326)

(isogenic for autosomes)

da-GAL4, UAS-HM-dPNUTS^{W726A} line1 (provided by Daimark Bennett)

(Overexpresses his-myc tagged non-PP1 binding PNUTS mutant in the pattern of the *daughterless* gene)

2.6.5. To make *dTOX4^{null}* allele (For crossing scheme see Appendix 3)

y^1w^{67c23};;P{EPgy2}CG12104^{EY02201} (Bloomington # 15089)

(P-element inserted in 5'UTR of CG12104)

w*; Dr^1/TMS, P{Δ2-3}99B (Transposase, Bloomington # 1610)

(Source of transposase for remobilisation of P-elements)

Dr^{Mio}/TMS, P{Δ2-3}99B (Transposase, Bloomington # 406)

(Source of transposase for remobilisation of P-elements)

w; Tft/CyO; MKRS/TM6B (gift from Shengjiang Tan)

(Source of balancer chromosomes)

2.6.6. For dTOX4 mutant analysis

w^{1118} (Bloomington # 6326)

(isogenic for autosomes)

w; +/CyO; $dTOX4^{null}$/ $dTOX4^{null}$ (homozygous dTOX4 mutant stock made in house by author, see 2.6.5)

w; +/CyO; $dTOX4^{null}$/ TM6B (heterozygous dTOX4 mutant stock made in house by author, see 2.6.5)

2.6.7. To make GFP-*dTOX4*^{wt} and GFP-*dTOX4*$^{P216\Delta}$ overexpression rescue strains (For crossing schemes see Appendix 4)

w; +/CyO; dTOX4 ^{null}/TM6B (made in house by author, see 2.6.5)

(heterozygous dTOX4 mutant allele)

w; Tft/Cyo; bam-GAL4-VP16 (gift from Helen White-Cooper)

(GAL4-VP16 fusion protein expressed under the control of the *bag of marbles* gene promoter)

w; maternal-α-tubulin-GAL4-VP16 (Bloomington # 7062)

(GAL4-VP16 fusion protein expressed under the control of the *maternal alpha tubulin* gene promoter)

w; Tft/CyO; MKRS/TM6B (gift from Shengjiang Tan)

(source of balancer chromosomes)

UAS-GFP-dTOX4^{wt} and UAS-dTOX4$^{P216\Delta}$ on second or third chromosomes (made by Cambridge fly facility over different balancers for author)

(For overexpression of GFP tagged wild type and mutant dTOX4)

w; da-GAL4/CyO (gift from Shengjiang Tan)

(To test expression of transgenic strains. Expresses GAL4 in the pattern of the *daughterless* gene)

2.6.8. For PNUTS, PTEN complementation analysis in the eye

(For crossing schemes see Appendix 5)

w; P[w+]30C, FRT40A (Bloomington stock # 1646)

(A strain carrying a P transposon that carries a wild type *white* gene to generate wild type clones in the wing disc)

w*; GMR-hid, FRT40A, l(2)CL/Cyo; eyGAL4, UAS-FLP (Bloomington stock # 5250)

(Eye specific expression of cell lethal mutation on GMR-hid chromosome)

w; P[w+]30C, PTEN[3], FRT40A/CyO (gift from Clive Wilson)

(PTEN mutant allele)

w; PNUTS^{13B}, FRT40A/Cyo; MKRS/TM6B (made in house by Daimark Bennett)

(PNUTS mutant allele)

w; PNUTS^{13B}, P[w+]30C, PTEN[3], FRT40A/Cyo (made by author, see Appendix 5 for crossing scheme)

(PNUTS^{13B} allele recombined with PTEN mutant allele)

Final genotypes of progeny screened (for crossing schemes see Appendix 5)

GMR-hid, FRT40, l(2)/ P[w^{+}]30c, FRT40A; ey-GAL4, UAS-FLP

GMR-hid, FRT40A, l(2)/dPNUTS^{13B}, FRT40A; ey-GAL4, UAS-FLP

GMR-hid, FRT40A, l(2)/dPTEN[3], FRT40A; ey-GAL4, UAS-FLP

GMR-hid, FRT40A, l(2)/dPNUTS^{13B}, P[w^{+}]30c, dPTEN[3], FRT40A, ey-GAL4, UAS-FLP

2.6.9. Strains used for PcG phenotypic screen in chapter 6

<u>TRiP Lines for RNAi of PcG proteins</u>

y^{1} v^{1}, P{TRiP.JF01392}attP2 (Bloomington stock # 31608)

(Expresses dsRNA for RNAi of *polyhomeotic proximal* under UAS control)

y^{1} v^{1}, P{TRiP.JF01705}attP2 (Bloomington stock # 31190)

(Expresses dsRNA for RNAi of *polyhomeotic distal* under UAS control)

y^1 sc* v^1, P{TRiP.HMS00082}attP2 (Bloomington stock # 33669)

(Expresses dsRNA for RNAi of *polyhomeotic proximal* under UAS control)

y^1 v^1, P{TRiP.HMS00016}attP2/TM3, Sb^1 (Bloomington stock # 33622)

(Expresses dsRNA for RNAi of *polycomb* under UAS control)

y^1 sc* v^1, P{TRiP.HMS00921}attP2 (Bloomington stock # 33964)

(Expresses dsRNA for RNAi of *polycomb* under UAS control)

y^1 v^1, P{TRiP.JF01581}attP2 (Bloomington stock # 31110)

(Expresses dsRNA for RNAi of *polycomb* under UAS control)

y^1 v^1, P{TRiP.JF01396}attP2 (Bloomington stock # 31612)

(Expresses dsRNA for RNAi of *sex combs extra* under UAS control)

VDRC Stocks for RNAi of PcG proteins

w^{1118}; P{GD17399}v50028 (VDRC stock # 50028)

(Expresses dsRNA for RNAi of *polyhomeotic* under UAS control)

P{KK108787}VIE-260B (VDRC stock # 100811)

(Expresses dsRNA for RNAi of *polyhomeotic* under UAS control)

P{KK109179}VIE-260B (VDRC stock # 106328)

(Expresses dsRNA for RNAi of *sex combs extra* under UAS control)

NIG-Fly Stocks for RNAi of PcG proteins

18414R-1

(Expresses dsRNA for RNAi of *polyhomeotic* under UAS control, inserted chromosome = 2)

18414R-2

(Expresses dsRNA for RNAi of *polyhomeotic* under UAS control, inserted chromosome = X)

32443R-1

(Expresses dsRNA for RNAi of *polycomb* under UAS control, inserted chromosome = 3)

5595R-1

(Expresses dsRNA for RNAi of *sex combs extra* under UAS control, inserted chromosome = 3)

***ey*-GAL4 strains**

w^{*}; P{GAL4-ey.H}4-8/Cyo (Bloomington stock # 5535)

(Strongly expresses GAL4 in the pattern of the *eyeless* gene)

w^{*}; P{GAL4-ey.H}3-8 (Bloomington stock # 5534)

(Moderately expresses GAL4 in the pattern of the *eyeless* gene)

y^{1} w^{1118}; P{ey3.5-GAL4.Exel}1 (Bloomington stock # 8221)

(Expresses GAL4 in the pattern of the *eyeless* gene)\

y^1 w^{1118}; P{ey3.5-GAL4.Exel}1 (Bloomington stock # 8220)

(Expresses GAL4 in the pattern of the *eyeless* gene)

Other strains used

w^*; P{tubP-GAL80^{ts}}20; TM2/TM6B (Bloomington stock # 7019)

(Temperature sensitive GAL80 expressed under the control of the alphaTub84B promoter)

w; UAS-*dicer-2/ UAS-dicer*-2; pin/Cyo (gift from Neville Cobbe)

(Expresses *dicer-2* under UAS control)

Final tester strain genotype

w; ey-GAL4/CyO; tubulin-GAL80^{ts}, Sce$^{IR5595R-2}$/TM6B (made by author)

(Please see Appendix 6 for crossing scheme to make this strain)

2.7. Generation of PNUTS^{13B} clones by FLP/FRT mediated recombination in the wing disc

Crosses (see section 2.6.1 for genotypes) were allowed to lay for 48 hours. Embryos were left to develop for a further 48 hours and then heat shocked in a 37°C water bath for 1 hour. Wing discs were dissected from third instar larvae at 48, 72 and 96 hours post heat shock for clones induced late, early and very early respectively.

2.8. Generation of PNUTS^{13B} and PP1 mutant clones by FLP/FRT mediated recombination in the salivary gland

Crosses were allowed to lay for 48 hours after which the embryos were heat shocked in a 37°C water bath. Salivary glands were dissected from third instar larvae when they emerged.

2.9. Immunostaining of wing imaginal discs and whole mount salivary glands

Tissues were dissected in cold 1 x PBS, transferred to a watch glass and fixed in 3.7% paraformaldehyde for 20 minutes at room temperature. Tissues were washed in 1 x PBS for 15 minutes and then blocked in blocking solution (see section 2.1) for 30 minutes at room temperature or a minimum of 2 hours at 4°C. Tissues were incubated with primary antibody (see Table 2.15) in blocking solution overnight at 4°C and then washed three times (10 minutes per wash) in PBST. Tissues were incubated with the secondary antibody (see Table 2.15) diluted in blocking solution for 2 hours at room temperature in the dark. They were then washed two times (10 minutes per wash) in PBST and incubated with TO-PRO®-3 Iodide (see Table 2.15) for ten minutes to visualise DNA. Tissues were mounted in 17.5μL of Vectashield mounting medium (Vector Laboratories) on a standard glass microscope slide and covered with a coverslip (22mm × 22mm). Wing discs were covered with a raised coverslip. The sides of the coverslip were sealed with clear nail polish and slides were stored in the dark at 4°C for no longer than a week.

2.10. Chromatin Immunoprecipitation (ChIP)

All equipment was autoclaved before use. Glass douncer was sterilised with 100% ethanol. Spatulas, pestles and mortars were stored at -80°C for at least 2 hours before

start of experiment. All steps were done on ice. A minimum of 3 biological replicates was done for each genotype. 1g of *Drosophila* third instar larvae were collected in 1 x PBS, frozen in liquid nitrogen and stored at -80°C for at least 2 hours before the experiment. Frozen larvae were ground in a mortar and pestle to a fine powder in liquid nitrogen and resuspended in 5ml Buffer A+ in precooled beaker on ice. The suspension was homogenised in a dounce homogeniser with pestle B on ice for 10 strokes then filtered through two layers of sterile Miracloth into a sterile beaker on ice. The remaining matter on the Miracloth was resuspended, homogenised in 2ml Buffer A+ in a dounce homogeniser for 10 strokes on ice and filtered through the same Miracloth with squeezing of the last liquid into a beaker using gloved hands. Homogenate was transferred over 2ml Buffer AS and nuclei were pelleted by centrifugation (3000rpm., 5 minutes, 4°C). The pellet was resuspended in 3ml Buffer A+ and homogenised in a dounce homogeniser with pestle A for 5 strokes on ice. The homogenate was transferred over 1ml Buffer AS and nuclei pelleted by centrifugation (3000rpm., 5 minutes, 4°C). The nuclear pellet was resuspended in 3ml Buffer A+ 0.1% NP-40 and cross-linked by adding 37% paraformaldehyde to a final concentration of 1.8% for 15 minutes at room temperature with gentle shaking. Crosslinking was stopped by addition of glycine to a final concentration of 0.125M and incubated for 5 minutes at room temperature with shaking. Nuclei were pelleted by centrifugation (2000rpm., 5 minutes 4°C) and washed two times with 10ml Buffer A+ 0.1% NP-40 (+ PIC). The supernatant was discarded and the pellet frozen in liquid nitrogen and stored at -80°C until use.

For sonication, nuclei were resuspended in 2-3 volumes of nuclei lysis buffer (+ PIC). Samples were split into 1.5ml tubes (300µL per tube) and sonicated for 35 x 30

seconds on and 30 seconds off using a high setting in a Diagenode Bioruptor. Samples were centrifuged (13000rpm, 1 minute, 4°C) and the supernatant transferred to a new tube. Concentration was measured as described in 2.15 and samples were stored at -80°C.

For input preparation, the iPure Kit (Diagenode) was used to reverse crosslink 30µg of sonicated chromatin by adding 115.4µl of Buffer A and 4.6µl Buffer B to the sample and incubating overnight at 65°C in a hot block. The samples were kept at 4°C until DNA purification was performed.

For immunoprecipitations 30µg of chromatin was diluted 10× with RIPA buffer and incubated overnight at 4°C with antibody (5-10µg/IP) on a rotary mixer set at 25rpm. The following day, 20µl of Magna ChIP™ protein A or G coated pre-blocked magnetic beads (Millipore) were added to each sample and incubated for a further 4 hours at 4°C on a rotary mixer set at 25rpm. Samples were then centrifuged at 4°C (2000rpm, 1 minute), placed on a cold magnetic rack (DiaMag 1.5, Diagenode) and the supernatant discarded. The beads were then washed 5 times with 500µl cold RIPA buffer (+ PMSF) followed by one wash with 500µl LiCl buffer and two washes with 500µl TE buffer. Each wash was 10 minutes at 4°C on a rotary mixer set at 25 rpm. Samples were centrifuged at 2000rpm. for 1 minute and the supernatant removed in between each wash.

For reverse cross-linking of immunoprecipitated chromatin, beads were resuspended in 115.4µl Buffer A and 4.6µl Buffer B from the iPure Kit (Diagenode) and

incubated overnight at 65°C. The following day samples were briefly centrifuged and placed on a magnetic rack. Supernatants were transferred to a fresh tube and kept on ice.

For DNA purification of input and IP samples 2µl of carrier (iPure Kit) was added to each sample, vortexed briefly and centrifuged briefly. 100µl of 100% isopropanol was added to each sample, then vortexed and centrifuged briefly. 15µl of magnetic beads (iPure Kit) were added to each sample and incubated for one hour at room temperature on a rotary mixer set at 40rpm. Samples were then briefly centrifuged, placed on the magnetic rack and the supernatant discarded. The beads were then washed in 100µl wash buffer 1 (iPure Kit) for 5 minutes at room temperature on a rotary mixer set at 40rpm. This process was repeated with wash buffer 2 (iPure Kit). Samples were eluted in 100µl ultrapure water and stored at -20°C until further use.

2.10.1. qPCR analysis of ChIP samples

For qPCR analysis input samples were diluted 100× in ultrapure water. Reactions were carried out in a total volume of 15µl made up of 7.5µl Power SYBR® Green PCR master mix (Life Technologies), 3µl DNA, 250nm primer 1, 250nm primer 2 and ultrapure water to 15µl. Reactions were carried out using the StepOnePlus™ Real Time PCR system (Applied Biosystems) using the conditions shown in Table 2.2. Reactions were done in duplicate per biological repeat and the quantity of immunoprecipitated DNA was calculated by % Input.

2.11. Oligonucleotides

Oligonucleotides were designed using primer3, synthesised by MWG Biotech and diluted in TE buffer (Sigma, pH 8.0) according to the manufacturer's recommendations to give 100µm stock solutions (stored at -80°C). A 10µm stock was made with ultrapure water for use in PCR and sequencing (stored at -20°C). A list of primers is given in Table 2.3. Primers used in Chapter 3 are listed in section 3.5.14.

Table 2.2. Thermal cycling conditions used for qPCR

Step	Time	Temperature (°C)	Cycles
AmpliTaq Gold® Enzyme Activation	10 minutes	95	1
Denature	15 seconds	95	
Anneal/Extend	60 seconds	60	40

Table 2.3. Primer list

Primer name	Sequence (5' to 3')	Purpose
TOX4 For	CACCATGAATCAGTTCCACACTCC	*Pfx* amplification of genes from cDNA vector clones to make tagged gene S2 or fly expression vector
TOX4 Rev	TGAGTTCATGGATATTACCCAGTGGTTG	
Wdr82 For	CACCATGAAGATAAAACTAATAGATTCGG	
Wdr82 Rev	CAAGCCCTCCTCGGATGTG	
ERR For	CACCATGTCCGACGGCGTCA	
ERR Rev	CCTGGCCAGCGGCTCGA	
MBD-R2 F	CACCATGGATACCGCGGAGAT	
MBD-R2 R	CTTGCTAGTGGCAGAATCTCTGAG	
M13-FP	TGTAAAACGACGGCCAGT (at GATC)	Sequencing TOX4, Wdr82 and ERR in pENTR
M13-RP	CAGGAAACAGCTATGACC (at GATC)	
ERR Forward	GCGTTCTTTAAACGCACCATCC	Sequencing ERR in pENTR
ERR Reverse	AGCTGGAGCGTCAGGATCTC	
MBD-R2 Forward 1	CAGCTTTCAGGCGTGGATGG	Sequencing MBD-R2 in pENTR
MBD-R2 Forward 2	CCATGGATGTGTCGATGAACTC	
MBD-R2 Forward 3	CTTTGGATGCTGGTCCAACTC	
TOX4 Primer 1	CGAGATGATGTTACTACCAGCAGAC	1,2 & 3 used to screen flies for deletion in *dTOX4*. 2 & 3 used to sequence $dTOX4^{null}$
TOX4 Primer 2	CATTCGGCTGGGAGGAGGAG	
TOX4 Primer 3	CAAGCACTGGCTTGCTCCTC	
TOX4fw	CACGGTGTCTCGAAAAGAACA	PCR on cDNA to determine transcript levels in mutant
TOX4rev	ACGAGGTGTTTGAGCTGACC	
GAPDH2 Fw	GGTGATCAACGACAACTTCG	Control for above
GAPDH2 Rev	CCAGTGGAAGCTGGAATGAT	
Jil-1/36727/F	TAATACGACTCACTATAGGGCCTCTCGGTTCTCGAACATTATG	dsRNA synthesis (first 19 bp = T7 promoter sequence)
Jil-1/36727/R	TAATACGACTCACTATAGGGGTGGTGGACAGCTCTACGG	
Jil-1/40737/F	TAATACGACTCACTATAGGGGAACGTCAACGGTTTTTCGTACG	
Jil-1/40737/R	TAATACGACTCACTATAGGGTGAACCAGAAACGACCTTCCG	
PP187B/27290/F	TAATACGACTCACTATAGGGCCTCCGAGAGCTGTACGTTTT	
PP187B/27290/R	TAATACGACTCACTATAGGGCGCAACAGCATACGAAGAAATTTTCA	
PP187B/23299/F	TAATACGACTCACTATAGGGCGGACTGCATTGTGGACGAA	
PP187B/23299/R	TAATACGACTCACTATAGGGACCGACCAACCATTCACCCA	
Jil-1/Forward	GAATCATTGGCTGCTCCTTC	Confirming gene knockdown in S2R+ cells
Jil-1/Reverse	TACCGCGGAGAATGAATACC	

PP187B/Forward	GAGGTCAAATCGGGACTGAG	Confirming gene knockdown in S2R+ cells
PP187B/Reverse	CGGAGAATTTCTTCCTGCTG	
$H3^{S10,28A}$ Forward	ACTACTTCCGCTACCTGGCC	Sequencing the $H3^{S10,28A}$ mutant probe
$H3^{S10,28A}$ Reverse	CGTCCAGTTCGACCAGAATC	

2.12. Transformation of TOP10 chemically competent cells

For every two transformations, one vial (50µl) of One Shot® TOP10 Chemically Competent Cells (Life Technologies) was thawed on ice split between two fresh microcentrifuge tubes. 1µl of DNA was added and mixed gently. The cells were incubated on ice for 30 minutes to 1 hour and then heat shocked at 42°C for exactly 30 seconds. Following heat shock, cells were placed on ice for two minutes and 200µl of pre-warmed S.O.C Medium (Life Technologies) was added to each transformation reaction. Reactions were shaken horizontally at 225rpm for 1 hour at 37°C and then spread on pre-warmed selective LB agar plates using sterile technique. The plates were inverted and incubated overnight at 37°C. The following day colonies were picked using sterile technique and propagated in 6ml LB broth plus selective antibiotic overnight at 37°C with shaking at 225rpm. Plasmid DNA was purified as in section 2.14.

2.13. Transformation of *dam*$^-$/*dcm*$^-$ competent *E.coli*

For each transformation a tube of *dam*$^-$/*dcm*$^-$ competent *E.coli* cells (New England Biolabs) was thawed on ice until the last ice crystals disappeared. Cells were mixed gently and 50µl transferred to a transformation tube on ice. 1µl (0.25ng) of plasmid DNA was added to the cells and the tube carefully flicked 4-5 times to mix. The sample was kept on ice for 30 minutes with no mixing and then heat shocked at 42°C for 30 seconds. The sample was kept on ice for a further 5 minutes followed by the addition of 950µl room temperature SOC medium. It was then incubated at 37°C for 60 minutes with shaking at 250rpm. Cells were then mixed by flicking the tube and inverting the tube and diluted 10-fold in SOC medium. Diluted sample was spread on

pre-warmed selective plates and incubated at 37°C overnight. The following day colonies were picked using sterile technique and propagated in 3ml LB broth plus selective antibiotic overnight at 37°C. Plasmid DNA was purified as described in 2.14.

2.14. DNA extraction from culture

Small-scale plasmid purification (<20μg) was carried out using the QIAprep Spin Miniprep Kit (Qiagen) and medium scale plasmid purification (≤ 100μg) was carried out using the QIAfilter Plasmid Midi Kit (Qiagen) according to the manufacturer's instructions. Briefly *E.coli* cells amplified overnight in selective LB broth were pelleted at approximately 4500rpm for 5 minutes and the supernatant removed. Cells were lysed under alkaline conditions and debris removed by centrifugation (mini) or filtering (midi). Clear cell lysates were applied to columns containing a silica gel membrane capable of binding DNA and washed to remove contaminants. DNA was eluted with an appropriate volume of Qiagen Elution Buffer or TE buffer. DNA concentration was measured using a NanoDrop™ (see section 2.15). DNA was stored at -20°C until use.

2.15. DNA/RNA quantification

DNA and RNA was quantified using the Thermo Scientific NanoDrop™ 1000 Spectrophotometer according to the manufacturers instructions. This measures the absorbance using a 1μl sample over a 220nm-750nm spectrum and gives an output of concentration and relative purity with 230/260 and 260/280ratio measurements.

2.16. DNA sequencing

DNA sequencing was carried out by GATC Biotech (Germany). DNA was provided at a concentration of 30-100ng/µl (typically 50ng/µl) in a total volume of 20µl (DNA diluted in ultrapure ddH_2O. Sequencing primers were designed with a theoretical melting temperature of 60°C and a G/C composition of approximately 50%.

2.17. Vector storage

Working purified DNA stocks were stored at -20°C. A frozen bacterial stock of each vector was prepared by adding glycerol to cultures to a final concentration of 15% and stored at -80°C.

2.18. PCR

The *Taq* PCR Master Mix Kit (Qiagen) was used for all PCR reactions where not specified. Reactions were set up in a final volume of 20µl as shown in Table 2.4. Conditions for most PCR reactions are shown in Table 2.5.

Table 2.4. PCR reaction components

Component	Volume (µl)
Mastermix	10
Forward Primer (10µM)	1
Reverse Primer (10µM)	1
cDNA (~2µg)	-
H_2O	to 20

Table 2.5. PCR Reaction conditions

Temperature (°C)	Time	No of Cycles
94	3 min	1
92	30s	
54	30s	30
72	40s	
72	40s	1
4	∞	-

2.19. Agarose Gel electrophoresis

DNA was separated by size using agarose gel electrophoresis. High gelling temperature agarose (Bioline) was heated in 1 × TAE buffer with Ethidium Bromide (0.2-0.5µg/ml). Samples were diluted with 1 x loading buffer (10x agarose loading buffer, 30% (v/v), 0.35% (v/v) bromophenol blue) and loaded onto the gel. The samples were electrophoresed at 100 volts for 45 minutes in 1×TAE buffer using Jencons Ltd gel electrophoresis equipment. 5µl of Smartladder (Eurogentec), 100bp DNA ladder (New England Biolabs, NEB) or Hyperladder I (bioline) was loaded as the molecular weight marker. DNA fragments were visualised using an ultraviolet light source (UVi-tech) and documented with a PULNiX TM-300 video camera system and Syngene UP-895MD video graphic printer.

2.20. Gel extraction

DNA fragments were cut from agarose gels using a scalpel blade under a UV light and purified using the QIAquick Gel Extraction Kit (Qiagen) according to the manufacturer's instructions. Briefly, agarose is dissolved in an optimised buffer containing a pH indicator, to determine the optimal pH for DNA binding. DNA is

purified by binding to an anion-exchange membrane, washed and eluted in an appropriate volume of TE buffer.

2.21. Restriction digestion

Restriction digests were performed using restriction endonuclease enzymes and their compatible buffers (New England Biolabs) according to the manufacturer's guidelines. Reactions were carried out in a volume of 20µl using 1×enzyme buffer, 0.4-1µl of each enzyme, 0.2µl BSA and 0.3/0.4µg DNA for diagnostic digests or 1µg DNA for gel purification. For double or triple digests, buffers compatible with all enzymes were used. Reactions were typically incubated at 37°C in a hot block or water bath for 2-3 hours or at 25°C (room temperature) overnight.

2.22. Yeast two-hybrid assay

Yeast two-hybrid screening was performed by Hybrigenics Services, Paris, France. An ULTImate Y2H screen was done using the full length coding sequence (amino acids 1-1135) of *Drosophila PNUTS* cloned into pB27 as a C-terminal fusion to LexA (N-LexA-*dPNUTS*-C) and checked by sequencing. This was used as a bait to screen a *Drosophila* third instar larvae cDNA library (Hybrigenics) constructed into pP6. For the cDNA library, RNA was extracted from third instar larvae in the Bennett lab by Dr Nick Lansdale and the library was prepared by Hybrigenics. Direct Y2H assays were also performed by Hybrigenics services. This is described in the results section of chapter 4 for each individual protein interaction.

2.23. Making the S2R+ cell expression constructs

Vector cDNA clones for *dTOX4* (CG12104), *dMBD-R2*, *dERR* and *dWdr82* were purchased from the *Drosophila* Genomics Resource Centre (DGRC). The open reading frame for each gene was amplified from the vector clones using *Pfx* mediated amplification (see section 2.23.1). Primers were designed with CACC at the 5' end of the forward primer to specify directional cloning. PCR products were separated on a 1% agarose gel (see section 2.19) to confirm amplification and then purified as in 2.23.2. Purified PCR products were cloned into the pENTR™ entry vector as described in 2.23.3. Reactions were transformed into One Shot® TOP10 Chemically Competent Cells and plated on kanamycin plates. 10 colonies were selected for each gene for colony PCR (see section 2.23.4) and PCR products separated on an agarose gel to check cloning was successful. The same colonies were amplified and three containing the gene were selected and purified as in section 2.14. A diagnostic digest was done on each gene in pENTR™ as described in 2.21. *dTOX4*, *dWdr82* and *dMBD-R2* were digested with *Not1* and *EcoRV* and *dERR* digested with *Not1* and *Nde1*. Digests were separated on an agarose gel. Each gene specific pENTR™ vector was sent for sequencing (see section 2.16). The *dTOX4*-pENTR vector was sent to BioPioneer (San Diego, USA) for site directed mutagenesis to generate a premature stop codon and thus remove the C-terminal PNUTS binding region.

A *dPNUTS* ORF conjugated to a C-terminal Myc tag had already been made by the Bennett lab in the pDONR221 entry vector. This together with the other genes in pENTR were subcloned into the desired destination vectors pAGW and pAFMW as well as pAW for *dPNUTS*-Myc using Gateway® technology (see section 2.23.5). 1µl

of each reaction was transformed into One Shot® TOP10 Chemically Competent Cells and plated on ampicillin plates (see section 2.12). DNA was purified as in section 2.14. A diagnostic digest of each gene specific destination vector was done to confirm subcloning of the gene sequence into the destination vector.

2.23.1. *Pfx* PCR

Pfx amplification was done using the Platinum® *Pfx* DNA Polymerase Kit (Invitrogen). Reactions were set up in a 20µl volume. Reaction components (Table 2.6) and reaction conditions (Table 2.7) are shown below. Extension time was calculated according to the manufacturers instructions of 2 minutes/kilobase.

Table 2.6. *Pfx* amplification reaction components

Component	Amount
10 × *Pfx* amplification buffer	2µl
50mM $MgSO_4$	0.4µl
10mM dNTPs (Qiagen)	0.6µl
10µM Forward Primer	1µl
10µM Reverse Primer	1µl
Pfx enzyme	0.25µl
Vector clone DNA	50ng
H_2O	to 20µl

Table 2.7. *Pfx* Reaction conditions

Temperature (°C)	Time	No of Cycles
94	3 min	1
92	20s	30
55	30s	
68	2min/kb	
68	10min	1
4	∞	-

2.23.2. PCR purification

PCR products were purified using the QIAquick® PCR Purification Kit (Qiagen). All buffers described in this protocol are from the kit. All centrifugation steps are carried out at 13,000rpm for 1 minute. 5 volumes of buffer PB was added to 1 volume of PCR reaction and mixed. If the colour of the mixture was orange or violet then 10µl 3M Sodium Acetate (pH 5.0) was added and mixed (colour should be yellow). The sample was applied to a QIAquick spin column in a 2ml collection tube and centrifuged. The flow through was discarded and 750µl buffer PE added to the column and centrifuged to wash. The flow through was discarded and the column centrifuged again to remove residual buffer. The column was placed in a clean 1.5ml tube and DNA eluted by adding 30µl buffer EB or TE directly onto the membrane and incubated for 5 minutes at room temperature followed by centrifugation. Samples were stored at -20°C until use.

2.23.3. pENTR™ directional cloning

The pENTR™/D-TOPO® Cloning Kit (Life Technologies) was used to clone gene products into the pENTR™ entry vector for subcloning into a destination vector. A 2:1 molar ratio of PCR product: TOPO Vector was used. To calculate the amount of PCR product to add the following equation was used:

((ng vector × kb PCR product/kb vector) × (2/1) = ng PCR product

The reaction was set up as shown in Table 2.8, mixed gently and incubated at room temperature for 15 minutes. The reaction was then put on ice and transformed into One Shot® competent *E.coli* as described in section 2.12.

DNA was purified as described in 2.14.

Table 2.8. TOPO® cloning reaction components

Reagent	Amount
Fresh PCR Product	0.5-4 µl
Salt Solution	1 µl
Sterile water	to 5 µl
TOPO® vector	1 µl

2.23.4. Colony PCR

Colonies were picked from agar plates using a pipette tip and a scratch of each colony was made at the bottom of a PCR tube. The BioMix™ Red PCR reaction mix (Bioline) was used to amplify DNA from bacterial plasmids using gene specific primers. Reaction components (Table 2.9) and reaction conditions (Table 2.10) for colony PCR are shown below.

Table 2.9. Colony PCR reaction components

Component	Volume (µl)
BioMix™ Red	25
Forward Primer (10µM)	2
Reverse Primer (10µM)	2
H_2O	21

Table 2.10. Colony PCR reaction conditions

Temperature (°C)	Time	No of Cycles
95	5 min	1
92	30s	30
55	30s	
72	30s	
72	5 min	1
4	∞	-

2.23.5. Gateway® LR Clonase™ II cloning

The Gateway® LR Clonase™ II Enzyme Mix (Life Technologies) was used to shuttle genes from the pDONR221 or pENTR™ into the desired destination vectors (pAGW, pAFMW, pAW and pPGW purchased from DGRC). 50-150ng of the entry clone containing the gene of interest was mixed with 1µl (150ng/µl) of the destination vector and TE buffer pH 8.0 to a final volume of 8µl. The LR Clonase™ II Enzyme Mix was thawed on ice for 2 minutes, vortexed briefly and 2µl added to the reaction. Reactions were incubated at 25°C for 1 hour and then 1µl of Proteinase K added to the reaction and incubated at 37°C for 10 minutes to stop the cloning reaction. 1µl was transformed into One Shot® TOP10 Chemically Competent Cells (see section 2.12).

2.23.6. Transient transfection of S2R+ cells with Effectene®

For transient transfection of S2R+ cells with gene expression vectors cells were plated at 2×10^6 cells in 4ml complete Schneider's medium (approximately 60% confluency) in 6 well dishes and allowed to adhere for a minimum of 2 hours under normal conditions. Before transfection, the Schneider's medium was removed and replaced with 1.6ml of fresh medium. Cells were either transfected or co-transfected with tagged expression constructs for each gene using the Effectene® Transfection Reagent (Qiagen) according to the manufacturer's protocols. Reagent ratios for the constructs were optimised for efficient transfection. Briefly 0.8µg of plasmid DNA was diluted to a volume of 100µl with EC buffer and condensed by adding 6.4µl of Enhancer. This was vortexed for one 1s and incubated at room temperature for 5 minutes followed by brief centrifugation. 20µl of Effectene transfection reagent was

added to the DNA-enhancer mixture, mixed by gently pipetting up and down five times and incubated for 15-20 minutes at room temperature to allow complex formation. 600µl of fresh complete Schneider's medium was added to the transfection tube, mixed by pipetting up and down twice and immediately added drop-wise onto the cells in the 6-well plates. Plates were gently swirled to ensure the transfection solution was properly diffused. Reagent amounts were doubled for co-transfections. Cells were left for 48-72 hours following transfection for suitable gene expression. Cells were then processed for western blot analysis as in section 2.24 or for fluorescence microscopy as in section 2.28.

2.24. GFP-Trap immunoprecipitation of GFP tagged proteins

Cells transfected with the same combination of plasmids were resuspended and pooled into a 15ml centrifuge tube. Cells were pelleted by centrifugation at 4000rpm for 3 minutes and the supernatant removed. The magnetic GFP-Trap®_M kit (Chromotek) was used to immunoprecipitate GFP tagged proteins. For each sample, cells were resuspended in 125µl of Chromotek lysis buffer (plus 1mM PMSF [SIGMA] and 1×Protease Inhibitor Cocktail [Roche]). Sample was kept on ice for 30 minutes with extensive pipetting every 5 to 10 minutes. The lysate was centrifuged at 13,000rpm for 10 minutes at 4°C and the supernatant transferred to a pre-cooled 1.5ml tube on ice. The supernatant was diluted to 500µl with ice-cold Chromotek dilution buffer (plus 1mM PMSF and 1×Protease Inhibitor Cocktail). 50µl of sample was kept as a positive control. Next, 20µl of GFP-Trap magnetic beads were equilibrated by washing three times in 500µl ice-cold dilution buffer. Between each wash step the beads were precipitated using a DiaMag 1.5 magnetic separator

(Diagenode) and the buffer removed. Once equilibrated the cell lysate (450µl) was added to the beads and incubated for 2 hours at 4°C on a rotating mixer set at 25rpm. The magnetic beads were pelleted using the magnetic separator and the supernatant removed. The beads were washed two times with 500µl ice-cold Chromotek wash buffer. Samples were then boiled at 95°C for 20 minutes in 2 × SDS sample buffer. Beads were pelleted using the magnetic separator and the remaining supernatant transferred to a 1.5ml tube and loaded onto a polyacrylamide gel for SDS-PAGE (see section 2.26) or stored at -20°C until use.

2.25. Protein extraction from *Drosophila* L1 larvae and adult flies for western blotting

For protein extraction from larvae 100-150 L1 larvae were collected in 1 × PBS. Excess buffer was removed and larvae were immediately frozen in liquid nitrogen and stored at -80°C until use. For protein extraction from adult flies 3 males and 3 females were transferred to a 1.5ml tube and frozen in liquid nitrogen. For protein extraction 100µl SDS buffer was added to the larvae/flies and homogenised in a 1.5ml tube using a small pestle. Samples were incubated at 95°C for 5 minutes and then centrifuged at 13,000rpm for 5 minutes to pellet the debris. The supernatant was transferred to a clean 1.5ml tube and stored at -20°C until use for western blotting.

2.26. SDS-PAGE

Proteins were separated based on their molecular weight on SDS-polyacrylamide gels as described in (Sambrook and Russell, 2001). Briefly protein extracts were run on Tris-buffered SDS-polyacrylamide gels, made according to Table 2.11 or

purchased from Bio-Rad (7.5% or 12% Mini-PROTEAN® TGX™ Precast Gels), in 1 × Running Buffer, with the acrylamide concentration of the separating gel varying depending on the size of the proteins being separated. 5µl Precision Plus Protein™ WesternC™ prestained protein standards (Bio-Rad) was used on each gel to determine protein size. Mini-Protean II Vertical Electrophoresis Apparatus (Bio-Rad) was used according to manufacturer's instructions. Samples were run at approximately 90 volts with time varying depending on the size and level of separation required

Table 2.11. Components for SDS-PAGE gels

Component	Separating Gel (10ml)					Stacking gel (5ml)
	6%	8%	10%	12%	14%	5%
40% Acrylamide (Sigma)	1.5ml	2.0ml	2.5ml	3.0ml	3.5ml	0.625ml
1.5M Tris-HCl pH 8.8	2.5ml	2.5ml	2.5ml	2.5ml	2.5ml	-
1M Tris-HCl pH 6.8	-	-	-	-	-	0.63ml
10% SDS	0.1ml	0.1ml	0.1ml	0.1ml	0.1ml	0.1ml
DdH_2O	5.9ml	5.3ml	4.8ml	4.4ml	3.9ml	3.6ml
10% APS	0.1ml	0.1ml	0.1ml	0.1ml	0.1ml	0.1ml
TEMED	5µl	5µl	5µl	5µl	5µl	5µl

2.27. Western blotting

After separation by SDS-PAGE proteins were transferred onto a nitrocellulose membrane (Amersham Hybond ECL, GE Healthcare) overnight at 25 volts and 4°C. Before setting up the transfer apparatus the membrane was pre-wetted with Tris-Glycine transfer buffer. After blotting, membranes were stained for 5 minutes with Ponceau S solution (Sigma Aldrich) to check transfer was successful and to label the lanes with a pencil. Membranes were washed in 0.1% TBST to remove the Ponceau stain.

Membranes were incubated in blocking buffer (5% milk) for 60-90 minutes at room temperature to reduce non-specific binding of the antibody before incubation with a suitable primary antibody (Table 2.12) diluted in blocking buffer (BSA) overnight at 4°C on a roller. Membranes were then washed four times, twice in 0.1% TBST followed by twice in 0.05% TBST for 10 minutes and incubated with an appropriate horseradish peroxidase (HRP) conjugated secondary antibody (Table 2.13) plus StrepTactin-HRP conjugate (1:10,000, Bio-Rad) for detection of the protein standards in blocking buffer (BSA) for 2 hours at room temperature on a roller. Membranes were then washed four times, twice in 0.1% TBST and twice in 0.05% TBST for 10 minutes.

SuperSignal® West Pico chemiluminescent substrate (Pierce) was used to detect the HRP-conjugated secondary antibodies on the membrane. The chemiluminescent signal was detected and imaged using the ImageQuant™ LAS 4000 Biomolecular Imager (GE Healthcare) or by exposure to Amersham Hyperfilm ELC (GE healthcare) for a length of time dependent on the signal intensity and then developed and fixed using Kodak GBX developer and fixer according to the manufacturers instructions.

Table 2.12. Primary antibodies used in western blots

Primary Antibody	Supplier	Species	Concentration
C-Myc (A14)	Santa Cruz	Rabbit	1μg/ml
FLAG (M2)	Sigma	Mouse	5μg/ml
GFP (JL-8)	Clontech	Mouse	1μg/ml
RNAPII CTD S2-P (3E10)	Chromotek	Rat	1:10
RNAPII CTD T4-P (6D7)	Chromotek	Rat	1:10
RNAPII CTD S5-P (3E8)	Chromotek	Rat	1:20
RNAPII S7-P (4E12)	Chromotek	Rat	1:10
Actin (clone C4)	Merck Millipore	Mouse	1:5000

Table 2.13. Secondary antibodies used in western blots

Secondary Antibody	Supplier	Species	Concentration
Anti-mouse HRP	Cell Signalling	Goat	1:2000 (anti GFP); 1:20,000 (anti-FLAG) 1:25,000 (anti-Actin)
Anti-rabbit HRP	Cell Signalling	Goat	1:20,000
Anti-rat HRP	Cell Signalling	Goat	1:2000

2.28. Fixing and staining transfected S2R+ cells

For imaging cells transfected with GFP-*dTOX4*^{wt} and GFP-*dTOX4*$^{P216\Delta}$ +/- RFP-*dPNUTS-Myc*. 48-72 hours after transfection with Effectene® in a 6 well dish, the medium was removed and cells resuspended in 2ml fresh complete Schneider's medium. 1ml was transferred to a 6 well dish with a glass-bottomed micro-well (10mm diameter) and cells allowed to adhere for a minimum of 2 hours. The medium was then removed and 500μl 10% paraformaldehyde added and incubated for 10 minutes to fix the cells. Cells were washed three times 5 minutes with 1 × PBS and blocked for 1 hour at room temperature or 2 hours at 4°C in blocking solution (5% FBS in 0.1% PBST). Cells were then incubated with Alexa Fluor® 633 Phalloidin (diluted in 0.1% PBST, see Table 2.15 for details) and incubated for 1 hour at room temperature in the dark. Cells were washed two times five minutes with

0.1% PBST and then final wash with DAPI (see Table 2.15) for ten minutes. 120µl Vectashield® mounting medium (Vector Labs) was added to the glass bottomed micro-well to preserve fluorescence. Dishes were stored at 4ºC in the dark for no longer than one week.

2.29. Making the *dTOX4*^{null} mutant strain

The *dTOX4*^{null} mutant strain was generated by imprecise excision of a *P*-element insertion (see section 2.6 for genotypes and Chapter 5 for details). A total of 82 crosses were set up and progeny screened as follows. For each cross 15 male and 15 female adult progeny were collected and snap frozen in liquid nitrogen. DNA was extracted as described in section 2.39. DNA from each cross was screened by PCR using primers mapped as shown in Figure 5.2 (see Table 2.2 for primer sequences). PCR was carried out using the *Taq* PCR Master mix kit with 4µl DNA (Table 2.4). Reaction conditions for these primers are shown in Table 2.14. Samples were separated on a 0.6% agarose gel for analysis. A band corresponding to an approximately 1200bp deletion (see Figure 5.2) was gel extracted as in section 2.20 and sent for sequencing (see section 2.16) to determine the extent of the deletion.

Table 2.14. PCR reaction conditions for screening the dTOX4^{null} mutant

Temperature (°C)	Time	No of Cycles
94	3 min	1
92	25s	30
57	30s	
72	60s (2&3), 100s (1 & 3)	
72	5 min	1
10	∞	-

To check the dTOX4 transcript levels were also affected in the mutant 3 male and 3 female adult flies were collected and RNA extracted as in section 2.40. cDNA was synthesised (see section 2.41) and PCR amplified (see section 2.18). Agarose gel electrophoresis (see section 2.19) was used to confirm absence of the transcript.

2.30. Making the tools for rescue experiments

For rescue by overexpressing GFP tagged *dTOX4*^{wt} or *dTOX4*$^{P216\Delta}$ genes were subcloned into a fly expression vector (pPGW) from pENTR as described in section 2.23.5. The pPGW gene specific expression vectors were sent to The Fly Facility at the university of Cambridge for *P*-element mediated transformation into the *Drosophila* genome. Transformants were analysed by crossing to a *daughterless* (*da*)-GAL4 strain for ubiquitous ectopic overexpression of GFP-*dTOX4*$^{wt/P216\Delta}$. Protein was extracted and analysed using western blotting with an anti-GFP antibody as described in section 2.25. For overexpression in the testis, the UAS constructs (on the 2nd chromosome) were recombined with *bam*-GAL4 on the 3rd chromosome, For overexpression in the ovaries, the UAS constructs were combined with *maternal-α-tubulin*-GAL4 on the second chromosome.

For genomic rescue, gene fragments encoding genomic *dTOX4*^{wt} and *dTOX4*$^{P216\Delta}$ (a 2714 bp fragment starting 459bp upstream of the transcription start site) with EGFP inserted immediately before the ATG start site, an *attB* site at the end of the fragment and restriction sites at either end of the fragment (5' *BamH1,* 3' *Not1*) was synthesised in pCaSpeR3 by GeneArt. This was amplified by transforming into One Shot® TOP10 Chemically Competent Cells as described in section 2.12 and sent to

The Fly Facility at the University of Cambridge for ΦC31 mediated *P*-element transformation into the *Drosophila* genome on the second chromosome.

2.31. *Drosophila* survival assay

Virgin males and females were collected over an 8 hour period for each genotype. Flies were then mated for 48 hours and then split into same sex vials of 10 flies on standard medium. Flies were kept at 25°C on standard yeast medium without dried yeast balls. Flies were transferred to fresh vials three times per week and the number of dead recorded.

2.32. Egg laying and fertility assay

10 female virgins were crossed to 6 males and allowed to mate for 48 hours at 25°C in 50ml vials on standard yeast medium with dried yeast balls. Flies were then transferred into 250ml bottles on apple juice agar plates with a small amount of yeast paste (dried yeast balls mixed with water) and kept at 25°C. After 24 hours the crosses were transferred onto new plates and the first collection of eggs was discarded. Recording of egg counts began with the second plate. Eggs were collected from the agar using a paintbrush and gently washed (to remove yeast paste) under a running tap over a nylon mesh to collect the eggs. They were then placed back onto the agar plates to be counted. The crosses were changed every 24 hours and the number of eggs counted. 48 hours after egg collection, the number of larvae emerged was counted and the percentage of eggs hatched calculated.

2.33. Dissection and staining of ovaries for fluorescence microscopy

Newly eclosed (0-1 day old) w^{1118} and *dTOX4*^{null}/ *dTOX4*^{null} adult females were transferred to new vials with yeast paste and allowed to fatten for 1-2 days. Ovaries were dissected in cold 1 × PBS and fixed for 30 minutes in 3.7% paraformaldehyde at room temperature. Ovaries were washed three times in 0.1% PBST for 10 minutes and blocked at 4°C in blocking solution for a minimum of 2 hours. Ovaries were washed two times 10 minutes in 0.1% PBST followed by another wash with TO-PRO®-3 Iodide (Life Technologies, diluted 1:1000 in 1 × PBS) for ten minutes. Tissues were mounted in 17.5μL of Vectashield mounting medium (Vector Laboratories) on a standard glass microscope slide and covered with a coverslip (22mm × 22mm). Coverslip slides were sealed with clear nail polish and slides were stored in the dark at 4°C for no longer than a week.

2.34. Dissection and staining of testes for fluorescence microscopy

Testes were dissected from *w*^{1118} and *dTOX4*^{null}/ *dTOX4*^{null} newly eclosed males (0-1 day old) in cold 1 × PBS and fixed for 30 minutes in 3.7% paraformaldehyde at room temperature. Testes were washed three times in 0.1% PBST for 10 minutes and blocked at 4°C in blocking solution for a minimum of 2 hours. Samples were incubated with the primary antibody (phH2AX, see Table 2.15) and Alexa Fluor® 555 Phalloidin (see section 2.14) diluted in blocking solution overnight at 4ºC in the dark. Testes were washed three times ten minutes in 0.1% PBST and then incubated with Alexa Fluor® 488 Goat Anti-Mouse antibody (anti-phH2AX, see Table 2.15 for details) for two hours at room temperature. Testes were washed two times 10 minutes in 0.1% PBST followed by another wash with TO-PRO®-3 Iodide (Life

Technologies, diluted 1:1000 in 1 × PBS) for ten minutes. Tissues were mounted in 17.5μL of Vectashield mounting medium (Vector Laboratories) on a standard glass microscope slide and covered with a coverslip (22mm × 22mm). Coverslip slides were sealed with clear nail polish and slides were stored in the dark at 4°C for no longer than a week.

2.35. Dissection, squashing and phase contrast microscopy of live testes

Testis of w^{1118} and $dTOX4^{null}$/ $dTOX4^{null}$ adult flies were dissected as described in (White-Cooper, 2004), protocol: Phase Contrast Microscopy of Live Testes. Testes were dissected from newly eclosed (0-1day old) males in fresh testis buffer with 2μg/ml of Hoechst 33342 (SIGMA, a vital dye for visualising DNA), on a 10cm petri dish. Testes were transferred to a small drop of testis buffer on a clean standard microscope slide and cut open using sharp forceps. The testes were incubated like this for 5 minutes and then a clean coverslip was placed on top to gently squash the cells. For better imaging testis buffer was removed from under the coverslip using Kim wipes to further squash the sample. This was done whilst looking down the microscope to ensure the sample was not over-squashed. Experiments were carried out together with Dr Helen White-Cooper using her facilities at Cardiff University. Images were captured using an Olympus BX50 microscope using a Hamamatsu Orca-05G camera and HCImage software.

2.36. Confocal microscopy

Fixed tissues were imaged using an LSM 710 or LSM 780 Confocal microscope (Zeiss) and Zen 2011 confocal software (Zeiss) equipped with 405nm, 488nm, 561nm and 633nm lasers. Tissues were imaged using a Plan Apochromat 40×/1.3NA oil immersion objective. Nurse cell nuclei were imaged using a Plan Apochromat 63x/1.0NA air objective. GFP was excited at 488nm and RFP was excited at 561nm.

Table 2.15. Antibodies and stains used for confocal microscopy

Name	Type	Supplier	Concentration	Laser (nm)
DAPI	Fluorescent stain	SIGMA	1:1000	405
TO-PRO®-3	Fluorescent stain	Life Technologies	1:1000	633
Alexa Fluor® 555 Phalloidin	Fluorescent dye	Life Technologies	1:500	561
Alexa Fluor® 633 Phalloidin	Fluorescent dye	Life Technologies	1:500	633
H2AX P-Ser 139 (JBW301)	Primary antibody (mouse)	Milliport	1:500	-
H3 Phospho S10	Primary antibody (Rabbit)	Abcam	1:100	-
H3 Phospho S28	Primary antibody (Rabbit)	Abcam	1:100	-
H3 Acetyl K27	Primary antibody (Rabbit)	Abcam	1:200	-
H3 dimethyl K4	Primary antibody (Rabbit)	Active motif	1:200	-
H3 trimethyl K4	Primary antibody (Rabbit)	Active motif	1:200	-
Alexa Fluor® 555 anti-mouse	Secondary antibody (Goat)	Life Technologies	1:500	561
Alexa Fluor® 555 anti-rabbit	Secondary antibody (Goat)	Life Technologies	1:500	561

2.37. Image analysis

Images were prepared using Fiji (ImageJ). For co-localisation analysis of imaged S2R+ cells Fiji was used to plot a profile of intensity for GFP and RFP across a specified section of the cell. For whole cell co-localisation analysis the JACoP (Just

Another Colocalisation Plugin) Plugin was used to perform M1 and M2 coefficients (see results in Chapter 4 for details) and generate a cytofluorogram.

2.38. Phylogenetic and alignment analysis

BLAST (Basic Local Alignment Search Tool) analysis was performed on *Drosophila* protein CG12104 and human LCP1/TOX4 using the NCBI (http://blast.ncbi.nlm.nih.gov/Blast.cgi) database to identify homologues in a range of species. The protein sequences of the top hits were aligned using MSAProbs (Liu *et al*., 2012) and then a distance matrix generated using Tree-Puzzle (Strimmer and von Haeseler, 1996). The distance matrix was then used to generate a minimum evolution tree using FastME (Lefort and Gascuel, 2015), which was used as a starting point to generate a maximum likelihood tree using PHYML (Guindon and Gascuel, 2003). The tree was visualised using FigTree 1.4 (http://tree.bio.ed.ac.uk/software/figtree/).

For the alignment, the amino acid sequence for dTOX4 (CG12104) was taken from flybase and the amino acid sequence for LCP1 (KIAA0737) taken from GenBank. The T-Coffee Multiple Alignment tool was used in the 'accurate' mode to align both sequences. The alignment was put into BoxShade to identify the conserved residues and Ali2D to map secondary structures.

2.39. DNA extraction from *Drosophila*

The DNeasy Blood and Tissue Kit (Qiagen) was used to extract DNA from adult flies. All buffers mentioned in this protocol are from the kit. Frozen flies were homogenised in a 1.5ml tube using a small pestle. 180µl of buffer ATL was added

and the flies further homogenised. 20µl of Proteinase K was added, mixed thoroughly by vortex and incubated at 56°C until the tissue was completely lysed (approximately 1-2 hours with occasional vortexing). 200µl of buffer AL was added to the supernatant and mixed by vortex and then 200µl 100% ethanol added and mixed immediately by vortex. Samples were centrifuged at 13,000rpm for approximately 30 seconds and the supernatant transferred to a fresh 1.5ml tube. Samples were treated with 3µl RNase A for 2 minutes at room temperature and then transferred onto a DNeasy mini spin column in a 2ml collection tube and centrifuged at 8000rpm for 1 minute. The column was transferred to a fresh collection tube and 500µl buffer AW1 added followed by centrifugation (8000rpm, 1 minute). This step was repeated with AW2 with centrifugation at 13,000rpm for 3 minutes. The column was placed in a clean 1.5ml tube and 100µl buffer AE added directly on to the column membrane. This was incubated at room temperature for 5 minutes before centrifugation at 8000rpm for 1 minute. The eluate was reloaded onto the column, incubated for another 1 minute at room temperature and centrifuged at 8000rpm for 1 minute.

2.40. RNA extraction from *Drosophila* adults and S2R+ cells

The RNeasy Mini Kit (Qiagen) was used to extract RNA from adult flies and S2R+ cells. All buffers mentioned in this protocol are from the kit. Frozen flies were homogenised in a 1.5ml tube using a small pestle and then 350µl buffer RLT (plus β-mercaptoethanol, 10µl/ml) added and homogenised further. S2R+ cells were pelleted by centrifugation for 5 minutes at 2500rpm after which the supernatant was removed and the cells lysed by adding 350µl buffer RLT (plus β-mercaptoethanol, 10µl/ml)

and mixing with the pipette. For complete homogenisation the sample was added directly on a Qiashredder spin column and centrifuged at maximum speed for 2 minutes. For adult flies the lysate was then centrifuged for 3 minutes at maximum speed to pellet any debris and the supernatant transferred to a clean 1.5ml tube. 1 volume of 70% ethanol was added and mixed immediately and the sample added to an RNeasy column and centrifuged for 15 seconds at 10,000rpm. The flow through was discarded and 700µl buffer RW1 added and the centrifugation step repeated. This was repeated again with 500µl buffer RPE and the flow through discarded. Another 500µl buffer RPE was added and centrifuged at 10,000rpm for 2 minutes. The column was transferred to a clean 1.5ml tube and 30µl RNase-free water added directly on to the membrane. This was then centrifuged at 10,000rpm for 1 minute to elute.

2.41. cDNA synthesis

The High Capacity RNA-to-cDNA (Applied Biosystems) kit was used according to the manufacturer's protocol to synthesise cDNA. Reaction components (Table 2.16) and reaction conditions (Table 2.17) are shown below. RT buffer includes dNTP's, random octamers and olido-dT-16. RT enzyme mix includes MuLV reverse transcriptase and RNase inhibitor protein.

Table 2.16. cDNA synthesis reaction components

Component	Amount
2 × RT buffer	10µl
20 × RT enzyme mix	1µl
RNA	1µg
H_2O	to 20µl

Table 2.17. cDNA synthesis reaction conditions

Temp (°C)	Time
37	60 min
95	5 min
4	∞

2.42. Making the $H3^{wt}$ and $H3^{S10,28A}$ phosphor FRET probes

The DNA sequence of the wild type probe and a smaller fragment encoding a serine to alanine amino acid change at S10 and S28 were sent to GENEART for synthesis in an entry vector (pDONR221/pMA-T respectively). The vectors were diluted in TE buffer to give a stock concentration of 0.25µg/µl.

2.42.1. $H3^{wt}$ probe

1.25×10^{-3}µg/µl of $H3^{wt}$ in pDONR221 was transformed into TOP10 competent *E.coli* (see 2.12) and DNA purified (see 2.14). A diagnostic digest with *Age1* and *Nco1* followed by gel electrophoresis on a 1% agarose gel confirmed the presence of the construct.

2.42.2 $H3^{S10,28A}$ probe

0.25ng/µl of $H3^{S10,28A}$ fragment in pMA-T was transformed into *dam*$^{-}$/*dcm*$^{-}$ competent *E.coli* (see 2.13) and DNA purified (see section 2.14). The $H3^{wt}$ probe in pDONR221 and $H3^{S10,28A}$ mutant fragment in pMA-T were digested with *StuI* and *SacI* (see section 2.21). Digests were chloroform extracted by adding 1 volume of chloroform, mixing vigorously and centrifuging at 13,000rpm for 3 minutes. The top phase was removed and separated on a 0.8% agarose gel. The bands corresponding to the $H3^{S10,28A}$ mutant fragment (insert) and $H3^{wt}$ backbone (vector) were gel extracted (see section 2.20). The formula below was used to calculate the amount of vector and insert to ligate together based on 40ng of vector and a 3 molar excess of insert:

((ng vector × kb insert)/kb vector) × (moles insert/moles vector) = ng insert

For ligation, the following protocol was used:

Table 2.18. Ligation reaction components

Component	Amount
Vector ($H3^{wt}$ backbone)	40ng
Insert ($H3^{S10,28A}$ fragment)	3M excess
10× Ligase buffer (NEB)	3µl
DNA Ligase (NEB)	1µl
H_2O	to 20µl

A reaction was also set up with double the amount of insert. All reactions were incubated at 16°C overnight followed by heat inactivation at 65°C for 25 minutes. 2µl of each reaction was transformed into TOP10 competent *E.coli* (see section 2.12). A diagnostic digest with *AgeI* (HF) and *EcoRV* (HF) (see 2.21) followed by

gel electrophoresis on a 1.2% agarose gel (see section 2.20) confirmed the presence of the mutant construct.

2.42.3. Cloning of $H3^{wt}$ and $H3^{S10,28A}$ (in pDONR221) into destination vector (pAW)

The Gateway® LR Clonase™ II enzyme mix (Invitrogen) was used (see section 2.23.5) to clone the wild type and mutant probes into the destination vector, pAW. This was transformed into TOP10 competent *E.coli* and processed as in section 2.12. Selective ampicillin (100μg/ml) plates were used. A diagnostic digest with *NcoI* (+ *AgeI* for mutant) followed by gel electrophoresis on a 1% agarose gel confirmed the presence of both constructs in pAW (see sections 2.21 and 2.20).

2.43. dsRNA synthesis (*PP187B* & *Jil-1*)

cDNA was synthesised from wild type *Drosophila* (L3 larvae or adult) RNA. The sequence of previously used amplicons for *PP187B* and *Jil-1* were taken from www.flyrnai.org and used to design primers (see Table 2.2 for primer list) for the amplification of wild type cDNA. After choosing the primer sequence, the T7 promoter sequence (TAATACGACTCACTATAGGG) was added to the 5' end of all primers. cDNA fragments were amplified using the *Taq* PCR Master Mix Kit (Qiagen) (Table 2.4). Reaction conditions are shown in Table 2.19.

Table 2.19. PCR conditions for dsRNA synthesis

Temp (°C)	Time	No of Cycles
95	2 min	1
92	20s	
55	30s	5
72	30s	
92	20s	25
72	40s	
72	5 min	1

Table 2.20. dsRNA synthesis reaction

Component	Amount
ATP solution	2µl
CTP solution	2µl
GTP solution	2µl
UTP solution	2µl
10 × Reaction Buffer	2µl
RNA Polymerase Enzyme Mix	2µl
Template DNA	0.1-1µg
Nuclease-free water	to 20µl

5µL of each sample was separated on a 1% agarose gel to check fragment size. PCR samples were cleaned up using the QIAquick PCR purification Kit (Qiagen) (see section 2.23.2). Ambion's MEGAscript kit was used according to the manufacturer's instructions to synthesise dsRNA fragments. Briefly a 20µl reaction was set up for each cDNA as shown in Table 2.20 using reagents from the MEGAscript kit. This was incubated at 37°C overnight (approximately 16 hours) and then briefly

centrifuged. 1µl of TURBO DNase was added, mixed well and incubated at 37°C for 15 minutes. A 20x dilution in DEPC-treated water of the dsRNA product was separated on a 1% agarose gel to check fragment size. dsRNA was purified using the RNAeasy Mini Kit (Qiagen) following the RNA clean-up protocol in the manufacturer's manual. The same protocol was used as for RNA extraction from S2R+ cells (see section 2.40) but with two changes at the beginning: 1) sample volume was adjusted to 100µl with RNase free water before addition of RLT 2) 250µl of 100% ethanol was added.

2.43.1. Testing the dsRNA (in S2R+ cells)

0.2-0.3µg of dsRNA was mixed with 30µl of Schneider's medium (Lonza) supplemented with 10% FCS and 100µg/ml penicillin-streptomycin (Gibco) (complete Schneider's medium). 3µl of Cellfectin II reagent (Invitrogen) was mixed with 30µl of complete medium. The two solutions were combined, gently mixed and incubated at room temperature (RT) for 15-30 minutes then 40µl of complete Schneider's medium was added. Adhered S2R+ cells were re-suspended in complete Schneider's medium. 3-8×10^4 cells in 100µl were aliquoted into wells of a 96-well plate. 100µl of the dsRNA/Cellfectin mix was added to the cells and incubated at 26°C in a tissue culture chamber for 3-4 days. Cells were then re-suspended, transferred to a 1.5ml tube and pelleted by centrifugation at 2500rpm for 5 minutes. RNA was extracted (see section 2.40) and cDNA synthesised (see section 2.41) followed by PCR (see section 2.18) with primers for *Jil-1* and *PP187B* (+GAPDH for control). Samples were separated on a 1.2% agarose gel to determine the extent of gene knockdown.

2.44. S2R+ transfections for FRET experiments

Initial transfection experiments were performed using Cellfectin® II Transfection Reagent (Life Technologies) in a 96 well format. 4×10^4 cells in 100µl was added to each well and allowed to adhere for at least 2 hours. 0.6µg of DNA +/- 0.6µg of dsRNA was mixed with 100µl Schneider's insect medium (without serum or antibiotics). 6µl Cellfectin® II Reagent was mixed with 100µl Schneider's insect medium (without serum or antibiotics) and added to the DNA/dsRNA mix and incubated at room temperature for 30 minutes then each reaction was split between 2 wells of cells. Cells were incubated under normal conditions for 4 days before imaging.

Due to problems with transfection efficiency using Cellfectin®, Effectene® was used. Each screen was performed by transfecting S2R+ cells with the $H3^{wt}$ and $H3^{S10,28A}$ probes 2 days prior to transfection with *PP187B* dsRNA. Qiagen's Effectene® transfection reagent kit was used as described in section 2.23.6 but with 0.4µg DNA, 3.2µl enhancer and 10µl Effectene reagent. 48 hours after transfection with the FRET probes cells were transfected with dsRNA for *PP187B* using the same protocol. Four days following transfection with dsRNA, the cells were imaged.

2.45. Live imaging of S2R+ cells for FRET experiments

The day before imaging, transfected S2R+ cells were re-suspended and 200µl transferred to an 8 chamber #1.0 Borosilicate cover glass system (Lab-Tek®) and incubated at 26°C in a tissue-culture chamber. Cells were imaged using a Zeiss 710 confocal microscope with a 40×oil immersion objective. For sensitised emission, ECFP was excited at 458nm alone and in combination with YPet excitation at

514nm. YPet was excited at 514nm and in combination with ECFP excitation at 458nm. The emission signal was measured for ECFP (479nm) and YPet (527nm). FRET was measured as a ratio of the mean ECFP/YPet intensity after excitation of ECFP at 458nm alone, using Image J software. For acceptor photobleaching 30 images were taken with bleaching of YPet at 514nm between images 4 and 5 and the emission signal for ECFP (479nm) and YPet (527nm) measured. The average nuclear intensity of ECFP and YPet was calculated before and after bleaching using Cell Tracker software.

2.46. Imaging of eyes

Flies were collected in 1.5ml tubes and immediately frozen with liquid nitrogen. They were stored at -20°C until imaging. Flies were imaged using a Leica MZ10F stereomicroscope (Leica).

3. Characterisation of *Drosophila* PNUTS

3.1 Introduction

The PP1 Nuclear Targeting Subunit (PNUTS) is a highly conserved, ubiquitously expressed metazoan protein and is one of the two most abundant PP1-binding proteins in the mammalian nucleus (Landsverk *et al*., 2005; Kreivi *et al*., 1997; Allen *et al*., 1998). It was first described as a regulatory subunit of PP1 in 1998, when it was isolated in a yeast two-hybrid screen against a rat brain cDNA library, identifying PP1 binding proteins (Allen *et al*., 1998). The human homologue of PNUTS, p99, had been identified the previous year when it was purified with PP1 from HeLa cell nuclear extracts (Kreivi *et al*., 1997). p99 was found to be expressed in the nucleus and sequence analysis revealed it contained a nuclear localisation signal (NLS) (Kreivi *et al*., 1997). Further analysis showed PNUTS/p99 is an RNA binding protein, and binds to RNA through several closely spaced RGG boxes in its C-terminus (Kreivi *et al*., 1997; Allen *et al*., 1998). Given PP1 has been linked to RNA processing, it was believed PNUTS may be responsible for anchoring PP1 to RNA complexes in the nucleus (Mermoud *et al*., 1994; Allen *et al*., 1998; Kim *et al*., 2003). Other domains identified included a cysteine/histidine rich zinc (Zn^{2+}) finger and a canonical PP1 binding motif (see Introduction, Section 1.3.2) (Kreivi *et al*., 1997).

Since then, the PNUTS-PP1 holoenzyme has been implicated in various nuclear processes including chromosome decondensation (Landsverk *et al*., 2005), cardiac aging (Boon *et al*., 2013) and the DNA damage response (Landsverk *et al*., 2010). As discussed in the introduction (see section 1.5) PP1 has been implicated in transcriptional regulation by targeting the CTD of RNAPII for dephosphorylation

(Washington *et al*., 2002). In 2011, Jerebtsova *et al.,* suggested both NIPP1 and PNUTS may regulate this process by showing they co-immunoprecipitate with RNAPII (Jerebtsova *et al*., 2011). They hypothesised that NIPP1 functions to reduce the rate of elongation by targeting PP1 to the CTD for active dephosphorylation, to allow coupling of transcription with splicing and RNA processing (Jerebtsova *et al*., 2011). Limited work has been done studying the physiological role of PNUTS and its role in RNAPII complexes.

In a yeast two-hybrid screen looking for PP1 binding proteins in *Drosophila* the Bennett lab isolated a protein with significant similarity (approximately 24%) to PNUTS/p99 (Bennett *et al*., 2006). Sequence analysis revealed the amino and carboxy termini of PNUTS/p99, together with the zinc finger and PP1 binding region are conserved in dPNUTS. The RGG motifs are not found in dPNUTS indicating that RNA-binding through these motifs is not conserved in the *Drosophila* orthologue, although dPNUTS might still bind RNA through numerous histidine/glycine repeats found in the C-terminus.

In the course of investigating phosphatases that might regulate gene expression through histone H3 phosphorylation, dPNUTS was selected as a candidate through its association with PP1, which is known to dephosphorylate serine 10 and serine 28 of histone H3 (see Chapter 6). In the Bennett lab, work was already underway to characterise dPNUTS and, given preliminary experiments showing that it is essential for development in *Drosophila*, focus shifted to understanding the molecular mechanisms underlying this phenotype. The association of mammalian PNUTS with RNAPII complexes led to the possibility of a similar complex existing in

Drosophila, therefore the role of dPNUTS in RNAPII phosphorylation and, ultimately, in gene expression was investigated.

The work performed in this chapter was recently published in *PLoS Genetics*. The manuscript is copied below together with a description of the contribution made by each author.

3.2 Paper

Ciurciu.A., Duncalf.L., Jonchere.V., Lansdale.N., Vasieva.O., Glenday.P., Rudenko.A., Vissi.E., Cobbe.N., Alphey.L. and Bennett.D. (2013). PNUTS/PP1 regulates RNAPII-Mediated Gene Expression and Is Necessary for Developmental Growth. *PLoS Genetics*, vol. 9.

Contributions of Authors:

Ciurciu.A.: Edited paper, characterised the mutant phenotype, prepared samples for RNA-seq, analysed RNA-Seq data, performed qPCR analysis, performed chromosome *in situ* stainings and western blots with mutant extracts, performed ChIP experiments. Figures: 1E-F, 2B-E, 4B, 5D, 6, 7B-E, S2, S5, S. Tables: S1, S2, S5.

Duncalf.L: Edited paper, characterised the mutant phenotype, performed qPCR analysis, performed *in vitro* binding assays, performed ChIP experiments, performed clonal analysis. Figures: 3K-R, S3, S6, S8.

Jonchere.V: Analysed RNA-Seq. Figures: 4A, S4. Table S3.

Lansdale.N: Performed localisation studies in whole mount samples. Figures 1B-D

Vasieva.O: Analysed RNA-Seq data. Table S4.

Glenday.P: Performed *in vivo* binding assays. Figure 5C

Rudenko.A: Performed initial chromosomal localisation studies in L. Alphey's laboratory.

Vissi.E: Performed *in vivo* binding assays. Figure 5B.

Cobbe.N: Analysed phylogenetic relationships

Alphey.L: Cloned the *dPNUTS* gene with Bennett, below.

Bennett.D: Wrote paper, cloned the *dPNUTS* gene, generated the null mutant alleles, characterised the mutant phenotypes, analysed RNA-seq data, performed *in vitro* and *in vivo* binding assays. Figures: 1A, 2A, 3A-J, 5A, 7A, S1.

OPEN ACCESS Freely available online

PLOS | GENETICS

PNUTS/PP1 Regulates RNAPII-Mediated Gene Expression and Is Necessary for Developmental Growth

Anita Ciurciu[1], Louise Duncalf[1], Vincent Jonchere[1], Nick Lansdale[1¤a], Olga Vasieva[1], Peter Glenday[1,2], Andreii Rudenko[2¤b], Emese Vissi[2¤c], Neville Cobbe[1], Luke Alphey[2¤d], Daimark Bennett[1]*

1 Institute of Integrative Biology, University of Liverpool, Liverpool, United Kingdom, **2** Department of Zoology, Oxford University, Oxford, United Kingdom

Abstract

In multicellular organisms, tight regulation of gene expression ensures appropriate tissue and organismal growth throughout development. Reversible phosphorylation of the RNA Polymerase II (RNAPII) C-terminal domain (CTD) is critical for the regulation of gene expression states, but how phosphorylation is actively modified in a developmental context remains poorly understood. Protein phosphatase 1 (PP1) is one of several enzymes that has been reported to dephosphorylate the RNAPII CTD. However, PP1's contribution to transcriptional regulation during animal development and the mechanisms by which its activity is targeted to RNAPII have not been fully elucidated. Here we show that the *Drosophila* orthologue of the PP1 Nuclear Targeting Subunit (dPNUTS) is essential for organismal development and is cell autonomously required for growth of developing tissues. The function of dPNUTS in tissue development depends on its binding to PP1, which we show is targeted by dPNUTS to RNAPII at many active sites of transcription on chromosomes. Loss of dPNUTS function or specific disruption of its ability to bind PP1 results in hyperphosphorylation of the RNAPII CTD in whole animal extracts and on chromosomes. Consistent with dPNUTS being a global transcriptional regulator, we find that loss of *dPNUTS* function affects the expression of the majority of genes in developing 1st instar larvae, including those that promote proliferative growth. Together, these findings shed light on the *in vivo* role of the PNUTS-PP1 holoenzyme and its contribution to the control of gene expression during early *Drosophila* development.

Citation: Ciurciu A, Duncalf L, Jonchere V, Lansdale N, Vasieva O, et al. (2013) PNUTS/PP1 Regulates RNAPII-Mediated Gene Expression and Is Necessary for Developmental Growth. PLoS Genet 9(10): e1003885. doi:10.1371/journal.pgen.1003885

Editor: Ana Pombo, Berlin Institute for Medical Systems Biology, Germany

Received November 27, 2012; **Accepted** September 3, 2013; **Published** October 31, 2013

Funding: This research was funded by Wellcome project grant 084659/Z/08/Z to DB, with additional support from Cancer Research UK, the Liverpool CRUK Centre, the North West Cancer Research Fund and the Royal Society; initial stages of the study were supported by BBSRC and MRC project grants and an MRC Senior Research Fellowship to LA. AR was supported by an Oxford University Scatcherd Scholarship, LD and PG were supported by BBSRC PhD Studentships and NL was supported by a Wellcome Trust Clinical Research Training Fellowship. The funders had no role in study design, data collection and analysis, decision to publish, or preparation of the manuscript.

Competing Interests: The authors have declared that no competing interests exist.

* E-mail: daimark.bennett@liverpool.ac.uk

¤a Current address: Department of Paediatric Surgery, Royal Manchester Children's Hospital, Manchester, United Kingdom.
¤b Current address: Picower Institute for Learning and Memory, Massachusetts Institute of Technology, Cambridge, Massachusetts, United States of America.
¤c Current address: Quintiles Hungary Ltd, Budapest, Hungary.
¤d Current address: Oxitec Limited, Oxford, United Kingdom.

Introduction

Development must be tightly coupled with cellular metabolism to ensure that necessary nutritional and energetic requirements are met and the available resources are utilised effectively to sustain appropriate levels of tissue growth. A particularly dramatic example of how development is coupled to metabolism is during the transition through the larval stages of *Drosophila* development, during which animals accumulate a 200-fold increase in body mass. The metabolic needs to sustain this rapid expansion are underpinned by transcriptional programmes initiated in the embryo; as maternal products become exhausted, large numbers of zygotically expressed genes, responsible for converting raw materials into cell mass, are induced to sustain developmental growth [1]. Elucidating what factors are necessary to drive these transcriptional programmes is not only critical for understanding tissue and organism size regulation during normal development, but is also important for understanding numerous disease processes characterized by inappropriate gene expression.

Reversible phosphorylation plays important roles in the regulation of transcriptional networks and in coordinating spatial and temporal patterns of gene expression. Phosphorylation of RNA polymerase II (RNAPII) at multiple sites on its C-terminal domain (CTD) is critical for gene expression and its regulation [2]. Different phospho-forms of the CTD appear at different stages of the transcription cycle, and these are thought to facilitate initiation, elongation and termination by recruiting specific histone and RNA modifiers [3,4]. The consensus view from studies of RNAPII occupancy in budding yeast is that there is a stereotypical pattern of phosphorylation at most gene loci during the transcription cycle [5,6]. However, numerous lines of evidence suggest that there is active control of CTD phosphorylation in response to environmental cues [7–9] and during developmental transitions, e.g. in which restriction of CTD phosphorylation to particular lineages [10] is used to control cell fate [11]. Furthermore, studies of the enzymes responsible for regulating CTD phosphorylation indicate that phosphorylation may be modified at specific loci to determine gene-specific patterns of expression [12,13].

Author Summary

During development, cells rely on appropriate patterns of gene expression to regulate metabolism in order to meet cellular demands and maintain rapid tissue growth. Conversely, dysregulation of gene expression is critical in various disease states, such as cancer, and during ageing. A key mechanism that is ubiquitously employed to control gene expression is reversible phosphorylation, a molecular switch that is used to regulate the activity of the transcriptional machinery. Here we identify an enzyme that binds to and regulates the phosphorylation state of RNA Polymerase II, a central component of the general transcription machinery. We also show that an essential role of this enzyme is to support normal patterns of gene expression that facilitate organismal growth. These findings are not only of relevance to the understanding of normal enzyme function but may also assist in the development of therapeutic strategies for the treatment of aberrant patterns of gene expression that occur during ageing and disease progression.

Serine/threonine protein phosphatase type 1 (PP1) is one of four protein phosphatases known to contribute to the regulation of CTD phosphorylation [14], the others being FCP1 [15], SCP1 [11] and Ssu72 [16]. In *Drosophila*, PP1 is found at multiple sites on chromosomes where it has been postulated to play important roles in regulating developmentally controlled gene expression [17,18]. However, analysing the role of PP1 in transcriptional regulation has been complicated by its pleiotropic roles [19] and broad *in vitro* substrate specificity. *In vivo*, PP1 has been shown to associate with different targeting subunits that restrict its activity towards particular substrates [20]. Therefore, a full understanding of PP1 function requires the identification and characterisation of these regulatory proteins.

In mammalian cells, the PP1 Nuclear Targeting Subunit (PNUTS) is one of the two most abundant PP1-interacting proteins in the nucleus [21] and is known to be chromatin-associated during interphase and not during mitosis [22,23]. Its reassociation with chromatin during telophase and its ability to augment chromosome decondensation *in vitro* [24] and *in vivo* [25] have indicated a possible role in cell cycle progression. Several lines of evidence also indicate that PNUTS is required for cell survival [26–30] and contributes to cellular responses to environmental stress, including hypoxia [31] and DNA damage [32]. These roles may be especially important during ageing since loss of PNUTS expression is associated with an age-dependent increase in cardiomyocyte apoptosis and decline in cardiac function [33]. Targeting of PNUTS to chromatin is likely to be in part through association with the DNA-binding factor Tox4/Lcp1 [25,34], which is capable of recognising DNA adducts generated by platinum anticancer drugs [35]. PNUTS and Tox4 have also been reported to form a stable multimeric complex with Wdr82 [25], which was previously identified as an integral component of a distinct complex containing Set histone H3-Lys4 methyltransferases. Although the role of Wdr82 bound to PNUTS is not known, Wdr82 may mediate interactions with initiating and early elongating RNAPII by recognising Ser5-phosphorylated CTD, as it does when it is associated with the Set1 complex [36]. A role for PNUTS in transcription has been further suggested by recent reports that it associates with RNAPII complexes [37]. Despite these insights, an understanding of the physiological roles of PNUTS remains incomplete.

Here we show that null mutants in the *D. melanogaster* orthologue of PNUTS (*dPNUTS*), display a larval growth defect and are larval lethal. Mutant clones show a cell autonomous growth defect and are eliminated from wild type epithelia due to cell competition. RNA-Sequencing (RNA-Seq) analysis indicates that *dPNUTS* affects the expression of the majority of genes in 1st instar larvae, including those that are highly expressed and are involved in cellular metabolism and larval development. The function of *dPNUTS* in tissue development is dependent on binding to the catalytic subunit of Protein phosphatase 1 (PP1), which is targeted by dPNUTS to RNA polymerase II in cell extracts and at many active sites of transcription on polytene chromosomes. Loss of *dPNUTS* function, or displacement of dPNUTS-PP1 using a non-PP1 binding mutant of *dPNUTS*, results in hyperphosphorylation of the C-terminal domain of RNA Polymerase II in whole animal extracts and on chromosomes. Taken together, these data suggest that dPNUTS-PP1 is a global regulator of gene expression via effects on RNAPII phosphorylation and is required in larvae to promote normal developmental growth.

Results

PNUTS is highly conserved across metazoa

Sequence homology searches have suggested that PNUTS is a metazoan PP1-binding protein [38]. However, its absence from species such as *C. elegans* indicates that it has not been retained in all metazoa. *D. melanogaster* contains one gene encoding PNUTS: *CG33526/dPNUTS*. Comparison of full-length PNUTS cDNA and genomic sequences shows that all four of d*PNUTS* intron/exon boundaries are shared with human *PNUTS* (hPNUTS; Figure S1), indicating that h*PNUTS* and d*PNUTS* are derived from a single ancestral gene. dPNUTS encodes two protein isoforms: dPNUTS and dPNUTS-S, a truncated version containing only the N-terminal region of dPNUTS. There is extensive homology between dPNUTS and mammalian PNUTS in a number of protein domains (Figure S1).

dPNUTS is expressed in developing tissues and localises to transcriptionally active sites on interphase chromosomes

PNUTS has been identified in all mammalian tissues so far examined [22,23], but the highest level of expression is reported to be in testis, brain, and intestine. *In situ* hybridisation revealed that *dPNUTS* transcripts are maternally provided and are uniformly distributed in most tissues during *Drosophila* embryogenesis. However, strikingly, there was stronger staining in the developing gut and in the nervous system during phases of rapid development (Figure 1A). To determine the subcellular distribution of dPNUTS, we generated transgenic fly lines capable of expressing epitope-tagged dPNUTS under UAS-GAL4 control. Ectopic dPNUTS shows a similar subcellular localisation to mammalian PNUTS: dPNUTS is nuclear and associates with chromatin during interphase when ectopically expressed in the wing disc, but is excluded from condensed chromosomes at metaphase (Figure 1B). In polytene nuclei, ectopic dPNUTS was visible in both the nucleoplasm and on polytene chromosomes as revealed by co-staining the DNA with Hoechst (Figure 1C,D). Strong Hoechst staining is associated with condensed chromosomal bands, which contain a high concentration of DNA, whilst weak, or no Hoechst signal is detected in interband regions of less tightly packed chromatin, which are thought to contain actively transcribed genes. dPNUTS is predominantly associated with regions of less condensed DNA corresponding to interbands that stain weakly with Hoechst (Figure 1D).

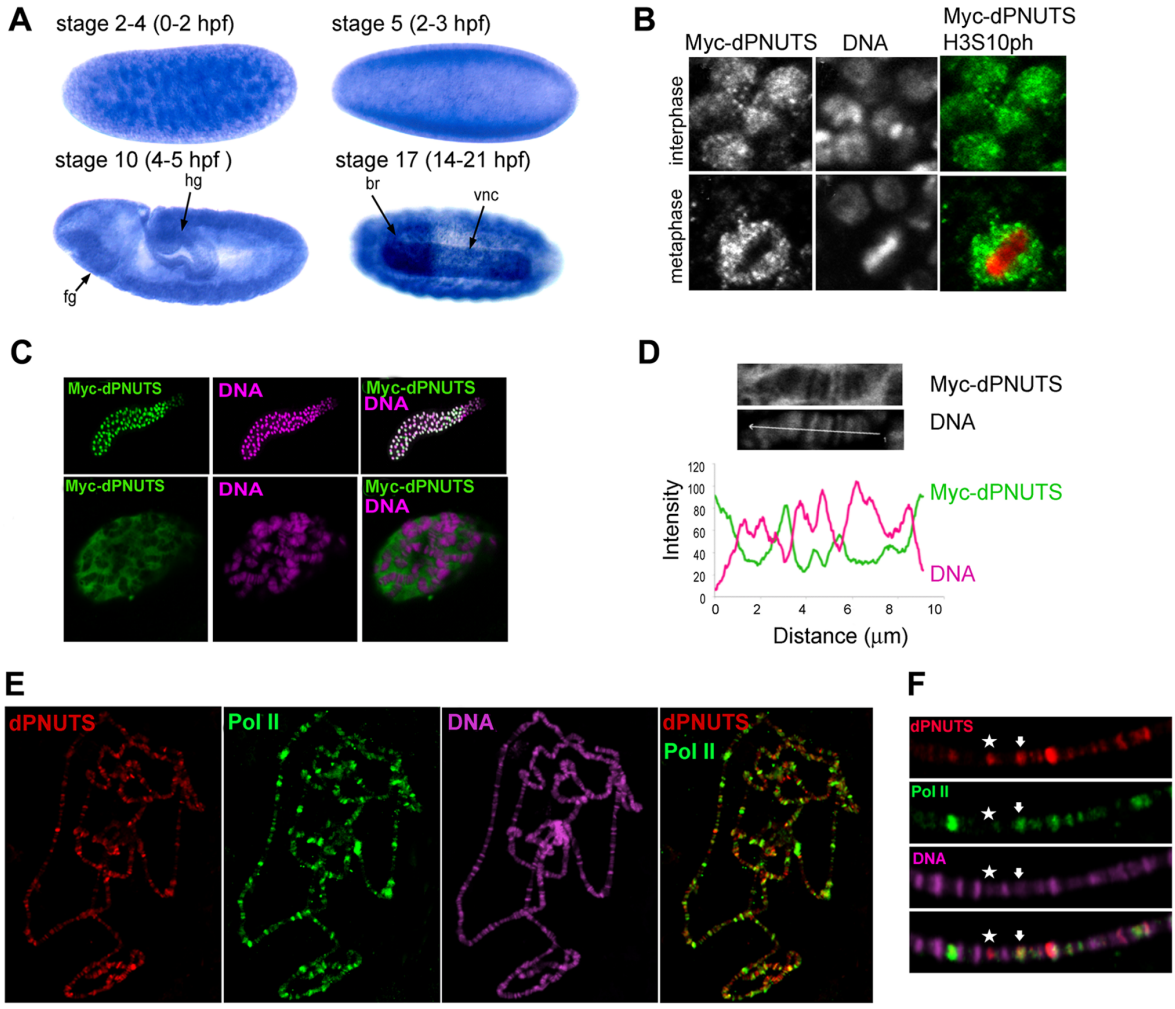

Figure 1. dPNUTS is a nuclear protein that colocalises with transcriptionally active RNAPII on salivary gland polytene chromosomes. A) Distribution of *dPNUTS* transcripts detected by RNA *in situ* hybridization; *dPNUTS* transcripts are maternally provided (top left) and are ubiquitously distributed in embryos at cellularisation (top right). At gastrulation, d*PNUTS* mRNA levels are enriched in the germband and in the fore- and hind-gut (fg and hg, respectively). Later, d*PNUTS* is highly expressed in the brain (br) and ventral nerve cord (vnc). Embryonic stage and approximate age, hours post fertilization (hpf), are indicated. B) 3rd instar wing discs stained to reveal the distribution of ectopically expressed Myc-tagged dPNUTS (green in merge), Histone H3S10ph (red in merge, marking mitotic nuclei) and DNA. C) Images of whole mount salivary gland and magnified images of an individual nucleus (below), stained to show the localization of Myc-tagged dPNUTS (green in merge) and DNA (magenta in merge). D) Line scans of images in C) reveal that Myc-tagged dPNUTS is localised to interbands that stain weakly for DNA. Fluorescence intensity of anti-Myc antibody and TOPRO-3 staining was measured along a line through the indicated chromosomal region in the images shown. The profile plot below shows that the peaks of Myc-PNUTS and DNA of staining do not overlap. E) Polytene chromosomes from salivary gland squashes showing that dPNUTS localises to a number of discrete bands that are broadly distributed. F) Merging of the green signal representing dPNUTS with the red signal representing RNAPII Ser2-P (H5) identifies sites where these two proteins co-localize (example indicated with arrow). The relative signals of dPNUTS and RNAPII Ser2-P vary between sites, but the majority dPNUTS loci colocalize with RNAPII Ser2-P staining (star indicates example where only dPNUTS staining is visible).
doi:10.1371/journal.pgen.1003885.g001

To examine the chromosomal association of dPNUTS further, we generated antibodies specific to dPNUTS and used them to stain polytene chromosomes from 3rd instar larval salivary glands. Although the dPNUTS antibodies worked well on polytene squash preparations we were unable to obtain a reliable signal from whole tissue mount preparations. We found that dPNUTS is localised at a large number of discrete sites of varying strength along all the chromosomes. To confirm the specificity of the dPNUTS antiserum on polytene squashes, we knocked down *dPNUTS* levels in salivary glands using heritable double-stranded RNA interference (RNAi). Flies carrying an inverted repeat (^{IR}) construct under UAS control were crossed to a salivary gland GAL4 source to induce expression of intron-spliced hairpin dsRNA for *dPNUTS* in the progeny. In squash preparations from relatively normal looking glands expressing *UAS-dPNUTS*^{IR} we found greatly reduced dPNUTS staining (Figure S2). To explore the possibility that dPNUTS may be associated with transcriptionally active sites, we performed double labelling experiments with antibodies against

the active form of RNA polymerase II (RNAPII). We found that the relative levels of dPNUTS and RNAPII vary at many sites, but, on close inspection, it is clear that the dPNUTS antibody marks a large number of transcriptionally active sites containing active RNAPII (H5 antibody, detecting RNAPII Ser2-P) (Figure 1E, F), suggesting that *dPNUTS* might have a role in transcriptional regulation.

dPNUTS loss of function results in larval growth arrest and defective tissue development

To determine the *in vivo* role of *Drosophila PNUTS*, we generated two deletion alleles, $dPNUTS^{9B}$ and $dPNUTS^{13B}$, by imprecise excision of a *P* element transposon ($P[SUPor\text{-}P]\ dPNUTS^{KG00572}$, referred to as $dPNUTS^{KG572}$ hereafter). Molecular analysis revealed that virtually all of the fourth coding exon of *dPNUTS* is deleted in $dPNUTS^{9B}$, and the entire coding region, including the translation start site, is deleted in $dPNUTS^{13B}$ (Figure 2A). Consistent with these findings, quantitative RT-PCR analyses revealed the absence or almost complete loss of *dPNUTS* transcripts in $dPNUTS^{9B}$ and $dPNUTS^{13B}$ homozygotes. *dPNUTS* levels were also greatly reduced in $dPNUTS^{KG572}$ homozygotes compared to revertant controls ($dPNUTS^{exKG}$) in which the *P* element had been precisely excised (Figure 2B). $dPNUTS^{9B}$ and $dPNUTS^{13B}$ are recessive lethal in combination with each other and over *Df(2L)ast4*, a deficiency that removes the *dPNUTS* gene. The phenotype of $dPNUTS^{9B}$ and $dPNUTS^{13B}$ homozygotes was indistinguishable from that of $dPNUTS^{9B}$ or $dPNUTS^{13B}/Df(2L)ast4$ hemizygotes, so we conclude that the excision alleles have little or no residual *dPNUTS* function. To confirm that disruption of the *dPNUTS* transcription unit is responsible for the larval lethality, we generated transgenic flies carrying a genomic fragment containing the entire *PNUTS* locus. A single copy of the transgenic construct was capable of fully rescuing the homozygous lethality of $dPNUTS^{9B}$ and $dPNUTS^{13B}$ mutants (Table S1).

To examine the lethal phase of *dPNUTS* mutants we combined the mutant alleles with a GFP-balancer chromosome and examined the development of mutant (non-GFP) larvae alongside their heterozygous (GFP marked) siblings. Homozygous $dPNUTS^{9B}$ and $dPNUTS^{13B}$ animals developed to 1st instar larvae but died in the ensuing 8 days without further growth and development (Figure 2C, D). To further assess the requirement for *dPNUTS* in tissue development we made use of the *ey-FLP* system to produce genetically mosaic flies that are otherwise heterozygous but in which the eye is composed exclusively of cells homozygous mutant for *dPNUTS*. Cells that are not derived from the homozygous mutant cells are eliminated by eye-specific expression of the pro-apoptotic gene *hid* [39]. Eyes of heterozygous $dPNUTS^{KG572}$, $dPNUTS^{9B}$ and $dPNUTS^{13B}$ flies resembled wild type. Flies with eyes homozygous for $dPNUTS^{KG572}$ were modestly reduced in size, with fewer and poorly organised ommatidia. Eyes homozygous for either $dPNUTS^{9B}$ or $dPNUTS^{13B}$ showed a more severe effect, indicating that cells lacking *dPNUTS* are incapable of developing into adult eyes (Figure 2E).

dPNUTS mutant cells fail to compete with wild type cells and are removed from developing epithelia

To understand more about the cellular role of *dPNUTS*, we generated clones of homozygous null *dPNUTS* mutant cells in otherwise *dPNUTS* heterozygous wing imaginal discs during early or mid-larval development using *Flp/FRT*-mediated recombination [40] and analysed them at the wandering 3rd instar larval stage. To do this we used a heat shock inducible Flipase (Flp) enzyme to induce mitotic recombination between two FRT chromatids, one of which carried a mutant *dPNUTS* allele and the other which expressed a GFP marker. Mitotic recombination events produce a GFP-negative cell clone that are homozygous for the mutant allele, together with a "twin-spot" marked by the presence of two copies of GFP. Surrounding heterozygous tissue is labelled with one copy of GFP. We failed to recover homozygous mutant cells when clones were induced in early 1st instar larvae, whereas wild type cells induced at the same stage proliferated to generate large clonal patches (Figure 3A, B). When we shortened the time between clone induction and analysis by inducing clones later on in 2nd instar larvae, we were able to observe very small patches of *dPNUTS* mutant cells (Figure 3C, D). However, in optical cross sections through the tissue it was apparent that mutant cells accumulated at the basal face of the epithelium and stained positive for cleaved caspase antibody (Figure 3E–J), indicating that *dPNUTS* mutant cells were undergoing cell death. This prompted us to examine whether clones were dying due to cell competition, a process in which slow-growing cells are eliminated by their faster-growing neighbours. To test this, we gave the *dPNUTS* mutant cells a growth advantage by generating them in tissues that were heterozygous for a dominant *Minute* (*M*) allele of *RpL27A*. Notably, under conditions in which *dPNUTS* mutant clones in a wild-type background are normally eliminated, we recovered *dPNUTS* clones in *M*/+ discs (Figure 3K, L and Figure S3) and mutant clones spanned the entire wing disc epithelium indicating they were not being eliminated (Figure 3Q, R and Figure S3). However, mutant clones colonised a significantly smaller area of *M*/+ discs compared with wild-type clones, indicating that they were still growth impaired (compare Figure 3K and 3L).

dPNUTS mutants deregulate the expression of the majority of genes in 1st instar larvae

To obtain an insight into the molecular basis for the growth defects in *dPNUTS* mutants and assess the impact of *dPNUTS* loss of function on gene expression, we analysed the transcriptomic signature of $dPNUTS^{9B}$ and $dPNUTS^{13B}$ mutant larvae by RNA-Seq. The control for these experiments was an isogenic strain that carried the same background mutation (w^{1118}) as the *dPNUTS* mutant strains. Homozygous $dPNUTS^{9B}$ and $dPNUTS^{13B}$ mutant 1st instar larvae had widespread changes in gene expression compared to control animals of the same stage (Figure 4A), with a comparable pattern of genes being affected in both mutants (Figure S4). In total, approximately 30% of genes (2819/9483) previously reported to be expressed in 1st instar larvae [40] were underexpressed, and a similar proportion (2850/9483) were overexpressed >1.5-fold in both $dPNUTS^{9B}$ and $dPNUTS^{13B}$ mutant animals relative to control larvae. Therefore, we conclude that disruption of *dPNUTS* function affects the expression of the majority of genes in developing 1st instar larvae.

To assess whether there was any enrichment of genes belonging to functionally-related biological processes, we analysed the distribution of Gene Ontology (GO) terms amongst differentially expressed genes. When compared to the frequency of GO terms amongst all genes encoded by the genome, we observed significant ($P \leq 10^{-4}$) enrichment of terms for cell death and stress responses amongst genes overexpressed in *dPNUTS* mutants (Figure S5, Table S2). Overexpression of these groups of genes might indicate that the animals are under stress and is consistent with their poor survival. The most significantly enriched GO terms amongst the underexpressed genes in *dPNUTS* mutants, were terms for cellular metabolic processes that drive proliferative growth, including ribosome biogenesis, rRNA processing, translation and metabolism of energy sources

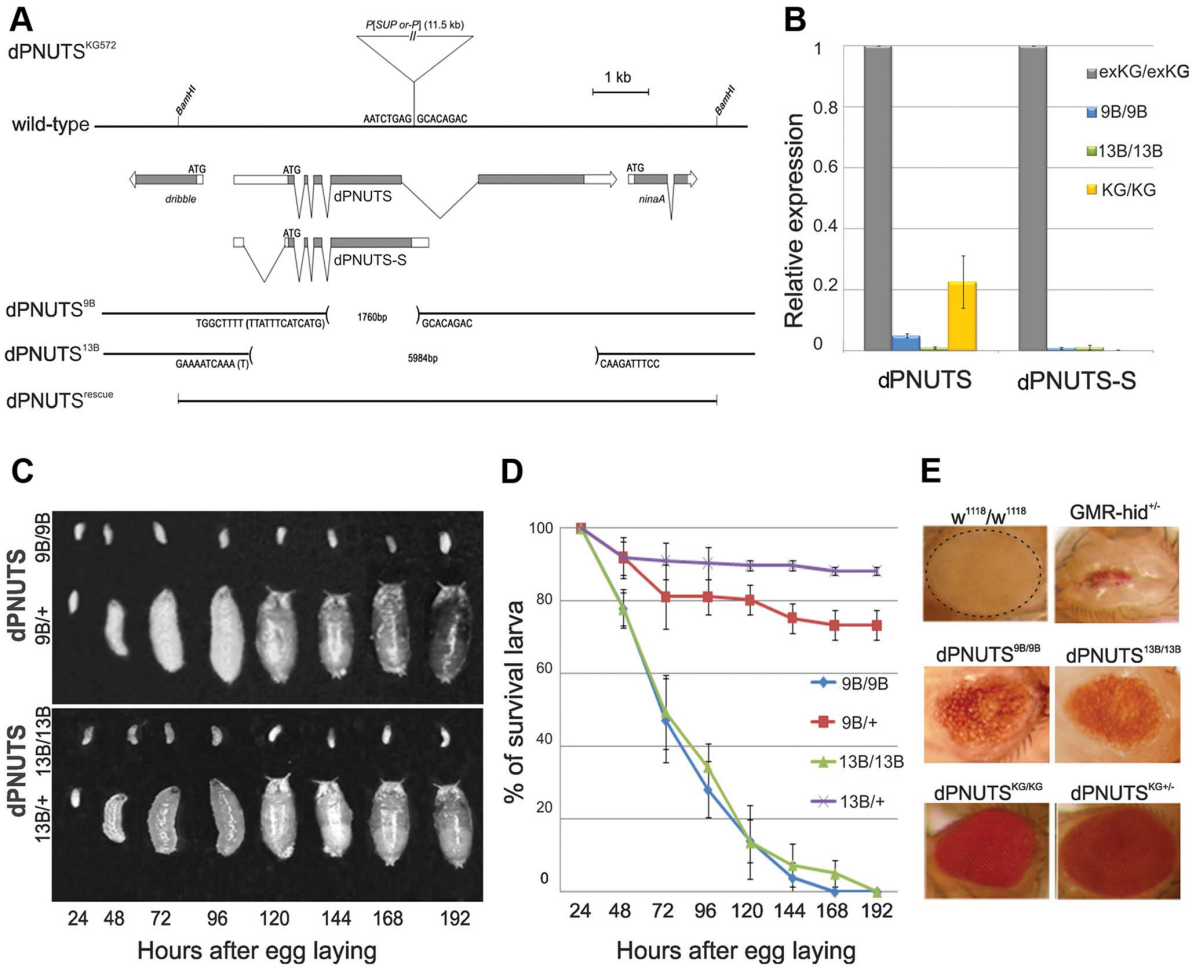

Figure 2. *dPNUTS* loss of function results in larval growth arrest and defective tissue development. A) Genomic region showing *dPNUTS* locus flanked by *dribble* and *ninaA*. Coding regions of the genes is represented by shading. *dPNUTS* produces two transcripts *dPNUTS* and *dPNUTS-S*. *ninaA* is a non-essential gene that is expressed solely in the eye to regulate rhodopsin synthesis [75,76]. *dPNUTS*^{KG572} contains a *P* element insertion in an untranslated region of *dPNUTS*. The extent of deletions in *dPNUTS*^{9B} and *dPNUTS*^{13B} resulting from imprecise excision of this element is indicated, together with the genomic sequence of the breakpoints. The *dPNUTS* genomic rescue construct, which contains the coding region of *ninaA*, and the 5′ end of *dribble*, is indicated. B) Levels of *dPNUTS* and *dPNUTS-S* transcripts produced in homozygous *dPNUTS*^{exKG}, *dPNUTS*^{KG572}, *dPNUTS*^{9B} and *dPNUTS*^{13B} larvae, as determined by qRT-PCR. *dPNUTSe*^{exKG} is a revertant strain in which the *P* element had precisely excised. C) Images of homozygous mutant and control (heterozygous sibling) larvae at different time points after egg laying as indicated. D) Graph showing percentage of surviving larvae over time for each genotype, as indicated. E) Images of adult female eyes. Homozygous *dPNUTS* mutant eyes are smaller than controls (isogenic *w*^{1118} strain), but are able to form some facets, unlike eyes expressing the proapototic gene *hid* under *GMR* control.
doi:10.1371/journal.pgen.1003885.g002

(Figure S5, Table S2). We observed a similar pattern of GO enrichment when comparing differentially expressed genes in the *dPNUTS* mutants to genes expressed in our developmentally matched control (Table S3). These patterns of transcriptional change are consistent with the larval growth defect exhibited by the *dPNUTS* mutants. In addition, Ingenuity analysis identified a number of different transcriptional networks involved in organismal growth that are likely to be affected by loss of *dPNUTS* (Table S4).

While these analyses provide biological insight into the likely processes underpinning the *dPNUTS* mutant phenotype, it is important to note that the enrichment of biologically-relevant GO categories is correlated with the expression level of the representative genes in 1st instar larvae (Figure 4A). Indeed, GO categories pertaining to cellular metabolism are also enriched amongst highly expressed genes in the control (median expression level >$(\log_2)$2.9 FPKM; data not shown). Taken together with the widespread effects on transcript abundance, these data indicate that *dPNUTS* globally affects gene expression and in 1st instar larvae is required to promote expression of highly expressed genes that support developmental growth.

To confirm the RNA-Seq results, we selected genes representative of enriched GO categories for quantitative real-time qRT-PCR analysis. Measurements of relative mRNA expression level determined by qRT-PCR were consistent with our RNA-Seq data (Figure 4B, Table S5).

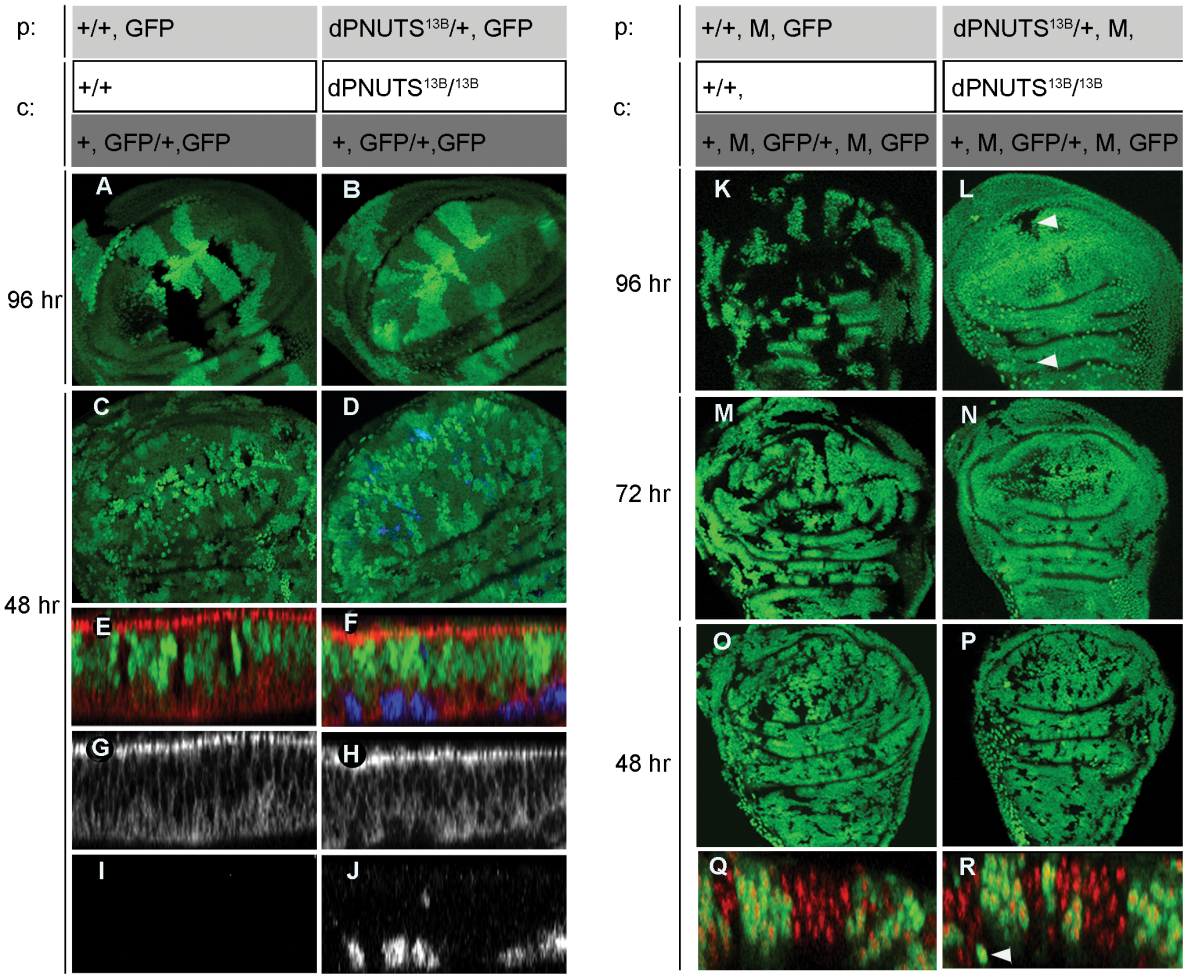

Figure 3. *dPNUTS* mutant clones reveal a cell autonomous growth defect in developing tissues. Clones (marked by absence of GFP) of either wild-type or *dPNUTS*^{13B} mutant cells are shown in wing imaginal discs obtained from 3rd instar larvae. Clones were induced in a wild type (A–J) or *Minute* (*M*) mutant background (K–R) 48 hr, 72 hr or 96 hr prior to dissection, as indicated. The parental (p) genotypes are indicated, along with the genotype of clones (c) generated by FLP-mediated mitotic recombination and are coded with grayscale to indicate the relative level of GFP expression. A–J, wing discs were stained for activated caspase shown in blue, and in cross sections (E–J), apico-lateral junctions are marked by discs-large staining in red; GFP is shown in green. In cross sections Q–R, DNA is shown in red. Arrowheads in panel L indicate the presence of *dPNUTS*^{13B} GFP-negative clones in a *Minute* (*M*) mutant background. +, *M*, GFP/+, *M*, GFP twinspot clones, indicated by arrowhead in panel R, were almost never observed because of a severe growth defect.
doi:10.1371/journal.pgen.1003885.g003

dPNUTS binds to and colocalises with PP1 on chromosomes

dPNUTS was originally isolated from a two-hybrid screen for putative PP1-binding proteins and contains a canonical PP1-binding motif - K/R, (x), V/I/L, x, F/W that in PNUTS/p99 is necessary for binding to, and inhibition of, PP1 [23,41]. This motif (residues 722–726) is also contained within all the *dPNUTS* two-hybrid clones, including the shortest interacting fragment encoding residues 608 to 1135 [42], (Figure 5A). When we retested binding in the two-hybrid system with full-length proteins, dPNUTS, but not dPNUTS-S, interacted strongly with all four *D. melanogaster* PP1 isoforms (Figure 5B), consistent with a role for this motif in binding PP1. To determine the importance of the putative PP1-binding motif for interaction with PP1, we compared binding of endogenous PP1, to ectopically expressed wild type dPNUTS (dPNUTS^{WT}) and a mutant form in which Trp726 was replaced with Ala (dPNUTS^{W726A}). Immunoprecipitation with antibodies against Myc-tagged dPNUTS, followed by immunoblotting with antibodies against PP1, showed that PP1 co-precipitated very efficiently with dPNUTS^{WT} but not dPNUTS^{W726A} (Figure 5C), indicating that Trp726 is crucial for interaction with PP1.

To further explore the association between PP1 and dPNUTS *in vivo*, we examined the distribution of dPNUTS and PP1 on polytene chromosomes from 3rd instar larvae. We previously reported that ectopic HA-tagged PP187B, the major PP1 isoform in *Drosophila* [43], localised to many discrete chromosomal loci [17,18]. Like the ectopic protein, we found a large number of

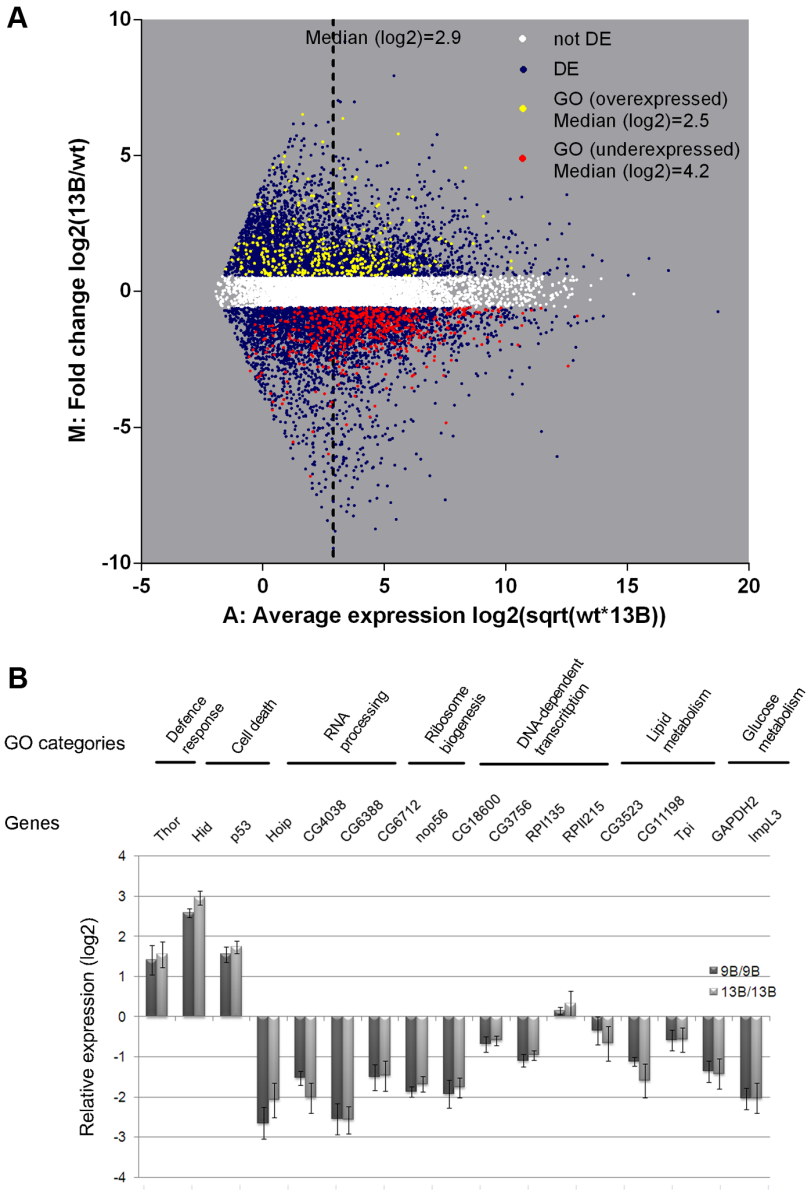

Figure 4. *dPNUTS* mutants deregulate the expression of the majority of genes in 1st instar larvae, including highly expressed genes involved in cellular metabolism and proliferative growth. A) MA plot of RNA-Seq data in which the $\log_2$ of the ratio of abundance of each transcript between *dPNUTS*^{13B} (13B) mutant and *w*^{1118} (WT) control (M) is plotted against the $\log_2$ geometric average of abundance (FPKM) in both conditions (A). Transcripts with an FPKM of less than 0.25, which are a source of noise in these plots, are not shown for clarity. Transcripts that are differentially expressed (DE) by <0.67 or >1.5 fold are shown in grey; unaffected transcripts are shown in white. Loci corresponding to enriched Gene Ontology (GO) terms amongst the differentially expressed genes relative to the entire genome are highlighted in yellow (enriched amongst overexpressed genes) or red (enriched amongst underexpressed genes). Log_2 median expression for genes expressed in WT and 13B is indicated with a dashed line. Log_2 median expression for genes belonging to GO categories is given in the legend. A complete list of GO categories is provided in the Supplementary information. B) Expression levels of the indicated genes in *dPNUTS*^{9B}/*dPNUTS*^{9B} and *dPNUTS*^{13B}/*dPNUTS*^{13B} mutant larvae, relative to control (*w*^{1118}) larvae, determined by qRT-PCR. Error bars represent the SE ($n \geq 3$ biological replicates). The GO categories to which the genes belong are shown at the top.
doi:10.1371/journal.pgen.1003885.g004

discrete sites widely dispersed along the chromosomes that were stained with an anti-peptide antibody to *Drosophila* PP1 (Figure 5D). When we co-stained for dPNUTS, we found that most sites staining for dPNUTS also stained strongly for PP1 although the relative staining varied greatly (Figure 5D).

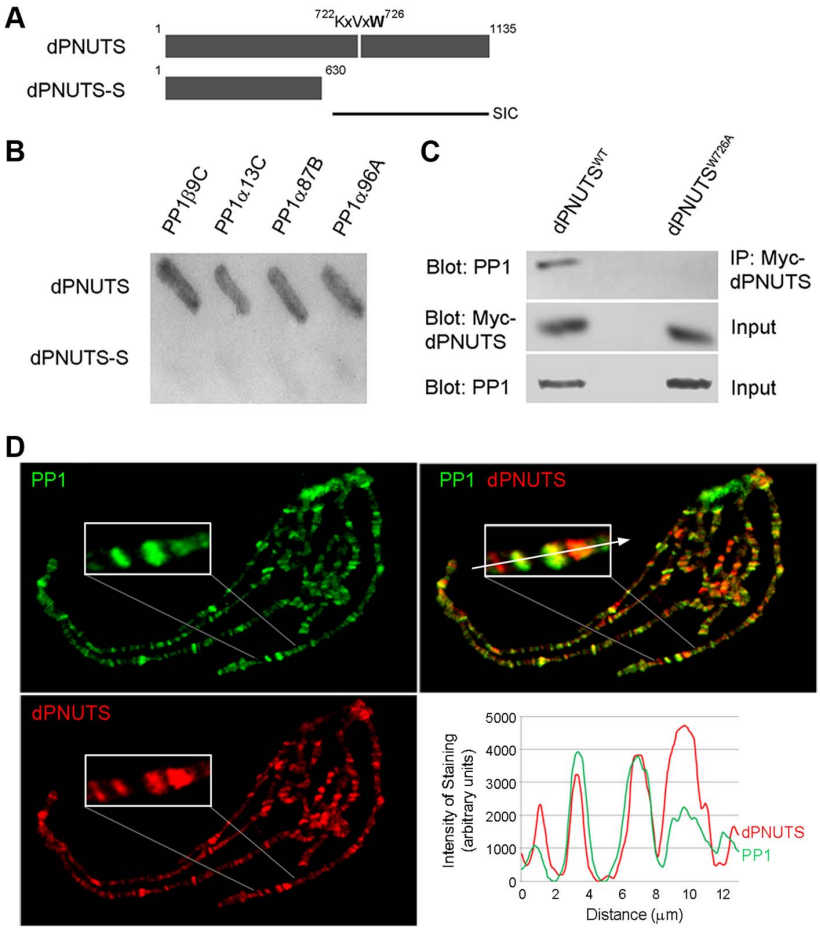

Figure 5. dPNUTS binds to and co-localises with PP1 on chromosomes. A) Predicted domain structure of dPNUTS and dPNUTS-S proteins, indicating the position of the putative PP1-binding motif (residues 722–726), which is located in the shortest yeast two-hybrid interacting clone (SIC) of dPNUTS. B) Beta-galactosidase assays showing binding of dPNUTS but not dPNUTS-S to all four *D. melanogaster* PP1 isoforms in the yeast two-hybrid system. C) dPNUTS^{WT}, but not dPNUTS^{W726A}, co-precipitates PP1 from nuclear extracts from adult flies. *da-GAL4 UAS-HM-dPNUTS^{WT}* and *da-GAL4 UAS-HM-dPNUTS^{W726A}* fly extracts were subjected to immunoprecipitation (IP) with Myc antibodies followed by immunoblotting with PP1 antibodies. Blots of total lysates confirmed levels of HM-tagged dPNUTS and PP1. D) dPNUTS and PP1 colocalise at many sites on polytene chromosomes. Inset is an enlarged view of the end of the X chromosome where this is clearly visible. Plot of fluorescence intensity of anti-PP1 and dPNUTS antibody staining, measured along a line through the indicated chromosomal region, reveal the degree of colocalisation between PP1 and dPNUTS.
doi:10.1371/journal.pgen.1003885.g005

dPNUTS recruits PP1 to chromosomes

Since salivary glands from 1st instar *dPNUTS* mutant larvae were too small to analyse in squash preparations, we were unable to test whether loss of *dPNUTS* function displaces PP1 from chromosomes. Therefore, to examine whether PP1 is dependent on dPNUTS for its localisation or *vice versa*, we utilised our transgenic overexpression construct *dPNUTS^{W726A}*, which exhibits reduced binding to PP1. We reasoned that if PP1 is necessary for dPNUTS localisation we would expect to observe loss of dPNUTS^{W726A} from chromosomes; conversely, if dPNUTS is responsible for recruiting PP1 then overexpressed dPNUTS^{W726A} should stoichiometrically compete with endogenous PNUTS-PP1 complexes for binding to chromosomes resulting in the displacement of PP1. Chromosomal PP1 staining, but not total PP1 levels, was reduced in glands overexpressing *dPNUTS^{W726A}* compared to those expressing *dPNUTS^{WT}* (Figure 6A). To quantify the effect on PP1 localisation, we performed line scans to measure fluorescence intensity at a readily identifiable site on the X chromosome, where endogenous PP1 and dPNUTS co-localise (Figure 5D). Intensity of PP1 staining at this site on chromosomes from animals overexpressing *dPNUTS^{W726A}* was on average reduced 0.6 fold (Figure 6B). Taken together, these data suggest that *dPNUTS* is responsible for targeting PP1 to many distinct chromosomal loci. Anti-Myc staining of ectopically expressed Myc-tagged dPNUTS was of relatively poor quality but, in general there was a comparable distribution of *dPNUTS^{W726A}* and *dPNUTS^{WT}* in squash preparations (Figure 6C). Levels of *dPNUTS^{W726A}* sometimes appeared weaker than *dPNUTS^{WT}* but this is accounted for by differences in the quality of squash preparations and a lower expression level of *dPNUTS^{W726A}* relative to *dPNUTS^{WT}*, as revealed by immunoblot-

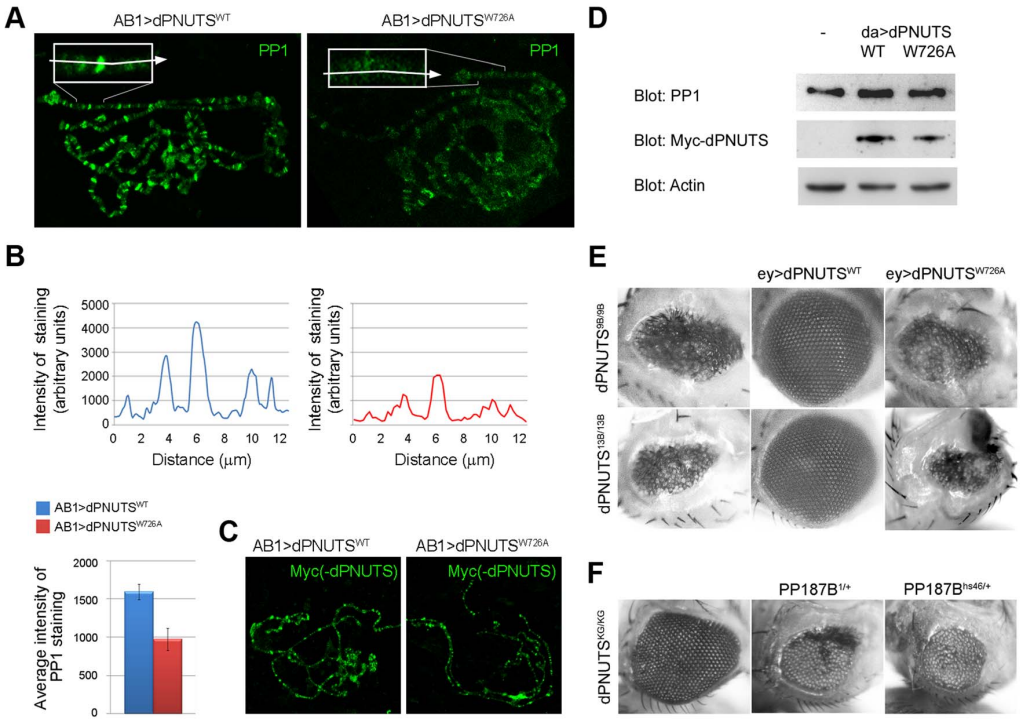

Figure 6. PP1 localisation is regulated by dPNUTS and binding to PP1 is important for dPNUTS function. A) Images of polytene chromosome squashes from salivary glands expressing either *dPNUTS*^{WT} or *dPNUTS*^{W726A} stained with PP1 (in green). Inset are enlarged views of the distal end of the X chromosome. Arrows indicate approximate lines along which quantitation of fluorescence (see B) was performed. B) Plots of line scans through the chromosomal region indicated in A, showing levels of PP1 staining in salivary glands expressing either *dPNUTS*^{WT} or *dPNUTS*^{W726A}. Bar graphs represent the average fluorescence in this region from 6 independent images/genotype. Genotypes are indicated by the colour key. C) Levels and distribution of Myc-dPNUTS on polytene chromosome squashes from salivary glands expressing either *dPNUTS*^{WT} or *dPNUTS*^{W726A}, as revealed by anti-Myc staining (green). D) Western blots showing levels of PP1 and Myc-dPNUTS, relative to Actin, in extracts from animals ectopically expressing *dPNUTS*^{WT} or *dPNUTS*^{W726A} under the control of *da-GAL4* (da>*dPNUTS*^{WT} and da>*dPNUTS*^{W726A}, respectively) compared to w^{1118} control (−). E) Images of adult female eyes showing that the severely reduced eye phenotype of homozygous *dPNUTS* mutant eyes is fully rescued by ectopic expression of *dPNUTS*^{WT} but not *dPNUTS*^{W726A}. F) Homozygous *dPNUTS*^{KG572} mutant eyes show a weaker phenotype than either *dPNUTS*^{9B} or *dPNUTS*^{13B}, and this can be enhanced by loss of one copy of *PP187B*.
doi:10.1371/journal.pgen.1003885.g006

ting (Figure 6D). Taken together these data suggest that PP1 binding is not necessary for dPNUTS localization to polytene chromosomes.

PP1-binding is important for dPNUTS function in tissue development

To elucidate the functional significance of the interaction between PP1 and dPNUTS *in vivo*, we examined whether *dPNUTS*^{W726A} was capable of rescuing the reduced eye phenotype exhibited by our *dPNUTS* mutants. *dPNUTS*^{WT} rescued the effect of both *dPNUTS*^{9B} and *dPNUTS*^{13B}. However, ectopic overexpression of *dPNUTS*^{W726A} failed to rescue either mutant (Figure 6E), indicating that binding to PP1 is critical for *dPNUTS* function in tissue development. We also took another approach to examine the effect of reducing PP1 activity in *dPNUTS* mutant eyes. For this, we generated flies that were homozygous for *dPNUTS*^{KG572}, which resulted in a modest reduction in eye size, and also heterozygous for mutations in *PP187B* that reduce the total PP1 activity by approximately 40% [44]. Reduced eye phenotypes caused by *dPNUTS*^{KG572} mutants were dominantly enhanced by *PP187B*, consistent with *dPNUTS* acting as a positive regulator of PP1 function during imaginal disc development (Figure 6F).

dPNUTS is complexed with and regulates the phosphorylation state of RNA Polymerase II

RNAPII has recently been reported to co-precipitate PNUTS from mammalian cell extracts [37]. Given the widespread effects of *dPNUTS* mutations on transcription and its colocalisation with active RNAPII at many transcriptionally active sites on chromosomes, we wondered whether dPNUTS also physically associates with RNAPII complexes. To test this, we immunoprecipitated endogenous dPNUTS from wild type embryo extracts and examined precipitates for the presence of RNAPII. Two RNAPII species, representing unphosphorylated (RNAPIIa) and phosphorylated RNAPII (RNAPIIo), can be detected using an antibody (ARNA-3) that recognises a peptide mapping to central region of RNAPII. Both these forms precipitated with dPNUTS-S, but only RNAPIIA co-precipitated efficiently with dPNUTS (Figure 7A). Since PP1 was previously shown to be capable of dephosphorylating RNAPIIo *in vitro* [14], we wondered whether the pattern of binding we observed was because dPNUTS is capable of binding PP1 and dPNUTS-S is not. To test the role of PP1 in endogenous dPNUTS complexes, we repeated our immunoprecipitations in the presence of Inhibitor-2 (I-2), a specific inhibitor of PP1 [45]. There was no apparent difference in the abundance of RNAPIIa or RNAPIIo in dPNUTS-S precipitates. However, when we

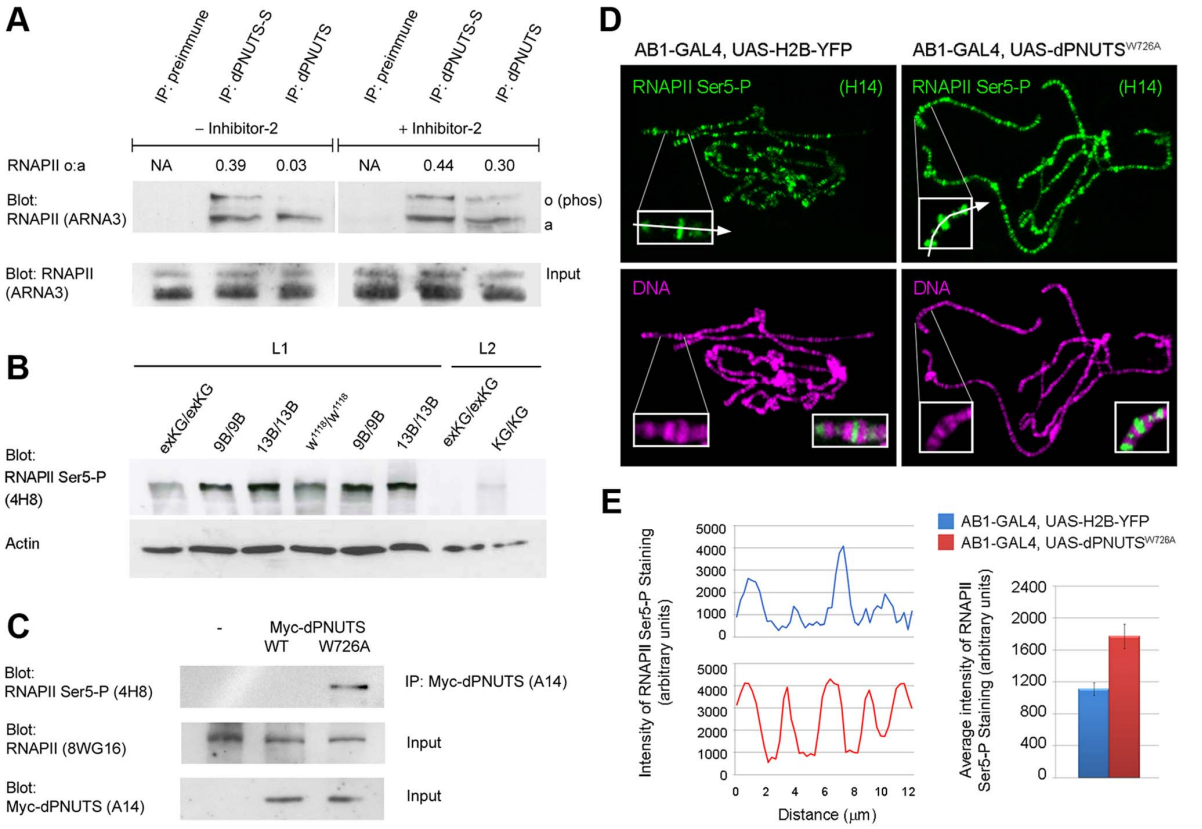

Figure 7. dPNUTS complexes with and regulates RNAPII phosphorylation. A) dPNUTS complexes contain RNAPII and PP1; inhibition of PP1 activity in dPNUTS complexes leads to hyperphosphorylation of RNAPII. dPNUTS-S and dPNUTS were immunoprecipitated (IP) from embryonic nuclear extracts and precipitates were probed with ARNA-3 anti-RNAPII antibody. Lane 1, neither hypo- or hyper-phosphorylated RNAPII (RNAPIIa and RNAPIIo respectively) precipitate with pre-immune serum; Lane 2, both RNAPIIa and RNAPIIo precipitate with dPNUTS-S; Lane 3, RNAPIIa, but almost no RNAPIIo, is detected in dPNUTS precipitates. Lane 4, pre-immune serum does not precipitate RNAPII; Lane 5, Inhibitor 2 does not affect the ability of RNAPIIa and RNAPIIo to associate with dPNUTS-S (compare Lane 2); Lane 6, inhibition of PP1 results in conversion of RNAPIIa to RNAPIIo in dPNUTS precipitates (compare Lane 3). Ratios of RNAPIIa and RNAPIIo levels, as derived from densitometry measurements of the respective bands, are shown above the blots. B) Western Blot showing levels of RNAPII CTD Ser5-P (4H8) in extracts from either 1st (L1) or 2nd (L2) instar larvae of the indicated genotypes: homozygous revertant $dPNUTS^{exKG}/dPNUTS^{exKG}$ (exKG/exKG); homozygous null mutant $dPNUTS^{9B}/dPNUTS^{9B}$ (9B/9B) or $dPNUTS^{13B}/dPNUTS^{13B}$ (13B/13B); isogenic control strain w^{1118}/w^{1118}; homozygous hypomorphic mutant $dPNUTS^{KG572}/dPNUTS^{KG572}$ (KG/KG). 1st instar larval samples from $dPNUTS^{9B/9B}$ and $dPNUTS^{13B/13B}$ were independent extracts run in parallel on the same gel. Blot with anti-Actin antibody shows relative loading. C) Precipitation of RNAPII Ser5-P with $dPNUTS^{W726A}$ but not $dPNUTS^{WT}$. dPNUTS complexes from *Drosophila* embryonic nuclear extracts expressing Myc-tagged $dPNUTS^{WT}$ or $dPNUTS^{W726A}$ under the control of *da-GAL4* were isolated by immunoprecipitation with anti-Myc antibody. Control precipitations were performed on w^{1118} extracts (−). This was followed by immunoblotting with anti-RNAPII CTD Ser5-P (4H8) antibody to test for co-immunoprecipitation. Lower panels show immunoblot analyses of total lysates, confirming the levels of total RNAPII and Myc-dPNUTS. D) Levels of RNAPII CTD Ser5-P (H14) on polytene chromosome squashes from salivary glands expressing either histone-H2B YFP or Myc-$dPNUTS^{W726A}$ prepared on the same slide to ensure identical staining conditions (H14 staining in green; DNA staining in magenta). Insets are enlarged views of the distal end of the X chromosome. Arrows indicate approximate lines along which quantitation of fluorescence (in E) was performed. E) Representative line scans through the regions illustrated in D, showing levels of RNAPII CTD Ser5-P staining in the two genotypes. Bar graphs represent the average fluorescence in this region from 6 independent images/genotype. Genotypes are indicated by the colour key.
doi:10.1371/journal.pgen.1003885.g007

precipitated dPNUTS in the presence of I-2, we found reduced levels of RNAPIIa and elevated levels of RNAPIIo (Figure 7A). I-2 selectively targets PP1 over PP2A, which is the next most closely related member of the PPP family of phosphatases [46]. Therefore, we conclude that PP1 is likely to be the major RNAPII phosphatase in these complexes.

Mammalian PNUTS has been reported to bind to Wdr82, which targets RNAPII phosphorylated on Ser5 of its CTD repeats (RNAPII CTD Ser5-P). Although the degree of functional conservation between mammalian and *Drosophila* Wdr82 (dWdr82) has not yet been fully determined, we found that dWdr82 co-precipitated with dPNUTS from *Drosophila* cell extracts indicating that the ability of Wdr82 to bind PNUTS is shared between fly and human orthologues (Figure S6A). This prompted us to assess the effect of *dPNUTS* loss of function on the levels of RNAPII CTD Ser5-P. Using an antibody (4H8) that recognizes the Ser5-phosphorylated C-terminal domain [47], we observed elevated levels of RNAPII CTD Ser5-P in total extracts from *dPNUTS* mutant larval extracts by Western Blotting compared to wild type (w^{1118}) or revertant ($dPNUTS^{exKG}/dPNUTS^{exKG}$) controls (Figure 7B). Using a panel of independent anti-phospho CTD antibodies [48,49] we further confirmed the effect of *dPNUTS* loss

of function on RNAPII CTD Ser5-P levels. We also observed a modest increase in levels of RNAPII CTD Ser2-P but little or no change in levels of RNAPII CTD Thr4-P or Ser7-P, in mutant extracts (Figure S6B). To test whether *dPNUTS* regulates RNAPII phosphorylation on chromosomes, we generated mutant clones in the salivary gland and examined RNAPII phosphorylation on polytene chromosomes in whole mount preparations. Levels of RNAPII CTD Ser5-P, as detected with an antibody (H14), which recognizes RNAPII Ser5-P in the context of Ser2 phosphorylation [48], were also elevated in this context (data not shown). Interestingly, on wild type polytene chromosome squashes, we observed relatively little co-localisation between dPNUTS and RNAPII Ser5-P (H14) (Figure S7), suggesting that the presence of dPNUTS at chromosomal loci is associated with a reduction of Ser5 phosphorylation at these sites. To confirm the role of dPNUTS-bound PP1, we expressed Myc-tagged $dPNUTS^{WT}$ and $dPNUTS^{W726A}$ in embryos, and tested their ability to bind to RNAPII CTD Ser5-P. Immunoprecipitation with anti-Myc antibodies, followed by immunoblotting with anti-RNAPII CTD Ser5-P (4H8) antibody, revealed that RNAPII CTD Ser5-P was only recovered in Myc-$dPNUTS^{W726A}$ and not Myc-$dPNUTS^{WT}$ precipitates (Figure 7C), further indicating that dPNUTS-bound PP1 dephosphorylates RNAPII Ser5-P.

Disruption of PP1-binding results in elevated RNAPII CTD Ser5-P at chromosomal loci

To further test the role of PP1-bound dPNUTS, we examined the effect of ectopic $dPNUTS^{W726A}$ on RNAPII phosphorylation on polytene chromosome spreads. Since $dPNUTS^{W726A}$ shows reduced binding to PP1, we predicted that ectopic expression of this mutant form would compete with endogenous PNUTS-PP1 complexes and thereby reduce RNAPII dephosphorylation by PP1. Correspondingly, we found that levels of RNAPII CTD Ser5-P appeared modestly elevated on chromosomes from glands overexpressing $dPNUTS^{W726A}$ (Figure 7D). To quantitate this effect, we compared the levels of RNAPII CTD Ser5-P staining on chromosomes from larvae with or without ectopic $dPNUTS^{W726A}$. Since RNAPII CTD Ser5-P staining was variable from slide to slide, chromosomes from animals over-expressing $dPNUTS^{W726A}$ were prepared alongside control samples labelled with histone-H2B YFP and stained on the same slides to ensure identical staining conditions between the two samples. Line scans and measurements of average signal intensity at a site at which $dPNUTS^{W726A}$ displaces endogenous PP1 (Figure 6A,B), indicated an average increase of 1.59 fold in RNAPII Ser5-P on chromosomes from larvae ectopically expressing $dPNUTS^{W726A}$ compared to wild type animals (Figure 7E). Ectopic $dPNUTS^{WT}$ on average had no effect on RNAPII Ser5-P staining relative to histone-H2B YFP labeled chromosomes (data not shown). Together, these results indicate that the dPNUTS-PP1 holoenzyme associates with RNAPII and regulates the dephosphorylation of its C-Terminal Domain.

Misregulation of gene expression, but not RNAPII distribution, is a consequence of disrupting dPNUTS-PP1 binding

Relatively little is known about the effect of RNAPII Ser5 hyperphosphorylation on gene expression, but it has been associated with decreased elongation rate or pausing of RNAPII when it occurs on the body of genes [50,51]. To assess whether effects on RNAPII occupancy might result from disrupting dPNUTS binding to PP1, we examined the effect of ectopic $dPNUTS^{W726A}$ on gene expression and the distribution of RNAPII at specific gene loci. Overexpression of $dPNUTS^{W726A}$ in 3rd instar larvae using *da-GAL4* (*da>*$dPNUTS^{W726A}$) had a similar, but weaker, effect on gene expression to that of *dPNUTS* loss-of-function in 1st instar larvae (Figure S8A). This might be because the transgenic line of $dPNUTS^{W726A}$ that we used had only a weak dominant-negative effect (animals expressing this construct were viable with *da-GAL4*) and/or because the regulation of some target loci is different at this later developmental stage. Amongst the genes we examined, *ImpL3*, *nop56* and *ACC* were underexpressed, whereas the stress response gene *Thor* was overexpressed in response to ectopic $dPNUTS^{W726A}$. Next, we examined the distribution of RNAPII at selected loci by Chromatin Immunoprecipitation (ChIP). For these experiments, chromatin was extracted from *da>*$dPNUTS^{W726A}$ or control larvae and precipitated with either mouse IgG or anti-total RNAPII antibody (8WG16). We determined the abundance of precipitated chromatin by qPCR with gene specific primers. Control precipitations with mouse IgG showed a low level of non-specific background in all of these experiments (Figure S8B–E). When we analysed the distribution of RNAPII at selected loci, we did not observe a significant change in the occupancy of total RNAPII at the 5′ ends or coding regions of genes in *da>*$dPNUTS^{W726A}$ samples. Together, these results provide evidence of the link between the disruption of PP1 binding to dPNUTS and the misregulation of RNAPII-mediated gene expression, but suggest that changes in gene expression that we have observed may be linked to effects on co-transcriptional processes, such as mRNA capping, rather than transcription *per se*. Indeed, Ser5-P has been shown to bind and stimulate the activity of mammalian capping enzyme (Mce1) [52,53]. Furthermore, in yeast, lethality resulting from substitution of all CTD Ser5 residues with Ala can be rescued by the tethering of Mce1 to the CTD, suggesting that the essential function of CTD Ser5 is in capping enzyme recruitment [54].

Discussion

dPNUTS is required for gene expression and for developmental growth

Here we report the functional analysis of *Drosophila* PNUTS, a regulatory subunit of PP1 that is highly conserved between flies and humans. We find that *dPNUTS* is essential for organismal growth, with mutant animals arresting early in larval development. Survival of the null zygotic mutants until the early larval stage is most likely due to perdurance of maternal *dPNUTS* gene products, raising the possibility of additional roles for *dPNUTS* during embryological development that we have not uncovered here. Clonal analysis indicates that *dPNUTS* has a cell autonomous effect on growth, with mutant clones failing to survive unless given a growth advantage. Transcriptomics characterisation of *dPNUTS* mutant animals indicates that the larval arrest phenotype is associated with the underexpression of many RNAPII-dependent genes, including those that normally support developmental growth. Of particular interest in this regard is the significant enrichment of genes involved in cellular metabolism. The underexpression of these genes suggests that an important role of *dPNUTS* during larval growth might be to ensure transcription of highly expressed metabolic pathways responsible for fuelling energy production and generating the macromolecular precursors for RNA and protein synthesis. Metabolic state is monitored in developing epithelia, ensuring that the fittest cells are selected as organ precursors [55]. The failure to compete with wild type neighbours is consistent with an altered metabolic state that is recognised by cell competition, triggering cells to be outcompeted by their neighbours and lost by caspase-dependent apoptosis.

Is the effect on RNAPII-dependent transcription the cause of growth defects? It is conceivable that roles that have been assigned to hPNUTS, e.g. in the DNA damage response and chromatin condensation, are conserved in dPNUTS and these might contribute to the larval lethality exhibited by *dPNUTS* mutants. Indeed the non-identical distribution of dPNUTS and RNAPII on chromosomes suggests that dPNUTS is present in chromatin-associated complexes lacking RNAPII. Notably we do not see any detectable condensation defects in *dPNUTS* mutant clones but we cannot exclude the possibility that *dPNUTS* may also contribute to other processes that underlie tissue growth, such as transcription-independent cell cycle control, as has been reported for other enzymes that regulate CTD phosphorylation, such as FCP1 [56]. Nevertheless, loss of expression of any one of the cell metabolism pathways affected by *dPNUTS* (Table S4) is sufficient to cause larval growth arrest and is likely to explain the failure of *dPNUTS* larvae to grow in size prior to their eventual demise.

dPNUTS associates with RNAPII at active sites of transcription

Like its mammalian counterpart, we have shown that dPNUTS is a nuclear protein that localises to chromatin during interphase. By utilising larval polytene chromosomes, which are readily visible by light microscopy, we have been able to extend this analysis by determining the distribution of dPNUTS on interphase chromosomes *in situ*. These analyses show co-localisation of dPNUTS with many transcriptionally active sites marked with RNAPII, suggesting that the widespread changes in gene expression that we observe upon loss of *dPNUTS* function are likely to be due to the direct involvement of *dPNUTS* in RNAPII-mediated transcriptional regulation. Correspondingly, we find that dPNUTS is complexed to the large subunit of RNAPII in cell extracts. However, it is important to note that not all RNAPII sites stain for dPNUTS (and *vice versa*) and the relative amounts of the two proteins vary widely amongst these sites. This suggests that the association of dPNUTS with RNAPII, or with associated factors, which may affect the availability of the dPNUTS epitope for detection by our antibody, may be differentially regulated. PNUTS contains a number of conserved macromolecular-interaction domains, which have led to the suggestion it might serve as a multivalent adapter protein. However, it has not yet been established to what extent the known interactors, Tox4 and Wdr82 aid in the recruitment of PNUTS to chromosomal loci. These issues will require investigation of the genome-wide sites of dPNUTS binding, as well as identification and comprehensive characterisation of dPNUTS-interacting proteins and their role in dPNUTS recruitment.

dPNUTS-PP1 regulates the phosphorylation state of RNAPII

Since we found that PP1-binding is necessary for dPNUTS function, we reasoned that dPNUTS affects transcription by targeting PP1 to specific substrates on chromosomes. Several lines of evidence indicate that one important target of dPNUTS-PP1 in this context is the CTD of RNAPII: i) dPNUTS is complexed with RNAPII in nuclear extracts and regulates RNAPII CTD phosphorylation in a PP1-dependent manner; ii) RNAPII CTD Ser5-P levels are elevated in *dPNUTS* mutant larval extracts and tissues; iii) dPNUTS colocalises with PP1 and RNAPII on chromosomes; iv) ectopic expression of a mutant version of dPNUTS that displaces PP1 from polytene chromosomes results in elevated RNAPII CTD Ser5-P levels on chromosomes. dPNUTS-PP1 appears to preferentially target Ser5-P of the CTD as we observed only a modest effect on Ser2-P levels and no effect on phosphorylation of other RNAPII-CTD residues in *dPNUTS* mutant larval extracts by Western blotting (Figure S6B). However, PNUTS/PP1 is not the only PP1 holoenzyme that has been implicated in regulation of RNAPII phosphorylation [37], raising the possibility that different PP1 holoenzymes possess different RNAPII CTD specificities.

Changes in the pattern of gene expression that we have observed in *dPNUTS* mutant animals are correlated with the normal expression level of the affected transcripts; these changes may also reflect the spatial distribution of *dPNUTS* expression during development. During embryogenesis we observed that the levels of *dPNUTS* expression in the gut and the ventral nerve cord correlates with stages in which these tissues are undergoing periods of rapid expansion and development. In an analogous fashion to SCP1, which restricts RNAPII dephosphorylation of neuronal genes to non-neuronal cells by virtue of its expression pattern [11], the enrichment of *dPNUTS* in proliferating tissues may function to promote expression of highly expressed transcripts, such as those involved in cellular metabolism, in these tissues, to support their development. In mammals, the gradual decrease from a high level of PNUTS during embryogenesis to a relatively low level in adults has been taken to imply that PNUTS could play a role in cortical development [22], but could equally reflect a requirement during growth of developing tissues. Notably, PNUTS is not found in some metazoans such as *C.elegans*, where strictly controlled cell lineage determines tissue architecture. An evolved function of PNUTS might therefore be to support proliferative states in organisms where compensatory mechanisms such as cell competition are at play.

How do dPNUTS and RNAPII hyperphosphorylation regulate gene expression? Studies of other enzymes that control CTD phosphorylation state indicate that maintaining correct levels of CTD phosphorylation is critical for normal levels of transcription and that hyperphosphorylation of RNAPII can increase or reduce gene expression depending on what stage of the transcriptional cycle phosphorylation is affected. For instance, FCP1 targets Ser2-P *in vivo* [57] and is thought to recycle RNAPII after the complex has dissociated from the transcribed region [58]. Correspondingly, conditional knockout of FCP1 in yeast results in a global defect in transcription affecting 77% of genes [59]. SCP1 and Ssu72 both target Ser5-P [16,60], but have contrasting roles in transcriptional regulation: knockdown of SCP1 unmasks neuronal gene expression, indicating it normally acts as a transcriptional repressor [11], whilst Ssu72 facilitates transcription by promoting the elongation stage of the transcription cycle [61]. ChIP experiments from larvae expressing $dPNUTS^{W726A}$ suggest that displacement of PP1 binding to dPNUTS does not result in accumulation of RNAPII on the coding region of affected loci. The precise mechanisms of how loss of *dPNUTS* function and RNAPII hyperphosphorylation disrupt gene expression require further investigation. However, we might expect processes dependent on normal CTD phosphorylation, including RNA processing, transcription-coupled chromatin modification and transcription-associated homologous recombination [4], to be affected. In this regard, it is notable that inhibition of TFIIH kinase activity, which phosphorylates promoter-bound RNAPII at Ser5, predominantly affects mRNA capping and stability rather than transcription *per se* [62–64].

In summary, the analysis of *dPNUTS* described here reveals an important function for this evolutionarily conserved chromatin-associated protein, via association with PP1, in the regulation of RNAPII phosphorylation and the appropriate expression of genes during larval development, which support organismal growth. These findings provide insight into the role of PNUTS and

RNAPII phosphorylation during normal development, and may also be of relevance to the understanding of aberrant gene expression patterns observed in disease processes and ageing.

Materials and Methods

Fly strains

Drosophila melanogaster stocks were kept at 18°C or 25°C on standard agar-cornmeal-yeast medium. Genotypes are provided in *Text S1*.

Isolation and characterisation of *dPNUTS* null alleles

Isolation of a null allele of *dPNUTS* by *P* element excision from $dPNUTS^{KG}$ was carried out by crossing *w*; $dPNUTS^{KG}/CyO$, *P{Delta2-3}* males to *y*, *w*; *Tft/CyO* females. From each cross, a single *w* revertant male in which the *P* element was excised, was individually crossed back to *w*; *Tft/CyO* females. To determine the molecular lesion in excisions, genomic DNA surrounding the original $dPNUTS^{KG}$ insertion site was amplified from heterozygous mutants by PCR using flanking primers (see *Text S1*) and sequenced. For genetic complementation tests, a 9.1 kb *Bam*HI restriction fragment from P1 clone DS02684, which contains all of the transcribed *dPNUTS* sequence, was subcloned into the *Bam*HI site in pW8 and injected into flies. Details of the growth arrest experiment can be found in *Text S1*.

Ectopic expression of wild type *dPNUTS* and $dPNUTS^{W726A}$

Full-length cDNAs for dPNUTS-S and PNUTS-L cloned into pNB40 were isolated from a 3rd instar larval library (see *Text S1*). $dPNUTS^{W726A}$ was generated by PCR-based site-directed mutagenesis. For ectopic expression in flies, full-length $dPNUTS^{WT}$ and $dPNUTS^{W726A}$ were subcloned into pUAS-HM, a modified of pUAST that contains an N-terminal 3× His 6× Myc (HM) tag. *UAS-HM-PNUTS* flies were made by *P* element-mediated germline transformation into a w^{1118} stain by Genetic Services Inc. (Cambridge, MA). Tagged $dPNUTS^{WT}$ and $dPNUTS^{W726A}$ were ectopically expressed ubiquitously using *da-GAL4* or in salivary glands using *AB1-GAL4*.

RNA *in situ* hybridisation

pNB40-dPNUTS clones were used to generate Digoxigenin (DIG)-labelled RNA probes. RNA *in situ* hybridisation was essentially performed as previously described [45,65]. Following hybridization, DIG-labelled probes were detected with an alkaline phosphatase conjugated anti-digoxygenin antibody in the presence of Nitro-blue tetrazolium salt (NBT) and X-phosphate/5-Bromo-4-chloro-3-indolyl-phosphate (BCIP).

RNA extraction and qRT-PCR

RNA was extracted using the Qiagen RNeasy Mini kit and was reverse transcribed using the High Capacity cDNA Reverse Transcription kit (Applied Biosystems). Quantitative PCR was performed following the incorporation of SYBRGreen (using the Applied Biosystem StepOnePlus Real Time PCR System). Primers are described in *Text S1*. All samples were normalized to 18S RNA. The $\Delta\Delta C_T$ method was used for the calculation of the relative abundances [66].

RNA-seq and bioinformatics

RNA from approximately 5000 1st instar larvae/genotype was extracted using the Qiagen RNeasy Mini kit following the manufacturer's instructions. Total RNA quality and quantity was verified on a NanoDrop1000 spectrophotometer (Thermofisher) and Bioanalyzer 2100. mRNA was polyA selected using Dynabeads mRNA Purification Kit for mRNA Purification from Total RNA Preps (Invitrogen). The libraries were prepared according to the SOLiD Total RNA-Seq Kit protocol (Part Number 4452437 Rev. A, Applied Biosystems). RNA samples were sequenced on an AB SOLiD sequencing platform with v4 chemistry, generating single-end 50 bp colour-space reads. More than 93M reads were generated for each sample. Reads were filtered for quality and mapped onto the dm3 *D. melanogaster* reference genome [67,68] using TOPHAT [69]. Only uniquely mapped reads were retained for analysis and reported as a BAM [70] file. Cufflinks [71] software took the BAM files to calculate expressions levels for annotated and predicted transcripts using FPKM (fragments per kilobase of transcript per million fragments mapped) values. Differentially expressed genes in the *dPNUTS* mutants were defined as genes with <0.67 or >1.5 fold change relative to controls. A significance threshold of 1 FPKM [72] was also applied. To analyse the enrichment of the genes belonging to specific biological processes, genes differentially expressed in both *dPNUTS* mutants were further analysed by Database for Annotation, Visualization and Integrated Discovery (DAVID) (http://david.abcc.ncifcrf.gov/) against the *D. melanogaster* database. To increase the reproducibility, enrichment of gene function was identified with EASE score ≤ 0.001, which is a conservative adjustment to Fisher exact probability, and a fold change enrichment (FE)≥ 1.5 in all samples. The GO terms were hierarchically classified using AMIGO. Human orthologues of differentially expressed genes were identified by BioMart (www.biomart.org) and used to reconstruct functional networks and predict upstream regulators using Ingenuity IPA (Ingenuity Systems Inc.), see *Text S1* for details.

Immunoprecipitation from *Drosophila* extracts and immunoblotting

Immunoprecipitation from 2–18 hr old *Oregon R Drosophila* embryonic nuclear extracts was performed as in [73], with minor modifications (see *Text S1*), using the following primary antibodies: rabbit anti-Myc (A14, Santa Cruz Biotechnology, 1:100); mouse anti-Myc (9E10, 1:50); guinea pig anti-dPNUTS and anti-dPNUTS-S (1:10). The following primary antibodies were used for Western Blotting: mouse anti-RNAPII (ARNA-3, Research Diagnostics/Millipore, 1:500), which recognizes both phosphorylated and unphosphorylated forms of RNAPII; mouse anti-RNAPII Ser5-P (4H8, Active Motif, 1:1000); purified rabbit anti-PP1 (1:500); rabbit anti-Myc (A14, Santa Cruz Biotechnology, 1:500); mouse anti-Actin (C4, Millipore, 1:5000). For quantitation, X-ray film was digitized with an ImageQuant biomolecular imager (GE Healthcare) and quantified using ImageJ (http://rsbweb.nih.gov/ij/).

Immunostaining of wing discs and whole mount salivary glands

Tissues were fixed and stained using standard approaches (see *Text S1*) with the following primary antibodies: rabbit anti-Cleaved Caspase-3 (Cell Signalling Technology, 1:100); mouse anti-Discs large (Developmental Studies Hybridoma Bank, 1:100); rabbit anti-Myc (A14, Santa Cruz Biotechnology, 1:100); mouse anti-phospho-Histone H3 (Millipore, 1:500). TO-PRO-3 (Invitrogen, 1:1000) was used to visualise DNA.

Immunostaining of polytene chromosomes

Polytene chromosome squashes were prepared as reported previously [74] (see also *Text S1*) and stained with the following

primary antibodies: guinea pig anti-dPNUTS (1:30); rabbit anti-PP1 (1:50); mouse anti-RNAPII Ser2-P (H5, Covance, 1:50); mouse anti-RNAPII Ser5-P (H14, Covance, 1:50); rabbit anti-Myc (A14, Santa Cruz Biotech, 1:100). For DNA staining, slides were incubated with either DAPI or TO-PRO-3.

Image analysis and quantitation

Images were captured on Zeiss 510 and 710 Confocal Microscopes equipped with 405 nm, 488 nm, 561 nm and 633 nm lasers using a Plan Apochromat 40x/1.3NA oil immersion objective. Images were imported to Adobe Photoshop and adjusted for brightness and contrast uniformly across entire fields. Projected images of wing discs in XY were generated using ImageJ. XZ projections were generated using the Cut function in Zen 2011 (Zeiss). Line scans of polytene chromosomes were generated using ImageJ. For this analysis, we imaged a region at end of the X chromosome that could be reliably identified on chromosomes from multiple squashes. Images were taken with identical microscope and laser settings, with signal intensities below the level of saturation. The mean intensity of RNAPII Ser5-P and PP1 fluorescence was determined for each genotype by calculating the average fluorescence intensity through the center of unprocessed images of the same chromosomal region from 6 samples, parallel to the long axis of the structure.

GenBank accession numbers

The accession numbers for the *dPNUTS* and *dPNUTS-S* nucleotide sequences reported in this paper are AJ580979 and AJ580980, respectively.

Supporting Information

Figure S1 Sequence comparison of dPNUTS and related proteins. A) Schematic representation of domains in human PNUTS (hPNUTS) and dPNUTS: Region similar to Domain 1 of TFIIS (and the corresponding domain in Elongin A); Ser-rich region; Central region, highly conserved in hPNUTS and dPNUTS containing a canonical PP1 binding motif; CCCH zinc-finger typical of NUP/Tis11 proteins. The positions of introns (arrowheads) in the coding regions are indicated. Identical intron-exon boundaries are shown with connecting arrows. B) Table of % identity and similarity of hPNUTS, Elongin A and Tis11 in the different domains relative to dPNUTS. NA, not applicable. Pairwise comparisons were performed using ALIGN [77].
(TIF)

Figure S2 Specificity of the dPNUTS antibody for immunofluorescent staining of polytene chromosomes. Chromosome squashes from salivary glands expressing either *histone H2B-YFP* (in green) or *dPNUTS RNAi* stained on the same slide for dPNUTS (in red) and DNA (in magenta). Levels of dPNUTS were greatly reduced on chromosomes from *dPNUTS RNAi* glands.
(TIF)

Figure S3 A) Expanded images of clones in panels K–P of Figure 3, showing DNA and GFP channels for each image. B) Magnified image of panel L of Figure 3, with cross section through a section of the epithelium containing a large *dPNUTS* mutant clone, which shows normal distribution of nuclei compared to neighbouring heterozygous (GFP positive) cells. In contrast, a rare *M, GFP/M, GFP* twinspot is located at the basal face of the epithelium and is being extruded.
(TIF)

Figure S4 Venn diagram showing overlap between differentially expressed up- and down-regulated genes in *dPNUTS* mutants.
(TIF)

Figure S5 Gene ontology (GO) term enrichment of the genes under-expressed (A) and over-expressed (B) in $dPNUTS^{9B}/dPNUTS^{9B}$ and $dPNUTS^{13B}/dPNUTS^{13B}$ mutant larvae relative to abundance of GO terms for all genes in the genome as determined by DAVID. The top GO categories for each gene set are grouped according to their hierarchical relationships along with the number of genes affected in that category, the total number of genes in that category (in parentheses), and the statistical significance of the match.
(TIF)

Figure S6 A) dPNUTS binds dWdr82 in S2 cell extracts. Cells were transfected with constructs expressing Flag-Myc-dWdr82 or GFP-dPNUTS-Myc or both. Ectopic dPNUTS was precipitated using GFP-Trap beads. Western Blotting with anti-Myc antibodies revealed the presence of ectopic GFP-dPNUTS-Myc in precipitates. Flag-Myc-dWdr82 co-precipitated with GFP-dPNUTS-Myc, but not from cells lacking ectopic dPNUTS. IN = Input (total lysate), NB = Non-bound, and IP = immuno-precipitated. B) Western Blot showing levels of RNAPII CTD Ser2-P, Thr4-P, Ser5-P, or Ser7-P in extracts from homozygous revertant $dPNUTS^{exKG}/dPNUTS^{exKG}$ (exKG/exKG) and homozygous null mutant $dPNUTS^{9B}/dPNUTS^{9B}$ (9B/9B) 1st instar larvae. mAb identity is indicated in parenthesis. Relative levels in the two conditions, as derived from densitometry measurements of the respective bands, are shown below the blots. C) Published conditions of recognition of phospho-CTD by mAbs, reproduced from [48,49]. Phosphorylation of red amino acids results in full or partial inhibition of mAb binding, whereas phosphorylation of other Tyr, Ser or Thr residues does not.
(TIF)

Figure S7 Polytene chromosomes from salivary gland squashes stained with dPNUTS and RNAPII Ser5-P (H14) antibodies. Merging of the green signal representing RNAPII Ser5-P with the red signal representing dPNUTS identifies sites where these two proteins co-localize. Insets, boxes 1–4, show enlarged view of chromosome regions. The relative signals of dPNUTS and RNAPII Ser5-P vary between sites, but only a minority of dPNUTS loci colocalize with RNAPII Ser5-P staining (indicated with arrows).
(TIF)

Figure S8 A) Expression levels of the indicated genes in larvae expressing $dPNUTS^{W726A}$ under the control of *da-GAL4* relative to control larvae, as determined by qRT-PCR. Error bars represent the SE (n≥3 biological replicates). B–E) Chromatin immunoprecipitation (ChIP) analyses of the indicated genes from 3rd instar larval extracts using anti-total RNAPII (8WG16) antibody and mouse IgG antibody. Immunoprecipitated DNA was amplified by qPCR. The distribution at four loci (*Thor*, *ImpL3*, *nop56* and *ACC*) was evaluated using primers positioned at the start (S) and middle (M), of the transcribed sequences. Percent input is the amount of precipitated DNA relative to input DNA. Error bars represent the SE of the mean (n≥3 biological replicates).
(TIF)

Table S1 Rescue of *dPNUTS* mutant lethality by genomic transgene. Expected and observed genotype frequencies of adult progeny from complementation crosses with two independent insertions of a *dPNUTS* wild type trangene (n≥350 progeny/cross).
(DOCX)

Table S2 Gene Ontology (GO) classification determined by DAVID. Biological process categories from GO analysis that are significantly overrepresented among the genes for which the expression was either decreased (downregulated worksheet) or increased (upregulated worksheet) in the *dPNUTS* mutants. Only the categories with a minimum of 4 genes per category and an EASE score ≤0.001 were considered.
(XLSX)

Table S3 Comparison of Gene Ontology (GO) outputs from DAVID and EASE. Shown are GO categories that were enriched amongst genes that are differentially expressed (DE) in *dPNUTS* mutants when compared against all genes in the genome (DAVID) or against genes expressed in matched w^{1118} controls (EASE). GO categories returned by the two approaches were not always identical because the programs used different versions of the *D. melanogaster* genome annotation for comparison (DAVID was updated Sept 2009; EASE used FlyBase annotation release 5.46 from July 2012).
(XLS)

Table S4 Ingenuity transcription factor analysis. The table shows the IPA predicted 'upstream regulators' for up- and down-regulated differentially expressed genes, ranked by an application of a z-score algorithm. Genes from each predicted regulator 'pool' present in the analyzed dataset are listed in a 'Target molecules' column.
(XLSX)

Table S5 Comparison of RNA-Seq and qRT-PCR data, showing $\log_2$ fold change in expression of the indicated loci in *dPNUTS* mutants relative to control.
(DOCX)

Text S1 Additional information including detailed genotypes and primer sequences as well as methodology for supplementary figures.
(DOCX)

Acknowledgments

We thank the Bloomington Stock Center, NIG-Fly Stock Center, Christophe Antoniewski and Daniela Grifoni for *Drosophila* strains, the Developmental Studies Hybridoma Bank for antibodies, the Centre for Cell Imaging University of Liverpool for assistance with image acquisition, Roy Chaudhuri, Xuan Liu and the Centre for Genomics Research, University of Liverpool for RNA-Seq and bioinformatic analysis, Mirel Lucaci for technical assistance, members of the Bennett lab and Mark Caddick for advice on the manuscript.

Author Contributions

Conceived and designed the experiments: AC LD VJ AR LA DB. Performed the experiments: AC LD NL PG AR EV DB. Analyzed the data: AC LD VJ OV NC DB. Contributed reagents/materials/analysis tools: LA DB. Wrote the paper: DB. Revised and approved the final version: AC LD VJ NL OV PG AR EV NC LA DB.

References

1. Tennessen JM, Thummel CS (2011) Coordinating growth and maturation - insights from Drosophila. Curr Biol 21: R750–757.
2. Brookes E, Pombo A (2009) Modifications of RNA polymerase II are pivotal in regulating gene expression states. EMBO Rep 10: 1213–1219.
3. Phatnani HP, Greenleaf AL (2006) Phosphorylation and functions of the RNA polymerase II CTD. Genes Dev 20: 2922–2936.
4. Hsin JP, Manley JL (2012) The RNA polymerase II CTD coordinates transcription and RNA processing. Genes Dev 26: 2119–2137.
5. Bataille AR, Jeronimo C, Jacques PE, Laramee L, Fortin ME, et al. (2012) A universal RNA polymerase II CTD cycle is orchestrated by complex interplays between kinase, phosphatase, and isomerase enzymes along genes. Mol Cell 45: 158–170.
6. Mayer A, Lidschreiber M, Siebert M, Leike K, Soding J, et al. (2010) Uniform transitions of the general RNA polymerase II transcription complex. Nat Struct Mol Biol 17: 1272–1278.
7. Patturajan M, Schulte RJ, Sefton BM, Berezney R, Vincent M, et al. (1998) Growth-related changes in phosphorylation of yeast RNA polymerase II. J Biol Chem 273: 4689–4694.
8. Ostapenko D, Solomon MJ (2003) Budding yeast CTDK-I is required for DNA damage-induced transcription. Eukaryot Cell 2: 274–283.
9. Sukegawa Y, Yamashita A, Yamamoto M (2011) The fission yeast stress-responsive MAPK pathway promotes meiosis via the phosphorylation of Pol II CTD in response to environmental and feedback cues. PLoS Genet 7: e1002387.
10. Seydoux G, Dunn MA (1997) Transcriptionally repressed germ cells lack a subpopulation of phosphorylated RNA polymerase II in early embryos of Caenorhabditis elegans and Drosophila melanogaster. Development 124: 2191–2201.
11. Yeo M, Lee SK, Lee B, Ruiz EC, Pfaff SL, et al. (2005) Small CTD phosphatases function in silencing neuronal gene expression. Science 307: 596–600.
12. Blazek D, Kohoutek J, Bartholomeeusen K, Johansen E, Hulinkova P, et al. (2011) The Cyclin K/Cdk12 complex maintains genomic stability via regulation of expression of DNA damage response genes. Genes Dev 25: 2158–2172.
13. Egloff S, Dienstbier M, Murphy S (2012) Updating the RNA polymerase CTD code: adding gene-specific layers. Trends Genet 28: 333–341.
14. Washington K, Ammosova T, Beullens M, Jerebtsova M, Kumar A, et al. (2002) Protein phosphatase-1 dephosphorylates the C-terminal domain of RNA polymerase-II. J Biol Chem 277: 40442–40448.
15. Bensaude O, Bonnet F, Casse C, Dubois MF, Nguyen VT, et al. (1999) Regulated phosphorylation of the RNA polymerase II C-terminal domain (CTD). Biochem Cell Biol 77: 249–255.
16. Krishnamurthy S, He X, Reyes-Reyes M, Moore C, Hampsey M (2004) Ssu72 Is an RNA polymerase II CTD phosphatase. Mol Cell 14: 387–394.
17. Rudenko A, Bennett D, Alphey L (2003) Trithorax interacts with type 1 serine/threonine protein phosphatase in Drosophila. EMBO Rep 4: 59–63.
18. Rudenko A, Bennett D, Alphey L (2004) PP1beta9C interacts with Trithorax in Drosophila wing development. Dev Dyn 231: 336–341.
19. Kirchner J, Gross S, Bennett D, Alphey L (2007) Essential, overlapping and redundant roles of the Drosophila protein phosphatase 1 alpha and 1 beta genes. Genetics 176: 273–281.
20. Bollen M, Peti W, Ragusa MJ, Beullens M (2010) The extended PP1 toolkit: designed to create specificity. Trends Biochem Sci 35: 450–458.
21. Beullens M, Van Eynde A, Stalmans W, Bollen M (1992) The isolation of novel inhibitory polypeptides of protein phosphatase 1 from bovine thymus nuclei. J Biol Chem 267: 16538–16544.
22. Allen PB, Kwon YG, Nairn AC, Greengard P (1998) Isolation and characterization of PNUTS, a putative protein phosphatase 1 nuclear targeting subunit. J Biol Chem 273: 4089–4095.
23. Kreivi JP, Trinkle-Mulcahy L, Lyon CE, Morrice NA, Cohen P, et al. (1997) Purification and characterisation of p99, a nuclear modulator of protein phosphatase 1 activity. FEBS Lett 420: 57–62.
24. Landsverk HB, Kirkhus M, Bollen M, Kuntziger T, Collas P (2005) PNUTS enhances in vitro chromosome decondensation in a PP1-dependent manner. Biochem J 390: 709–717.
25. Lee JH, You J, Dobrota E, Skalnik DG (2010) Identification and characterization of a novel human PP1 phosphatase complex. J Biol Chem 285: 24466–24476.
26. De Leon G, Cavino M, D'Angelo M, Krucher NA (2010) PNUTS knockdown potentiates the apoptotic effect of Roscovitine in breast and colon cancer cells. Int J Oncol 36: 1269–1275.
27. De Leon G, Sherry TC, Krucher NA (2008) Reduced expression of PNUTS leads to activation of Rb-phosphatase and caspase-mediated apoptosis. Cancer Biol Ther 7: 833–841.
28. Grana X (2008) Downregulation of the phosphatase nuclear targeting subunit (PNUTS) triggers pRB dephosphorylation and apoptosis in pRB positive tumor cell lines. Cancer Biol Ther 7: 842–844.
29. Krucher NA, Rubin E, Tedesco VC, Roberts MH, Sherry TC, et al. (2006) Dephosphorylation of Rb (Thr-821) in response to cell stress. Exp Cell Res 312: 2757–2763.
30. Udho E, Tedesco VC, Zygmunt A, Krucher NA (2002) PNUTS (phosphatase nuclear targeting subunit) inhibits retinoblastoma-directed PP1 activity. Biochem Biophys Res Commun 297: 463–467.
31. Lee SJ, Lim CJ, Min JK, Lee JK, Kim YM, et al. (2007) Protein phosphatase 1 nuclear targeting subunit is a hypoxia inducible gene: its role in post-translational modification of p53 and MDM2. Cell Death Differ 14: 1106–1116.
32. Landsverk HB, Mora-Bermudez F, Landsverk OJ, Hasvold G, Naderi S, et al. (2010) The protein phosphatase 1 regulator PNUTS is a new component of the DNA damage response. EMBO Rep 11: 868–875.
33. Boon RA, Iekushi K, Lechner S, Seeger T, Fischer A, et al. (2013) MicroRNA-34a regulates cardiac ageing and function. Nature 495: 107–110.
34. Lee SJ, Lee JK, Maeng YS, Kim YM, Kwon YG (2009) Langerhans cell protein 1 (LCP1) binds to PNUTS in the nucleus: implications for this complex in transcriptional regulation. Exp Mol Med 41: 189–200.

35. Bounaix Morand du Puch C, Barbier E, Kraut A, Coute Y, Fuchs J, et al. (2011) TOX4 and its binding partners recognize DNA adducts generated by platinum anticancer drugs. Arch Biochem Biophys 507: 296–303.
36. Lee JH, Skalnik DG (2008) Wdr82 is a C-terminal domain-binding protein that recruits the Setd1A Histone H3-Lys4 methyltransferase complex to transcription start sites of transcribed human genes. Mol Cell Biol 28: 609–618.
37. Jerebtsova M, Klotchenko SA, Artamonova TO, Ammosova T, Washington K, et al. (2011) Mass spectrometry and biochemical analysis of RNA polymerase II: targeting by protein phosphatase-1. Mol Cell Biochem 347: 79–87.
38. Ceulemans H, Stalmans W, Bollen M (2002) Regulator-driven functional diversification of protein phosphatase-1 in eukaryotic evolution. Bioessays 24: 371–381.
39. Stowers RS, Schwarz TL (1999) A genetic method for generating Drosophila eyes composed exclusively of mitotic clones of a single genotype. Genetics 152: 1631–1639.
40. Theodosiou NA, Xu T (1998) Use of FLP/FRT system to study Drosophila development. Methods 14: 355–365.
41. Kim YM, Watanabe T, Allen PB, Kim YM, Lee SJ, et al. (2003) PNUTS, a protein phosphatase 1 (PP1) nuclear targeting subunit. Characterization of its PP1- and RNA-binding domains and regulation by phosphorylation. J Biol Chem 278: 13819–13828.
42. Bennett D, Lyulcheva E, Alphey L, Hawcroft G (2006) Towards a comprehensive analysis of the protein phosphatase 1 interactome in Drosophila. J Mol Biol 364: 196–212.
43. Dombradi V, Axton JM, Barker HM, Cohen PT (1990) Protein phosphatase 1 activity in Drosophila mutants with abnormalities in mitosis and chromosome condensation. FEBS Lett 275: 39–43.
44. Baksa K, Morawietz H, Dombrádi V, Axton M, Taubert H, et al. (1993) Mutations in the protein phosphatase 1 gene at 87B can differentially affect suppression of position-effect variegation and mitosis in *Drosophila melanogaster*. Genetics 135: 117–125.
45. Bennett D, Szoor B, Alphey L (1999) The chaperone-like properties of mammalian inhibitor-2 are conserved in a Drosophila homologue. Biochemistry 38: 16276–16282.
46. Watanabe T, Huang HB, Horiuchi A, da Cruze Silva EF, Hsieh-Wilson L, et al. (2001) Protein phosphatase 1 regulation by inhibitors and targeting subunits. Proc Natl Acad Sci U S A 98: 3080–3085.
47. Stock JK, Giadrossi S, Casanova M, Brookes E, Vidal M, et al. (2007) Ring1-mediated ubiquitination of H2A restrains poised RNA polymerase II at bivalent genes in mouse ES cells. Nat Cell Biol 9: 1428–1435.
48. Chapman RD, Heidemann M, Albert TK, Mailhammer R, Flatley A, et al. (2007) Transcribing RNA polymerase II is phosphorylated at CTD residue serine-7. Science 318: 1780–1782.
49. Hintermair C, Heidemann M, Koch F, Descostes N, Gut M, et al. (2012) Threonine-4 of mammalian RNA polymerase II CTD is targeted by Polo-like kinase 3 and required for transcriptional elongation. Embo J 31: 2784–2797.
50. Alexander RD, Innocente SA, Barrass JD, Beggs JD (2010) Splicing-dependent RNA polymerase pausing in yeast. Mol Cell 40: 582–593.
51. Batsche E, Yaniv M, Muchardt C (2006) The human SWI/SNF subunit Brm is a regulator of alternative splicing. Nat Struct Mol Biol 13: 22–29.
52. Ghosh A, Shuman S, Lima CD (2011) Structural insights to how mammalian capping enzyme reads the CTD code. Mol Cell 43: 299–310.
53. Ho CK, Shuman S (1999) Distinct roles for CTD Ser-2 and Ser-5 phosphorylation in the recruitment and allosteric activation of mammalian mRNA capping enzyme. Mol Cell 3: 405–411.
54. Schwer B, Shuman S (2011) Deciphering the RNA polymerase II CTD code in fission yeast. Mol Cell 43: 311–318.
55. Baker NE (2011) Cell competition. Curr Biol 21: R11–15.
56. Visconti R, Palazzo L, Della Monica R, Grieco D (2012) Fcp1-dependent dephosphorylation is required for M-phase-promoting factor inactivation at mitosis exit. Nat Commun 3: 894.
57. Cho EJ, Kobor MS, Kim M, Greenblatt J, Buratowski S (2001) Opposing effects of Ctk1 kinase and Fcp1 phosphatase at Ser 2 of the RNA polymerase II C-terminal domain. Genes Dev 15: 3319–3329.
58. Fuda NJ, Buckley MS, Wei W, Core LJ, Waters CT, et al. (2012) Fcp1 Dephosphorylation of the RNA Polymerase II C-Terminal Domain Is Required for Efficient Transcription of Heat Shock Genes. Mol Cell Biol 32: 3428–3437.
59. Kobor MS, Archambault J, Lester W, Holstege FC, Gileadi O, et al. (1999) An unusual eukaryotic protein phosphatase required for transcription by RNA polymerase II and CTD dephosphorylation in S. cerevisiae. Mol Cell 4: 55–62.
60. Yeo M, Lin PS, Dahmus ME, Gill GN (2003) A novel RNA polymerase II C-terminal domain phosphatase that preferentially dephosphorylates serine 5. J Biol Chem 278: 26078–26085.
61. Reyes-Reyes M, Hampsey M (2007) Role for the Ssu72 C-terminal domain phosphatase in RNA polymerase II transcription elongation. Mol Cell Biol 27: 926–936.
62. Hong SW, Hong SM, Yoo JW, Lee YC, Kim S, et al. (2009) Phosphorylation of the RNA polymerase II C-terminal domain by TFIIH kinase is not essential for transcription of Saccharomyces cerevisiae genome. Proc Natl Acad Sci U S A 106: 14276–14280.
63. Kanin EI, Kipp RT, Kung C, Slattery M, Viale A, et al. (2007) Chemical inhibition of the TFIIH-associated kinase Cdk7/Kin28 does not impair global mRNA synthesis. Proc Natl Acad Sci U S A 104: 5812–5817.
64. Schwer B, Sanchez AM, Shuman S (2012) Punctuation and syntax of the RNA polymerase II CTD code in fission yeast. Proc Natl Acad Sci U S A 109: 18024–18029.
65. Bennett D, Alphey L (2004) Cloning and expression of mars, a novel member of the guanylate kinase associated protein family in Drosophila. Gene Expr Patterns 4: 529–535.
66. Winer J, Jung CK, Shackel I, Williams PM (1999) Development and validation of real-time quantitative reverse transcriptase-polymerase chain reaction for monitoring gene expression in cardiac myocytes in vitro. Anal Biochem 270: 41–49.
67. Adams MD, Celniker SE, Holt RA, Evans CA, Gocayne JD, et al. (2000) The genome sequence of Drosophila melanogaster. Science 287: 2185–2195.
68. Celniker SE, Wheeler DA, Kronmiller B, Carlson JW, Halpern A, et al. (2002) Finishing a whole-genome shotgun: release 3 of the Drosophila melanogaster euchromatic genome sequence. Genome Biol 3: RESEARCH0079.
69. Trapnell C, Pachter L, Salzberg SL (2009) TopHat: discovering splice junctions with RNA-Seq. Bioinformatics 25: 1105–1111.
70. Li H, Handsaker B, Wysoker A, Fennell T, Ruan J, et al. (2009) The Sequence Alignment/Map format and SAMtools. Bioinformatics 25: 2078–2079.
71. Trapnell C, Williams BA, Pertea G, Mortazavi A, Kwan G, et al. (2010) Transcript assembly and quantification by RNA-Seq reveals unannotated transcripts and isoform switching during cell differentiation. Nat Biotechnol 28: 511–515.
72. Graveley BR, Brooks AN, Carlson JW, Duff MO, Landolin JM, et al. (2011) The developmental transcriptome of Drosophila melanogaster. Nature 471: 473–479.
73. Rozenblatt-Rosen O, Rozovskaia T, Burakov D, Sedkov Y, Tillib S, et al. (1998) The C-terminal SET domains of ALL-1 and TRITHORAX interact with the INI1 and SNR1 proteins, components of the SWI/SNF complex. Proc Natl Acad Sci U S A 95: 4152–4157.
74. Ciurciu A, Komonyi O, Pankotai T, Boros IM (2006) The Drosophila histone acetyltransferase Gcn5 and transcriptional adaptor Ada2a are involved in nucleosomal histone H4 acetylation. Mol Cell Biol 26: 9413–9423.
75. Schneuwly S, Shortridge RD, Larrivee DC, Ono T, Ozaki M, et al. (1989) Drosophila ninaA gene encodes an eye-specific cyclophilin (cyclosporine A binding protein). Proc Natl Acad Sci U S A 86: 5390–5394.
76. Shieh BH, Stamnes MA, Seavello S, Harris GL, Zuker CS (1989) The ninaA gene required for visual transduction in Drosophila encodes a homologue of cyclosporin A-binding protein. Nature 338: 67–70.
77. Myers EW, Miller W (1988) Optimal alignments in linear space. Comput Appl Biosci 4: 11–17.

3.3. Supplementary Figures

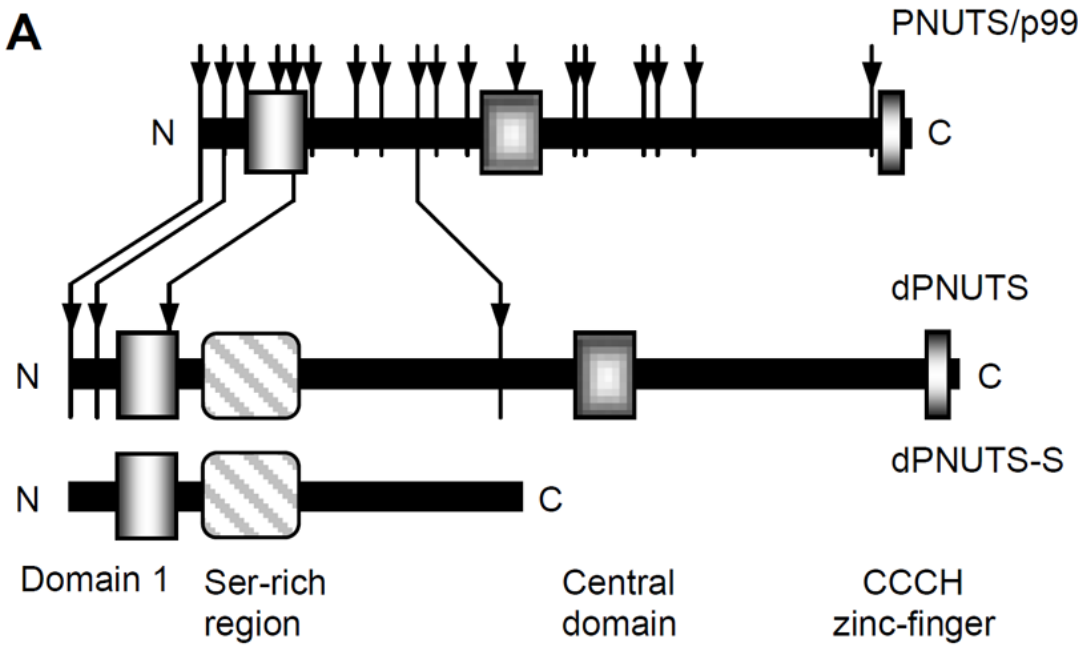

B

dPNUTS domains	% Identity/ Similarity over domain		
	PNUTS	Elongin A	Tis11
N-terminus (residues 1-788)	38/63	NA	NA
Domain 1 (residues 65-147)	37/63	27/45	NA
Central region (residues 705-789)	46/61	NA	NA
CCCH zinc-finger (residues 1110-1130)	45/73	NA	32/64

Figure S1. Sequence comparison of dPNUTS and related proteins. A) Schematic representation of domains in human PNUTS (hPNUTS) and dPNUTS: Region similar to Domain 1 of TFIIS (and the corresponding domain in Elongin A); Ser-rich region; Central region, highly conserved in hPNUTS and dPNUTS containing a canonical PP1 binding motif; CCCH zinc-finger typical of NUP/Tis11 proteins. The positions of introns (arrowheads) in the coding regions are indicated. Identical intron-exon boundaries are shown with connecting arrows. B) Table of % identity and similarity of hPNUTS, Elongin A and Tis11 in the different domains relative to dPNUTS. NA, not applicable. Pairwise comparisons were performed using ALIGN [77].

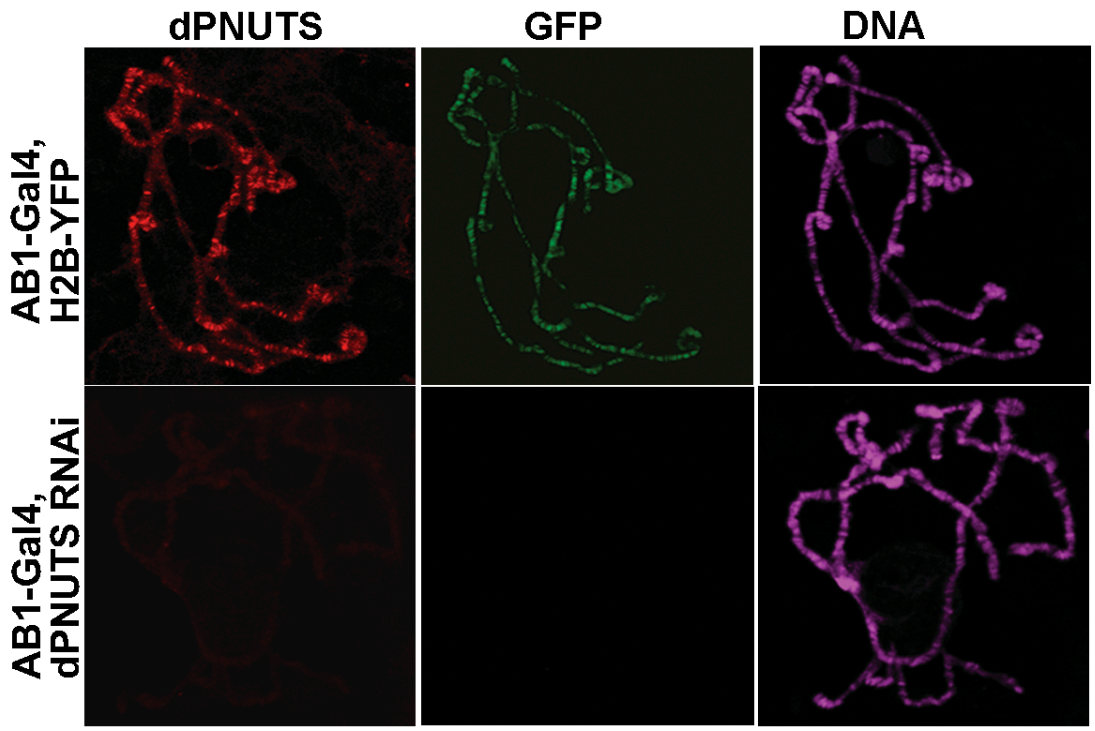

Figure S2. Specificity of the dPNUTS antibody for immunofluorescent staining of polytene chromosomes. Chromosome squashes from salivary glands expressing either *histone H2B-YFP* (in green) or *dPNUTS RNAi* stained on the same slide for dPNUTS (in red) and DNA (in magenta). Levels of dPNUTS were greatly reduced on chromosomes from *dPNUTS RNAi* glands.

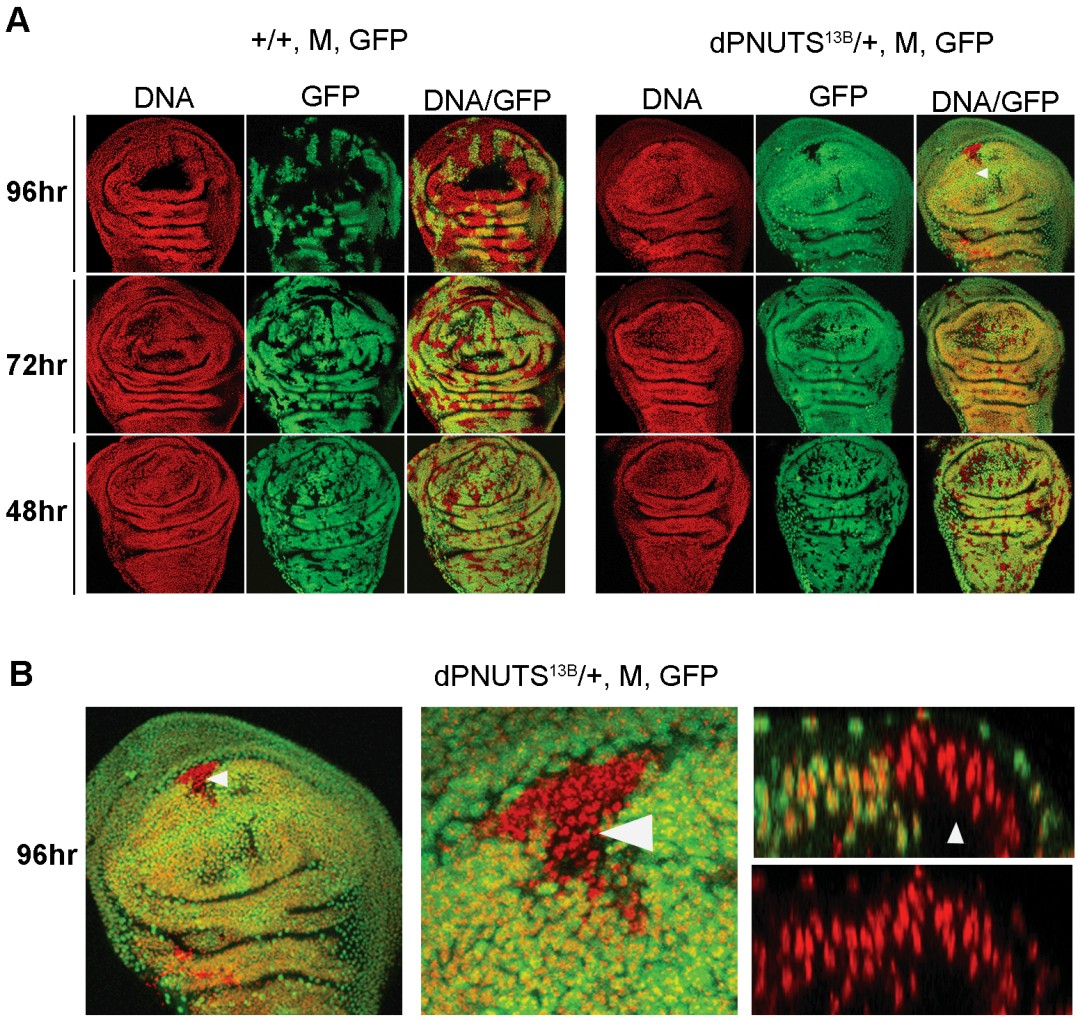

Figure S3. A) Expanded images of clones in panels K–P of Figure 3, showing DNA and GFP channels for each image. B) Magnified image of panel L of Figure 3, with cross section through a section of the epithelium containing a large *dPNUTS* mutant clone, which shows normal distribution of nuclei compared to neighbouring heterozygous (GFP positive) cells. In contrast, a rare *M, GFP*/*M, GFP* twinspot is located at the basal face of the epithelium and is being extruded.

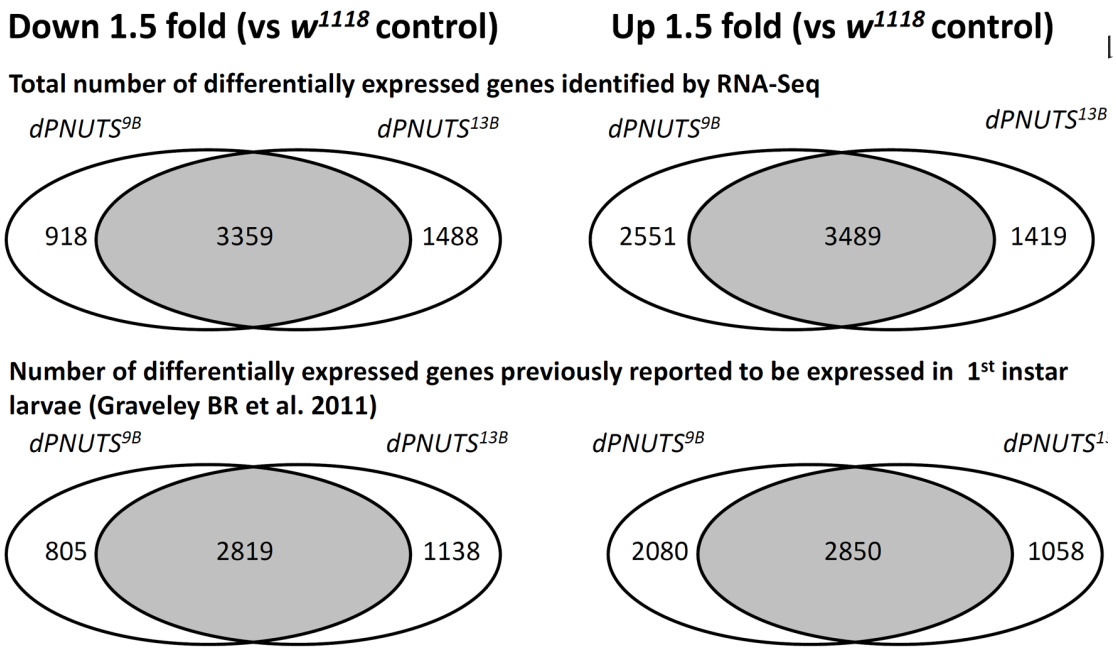

Figure S4. Venn diagram showing overlap between differentially expressed up- and down-regulated genes in *dPNUTS* mutants.

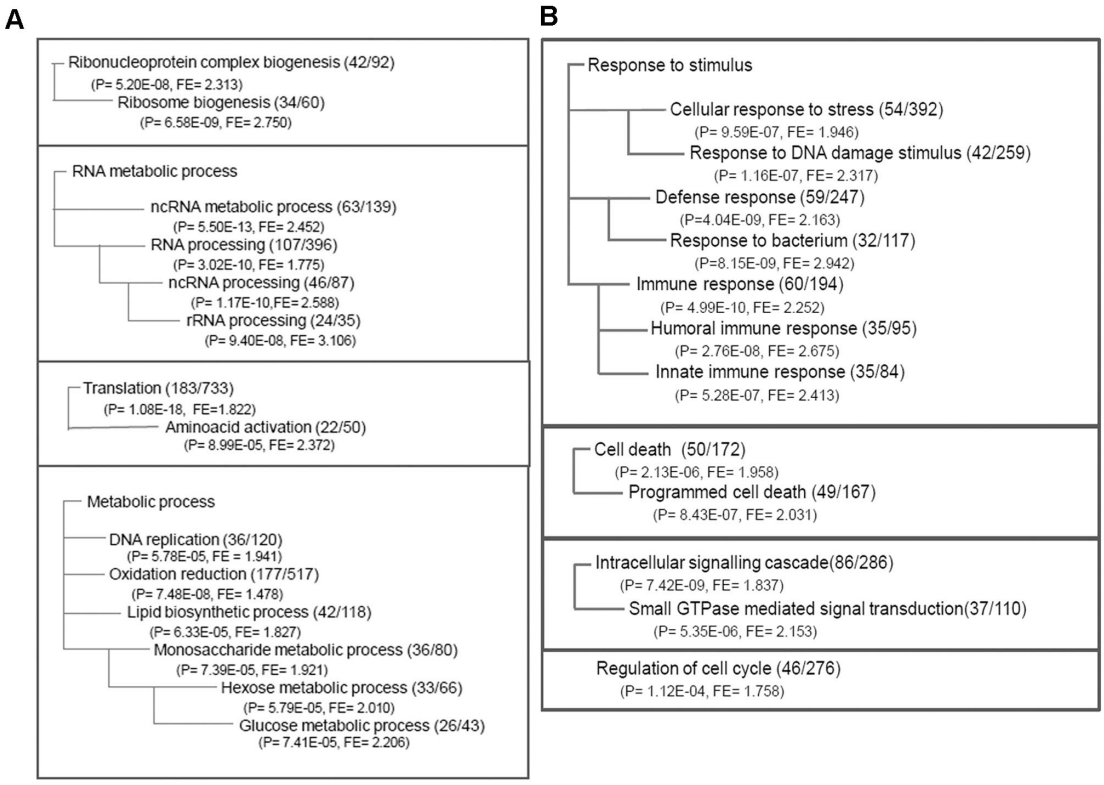

Figure S5. Gene ontology (GO) term enrichment of the genes under-expressed (A) and over-expressed (B) in *dPNUTS*^{9B}/*dPNUTS*^{9B} and *dPNUTS*^{13B}/*dPNUTS*^{13B} mutant larvae relative to abundance of GO terms for all genes in the genome as determined by DAVID. The top GO categories for each gene set are grouped according to their hierarchical relationships along with the number of genes affected in that category, the total number of genes in that category (in parentheses), and the statistical significance of the match.

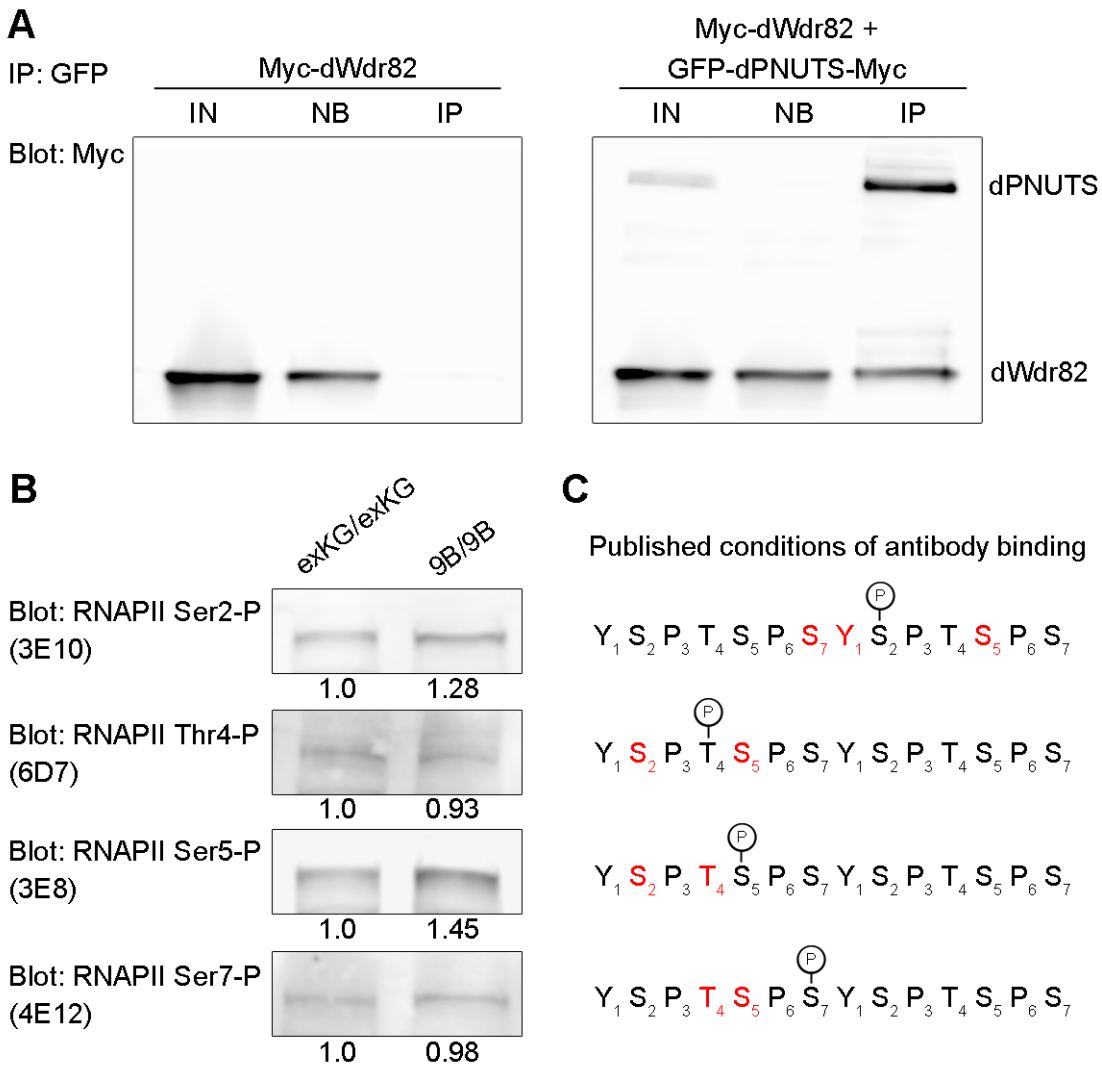

Figure S6. A) dPNUTS binds dWdr82 in S2 cell extracts. Cells were transfected with constructs expressing Flag-Myc-dWdr82 or GFP-dPNUTS-Myc or both. Ectopic dPNUTS was precipitated using GFP-Trap beads. Western Blotting with anti-Myc antibodies revealed the presence of ectopic GFP-dPNUTS-Myc in precipitates. Flag-Myc-dWdr82 co-precipitated with GFP-dPNUTS-Myc, but not from cells lacking ectopic dPNUTS. IN = Input (total lysate), NB = Non-bound, and IP = immunoprecipitated. B) Western Blot showing levels of RNAPII CTD Ser2-P, Thr4-P, Ser5-P, or Ser7-P in extracts from homozygous revertant $dPNUTS^{exKG}/dPNUTS^{exKG}$ (exKG/exKG) and homozygous null mutant $dPNUTS^{9B}/dPNUTS^{9B}$ (9B/9B) 1st instar larvae. mAb identity is indicated in parenthesis. Relative levels in the two conditions, as derived from densitometry measurements of the respective bands, are shown below the blots. C) Published conditions of recognition of phospho-CTD by mAbs, reproduced from [48], [49]. Phosphorylation of red amino acids results in full or partial inhibition of mAb binding, whereas phosphorylation of other Tyr, Ser or Thr residues does not.

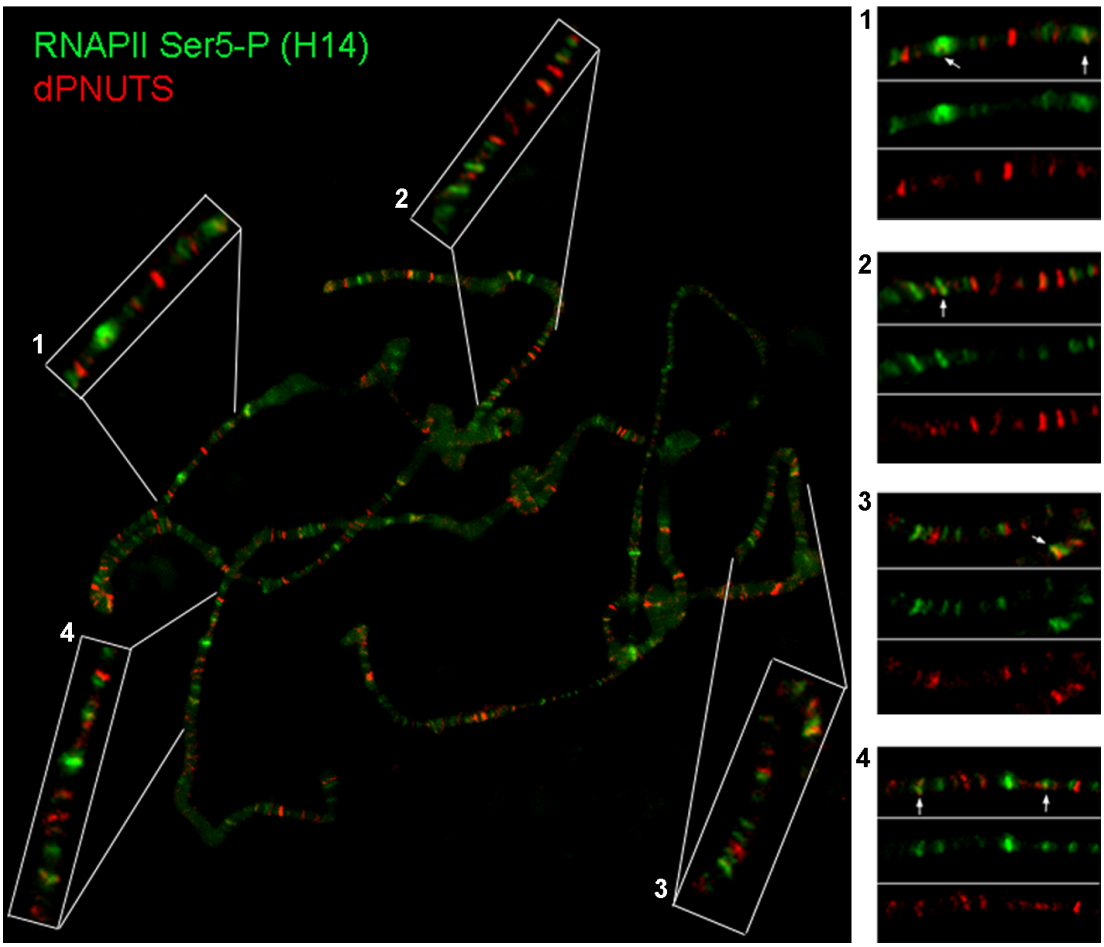

Figure S7. Polytene chromosomes from salivary gland squashes stained with dPNUTS and RNAPII Ser5-P (H14) antibodies. Merging of the green signal representing RNAPII Ser5-P with the red signal representing dPNUTS identifies sites where these two proteins co-localise. Insets, boxes 1–4, show enlarged view of chromosome regions. The relative signals of dPNUTS and RNAPII Ser5-P vary between sites, but only a minority of dPNUTS loci co-localise with RNAPII Ser5-P staining (indicated with arrows).

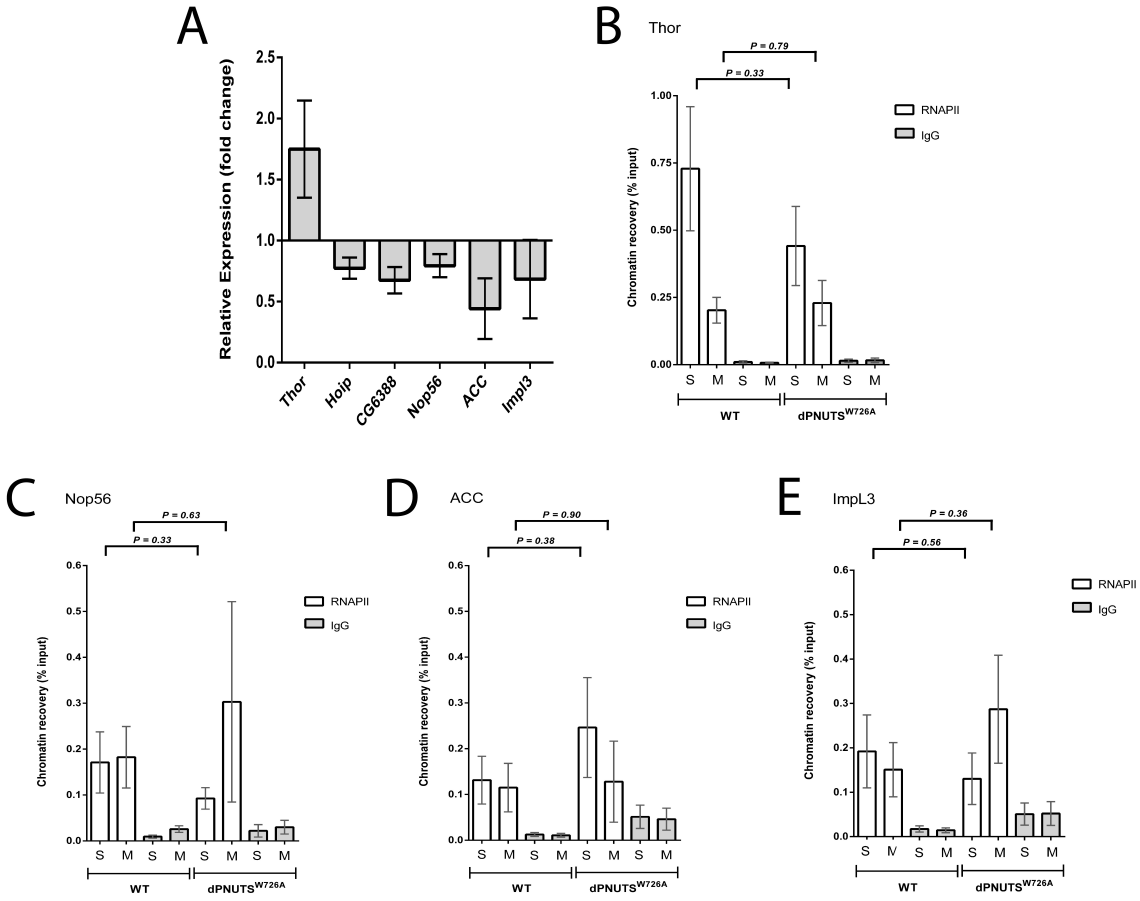

Figure S8. A) Expression levels of the indicated genes in larvae expressing *dPNUTS*^{W726A} under the control of *da-GAL4* relative to control larvae, as determined by qRT-PCR. Error bars represent the SE (n≥3 biological replicates). B–E) Chromatin immunoprecipitation (ChIP) analyses of the indicated genes from 3rd instar larval extracts using anti-total RNAPII (8WG16) antibody and mouse IgG antibody. Immunoprecipitated DNA was amplified by qPCR. The distribution at four loci (*Thor*, *ImpL3*, *nop56* and *ACC*) was evaluated using primers positioned at the start (S) and middle (M), of the transcribed sequences. Percent input is the amount of precipitated DNA relative to input DNA. Error bars represent the SE of the mean (n≥3 biological replicates).

Note: Table S2 and S4 can be found online at

http://www.plosgenetics.org/article/info%3Adoi%2F10.1371%2Fjournal.pgen.1003885.

Table S1. Rescue of *dPNUTS* mutant lethality by genomic transgene. Expected and observed genotype frequencies of adult progeny from complementation crosses with two independent insertions of a *dPNUTS* wild type transgene (n≥ 350 progeny/cross)

Cross No.	Genotype	Expected (no rescue) %	Expected (complete rescue) %	Observed %
1.	PNUTS13B/Cyo; P[PNUTS^{+} genomic, Line09]/TM6B X PNUTS13B /Cyo; P[PNUTS^{+} genomic, Line09]/TM6B			
	PNUTS^{13B} /PNUTS^{13B}; P[PNUTS^{+} genomic, Line09]/TM6B	0	22.2	18.6
	PNUTS^{13B} /PNUTS^{13B}; P[PNUTS^{+} genomic, Line09]/ P[PNUTS^{+} genomic, Line09]	0	11.1	11.8
	PNUTS^{13B} /Cyo; P[PNUTS^{+} genomic, Line09]/TM6B	66.6	44.4	37.05
	PNUTS^{13B} /Cyo; P[PNUTS^{+} genomic, Line09]/ P[PNUTS^{+} genomic, Line09]	33.3	22.2	32.4
2.	PNUTS^{13B} /Cyo; P[PNUTS^{+} genomic, Line03]/TM6B X PNUTS^{13B} /Cyo; P[PNUTS^{+} genomic, Line03]/TM6B			
	PNUTS^{13B} / PNUTS^{13B}; P[PNUTS^{+} genomic, Line03]/TM6B	0	22.2	19.2
	PNUTS^{13B} / PNUTS^{13B}; P[PNUTS^{+} genomic, Line03]/ P[PNUTS^{+} genomic, Line03]	0	11.1	12.8
	PNUTS^{13B} /Cyo; P[PNUTS^{+} genomic, Line03]/TM6B	66.6	44.4	42.4
	PNUTS^{13B} /Cyo; P[PNUTS^{+} genomic, Line03]/ P[PNUTS^{+} genomic, Line03]	33.3	22.2	25.6

Table S3. Comparison of Gene Ontology (GO) outputs from DAVID and EASE. Shown are GO categories that were enriched amongst genes that are differentially expressed (DE) in *dPNUTS* mutants when compared against all genes in the genome (DAVID) or against genes expressed in matched w^{1118} controls (EASE). GO categories returned by the two approaches were not always identical because the programs used different versions of the *D.melanogaster* genome annotation for comparison (DAVID was updated Sept 2009; EASE used FlyBase annotation release 5.46 from July 2012).

Under-expressed genes in *dPNUTS* mutants								
	EASE (DE vs genes expressed in w1118)					**DAVID (DE vs all genes in the genome)**		
Term	**List Hits**	**List Size**	**Pop. Hits**	**Pop.Size**	**EASE Score**	**List Hits**	**List Size**	**EASE Score**
Ribonucleoprotein complex biogenesis						42	92	5.20E-08
Ribonucleoprotein complex	12	1881	23	10256	1.18E-03			
Ribosome biogenesis	12	2189	22	11715	8.67E-04	34	60	6.58E-09
ncRNA metabolic process						63	139	5.50E-13
RNA processing	10	2189	38	11715	2.70E-01	107	396	3.02E-10
rRNA processing	20	2189	26	11715	2.28E-09	24	35	9.40E-08
Translation	87	2189	190	11715	2.55E-17	183	733	1.08E-18
Amino acid activation						22	50	8.99E-05
tRNA aminoacetylation for protein translation	14	2189	32	11715	3.23E-03			
DNA replication	29	2189	54	11715	3.94E-08	36	120	5.78E-05
Oxidation reduction						177	517	7.48E-08
Oxidation-reduction process	131	2189	459	11715	1.82E-07			
Lipid biosynthetic process						42	118	6.33E-05

Phospholipid biosynthetic process	5	2189	14	11715	2.57E-01			
Monosaccharide metabolic process						36	80	7.39E-05
Glucose metabolic process	5	2189	9	11715	6.91E-02	26	43	7.41E-05

Over-expressed genes in *dPNUTS* mutants								
	EASE (DE vs genes expressed in w1118)					**DAVID (DE vs all genes in the genome)**		
Term	**List Hits**	**List Size**	**Pop. Hits**	**Pop.Size**	**EASE Score**	**List Hits**	**List Size**	**EASE Score**
Response to DNA damage stimulus	31	2242	95	11715	2.49E-03	42	259	1.16E-07
Defense response	30	2242	98	11715	8.08E-03	59	247	4.04E-09
Response to bacterium	8	2242	20	11715	7.09E-02	32	117	8.15E-09
Immune response	18	2242	48	11715	5.82E-03	60	194	4.99E-10
Programmed cell death	12	2242	16	11715	2.07E-05	49	167	8.43E-07
Intracellular signalling cascade						86	286	7.42E-09
Signal transduction	61	2242	208	11715	4.11E-04			
Small GTPase mediated signal transduction	34	2242	91	11715	9.05E-05	37	110	5.35E-06
Regulation of cell cycle	13	2242	46	11715	1.55E-01	46	276	1.12E-04

Key: List Hits = number of genes in differentially expressed (DE) group belonging to the respective GO category; List Size = number of genes differentially expressed group; Pop. Hits (EASE) = number of genes in control group belonging to the respective GO category; Pop. Size (EASE) = number of genes in control group

Table S5. Comparison of RNA-Seq and qRT-PCR data, showing $\log_2$ fold change in expression of the indicated loci in *dPNUTS* mutants relative to control

		dPNUTS[9B]/ dPNUTS[9B]		dPNUTS[13B]/ dPNUTS[13B]	
	Gene name	**RNA-seq**	**qRT-PCR**	**RNA-seq**	**qRT-PCR**
UP	Thor	1.55	1.4	1.58	1.55
	Hid	1.53	2.58	1.96	2.96
	p53	1.76	1.55	2.137	1.73
DOWN	Hoip	1.64	2.65	2.117	2.07
	CG4038	0.73	1.53	1.434	2.02
	CG6388	2.608	2.55	3.49	2.57
	CG6712	1.39	1.51	1.68	1.47
	nop56	1.415	1.87	1.32	1.68
	CG18600	1.36	1.92	1.717	1.76
	CG3756	1.44	0.68	1.31	0.59
	RPI135	0.55	1.09	1.08	0.96
	RPII215	0.08	0.14	0.014	0.32
	CG3523	1.217	0.34	1.68	0.66
	CG11198	1.18	1.12	1.49	1.59
	Tpi	0.35	0.59	0.86	0.57
	GAPDH2	1	1.36	1.81	1.42
	ImpL3	1.45	2.04	1.21	2.02

3.4. Supplementary Text

List of genotypes

Fig.2B-D
w^{1118}; $dPNUTS^{exKG}/dPNUTS^{exKG}$
w^{1118}; $dPNUTS^{9B}$/CyO, twi-GFP
w^{1118}; $dPNUTS^{9B}/dPNUTS^{9B}$
w^{1118}; $dPNUTS^{13B}$/CyO, twi-GFP
w^{1118}; $dPNUTS^{13B}/dPNUTS^{13B}$
w^{1118}; $dPNUTS^{KG}$/CyO, twi-GFP
w^{1118}; $dPNUTS^{KG}/dPNUTS^{KG}$

Fig.2E
w^{1118} (isogenic for autosomes)
GMR-hid, FRT40A, l(2)/CyO; ey-GAL4, $UAS\text{-}FLP^{1}$
GMR-hid, FRT40A, l(2)/ $dPNUTS^{9B}$, FRT40A; ey-GAL4, $UAS\text{-}FLP^{1}$
GMR-hid, FRT40A, l(2)/ $dPNUTS^{13B}$, FRT40A; ey-GAL4, $UAS\text{-}FLP^{1}$
GMR-hid, FRT40A, l(2)/ $dPNUTS^{KG}$, FRT40A; ey-GAL4, $UAS\text{-}FLP^{1}$
GMR-hid, FRT40A, l(2)/ $dPNUTS^{exKG}$, FRT40A; ey-GAL4, $UAS\text{-}FLP^{1}$

Fig.3 and Fig.S3
$hsFLP^{122}$; $dPNUTS^{13B}$, FRT40A/ Ubi-GFPnls, FRT40A
$hsFLP^{122}$; $dPNUTS^{13B}$, FRT40A/ Ubi-GFPnls, FRT40A, M(RpL27A)

Fig. 5C
da-GAL4/+; UAS-HM-$dPNUTS^{WT}$ line3/+
da-GAL4/+; UAS-HM-$dPNUTS^{W726A}$ line1/+

Fig. 6A-C
AB1-GAL4, UAS-HM-$dPNUTS^{WT}$ line3
AB1-GAL4, UAS-HM-$dPNUTS^{W726A}$ line1

Fig. 6D
w^{1118}
da-GAL4, UAS-HM-$dPNUTS^{WT}$ line3
da-GAL4, UAS-HM-$dPNUTS^{W726A}$ line1

Fig. 6E
GMR-hid, FRT40A, l(2)/ $PNUTS^{9B}$, FRT40A; ey-GAL4, $UAS\text{-}FLP^{1}$/+
GMR-hid, FRT40A, l(2)/ $PNUTS^{9B}$, FRT40A; ey-GAL4, $UAS\text{-}FLP^{1}$/ UAS-HM-$dPNUTS^{WT}$ line3
GMR-hid, FRT40A, l(2)/ $PNUTS^{9B}$, FRT40A; ey-GAL4, $UAS\text{-}FLP^{1}$/ UAS-HM-$dPNUTS^{W726A}$ line1

GMR-hid, FRT40A, l(2)/ $PNUTS^{13B}$, FRT40A; ey-GAL4, $UAS\text{-}FLP^{1}$/+
GMR-hid, FRT40A, l(2)/ $PNUTS^{13B}$, FRT40A; ey-GAL4, $UAS\text{-}FLP^{1}$/ UAS-HM-$dPNUTS^{WT}$ line3
GMR-hid, FRT40A, l(2)/ $PNUTS^{13B}$, FRT40A; ey-GAL4, $UAS\text{-}FLP^{1}$/ UAS-HM-$dPNUTS^{W726A}$ line1

Fig. 6F
GMR-hid, FRT40A, l(2)/ PNUTS ^{KG572}, FRT40A; ey-GAL4, UAS-FLP^{1}/+
GMR-hid, FRT40A, l(2)/ PNUTS^{KG572}, FRT40A; ey-GAL4, UAS-FLP^{1}/ PP187B^{1}
GMR-hid, FRT40A, l(2)/ PNUTS^{KG572}, FRT40A; ey-GAL4, UAS-FLP^{1}/ PP187B^{hs46}

Fig. 7B
w^{1118} (isogenic for autosomes)
w^{1118}; dPNUTS^{9B}/dPNUTS^{9B}
w^{1118}; dPNUTS^{13B}/dPNUTS^{13B}
w^{1118}; dPNUTS^{KG}/dPNUTS^{KG}
w^{1118}; dPNUTS^{exKG}/dPNUTS^{exKG}

Fig. 7C
w^{1118}
da-GAL4, UAS-HM-dPNUTS^{WT} line3
da-GAL4, UAS-HM-dPNUTS^{W726A} line1

Fig. 7D,E
AB1-GAL4, UAS-H2B-YFP
AB1-GAL4, UAS-HM-dPNUTS^{W726A} line1

Fig.S2
AB1-GAL4, UAS-H2B-YFP
AB1-GAL4, UAS-PNUTS RNAi (NIG-FLY, 31657R-3)

Fig.S8
w^{1118}
da-GAL4, UAS-HM-dPNUTS^{W726A} line1

3.5. Supplementary Methods

Growth arrest experiment

PNUTS^{9B} and *PNUTS^{13B}* were balanced with *Cyo, twi-GFP*. For each genotype, 10 females and 6 males were allowed to mate for 2 days and were then transferred to plates with laying apple juice medium at 25°C. The first-day egg collections were discarded, and, starting on the second day, a 4 hr egg collection regimen was established. After 24 hr, 30 homozygous (GFP negative) and 30 heterozygous (GFP positive) eggs from each genotype were transferred to separate fresh agar plates. After each 24 hr, the number of living larvae was counted and their size was compared until all larvae died.

Imaging of adult eyes

Flies were collected in micro-centrifuge tubes and frozen and stored at -20°C until imaging. Flies were imaged using a Leica MZ10F stereomicroscope (Leica).

***dPNUTS* cDNA isolation and sequence analysis**

5 x 10^6 *Drosophila* 3rd instar larval cDNAs were screened using PP1β9C as bait in the two-hybrid assay as [1, 2]. cDNAs containing the complete dPNUTS open reading frame were obtained by hybridisation using the screening procedure described in [3]. In brief, 1 x 10^6 clones from a 3rd instar larval library [4] were screened in pools by Southern Blotting and PCR, using the longest two-hybrid clone (DB388: nucleotides 1894-4831 of dPNUTS or a PCR product from the 3' end of DB388 (nucleotides 3239-4096 of dPNUTS) as probes. These approaches identified full-length clones of dPNUTS-S and dPNUTS, respectively, representing the two alternative mRNA splice variants of the d*PNUTS* gene. Identification of the intron and exon structures of PNUTS and dPNUTS was done by comparison of the following sequences: d*PNUTS* cDNA reported in this study; AE003588, d*PNUTS* genomic; AJ544537, human *PNUTS* mRNA; AB088097, human *PNUTS* genomic.

Yeast two-hybrid assays

GAL4 activation domain-dPNUTS fusion constructs were made as follows: A *Bam*HI site was introduced immediately 5' of the translation start and a *Sal*I site at the 3' end of both *dPNUTS* and *dPNUTS-S* by PCR using the following primers: (+) 5'-CTAAGGATCCAAATGCCTCGTATAGTTCC-3',(-)5'-GGGGTCGACAGACCGGAATTCGGCGG-3'. The whole open reading frames of *dPNUTS* and *dPNUTS-S* were then introduced as *Bam*HI/*Sal*I fragments into the *Bam*HI/*Xho*I sites of pACT. For the 2-hybrid assays: GAL4 DNA-binding domain-PP1c fusion constructs pAS2-PP1α87B, pAS2-PP1α13C, pAS2-PP1α96A and pAS2-PP1β9C have been previously described [2, 5]. Y190 yeast cells were transformed with pAS2 and pACT constructs and transformed cells were selected on drop-out base with agar plates (BIO 101) lacking leucine, tryptophan and histidine. Colonies appearing after 4-5 days of incubation at 30^{o}C were tested for β-galactosidase activity using a filter lift assay described by Clontech.

dPNUTS and PP1 antisera

Guinea pig anti-PNUTS and rabbit anti-PP1 antibodies were generated by Moravian-Biotechnology and Eurogentec respectively using the following peptides as antigens: KLEVDNVPDHPNGNL (residues 789-792 of dPNUTS); KLFSILFHSPRTLVA (residues 581-594 of dPNUTS-S); RGARPGKNVQLSEGE and SDPDKDTMGWGENDR (residues 18-32 and 205-219, respectively of PP187B).

Analysis of RNAPII CTD phosphorylation levels by Western Blotting

The following monoclonal antibodies directed against phospho-CTD marks were obtained from Chromotek: 3E10 (Ser2-P); 6D7 (Thr4-P); 3E8 (Ser5-P); 4E12 (Ser7-P). For relative quantitation, signals were captured using an ImageQuant biomolecular imager (GE Healthcare) and quantified using ImageJ (http://rsbweb.nih.gov/ij/).

Co-immunoprecipitation from *Drosophila* extracts

Nuclear extracts, prepared from approximately 200 µl of dechorionated embryos of each genotype, were incubated with primary antibodies overnight and then another 2-4 hours the next day with either GammaBind Plus Sepharose (Amersham) or protein A-coated magnetic beads (Millipore).

Co-immunoprecipitation from S2 cell extracts

2 x 10^6 S2R+ cells in 2ml Schneider's were seeded out 2-3 hours before transfection. Cells were either transfected or co-transfected with constructs containing Flag-Myc-dWdr82 or GFP-dPNUTS-Myc using Effectene transfection reagent (Qiagen) according to the manufacturer's protocol for the transient transfection of adherent cells. After 48-72 hours incubation, cells were harvested at 4000 rpm for 3 mins. Immunoprecipitation was carried out using magnetic GFP-Trap beads (Chromotek) according to the manufacturer's protocol. Anti-Myc antibody (A14, 1:1000) was used for immunoblotting of S2 cell extracts.

Chromatin Immunoprecipitation (ChIP) from larval extracts

ChIP experiments were performed from wandering 3rd instar larvae, as described previously [7]. For the immunoprecipitations, 25 µg of chromatin was incubated overnight with antibody and another 4 hours the next day with protein A or G coated

magnetic beads (Diagenode or Millipore). The antibodies used in the IP were: mouse anti-total RNAPII (8WG16, Covance) and mouse IgG. A minimum of 3 biological replicates was done for each genotype. For the qPCR analysis, reactions were done in duplicates and the quantity of DNA bound by specific antibodies was calculated by % Input. Primers used for PCR are given in the table below.

Immunostaining of wing discs and whole mount salivary glands

Tissues were dissected from 3rd instar larvae were fixed in 3.7% paraformaldehyde in 1x phosphate-buffered saline (PBS) for 20 minutes. Tissues were washed in 1x PBS for 15 minutes and then blocked in 1x PBS, 5% bovine serum albumin (BSA), 0.1% Triton X-100 (blocking solution) for 30 minutes at room temperature or a minimum of 2 hours at 4°C. Tissues were incubated with primary antibody in blocking solution overnight at 4°C. Tissues were washed in PBST (1x PBS, 0.1% Triton X-100) and incubated with secondary antibody conjugated to Alexa-Fluor 488, 555 or 633 (1:500, Molecular Probes) for 2 hours at room temperature in the dark. Tissues were washed two times in PBST for 10 minutes each time followed by incubation with TO-PRO-3 (Invitrogen, 1:1000 in 1x PBS) for visualising DNA. Tissues were mounted in Vectashield mounting medium (Vector Laboratories).

Immunostaining of polytene chromosomes

Polytene chromosome squashes were done as described previously [8]. In brief, salivary glands of wandering larvae were fixed with 3.7% paraformaldehyde dissolved in phosphate-buffered saline (PBS) and then incubated in 45% acetic acid for 1 minute. Slides were blocked in PBST (PBS+ 0.1% Tween-20) + 5% BSA for 1 hour at 25°C and incubated overnight at 4°C with primary antibodies. Slides were washed in PBST and incubated with secondary antibodies for 1 hour at 25°C: Alexa-Fluor 488-conjugated goat anti-mouse IgG, Alexa-Fluor 488-conjugated goat anti-guinea pig IgG and Alexa-Fluor 555-conjugated goat anti-rabbit IgG (Molecular Probes), were used at 1:500 dilutions. For DNA staining, slides were incubated with DAPI or TO-PRO-3 in PBST for 10 minutes at 25°C, washed again and covered with Vectashield.

Expression Analysis Systematic Explorer (EASE) analysis

Statistical measurement of GO term enrichment comparing genes differentially expressed to genes expressed in developmentally matched w^{1118} controls was determined using an EASE score ($P < 0.05$) [9].

Ingenuity IPA analysis

Data sets containing identifiers for the human orthologues of differentially expressed (DE) *Drosophila* genes were uploaded into Ingenuity IPA. Each identifier was mapped to its corresponding object in the Ingenuity Knowledge Base. Network Eligible molecules, were overlaid onto a global molecular network developed from information contained in the Ingenuity Knowledge Base. Networks were algorithmically generated from Network Eligible Molecules based on their connectivity. All edges are supported by at least one reference from the literature, from a textbook, or from canonical information stored in the Ingenuity Knowledge Base. The generated networks were used by IPA to automatically predict 'upstream regulators' of DE genes. The term "upstream regulator" refers to any molecule that can affect the expression of another molecule. Upstream regulators cover the gamut of molecule types founds in the literature, from transcription factors, to cytokines, microRNAs, receptors, kinases, chemicals and drugs. Upstream Regulator Analysis is based on expected causal effects between Upstream regulators and targets; the expected causal effects are derived from the literature compiled in the Ingenuity Knowledge Base. The analysis examines the known targets of each upstream regulator in the dataset, compares the targets' actual direction of change to expectations derived from the literature, then issues a prediction for each upstream regulator. IPA uses a z-score algorithm to make predictions. The z-score algorithm is designed to reduce the chance that random data will generate significant predictions.

Oligonucleotide primer sequences

Name	Sequence (5'-3')	Purpose
PNUTSATGex+	ACGCAGGAGTTTTCGGAGAG	Mutant characterisation
PNUTSATGex-	ATTGTGGAGACCCTCGGTGA	Mutant characterisation
PNUTS3ex+	GCTGCCCGAGTGTGAGTCTA	Mutant characterisation
PNUTS3ex-	GTTCGGTTTAATGGCAAACGTAATG	Mutant characterisation
PNUTS Fw	GCCAAGATCGACATCAACAA	qRT-PCR
PNUTS Rev	CTTGCGCTTCACCACCTT	qRT-PCR
dPNUTS-S Fw	GGATCGAGTTTGAACTGCAAG	qRT-PCR
dPNUTS-S Rev	AACATCAGGCAGCGACAAC	qRT-PCR
Thor Fw	AACCCTCTACTCCACCACTCC	qRT-PCR
Thor Rev	ACTTGCGGAAGGGAGTACG	qRT-PCR
Hid Fw	GGCCGTAAAGTTGTCGTAGC	qRT-PCR
Hid Rev	GACCTCCACGCCGTTATC	qRT-PCR
RPI135 Fw	ACCGTGCGGACTGTTAAATC	qRT-PCR
RPI135 Rev	GACCCAAGTGTTTGCCATCT	qRT-PCR
Nop56 Fw	CAACTGATCCAGCAAAGCAA	qRT-PCR
Nop56 Rev	TCCAGTGCAGTCACTTTGGA	qRT-PCR
Hoip Fw	CCATCGAGATTCTGCTCCAT	qRT-PCR
Hoip Rev	GTGATCTGCGACTTGAGCTG	qRT-PCR
CG6712 Fw	CGACGACAAGAAGACACGAA	qRT-PCR
CG6712 Rev	AGATTGGCCACCTCTGTTTG	qRT-PCR
CG4038 Fw	GAGGAGGACGAGGATTTGGT	qRT-PCR
CG4038 Rev	GGTCGTTTTGGCAGGAGTAA	qRT-PCR
CG6388 Fw	ATCCGGATATTTGTGCGTGT	qRT-PCR
CG6388 Rev	CTTCAGCTGCTGGGGATTAC	qRT-PCR
CG18600 Fw	GGCCAAACATGACTTGAGGT	qRT-PCR
CG18600 Rev	ACAAGGAGGCAACCAAAGTG	qRT-PCR
CG3756 Fw	GAGGAGTATCGGGTGAAGCA	qRT-PCR
CG3756 Rev	ATTTGCAATGGCGGGATAC	qRT-PCR
Tpi FW	CTTGGAGATGTTGTCGCTCA	qRT-PCR
Tpi Rev	CCTACGCCCAGAAGATCAAG	qRT-PCR
GAPDH2 Fw	GGTGATCAACGACAACTTCG	qRT-PCR
GAPDH2 Rev	CCAGTGGAAGCTGGAATGAT	qRT-PCR
ImpL3 Fw	CTTGACCACGGATGTCACAC	qRT-PCR
ImpL3 Rev	GATACACCTCCTGGGCCATT	qRT-PCR
CG3523 Fw	CCACCATCGAGGAGTTCAAG	qRT-PCR
CG3523 Rev	CACCGAAGAACTGTTGGTCA	qRT-PCR
CG11198 Fw	TACGAGAGCCAGTCGAGGAT	qRT-PCR
CG11198 Rev	GGCTATGCTGCGCTTAACA	qRT-PCR
18S Fw	CGCAAGATCGTTATATTGGTTG	qRT-PCR
18S Rev	GCTGCCTTCCTTAGATGTGG	qRT-PCR
RpII215 Fw	ACCAGCTAGGCGACATTCC	qRT-PCR
RpII 215 Rev	GATCGACACCGAGCATGAC	qRT-PCR

p53 Fw	GGACTTGCGCTTCTTGCTAT	qRT-PCR
p53 Rev	TGTATCGGGCGAAAAGAAAC	qRT-PCR
Thor-S Fw	CATAGCAGCCACACAAGCTC	qPCR (from ChIP)
Thor-S Rev	GGTGAAGCGGACATCTTAGC	qPCR (from ChIP)
Thor-M Fw	TTATCTACGAGCGGGCTTTC	qPCR (from ChIP)
Thor-M Rev	ACTTGCGGAAGGGAGTACG	qPCR (from ChIP)
ImpL3-S Fw	GGGCCAACAGACTGTCCTTA	qPCR (from ChIP)
ImpL3-S Rev	AATCATAGGCACGTGATAGCAA	qPCR (from ChIP)
ImpL3-M Fw	ATCACCTCGTAGGCGGAGT	qPCR (from ChIP)
ImpL3-M Rev	CGTTTGGTCTGGAGTGAACA	qPCR (from ChIP)
nop56-S Fw	TGCCGAATATATGCCGATTT	qPCR (from ChIP)
nop56-S Rev	GGCTTGCTATGGTCACACTTG	qPCR (from ChIP)
nop56-M Fw	CGTATTGGAGCGGGTCTTTA	qPCR (from ChIP)
nop56-M Rev	GCACCCAATCTGCAGTCTTT	qPCR (from ChIP)
CAA-S Fw	AGCTCGCTTTACCACTCTGC	qPCR (from ChIP)
CAA-S Rev	CATCTACAAATCGTGCGGAAC	qPCR (from ChIP)
CAA-M Fw	CCACGCATTTGTCGTAGTGT	qPCR (from ChIP)
CAA-M Rev	CAGCGCTATAGGAACGGAAT	qPCR (from ChIP)

3.6. Supplementary References

1. Bennett, D. and L. Alphey, *PP1 binds Sara and negatively regulates Dpp signaling in Drosophila melanogaster.* Nat. Genet., 2002. **31**(4): p. 419-423.

2. Bennett, D., B. Szöor, and L. Alphey, *The chaperone-like properties of mammalian Inhibitor-2 are conserved in a Drosophila homologue.* Biochemistry, 1999. **38**(49): p. 16276-16282.

3. Alphey, L., *PCR-based method for isolation of full-length clones and splice variants from cDNA libraries.* BioTech., 1997. **22**: p. 481-486.

4. Brown, N. and F. Kafatos, *Functional cDNA libraries from Drosophila embryos.* J. Mol. Biol., 1988. **203**: p. 425-437.

5. Alphey, L., *et al*., *KLP38B: a mitotic kinesin-related protein that binds PP1.* J. Cell Biol., 1997. **138**(2): p. 395-409.

6. Stock, J.K., *et al*., *Ring1-mediated ubiquitination of H2A restrains poised RNA polymerase II at bivalent genes in mouse ES cells.* Nat Cell Biol, 2007. **9**(12): p. 1428-35.

7. Zsindely, N., *et al*., *The loss of histone H3 lysine 9 acetylation due to dSAGA-specific dAda2b mutation influences the expression of only a small subset of genes.* Nucleic Acids Res, 2009. **37**(20): p. 6665-80.

8. Ciurciu, A., *et al*., *The Drosophila histone acetyltransferase Gcn5 and transcriptional adaptor Ada2a are involved in nucleosomal histone H4 acetylation.* Mol Cell Biol, 2006. **26**(24): p. 9413-23.

9. Hosack, D.A., *et al*., *Identifying biological themes within lists of genes with EASE.* Genome Biol, 2003. **4**(10): p. R70.

3.7. Further discussion

The work in this chapter reports on the characterisation of *dPNUTS* function, showing it is essential for proper growth and development through regulation of genes involved in various metabolic pathways necessary for sustainable growth. RNAPII was identified as a dPNUTS-associated protein and a potential substrate of dPNUTS-PP1, specifically Serine 5 in the CTD of RNAPII. It was originally hypothesised that dPNUTS regulates gene expression through control of RNAPII CTD phosphorylation and occupancy. However, ChIP analysis did not provide any evidence of this, as the distribution of chromatin-bound RNAPII was not affected in regulated genes. It is possible the genes studied are not direct targets of dPNUTS. Mapping of chromatin sites bound by PNUTS would need to be done using either ChIP or DNA adenine methyltransferase Identification (DamID). Mathieu Bollen and his lab are currently taking the latter approach for mammalian PNUTS (communication from Daimark Bennett). DamID is a powerful tool for studying chromatin-protein interactions. It allows detection of binding sites using a methylation-based approach whereby a protein of interest is fused to a bacterial DNA adenine methyltransferase and expressed in cells or transgenic animals (Orian, 2006; Greil *et al*., 2006). Any sites bound by the protein of interest become methylated and subsequently identified using the Dpn1 restriction enzyme, which cleaves the sequence GATC when adenine is methylated (Orian, 2006; Greil *et al*., 2006). Microarray analysis can then be used to identify these fragments (Orian, 2006).

The interaction of PNUTS with Wdr82 and TOX4 may offer more insight into the mechanisms underlying the observed effects on gene expression given that this complex has been implicated in transcriptional regulation (Lee *et al*., 2010; Lee *et*

al., 2009). Wdr82 is a highly conserved WD40 repeat protein with human Wdr82 being 93% similar to *Drosophila* Wdr82 (Lee and Skalnik, 2008). It is involved in the regulation of H3K4 di- and tri-methylation by directly recruiting the Set1 methyltransferase complex, COMPASS. H3K4 di- and tri-methylation is necessary for the recruitment of RNAPII to promoter regions (Chen, *et al*. 2011; Lee and Skalnik, 2008). It is possible that under normal conditions Wdr82 recruits PNUTS-PP1 to actively dephosphorylate RNAPII Ser5 and allow progression through the transcription cycle. However, PP1 is not the only Ser5 phosphatase, for example the Ssu72 phosphatase also targets Ser5 for dephosphorylation and redundant mechanisms may be in place such that RNAPII occupancy is not affected in the *dPNUTS* mutant (Rosado-Lugo and Hampsey, 2014; Krishnamurthy *et al*., 2004). Interestingly, depletion of human Wdr82 in mammalian cells also does not affect RNAPII occupancy (Lee and Skalnik, 2008).

It is possible other processes that determine gene expression are affected in the *dPNUTS* mutants especially considering RNAPII CTD phosphorylation is responsible for coupling transcription to RNA processing predominantly through recruitment of 5' capping factors via phosphorylated Ser5 (Bentley, 2005). Determining the effect of PNUTS on capping using cap trapping approaches, whereby 5' caps are tagged for subsequent purification and identification of capped mRNAs, may offer more insight into its role in RNAPII mediated gene expression (Efimov *et al*., 2001).

The fact there is not complete co-localisation of RNAPII and dPNUTS on chromosomes suggests other chromatin bound dPNUTS-PP1 complexes may exist to

regulate gene expression. However, the factors responsible for recruiting dPNUTS to these sites, remains to be determined. In the case of the PNUTS-PP1/Wdr82/TOX4 complex reported in mammals, both TOX4 and Wdr82 as well as PNUTS were shown to associate with chromatin, therefore Wdr82 or TOX4 could mediate the interaction with chromatin (Lee *et al*., 2010). If the relationship between PNUTS and TOX4/Wdr82 is conserved in *Drosophila*, this could provide a mechanistic insight into the role of dPNUTS in gene expression. Identification of dPNUTS interacting proteins is necessary to understand the mechanisms underlying its role in gene expression as well as its association with chromosomal sites not marked by RNAPII.

4. Identifying PNUTS interacting proteins in *Drosophila*

4.1. Introduction

Human PNUTS associates with chromatin during interphase and telophase (Landsverk *et al*., 2005). It has been reported to be capable of binding RNA and ssDNA through RGG motifs, histidine/glycine repeats and a Zinc-finger motif at its extreme C-terminus (Kim *et al*., 2003). However, it is unclear what role these domains of PNUTS play in chromatin binding. dPNUTS is also chromosome-associated (Ciurciu *et al*., 2013). Notably, the short dPNUTS isoform, which lacks the C-terminal half of the protein, shows a similar distribution to the full-length dPNUTS isoform on chromosomes. Since this region does not possess DNA-binding ability, it has raised the possibility that the N-terminus of dPNUTS associates with other proteins that are responsible for directing the PP1 binding protein to particular substrates and chromatin-associated processes. The identification of dPNUTS-interacting proteins may offer further insight into mechanisms behind its role in RNAPII-mediated gene expression and cell growth.

In vitro studies using mammalian cell lines have identified a small number of proteins that interact with PNUTS and revealed complexes PNUTS-PP1 may be involved in that have implicated the protein in novel processes (Lee *et al*., 2010; Kavela *et al*., 2013). In a screen looking for PTEN-associated proteins, Kavela *et al.,* found that PNUTS directly interacts with the lipid binding domain (C2 domain) of PTEN and sequesters it to the nucleus, away from its normal membrane-associated location (Kavela *et al*., 2013). *PTEN* is a well-described tumour suppressor gene that negatively regulates the ability of the PI3K/Akt pathway to promote cell growth and survival (Maehama and Dixon, 1998). PTEN is a dual specificity phosphatase that

has many protein and lipid targets, but its tumour suppressor activity is mediated through one of its lipid substrates, phosphatidylinositol-4,5-triphosphate (PIP3), which is required for the downstream activation of the Akt pathway (Maehama *et al*., 2004; Myers *et al*., 1997). PTEN dephosphorylates PIP3 to phosphatidylinositol-4,5-bisphosphate (PIP2) at the cellular membrane, thus preventing activation of the Akt pathway and cell growth. Due to its ability to negatively regulate PTEN by sequestration, PNUTS has been described as a proto-oncogene (Kavela *et al*., 2013). Currently it is not known if the interaction between PNUTS and PTEN is conserved in *Drosophila*, which might have relevance to the growth phenotype observed in animals mutant for *dPNUTS*.

There is an increasing amount of evidence that PNUTS-PP1 exists in a complex with TOX4/Langerhans Cell Protein 1 (LCP1) and Wdr82. In 2006, Trinkle-Mulcahy *et al.*, identified PNUTS, LCP1 and Wdr82 as PP1-associated proteins by mass spectrometry analysis (Trinkle-Mulcahy *et al*., 2006). Then in 2009, Lee *et al.*, reported that the N-terminus of PNUTS binds to the C-terminus of LCP1 and suggested the complex has a role in mediating transcriptional activation (Lee *et al*., 2009). Using a GAL4-based transcription assay they showed the N-terminus of LCP1 has a trans-activation domain that is inhibited by its interaction with PNUTS (Lee *et al*., 2009). It has since been shown that PNUTS-PP1 exists in a complex with TOX4 (LCP1) and Wdr82, with PNUTS acting as a molecular platform for complex formation (Lee *et al*., 2010). They suggested PNUTS predominantly associates with this complex therefore it may mediate the activity of PNUTS in different cellular processes such as chromosome decondensation and cell cycle progression as biochemical analysis showed all three proteins associate with chromatin (Lee *et al*.,

2010). PNUTS, TOX4 and Wdr82 were also identified in a screen looking for proteins that associate with sites of damaged DNA, implicating the complex in the DNA damage response (Puch *et al*., 2011). LCP1 (TOX4) is a HMG-box protein, which physically binds to DNA (see Chapter 5 for more details) (O'Flaherty and Kaye, 2003; Lee *et al*., 2009). It is therefore conceivable that TOX4 recruits PNUTS to chromatin.

In an attempt to understand more about dPNUTS-PP1 and the complexes it associates with, a yeast two-hybrid (Y2H) approach was used to identify proteins that interact with dPNUTS in *Drosophila.* Y2H assays (both an initial screen and subsequent experiments in this system) were carried out on a collaborative basis by Hybrigenics Services (Paris, France). Although PNUTS-binding proteins have been characterised to some extent in mammalian cells, *Drosophila* offers a more practical system in which to study interacting proteins due to its genetic tractability and the availability of various tools for cell biology experiments.

4.1.1. Identifying protein interactions using the Y2H system

Since its development by Fields and Song in 1989, the Y2H system has become a powerful and popular technique for identifying protein-protein interactions. It allows detection of binding partners using living yeast cells (*Saccharomyces cerevisiae*) and a transcriptional activation response that exploits the properties of the GAL4 transcriptional activator (Brückner *et al*., 2009). GAL4 has an N-terminal DNA binding domain (DBD) and a C-terminal activation domain (AD), which are both required for transcriptional activation of target genes. The original Y2H assay involved fusing two proteins of interest, X and Y, to the DBD and AD of GAL4

respectively, creating a functional GAL4, which drives the expression of a reporter gene through RNAPII mediated transcription, if the two proteins bind (Fields and Song, 1989). The most common reporter genes used encode proteins that allow growth on minimal media (auxotrophic markers) and include genes such as *HIS3*, which encodes imidazole glycerol phosphate (IGP) dehydratase, and allows growth on media lacking histidine (Brückner *et al*., 2009). Since then, other DNA binding proteins have been exploited including the *E.coli* transcription factor LexA, the DBD of which can be fused to the AD of GAL4 to form a fully functional transcription activator in yeast (Van Criekinge and Beyaert, 1999).

The main advantage of using the Y2H assay is it allows detection of proteins that bind directly, unlike other methods for studying protein-protein interactions, such as immunoprecipitation, which do not provide conclusive evidence of a direct interaction. Nevertheless it is important to recognise there are several limitations of this approach; the Y2H assay is based on overexpression of proteins of interest in yeast and may lead to false positives due to high concentrations of fusion proteins, which may under normal conditions not bind or be co-expressed.

4.1.2. Aims

The aim of this chapter was to validate and better characterise dPNUTS-interacting proteins, which were identified in the Y2H system, using biochemical techniques. In parallel, interactions between *Drosophila* orthologues of PTEN and PNUTS were examined to determine whether binding between these proteins is conserved in flies.

4.2. Identification of PNUTS interacting proteins by Y2H

To identify proteins that bind to dPNUTS the Y2H method was used to screen a *Drosophila* 3rd instar larvae cDNA library using the full-length dPNUTS (amino acids 1-1135) protein as 'bait' fused to the LexA DBD of plasmid pB27. The screen, carried out by Hybrigenics Services (Paris, France), analysed $6.1x10^7$ interactions and 351 positive clones were processed, and found to encode a total of 54 proteins. Each protein identified was assigned a Predicted Biological Score (PBS), which assesses the reliability of the interaction and is an e-value ranging from 0 to 1 calculated by comparing the number of prey fragments identified for each interacting proteins to the probability of finding them at random (Rain *et al*., 2001; Formstecher, 2005). For practicality, the e-values are arbitrarily defined into ranks from A to E with A being the highest confidence rank (closest to 0) and E most likely being artefacts from the assay (Rain *et al*., 2001). Hybrigenics also carried out domain analysis on each identified protein and provided information on the selected interaction domain, which corresponds to the minimal fragment capable of binding to dPNUTS. The majority of proteins (n=40) identified were assigned a predicted biological score of D, meaning they have a higher chance of being a false positive interaction as they were generally only identified through one unique prey fragment. All proteins assigned a score of A, B or C are shown in Table 4.1.

61 of the 351 positive clones encoded the same unnamed protein, CG12104 (250 aa), which was the only protein given a confidence score of A. Domain analysis identified this as a High Mobility Group Box protein (Appendix 7) and fragment analysis revealed dPNUTS interacts with the C-terminus (amino acids 206-246) (Table 4.1). Phylogenetic analysis and sequence alignments indicate that CG12104 is

the *Drosophila* orthologue of LCP1/TOX4 (see Chapter 5). It is possible CG12104 is the only orthologue as other *Drosophila* proteins have not been identified that contain a HMG-box with similarity to the TOX family (O'Flaherty and Kaye, 2003). Therefore CG12104 will be referred to as dTOX4 hereafter. Another HMG-box containing protein, Sox14, was also identified (represented by 8 clones and given a confidence score of B). Other proteins given a confidence score of B included P32, a mitochondrial protein that may function in RNA splicing and apoptosis; MBD-R2, a component of the Non-specific Lethal (NSL) complex which binds DNA and is associated with active transcription; and Msr-110, which may be a target of microRNA miR-1-mediated post-transcriptional regulation (see Table 4.1 for references). Finally, two proteins identified were given a confidence score of C: Estrogen-Related Receptor (ERR, CG7404), a nuclear receptor involved in transcription and metabolism and ArgK, an arginine kinase (see Table 4.1 for references).

Table 4.1. The top hits from a Y2H screen using full length PNUTS as bait. The number of clones identified in the screen for each protein together with predicted biological score (assigned by Hybrigenics) and the selected interaction domain is shown.

Protein Name (FlyBase)	Length (aa)	Number of clones Identified	Predicted Biological Score	Selected Interaction Domain	Description	Reference
CG12104	250	61	A	206-246	*Drosophila* TOX4, HMG-box domain binds to sequence independent DNA structures, DNA bending	(O'Flaherty and Kaye, 2003; Stros *et al*., 2007)
MBD-R2 (CG10042)	1081	4	B	862-1081	Part of NSL complex involved in transcription regulation, DNA binding, associated with active chromatin states	(Raja *et al*., 2010; Lam *et al*., 2012)
Sox14 (CG3090)	669	8	B	161-282	Transcription factor, HMG-box domain, component of 20E signalling pathway – regulates metamorphosis	(Ritter and Beckstead, 2010)
P32 (CG6459)	263	6	B	145-263	Mitochondrial protein, may function in RNA splicing, mitochondrial oxidative phosphorylation and apoptosis	(Lutas *et al*., 2012)
Msr-110 (CG10596)	608	3	B	147-244	Target of microRNA miR-1, post-transcriptionally regulated by miR-1	(Easow *et al*., 2007)
Estrogen-Related Receptor (ERR) (CG7404)	496	3	C	93-292	Nuclear receptor, transcription factor, regulates growth and metabolism	(Tennessen *et al*., 2011)
Argk (CG32031)	396	3	C	371-396	Arginine kinase activity	

4.3. Characterisation of the interaction between dPNUTS and dTOX4

To verify the interaction between dPNUTS and the C-terminal region of dTOX4 a direct one-by-one Y2H assay was performed using full length dPNUTS (aa 1-1135) cloned in frame with the LexA DNA binding domain into plasmid pB27 and a dTOX4 fragment (aa 179-250) extracted from the original screen (see 4.2) cloned in frame with the Gal4 Activation Domain into plasmid pP7. Selective medium without tryptophan and leucine (DO-2) was used to select for the presence of the two plasmids and selective medium without tryptophan, leucine and histidine (DO-3) was used to select for an interaction. To increase stringency and reduce autoactivation by PNUTS an inhibitor (3-aminotriazol [3-AT]) of the reporter gene, *HIS3*, was used at increasing concentrations. Figure 4.1 shows that even at the highest concentration of 3-AT (50mM) and on selective medium, an interaction between dPNUTS and the C-terminus of dTOX4 is still detectable suggesting they bind with high affinity.

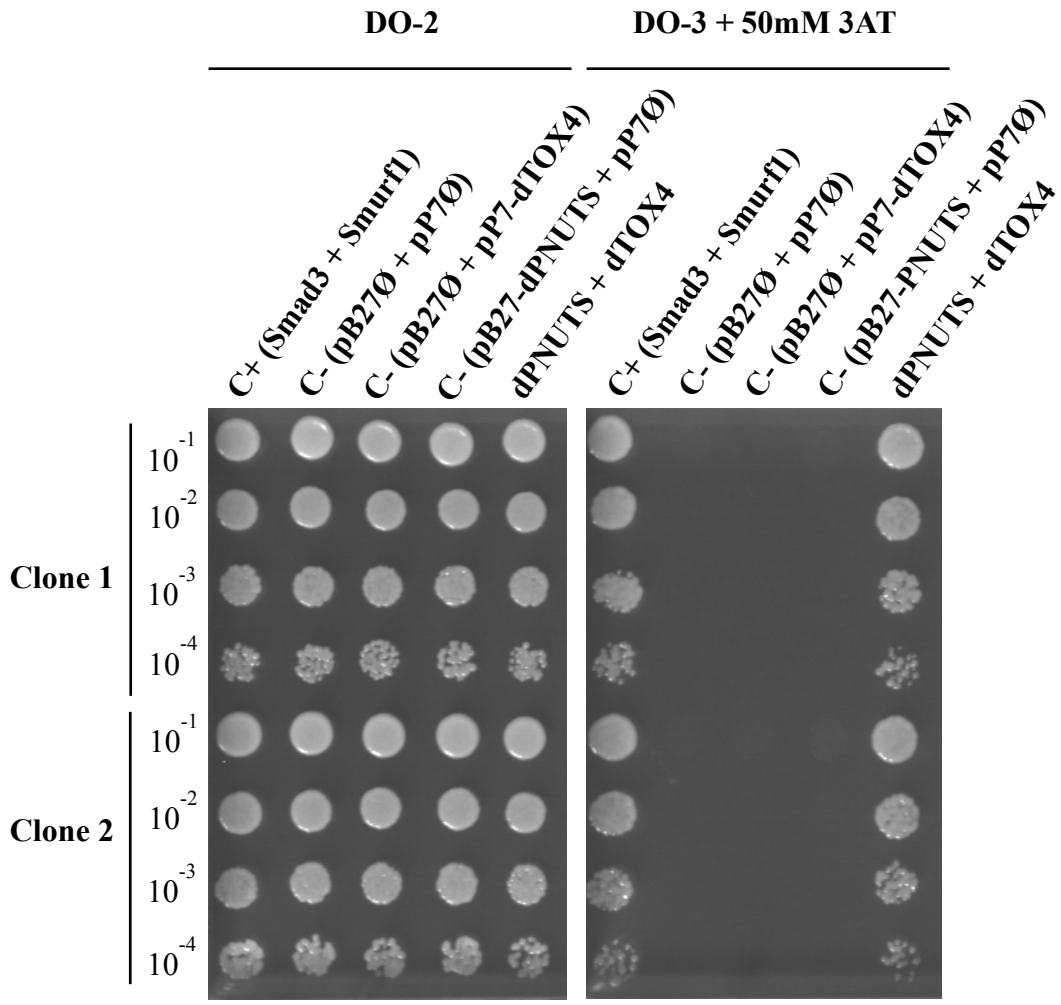

Figure 4.1. dPNUTS binds to the C-terminus of dTOX4 in the Y2H assay. Yeast two hybrid analysis showing presence of interaction between dPNUTS (in pB27) and dTOX4 (in pP7). Interaction pairs were tested in duplicate (clone 1 and clone 2) on several dilutions (10^{-1}, 10^{-2}, 10^{-3}, 10^{-4}, normalised at $5x10^4$ cells). Cells were grown on selective medium without tryptophan and leucine (DO-2) and selective medium without tryptophan, leucine and histidine (DO-3). 3-aminotriazol (3-AT) was used at various concentrations to increase stringency and test the affinity of binding. The highest concentration used (50mM) is shown. C+ = Hybrigenics interaction positive control, C- = negative controls. ∅ specifies empty vector.

Having confirmed the C-terminus of dTOX4 is essential for its interaction with dPNUTS, a dTOX4 mutant construct was made by site-directed mutagenesis to remove the dPNUTS-binding region for future characterisation of the interaction. To do this, a two base pair change was introduced that generated a premature stop codon in place of Proline 216, removing the last 34 residues of dTOX4 and the dPNUTS-binding region (Figure 4.2). Mutagenesis was performed by BioPioneer (San Diego, USA) on a pENTR^{TM} entry (Gateway®) vector containing the *Drosophila* dTOX4 coding sequence.

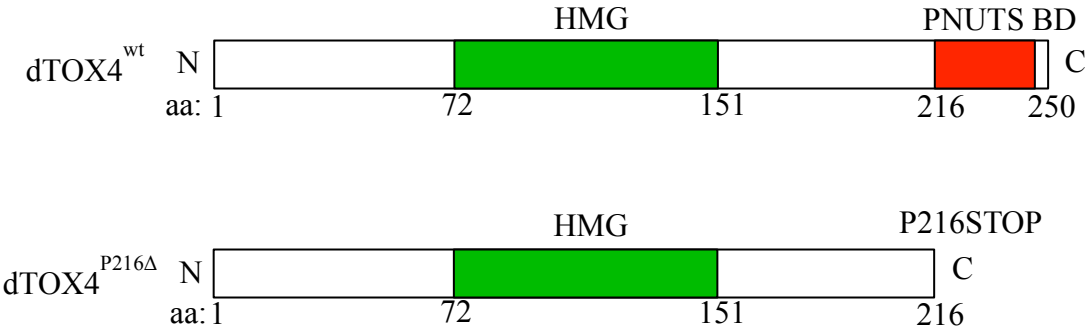

Figure 4.2. Map of dTOX4. Map of wild type dTOX4 (dTOX4^{wt}) protein with the PNUTS Binding Domain (BD) in red and the site-directed mutant (dTOX4$^{P216\Delta}$) with a premature stop codon, which gives a truncated protein lacking the PNUTS binding domain.

To provide further confirmation that dPNUTS binds dTOX4 and to test binding of dPNUTS to the dTOX4$^{P216\Delta}$ construct, tagged expression constructs were made that could be used in co-immunoprecipitation (co-IP) experiments and co-localisation studies. The Bennett lab had already generated a construct for dPNUTS conjugated

to a C-terminal Myc tag in the Gateway® entry vector pDONR221, so this was subcloned into an appropriate S2 cell expression vector, pAW, for co-IP experiments. For the purposes of co-localisation studies in S2 cells, the dPNUTS-Myc construct was also cloned into an N-terminal Red Fluorescent Protein (RFP) tagged S2 cell expression vector, pARW. The dTOX4 cDNA sequence was PCR amplified from the BDGP gold cDNA clone LP01188 and cloned into the pENTR entry vector, which was also used to generate the dTOX4$^{P216\Delta}$, as previously described and checked by sequencing. The dTOX4^{wt} and dTOX4$^{P216\Delta}$ were then subcloned into an N-terminal GFP tagged S2 cell expression vector, pAGW for the purposes of co-IP experiments and co-localisation studies.

4.3.1. Co-immunoprecipitation of dPNUTS and dTOX4 in S2R+ cells

For co-IP experiments, *Drosophila* S2R+ cells were transiently transfected with either GFP-dTOX4^{wt}, dPNUTS-Myc (control in figure 4.3) or co-transfected with GFP-dTOX4^{wt} and dPNUTS-Myc. Immunoprecipitation of GFP-dTOX4^{wt} from transfected cells, using a magnetic GFP trap resulted in co-precipitation of dPNUTS-Myc as detected by an anti-Myc antibody on a Western blot (Figure 4.3a). The same experiment was done using GFP-dTOX4$^{P216\Delta}$, which showed the site-directed mutant was unable to co-precipitate dPNUTS-Myc (Figure 4.3a), confirming it lacks the dPNUTS binding domain. The experiment was repeated to confirm the results and also to check expression of the GFP-dTOX4 constructs, having found a suitable anti-GFP antibody (Figure 4.3b). Again dPNUTS-Myc was detected in immunoprecipitated GFP-dTOX4^{wt} extracts when blotted with an anti-Myc antibody but not in GFP-dTOX4$^{P216\Delta}$ extracts (Figure 4.3b). Blotting with an anti-GFP antibody (Clontech) confirmed expression of the GFP-dTOX4 constructs and also

revealed dTOX4$^{P216\Delta}$ expresses a truncated protein with a lower molecular weight (Figure 4.3b, 67kDa vs. 59kDa).

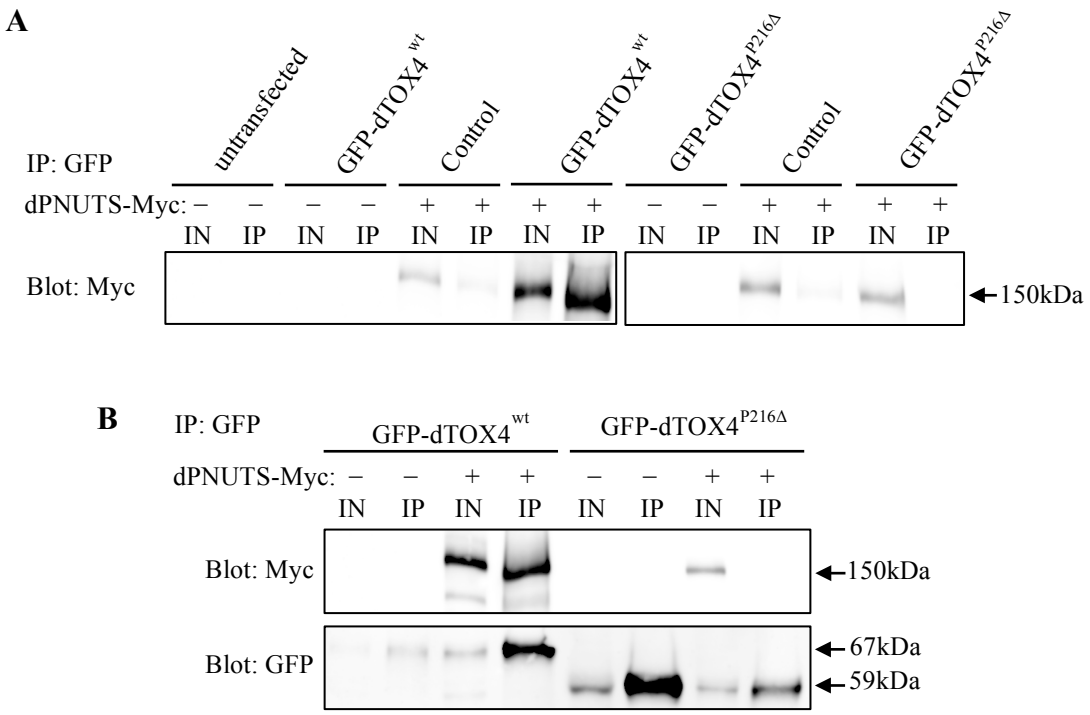

Figure 4.3. dPNUTS binds to dTOX4 in *Drosophila* S2R+ cells. a) Western blot showing Myc-tagged dPNUTS co-immunoprecipitates with GFP-tagged dTOX4^{wt} but not GFP-dTOX4$^{P216\Delta}$. Immunoblot analysis of total protein extract (IN) and immunoprecipitated protein extract (IP) from S2R+ cells co- transfected with GFP-dTOX4 (^{wt} or $^{P216\Delta}$) and dPNUTS-Myc or with each expression vector alone and blotted with anti-Myc antibody. b) A repeat of experiment in (a) showing dPNUTS precipitates with dTOX4^{wt} but not dTOX4$^{P216\Delta}$ as shown by immunoblotting with anti-Myc. Immunoblotting with anti-GFP shows presence of GFP-dTOX4 constructs in total extracts.

4.3.2. Nuclear colocalisation of dPNUTS and dTOX4 in S2R+ cells

dPNUTS is a nuclear protein that binds to chromosomes during interphase (Ciurciu *et al*., 2013). To confirm that dTOX4 binds to dPNUTS in the nucleus, S2R+ cells were transiently co-transfected with RFP-dPNUTS-Myc and GFP-dTOX4^{wt} or with GFP-dTOX4^{wt} alone and imaged using confocal microscopy. Single transfection of dTOX4^{wt} revealed it is localised in the nucleus and the cytoplasm, with a higher level of localisation in the nucleus (Figure 4.4a, top row, GFP panel). Upon co-transfection with RFP-dPNUTS, GFP-dTOX4^{wt} became exclusively localised in the nucleus and co-localised with RFP-dPNUTS (Figure 4.4a top and second rows). To confirm this was due to the interaction between dPNUTS and dTOX4 and not a consequence of the GFP or RFP tags, GFP-dTOX4$^{P216\Delta}$ was co-transfected with RFP-dPNUTS. Similar to GFP-dTOX4^{wt}, GFP-dTOX4$^{P216\Delta}$ was localised in the nucleus and cytoplasm (Figure 4.4a, third row, GFP panel). However, upon co-transfection with RFP-dPNUTS, GFP-dTOX4$^{P216\Delta}$ did not relocate to the nucleus (Figure 4.4a, fourth row, RFP and GFP panels), indicating that the ability of ectopic dPNUTS to sequester dTOX4 in the nucleus is dependent on the presence of the dPNUTS-binding region in dTOX4.

To quantify the degree of co-localisation in co-transfected cells a line scan was performed to measure the fluorescent intensity of both GFP and RFP signals across the cell. In cells coexpressing GFP-dTOX4^{wt} and RFP-dPNUTS, the signal from each fluorescent tag largely overlapped, showing a large peak of co-localisation in the nucleus (Figure 4.4b). In cells coexpressing GFP-dTOX4$^{P216\Delta}$ and RFP-dPNUTS, the co-localisation plot showed a strong overlap in the nucleus followed by a drop in RFP-dPNUTS signal in the cytoplasm where the GFP-dTOX4$^{P216\Delta}$ signal remained

relatively high (Figure 4.4c). To determine the degree of overlap in the whole cell, co-localisation analysis was carried out using the JaCOP plugin in Fiji and Manders' coefficient analysis performed (Manders *et al*., 1993). Figure 4.4c shows GFP-dTOX4^{wt} signal strongly correlates with RFP-dPNUTS signal in the whole cell (Manders' coefficient M1=0.982, M2= 0.995). Figure 4.4e shows correlation is weaker in cells co-transfected with GFP-dTOX4$^{P216\Delta}$ and RFP-dPNUTS (Manders' coefficient M1= 0.488, M2=0.934). M1 is a ratio of the amount of GFP-dTOX4 overlapping with RFP-dPNUTS and M2 is a ratio of the amount of RFP-dPNUTS that overlaps with GFP-dTOX4. A value of 1 represents complete co-localisation.

Figure 4.4 (next page). dTOX4^{wt} relocates to the nucleus when co-expressed with dPNUTS. a) S2R+ cells were transfected with GFP-dTOX4^{wt} or GFP-dTOX4$^{P216\Delta}$ alone or in combination with RFP-dPNUTS. Staining with anti-actin was used to identify cell borders and staining with DAPI was used to identify the position of the nucleus. Cells were imaged using confocal microscopy. Scale bar = 5μm. b) Plot of normalised fluorescence intensity for GFP-dTOX4^{wt} and RFP-dPNUTS co-transfected cell measured along a line through the indicated cell in the image to the left (white arrow). c) Cytofluorogram showing fluorescence intensity across whole cell transfected with GFP-dTOX4^{wt} and RFP-dPNUTS. d) Plot of normalised fluorescence intensity for GFP-dTOX4$^{P216\Delta}$ and RFP-dPNUTS co-transfected cell measured along a line through the indicated cell in the image to the left (white arrow). e) Cytofluorogram showing fluorescence intensity across whole cell transfected with GFP-dTOX4$^{P216\Delta}$ and RFP-dPNUTS.

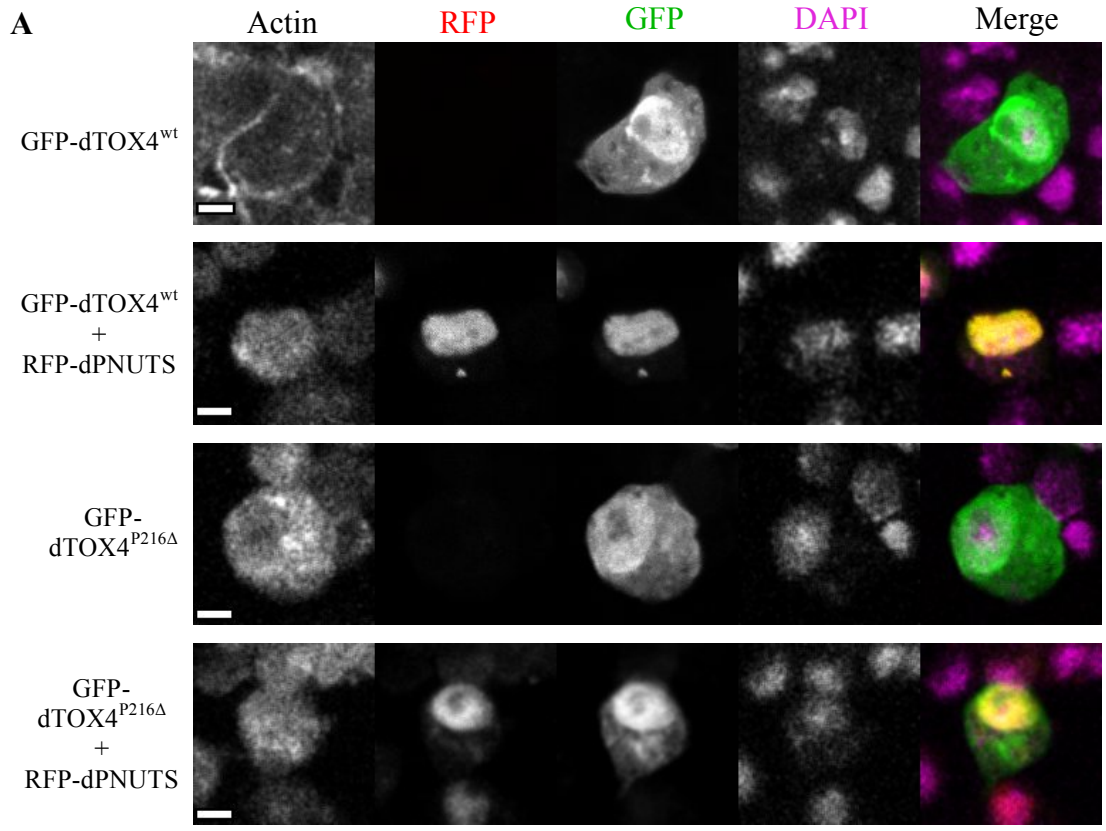
A
Actin
RFP
GFP
DAPI
Merge
GFP-dTOX4wt
GFP-dTOX4wt + RFP-dPNUTS
GFP-dTOX4P216Δ
GFP-dTOX4P216Δ + RFP-dPNUTS

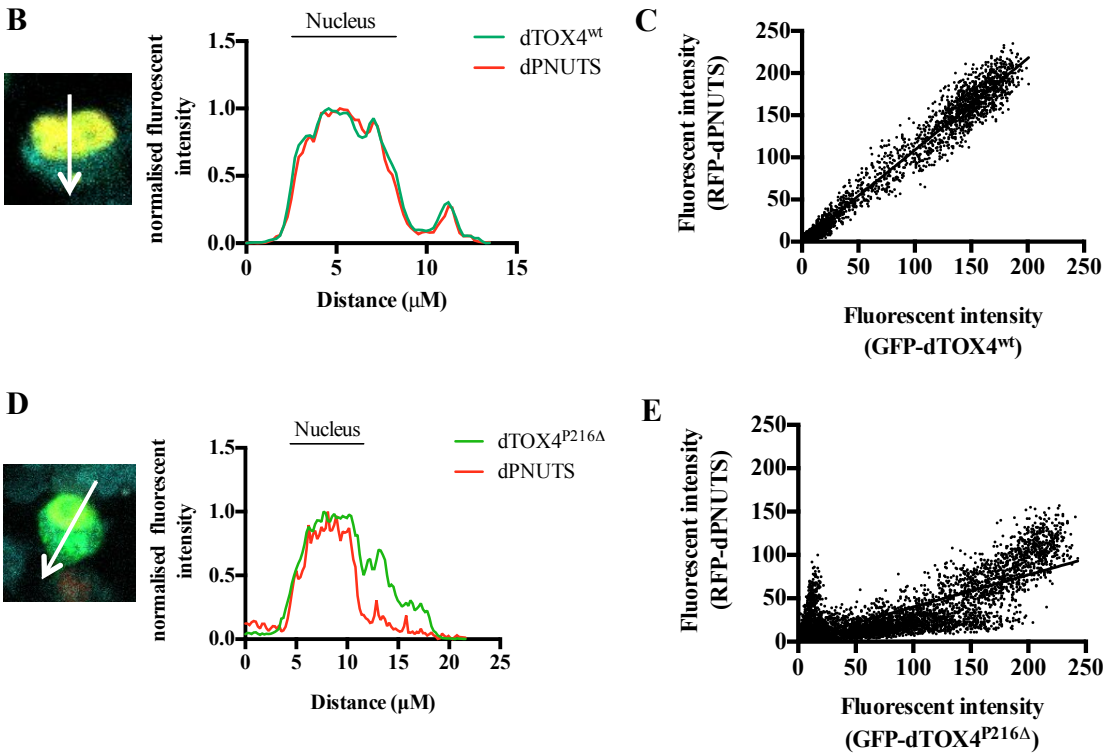
B
Nucleus
dTOX4wt
dPNUTS
normalised fluorescent intensity
Distance (μM)
C
Fluorescent intensity (RFP-dPNUTS)
Fluorescent intensity (GFP-dTOX4wt)
D
Nucleus
dTOX4P216Δ
dPNUTS
normalised fluorescent intensity
Distance (μM)
E
Fluorescent intensity (RFP-dPNUTS)
Fluorescent intensity (GFP-dTOX4P216Δ)

4.4. Characterisation of the interaction between dPNUTS and dMBD-R2

Only four clones of dMBD-R2 were identified in the initial yeast two-hybrid screen but, given its role transcription, the interaction between dPNUTS and dMBD-R2 was investigated further. In the initial screen it was found that dPNUTS binds to the C-terminus of dMBD-R2 (Table 4.1). To determine which part of dPNUTS interacts with dMBD-R2, a direct Y2H domain-mapping assay was done by Hybrigenics using fragments of dPNUTS and a fragment of dMBD-R2 (aa 950-1169) incorporating the minimal PNUTS-binding region, which was determined from the initial screen. The dMBD-R2 fragment was cloned in-frame with the Gal4 AD in plasmid pP7 and the dPNUTS fragments were cloned in-frame with the LexA DBD in plasmid pB27. Figure 4.5 gives a map of the dPNUTS fragments used in the assay and a summary of the interactions observed.

Figure 4.5. Schematic representation of the dPNUTS fragments used to determine dMBD-R2 binding site. Fragments with a positive interaction are indicated with a red + sign, fragments with a negative interaction are indicated with – sign.

Cells were grown on selective DO-2 and DO-3 medium with increasing concentrations of 3-AT. Figure 4.6 shows only full-length dPNUTS (fragment 1) and a fragment consisting of the first 147 amino acids of dPNUTS (fragment 2) binds to dMBD-R2 in the yeast two-hybrid assay. This interaction was only detectable when grown on plates with 1mM 3-AT suggesting the interaction is weak compared to binding between dPNUTS and dTOX4. Surprisingly fragment 7, which incorporates the N-terminus of dPNUTS, did not interact with dMBD-R2 (Figure 4.6). This is unexpected given fragment 1 and full-length dPNUTS do interact but might be because fragment 7 isn't expressed, it's unstable or it doesn't fold correctly. Together, these results confirm that dMBD-R2 binds to dPNUTS in the Y2H assay, albeit with low affinity, and indicate that binding is mediated by the N-terminus of dPNUTS.

DO-2
DO-3 + 1mM 3-AT
C+ (Smad/Smurf)
C- (pB27Ø/pP7Ø)
C- (pB27-dPNUTS frag 1 + pP7Ø)
C- (pB27-dPNUTS frag 3 + pP7Ø)
C- (pB27-dPNUTS frag 6 + pP7Ø)
dPNUTS frag 1 +-dMBD-R2
dPNUTS frag 2 + dMBD-R2
dPNUTS frag 3 + dMBD-R2
dPNUTS frag 4 + dMBD-R2
dPNUTS frag 6 + dMBD-R2
dPNUTS frag 7 + dMBD-R2
10-1
10-2
10-3
10-4
(Smad/Smurf) C+
(pB27Ø + pP7-dMBD-R2) C-
(pB27-dPNUTS frag 2 + pP7Ø) C-
(pB27-dPNUTS frag 4 + pP7Ø) C-
(pB27-dPNUTS frag 7 + pP7Ø) C-

Figure 4.6 (previous page). dMBD-R2 binds to the N-terminus of dPNUTS in a Y2H assay. Yeast two-hybrid analysis showing full-length dPNUTS (frag 1) and a dPNUTS fragment consisting of amino acids 1-147 (frag 2) bind to dMBD-R2. Interaction pairs were tested in duplicate on several dilutions (10^{-1}, 10^{-2}, 10^{-3}, 10^{-4}, normalised at $5x10^4$ cells). Cells were grown on selective medium without tryptophan and leucine (DO-2) and selective medium without tryptophan, leucine and histidine (DO-3). 3-aminotriazol (3-AT) was used at various concentrations to increase stringency and test the affinity of binding. Only the results for 1mM 3-AT are shown as no interaction was detected at higher concentrations. C+ = Hybrigenics interaction positive control, C- = negative controls. ∅ specifies empty vector.

4.4.1. Co-immunoprecipitation of dPNUTS and dMBD-R2 in S2R+ cells

To provide further confirmation that dPNUTS and dMBD-R2 bind to each other, a tagged expression construct was made for use in co-IP experiments. The dMBD-R2 cDNA sequence was PCR amplified from the BDGP gold cDNA clone SD10773, cloned into the pENTR Gateway® entry vector and checked by sequencing. This was then subcloned into an amino-terminal GFP tagged S2 cell expression vector, pAGW (DGRC) for co-IP experiments.

Immunoprecipitation of GFP-dMBD-R2 from transfected cells, using a magnetic GFP trap (Chromotek) resulted in co-precipitation of dPNUTS-Myc as detected by an anti-Myc antibody on a Western blot (Figure 4.7). It is important to note that problems with transfection efficiencies and controls meant that this result could not be repeated. However, this does provide preliminary evidence that dPNUTS and dMBD-R2 bind in S2R+ cells.

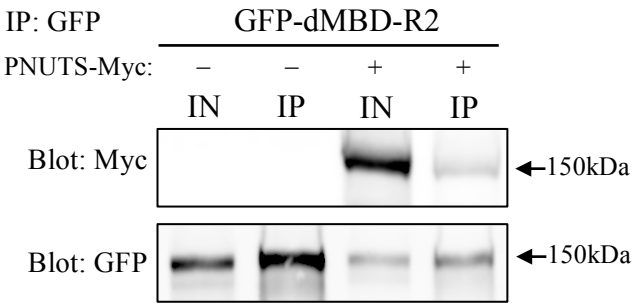

Figure 4.7. dPNUTS binds to dMBD-R2 in S2R+ cells. Western blot showing Myc tagged dPNUTS co-immunoprecipitates with GFP tagged MBD-R2. Immunoblot analysis of total protein extract (IN) and immunoprecipitated protein extract (IP) from S2R+ cells co- transfected with GFP-dMBD-R2 and dPNUTS-Myc or with GFP-dMBD-R2 alone and blotted with anti-Myc antibody. Immunoblotting with anti-GFP shows presence of GFP-dMBD-R2 in transfected cell extracts.

4.5. Characterisation of the interaction between dPNUTS and dERR

The estrogen related receptor is a nuclear hormone receptor that plays an important role in regulating development, growth and metabolism (Chawla *et al*., 2001). Given that genes involved in metabolism and proliferative growth were found to be significantly underexpressed in *dPNUTS* mutants (see Chapter 1), the interaction between dERR and dPNUTS was further characterised. Only three clones were identified in the initial screen and the interaction was only given a confidence score of C (Table 4.1). Therefore to confirm the interaction, a direct one-by-one yeast two-hybrid assay was done using full-length dPNUTS and fragments of dERR. dPNUTS was cloned in frame with the LexA DBD into plasmid pB27 and checked by sequencing. A prey fragment consisting of amino acids 93-309 of dERR (incorporating the Selected Interaction Domain) was extracted from the initial

screen, cloned in frame with the Gal4 AD into plasmid pP7 and checked by sequencing. The coding sequences for different dERR fragments were also cloned in frame with the Gal4 AD into plasmid pP7. Figure 4.8 gives a map of the dERR fragments used in the assay and a summary of the interactions observed.

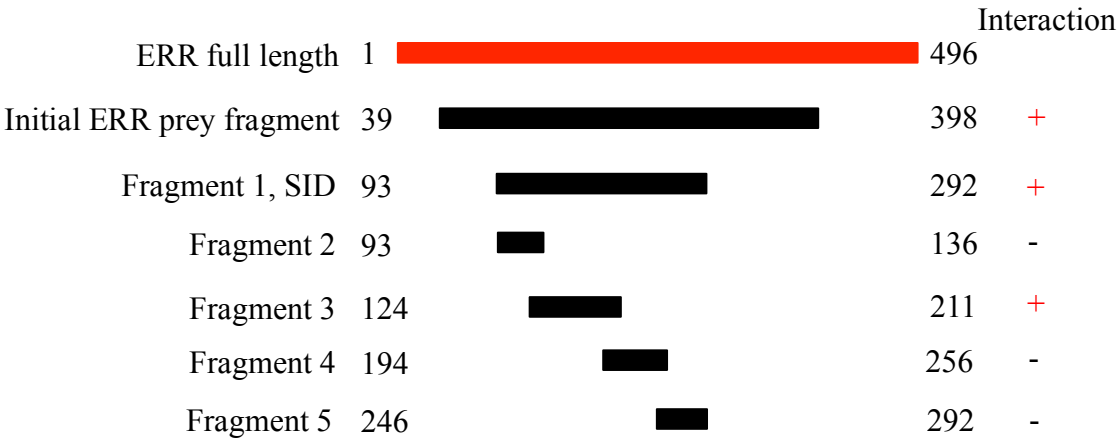

Figure 4.8. Schematic representation of the dERR fragments used to determine the dPNUTS-binding site. Fragments with a positive interaction are indicated with a red + sign, fragments with a negative interaction are indicated with – sign.

Cells were grown on selective DO-2 and DO-3 medium. Figure 4.9 shows an interaction was detectable between the initial dERR prey fragment and dPNUTS, confirming the results from the original screen. Fragment 1, the selected interaction domain identified in the original screen, also bound to dPNUTS together with fragment 3, which incorporates amino acids 124-211. Fragments 2, 4 and 5 did not interact with dPNUTS suggesting amino acids 124-211 are sufficient for dPNUTS binding.

Figure 4.9 (next page). dERR binds to dPNUTS in a Y2H assay. Yeast two hybrid analysis showing full-length dPNUTS and the initial prey fragment from the original screen (aa 39-398) interact with dPNUTS as does fragment 1 (aa 93-292) and fragment 3 (aa 124-211). Interaction pairs were tested in duplicate using several dilutions (10^{-1}, 10^{-2}, 10^{-3}, 10^{-4}, normalised at $5x10^4$ cells). Cells were grown on selective medium without tryptophan and leucine (DO-2) and selective medium without tryptophan, leucine and histidine (DO-3). C+ = Hybrigenics interaction positive control, C- = negative controls. ∅ specifies empty vector.

DO-2
dPNUTS + dERR initial prey clone
C- (pB27-dPNUTS + pP7Ø)
dPNUTS + dERR frag 1
C- (pB27Ø + dERR frag 1)
dPNUTS + dERR frag 2
C- (pB27Ø + dERR frag 2
dPNUTS +d ERR frag 3
C- (pB27Ø + dERR frag 3)
dPNUTS + dERR frag 4
C- (pB27Ø + dERR frag 4)
dPNUTS + dERR frag 5
C- (pB27Ø + dERR frag 5)
10-1
10-2
10-3
10-4
10-1
10-2
10-3
10-4
(pB27Ø + dERR initial prey clone) C-
DO-3
dPNUTS + dERR initial prey clone
C- (pB27-dPNUTS + pP7Ø)
dPNUTS + dERR frag 1
C- (pB27Ø + dERR frag 1)
dPNUTS + dERR frag 2
C- (pB27Ø + dERR frag 2
dPNUTS +d ERR frag 3
C- (pB27Ø + dERR frag 3)
dPNUTS + dERR frag 4
C- (pB27Ø + dERR frag 4)
dPNUTS + dERR frag 5
C- (pB27Ø + dERR frag 5)
10-1
10-2
10-3
10-4
10-1
10-2
10-3
10-4
(pB27Ø + dERR initial prey clone) C-

An attempt was made to identify the dERR-binding site in dPNUTS using a direct Y2H assay. Fragments of dPNUTS (Figure 4.10) were cloned in frame with the LexA DBD into plasmid pB27 and a fragment of dERR (aa 93-309) incorporating the PNUTS binding domain, which was extracted from the initial screen was cloned in frame with the Gal4 AD into plasmid pP7. Figure 4.10 gives a map of the dPNUTS fragments used in the assay and a summary of the interactions observed.

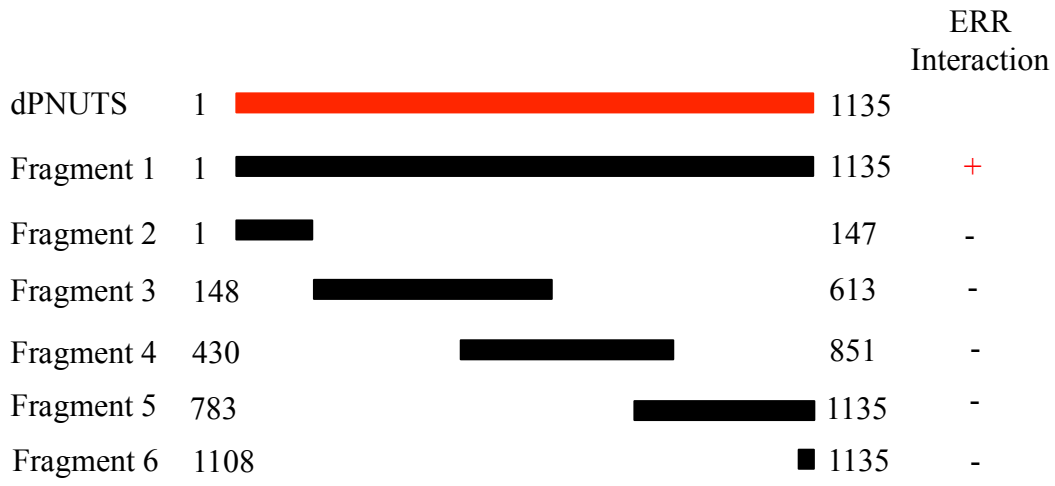

Figure 4.10. Schematic representation of the dPNUTS fragments used to determine dERR-binding site. Fragments with a positive interaction are indicated with a red + sign, fragments with a negative interaction are indicated with – sign.

Cells were grown on selective DO-2 and DO-3 medium with increasing concentrations of 3-AT. Figure 4.11 shows only full-length dPNUTS (fragment 1) binds to dERR in the Y2H assay. This interaction was detectable when grown on plates with up to 10mM 3-AT (only 1mM 3-AT shown) suggesting they bind with high affinity.

Figure 4.11 (next page). dERR binds to dPNUTS in a Y2H assay. Yeast two hybrid analysis showing full-length dPNUTS binds to a dERR prey fragment (aa 93-309). Interaction pairs were tested in duplicate using several dilutions (10^{-1}, 10^{-2}, 10^{-3}, 10^{-4}, normalised at $5x10^4$ cells). Cells were grown on selective medium without tryptophan and leucine (DO-2) and selective medium without tryptophan, leucine and histidine (DO-3). 3-aminotriazol (3-AT) was used at various concentrations to increase stringency and test the affinity of binding. Only the results for 1mM 3-AT are shown. C+ = Hybrigenics interaction positive control, C- = negative controls. ∅ specifies empty vector.

DO-2
dPNUTS frag 1+ dERR
C- (pB27-dPNUTS frag 1 + pP7Ø)
C- (pB27Ø + dERR)
C- (pB27-dPNUTS frag 3+ pP7Ø)
C- (pB27-dPNUTS frag 5+ pP7Ø)
dPNUTS frag 2 + dERR
dPNUTS frag 3 + dERR
dPNUTS frag 4 + dERR
dPNUTS frag 5 + dERR
dPNUTS frag 6 + dERR
10-1
10-2
10-3
10-4
10-1
10-2
10-3
10-4
(pB27-dPNUTS frag 2 + pP7Ø) C-
(pB27-dPNUTS frag 4 + pP7Ø) C-
(pB27-dPNUTS frag 6 + pP7Ø) C-

DO-3 + 1mM 3AT
dPNUTS frag 1+ dERR
C- (pB27-dPNUTS frag 1 + pP7Ø)
C- (pB27Ø + dERR)
C- (pB27-dPNUTS frag 3+ pP7Ø)
C- (pB27-dPNUTS frag 5+ pP7Ø)
dPNUTS frag 2 + dERR
dPNUTS frag 3 + dERR
dPNUTS frag 4 + dERR
dPNUTS frag 5 + dERR
dPNUTS frag 6 + dERR
10-1
10-2
10-3
10-4
10-1
10-2
10-3
10-4
(pB27-dPNUTS frag 2 + pP7Ø) C-
(pB27-dPNUTS frag 4 + pP7Ø) C-
(pB27-dPNUTS frag 6 + pP7Ø) C-

4.5.1. Co-immunoprecipitation of dPNUTS and dERR in S2R+ cells

To provide further confirmation that dPNUTS binds dERR, an epitope tagged expression construct of dERR was made that could be used in co-IP experiments. The dERR cDNA sequence was PCR amplified from the BDGP gold cDNA clone GH28308, cloned into the pENTR entry vector and checked by sequencing. This was then subcloned into an amino-terminal Flag-Myc tagged S2 cell expression vector, pAFMW. dPNUTS-Myc was subcloned into a GFP S2 cell expression vector, pAGW.

Cells were transiently transfected with either Flag-Myc-dERR alone or in combination with GFP-dPNUTS-Myc. Immunoprecipitation of GFP-dPNUTS-Myc from transfected cells, using a magnetic GFP trap resulted in co-precipitation of Flag-Myc-dERR as detected by an anti-Flag antibody on a Western blot (Figure 4.12). However, when the experiment was repeated using an anti-Myc antibody an interaction was not detected. Problems with transfection efficiencies in co-transfected samples could be one possible explanation for the lack of immunoprecipitation in the repeat experiment. Due to time constraints more repeats were not done.

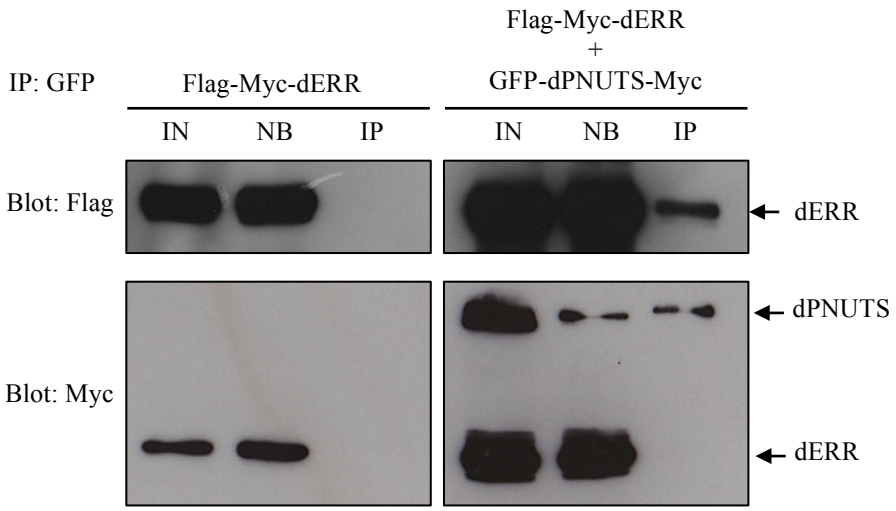

Figure 4.12. dPNUTS binds to dERR in S2R+ cells. Cells were transfected with S2 constructs expressing Flag-Myc-dERR or co-transfected with Flag-Myc-dERR and GFP-dPNUTS-Myc. Ectopic dPNUTS was precipitated using a magnetic GFP trap (Chromotek). Western blotting with an anti-Flag antibody shows dERR co-immunoprecipitates with GFP-dPNUTS. A repeat experiment immunoblotted with anti-Myc antibody (bottom panels) did not detect an interaction. IN= input (total protein extract), NB = non-bound and IP = immunoprecipitated.

4.6. Characterisation of the interaction between dPNUTS and dWdr82

dWdr82 was not identified as a dPNUTS-interacting protein in the initial Y2H screen. However Lee *et al.*, 2010 showed human PNUTS binds to human Wdr82 and they exist in a stable complex with TOX4 and PP1 (Lee *et al*., 2010). dWdr82 may not have been represented in the cDNA library used in the original screen therefore a direct one-by-one assay between full-length dPNUTS and full-length dWdr82 was done. Both genes were PCR amplified and cloned in frame with the LexA DBD into plasmid pB27 and the Gal4 AD into plasmid pP7 and checked by sequencing. Cells

were grown on selective DO-2 and DO-3 medium. Figure 4.13 shows an interaction could not be detected in either reciprocal interaction assay.

Figure 4.13 (next page). dPNUTS does not bind dWdr82 in the yeast two-hybrid system. Yeast two-hybrid analysis showing that an interaction between full-length dPNUTS and full-length dWdr82 was not detected. Interaction pairs were tested in triplicate in the form of streaks. Cells were grown on selective medium without tryptophan and leucine (DO-2) and selective medium without tryptophan, leucine and histidine (DO-3) to select for an interaction. C+ = Hybrigenics interaction positive control, C- = negative controls. ∅ specifies empty vector.

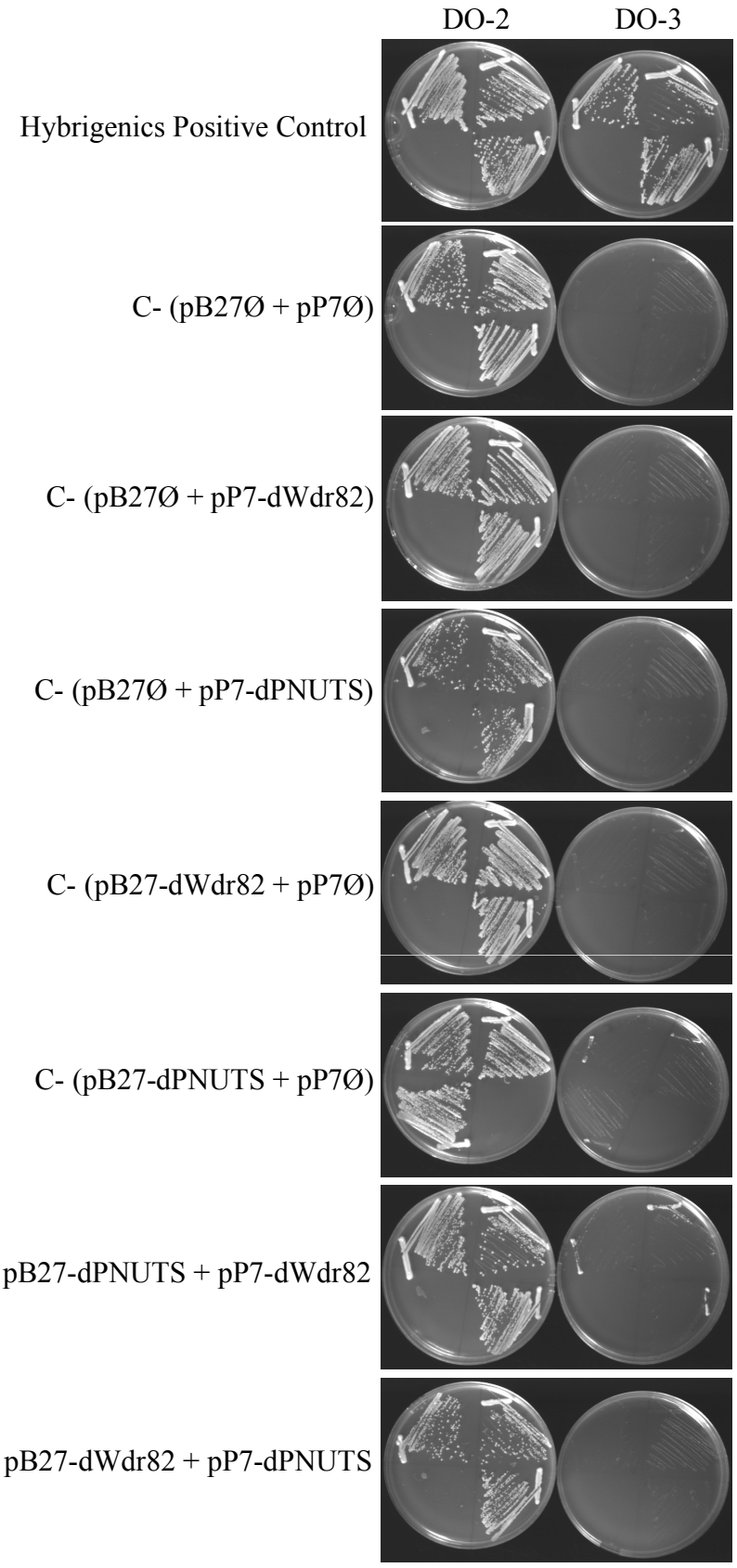
DO-2
DO-3
Hybrigenics Positive Control
C- (pB27Ø + pP7Ø)
C- (pB27Ø + pP7-dWdr82)
C- (pB27Ø + pP7-dPNUTS)
C- (pB27-dWdr82 + pP7Ø)
C- (pB27-dPNUTS + pP7Ø)
pB27-dPNUTS + pP7-dWdr82
pB27-dWdr82 + pP7-dPNUTS

4.6.1. Co-immunoprecipitation of dPNUTS and dWdr82 in S2R+ cells

Despite not detecting an interaction in the Y2H assay, the evidence in the literature warranted biochemical analysis of this potential interaction in *Drosophila*. Therefore tagged expression constructs were made for co-IP experiments in *Drosophila* S2R+ cells. The dWdr82 cDNA sequence was PCR amplified from the BDGP gold cDNA clone GH09638, subcloned into the pENTR Gateway® entry vector and checked by sequencing. This was then subcloned into an amino-terminal FLAG-Myc tagged S2 cell expression vector, pAFMW and an amino-terminal GFP tagged S2 cell expression vector, pAGW. Similarly dPNUTS-Myc was subcloned into an untagged vector (pAW) as previously described and also pAGW for biochemical analysis using reciprocal tags. *Drosophila* S2R+ cells were transiently transfected with GFP-dWdr82 with and without dPNUTS-Myc and FLAG-myc-dWdr82 with or without GFP-PNUTS-Myc. Immunoprecipitation of GFP-dWdr82 from co-transfected cells, using a magnetic GFP trap resulted in co-precipitation of dPNUTS-Myc as detected by an anti-Myc antibody on a Western blot (Figure 4.14). This was confirmed in the reciprocal experiment as immunoprecipitation of GFP-dPNUTS-Myc from co-transfected cells, was able to pull down FLAG-myc-dWdr82 (see Figure S6 in section 3.2 of Chapter 3). This suggests that dPNUTS binds to dWdr82 despite the inability to detect a direct interaction between these proteins in the two-hybrid assay.

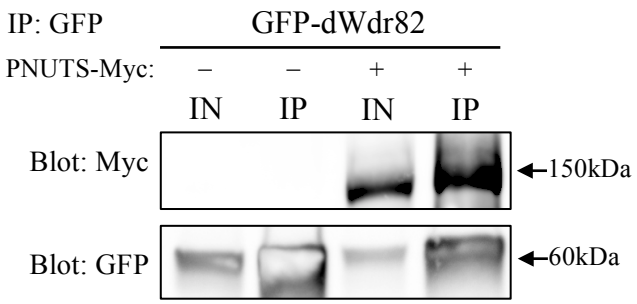

Figure 4.14. dPNUTS binds to dWdr82 in S2R+ cells. Western blot showing Myc tagged dPNUTS co-immunoprecipitates with GFP tagged MBD-R2. Immunoblot analysis of total protein extract (IN) and immunoprecipitated protein extract (IP) from S2R+ cells co- transfected with GFP-dWdr82 and dPNUTS-Myc or with GFP-dWdr82 alone and blotted with anti-Myc antibody. Immunoblotting with anti-GFP shows presence of GFP-dWdr82 in transfected cell extracts.

4.7. Characterisation of the interaction between dPNUTS and dPTEN

dPTEN was not identified as a dPNUTS binding protein in the original Y2H screen. However, recent evidence indicates that an interaction between the orthologous proteins occurs in human cells (Kavela *et al*., 2013). Binding between dPNUTS and dPTEN, if it could be demonstrated, could provide an alternative mechanism by which dPNUTS promotes developmental growth. Therefore *in vitro* and *in* vivo analysis was carried out to determine whether the interaction between PTEN and PNUTS is conserved in *Drosophila.*

4.7.1. *in vitro* analysis of dPNUTS and dPTEN interaction

Biochemical analysis in *Drosophila* S2R+ cells was done by subcloning dPNUTS-Myc into an empty *Drosophila* expression vector (pAW) as previously described.

Drosophila expression vectors (pDEX) containing GFP tagged dPTEN splice variants (dPTEN1, dPTEN2 and dPTEN3) along with an empty pDEX-GFP vector were provided by T. Maehama (as reported in Maehama *et al*., 2004). The three splice variants were identified by (Smith *et al*., 1999) and differ at the C-terminus, with dPTEN2/3 having an extended C-terminus compared to dPTEN1, which lacks the majority of this region (Smith *et al*., 1999; Maehama *et al*., 2004). dPTEN1 encodes a 418aa protein (predicted MW=48.1kDa), dPTEN2 encodes a 514aa protein (predicted MW=59.0kDa) and dPTEN3 encodes a 509aa protein (predicted MW=58.4kDa) (Smith *et al*., 1999; Maehama *et al*., 2004). dPTEN3 is the predominant isoform involved in PIP3 mediated signalling in *Drosophila* (Maehama *et al*., 2004). S2R+ cells were transfected with pDEX, pDEX-GFP-dPTEN1 or pDEX-GFP-dPTEN2 alone or together with dPNUTS-Myc. Precipitation of GFP-dPTEN1 or GFP-dPTEN2 using a magnetic GFP trap was unable to co-precipitate dPNUTS-Myc as shown by anti-Myc blotting on a Western blot (Figure 4.15). Unfortunately transfection with pDEX-GFP-dPTEN3 was unsuccessful as transfection efficiency varied between each experiment and it proved very difficult to achieve high transfection efficiencies suitable for biochemical analysis. This also made it difficult to repeat the biochemical analysis. It is also worth noting the band sizes seen in these experiments are different to the ones originally seen in (Maehama *et al*., 2004). For GFP-dPTEN2 and GFP-dPTEN1, band sizes of 78kDa and 68kDa were observed respectively, whereas Maehama *et al* reported band sizes of approximately 115kDa for GFP-dPTEN2 and 104kDa for GFP-dPTEN1 (Maehama *et al*., 2004). The band sizes reported here appear to be closer to the predicted molecular weight, if the molecular weight for the empty vector (pDEX-GFP, MW = approximately 25kDa, Figure 4.15) is accounted for. It is possible different

percentage gels were used, which could be one explanation for the differences in MW. However more analysis would need to be done to further characterise this interaction in *Drosophila*, in particular the relationship between PNUTS and dPTEN3, which may bind considering it is the predominant isoform involved in regulating the dAkt growth promoting pathway (Maehama *et al*., 2004).

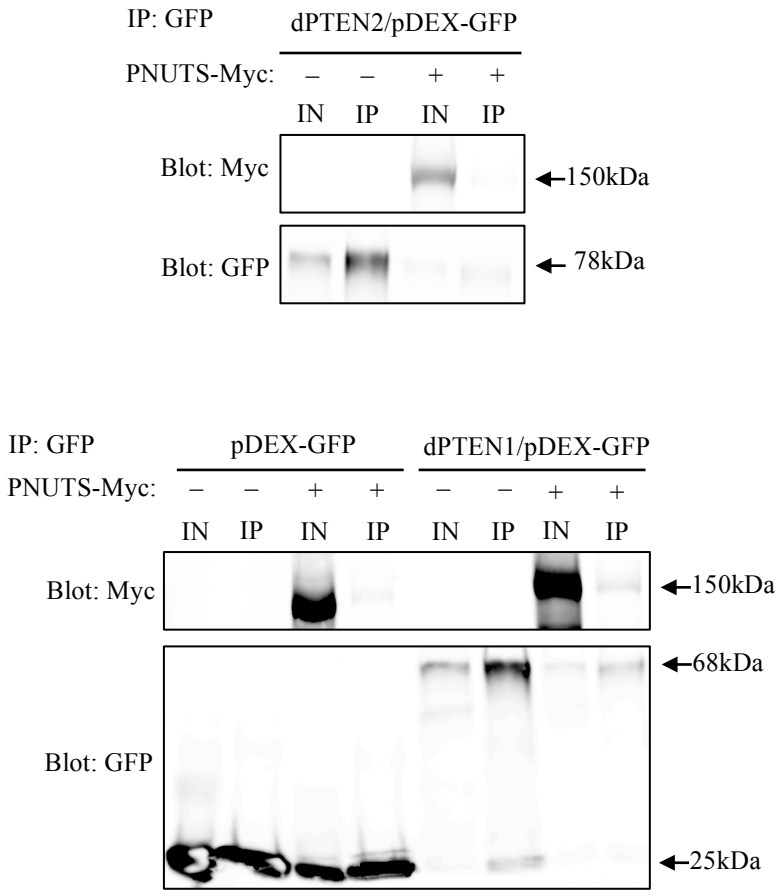

Figure 4.15. dPNUTS does not bind to dPTEN in *Drosophila* S2R+ cells. Western blot showing Myc tagged dPNUTS does not co-immunoprecipitate with GFP tagged dPTEN1 or dPTEN2 splice variants. Immunoblot analysis of total protein extract (IN) and immunoprecipitated protein extract (IP) from S2R+ cells co-transfected with dPTEN1/pDEX-GFP or dPTEN2/pDEX-GFP and dPNUTS-Myc or with each expression vector alone and blotted with anti-Myc antibody. pDEX-GFP is

an empty expression vector (negative control). Blotting with anti-GFP shows expression of GFP constructs in extracted samples.

4.7.2. *in vivo* analysis of dPNUTS and dPTEN interaction

To determine if a functional interaction exists *in vivo* the *ey-FLP* system was used to establish if a dPTEN mutant allele could suppress the dPNUTS mutant phenotype observed in developing adult eyes (see chapter 3). The *ey-FLP* system combines the *UAS/GAL4* and *FLP/FRT* systems to generate eyes made up exclusively of homozygous mutant cells, in an otherwise heterozygous fly. Any cell that is not homozygous for the mutant allele is eliminated by apoptosis due to eye-specific expression of the gene *hid* (Stowers and Schwarz, 1999). A dPTEN mutant allele ($dPTEN^3$) was provided by Clive Wilson (Goberdhan *et al*., 1999). Eyes composed of homozygous $dPTEN^3$ cells exhibit normal growth but with slightly enlarged and disorganised ommatidial facets whereas homozygous $dPNUTS^{13B}$ eyes are small with disorganised and aberrant ommatidial facets (Figure 4.16). Upon recombination of the two mutant alleles, eyes remained small and disorganised suggesting $dPTEN^3$ was unable to suppress the *dPNUTS* mutant eye phenotype (Figure 4.16). Together these results indicate that the *dPNUTS* loss-of-function phenotype in the developing eye is not due to an excess of PTEN activity.

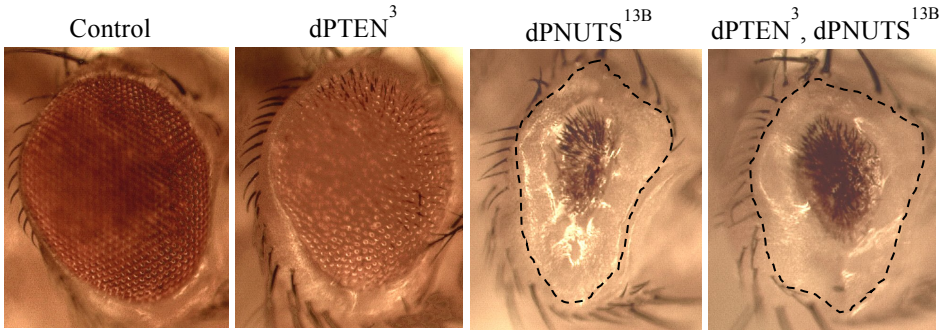

Figure 4.16. Loss of dPTEN does not suppress dPNUTS homozygous mutant eye phenotype. Images of adult female eyes showing eyes homozygous for dPTEN^{3} are able to develop into normal eyes, whereas eyes composed of homozygous dPNUTS^{13B} cells are smaller and less organised than a wild type control. Co-expression of both mutant alleles shows the effect of loss of dPNUTS cannot be suppressed by loss of dPTEN.

4.8. Discussion

A Y2H assay looking for dPNUTS interactors identified the *Drosophila* protein CG12104 (referred to as dTOX4) as the most abundant binding partner with 61 out of 351 clones and a predicted biological score of 'A'. Domain analysis revealed dTOX4 contains a centrally located HMG-box, a highly conserved DNA binding domain that is characteristic of proteins belonging to the HMG group, the members of which are often implicated in transcriptional regulation (see Chapter 5, which reports on the functional characterisation of *dTox4*) (Ueda and Yoshida, 2010). A Y2H assay and biochemical analysis confirmed the interaction in *Drosophila* and revealed dTOX4 tightly associates with dPNUTS through its C-terminus (aa 216-246). Immunofluorescence analysis showed dTOX4 is localised throughout the cell with a higher expression in the nucleus. Upon co-transfection with dPNUTS it is exclusively present in the nucleus and co-localises with dPNUTS protein, suggesting that ectopic dPNUTS sequesters dTOX4 in the nucleus. These data support the biochemical evidence that the two proteins physically interact. Interestingly in humans the HMG-box protein LCP1 (human TOX4) also binds to PNUTS in a Y2H assay using a human brain cDNA library and using biochemical analysis (Lee *et al*., 2009). Mapping of the dTOX4 binding region in dPNUTS was not done however two studies show human TOX4 binds to the N-terminus of PNUTS (Lee *et al*., 2010; Lee *et al*., 2009), which is separate from its PP1 binding domain. Together these results reveal a novel PNUTS binding partner in *Drosophila* and suggest the human PNUTS-LCP1 interaction is conserved in flies. This highlights the likely biological significance of the relationship between TOX4 and PNUTS and techniques available in *Drosophila* will aid in further characterisation of this interaction.

TOX4 and PNUTS-PP1 have been shown to exist in a complex with Wdr82, which is more well known for its role in regulating histone H3 lysine 4 methylation through association with the histone methyltransferase containing complex, COMPASS (Lee *et al*., 2010). Two-hybrid screening did not identify dWdr82 as a dPNUTS binding protein however biochemical analysis did confirm an association in *Drosophila,* suggesting this complex is conserved in flies. Interestingly Wdr82 was not identified in a Y2H screen looking for PNUTS-binding partners in humans, despite biochemical analysis showing they directly interact (Lee *et al*., 2010; Lee *et al*., 2009). This suggests Wdr82 may not be detectable using a Y2H approach, possibly because it is toxic to yeast or because of other limitations of the Y2H method. Yeast has a different post-translational modification system, which often means proteins of higher eukaryotes aren't modified correctly and cannot be detected (Brückner *et al*., 2009; Osborne *et al*., 1996). Furthermore Wdr82 is known to associate with multiple complexes but whether its association in these complexes is mutually exclusive is unknown (Lee *et al*., 2010). Therefore it is plausible its interaction with dPNUTS is transient and transient interactions can go undetected in Y2H assays (Brückner *et al*., 2009).

Other proteins identified in the screen include dMBD-R2. A direct Y2H assay confirmed binding and revealed dMBD-R2 associates with the N-terminus of PNUTS. Initial biochemical analysis confirmed binding, however the results have to be taken with caution due to the lack of repeats. Problems with transfection efficiencies with the dMBD-R2 tagged expression vector alone and together with the dPNUTS expression vector made it difficult to obtain repeatable results therefore further biochemical and functional analysis is necessary. As a commercial antibody

against dMBD-R2 is available, one way to address this would be to test the interaction between dPNUTS and dMBD-R2 in immunoprecipitated fly extracts.

dMBD-R2 is part of the non-specific lethal (NSL) complex that plays a major role in active transcription in *Drosophila* through recruitment of RNAPII and the histone H4 lysine 16 methyltransferase, Males absent On First (MOF) (Raja *et al*., 2010). Interestingly disruption of dMBD-R2 and other NSL genes by *P*-element insertion causes early larval lethality in *Drosophila*. If the interaction with dMBD-R2 could be confirmed, it would be interesting to determine whether *dMBD-R2* mutant larvae display a similar growth arrest phenotype to *dPNUTS* (see Chapter 3) (Mendjan *et al*., 2006; Raja *et al*., 2010). Functional analysis of dMBD-R2 and its interaction with dPNUTS may offer insights into the mechanisms by which dPNUTS is recruited to chromatin.

The *Drosophila* Estrogen Related Receptor (dERR) was also identified in the Y2H screen as a dPNUTS-binding partner. Only 3 out of 351 clones were recovered, however fragment analysis confirmed binding and showed dPNUTS interacts with a region near the N-terminus of dERR that contains a Zinc-finger DNA binding domain (Appendix 7). In *Drosophila*, ERR directs a metabolic switch to ensure proper carbohydrate metabolism during embryogenesis and support rapid growth during larval development (Tennessen *et al*., 2011). *dERR* mutants die as second instar larvae due to metabolic defects caused by the absence of a *dERR*-dependent transcriptional programme (Tennessen *et al*., 2011). Notably, transcriptomic analysis revealed that genes involved in glucose metabolism, which are regulated by *dERR*, are also underexpressed in *dPNUTS* mutants (see Figure S5, Chapter 3). Not all

genes controlled by *dERR* are similarly affected by dPNUTS, but this might reflect the difference in the developmental stage at which the transcriptomes were determined (1st instar larvae for *dPNUTS*, 2nd instar for *dERR* mutants). It is interesting to speculate that an association with sequence-specific DNA-binding proteins such as dERR may direct PNUTS-PP1 to specific transcriptional targets e.g. to control the metabolic status of the organism.

PTEN was studied as a potential dPNUTS interactor based on evidence from studies of the mammalian counterparts (Kavela *et al*., 2013). PTEN was not identified in the initial Y2H screen but this could be because PTEN is predominantly associated with the cell membrane and membrane proteins often go undetected in Y2H assays because of poor recruitment to the nucleus where interactions must take place to be observed (Brückner *et al*., 2009). Co-IP experiments also failed to detect an interaction between dPNUTS and dPTEN1 and dPTEN2, however problems with transfection efficiencies made these analyses difficult to interpret. Furthermore, transfection with dPTEN3, which may be the predominant PTEN isoform in *Drosophila*, was unsuccessful, therefore an interaction between dPNUTS and dPTEN3 can't be ruled out. Due to the problems with biochemical approaches, *in vivo* functional analysis using the *ey-FLP* system was used to study the interaction between *dPNUTS* and *dPTEN*. Loss of *dPTEN* function in the developing eye failed to rescue the reduced eye phenotype caused by *dPNUTS* loss-of-function. Taken at face value, these results appear to indicate that *PNUTS* and *PTEN* do not functionally interact in *Drosophila*. However, *dPNUTS* is likely to have pleiotropic roles and the *dPNUTS* alleles used in these experiments were null mutations. Consequently, it

would be worth repeating these experiments with a weaker (hypomorphic) *dPNUTS* mutant allele that might allow suppression of the growth phenotype to be revealed.

Surprisingly PP1 was not identified as a dPNUTS-binding protein in the Y2H screen. A possible reason is that PP1 may be toxic to yeast when the PNUTS-PP1 holoenzyme is reconstituted and in combination with the plasmids used for expression. For example, overexpression of PP1 in the vector pAS2 has previously been reported to be toxic in the Y2H system (Bennett and Alphey, 2007).

Analysis of overlapping cDNA clones isolated from the Y2H screen highlighted the selected interaction domain (SID) for each identified protein. Interestingly the SID in dERR and dMBD-R2, as well as other identified proteins, contain a Zinc-finger domain (Appendix 7). Zinc-fingers are well known for facilitating DNA binding but some, such as the PHD Zinc-finger found in dMBD-R2 (Appendix 7) facilitate protein-protein interactions. The PHD Zinc-finger is known to bind both modified and unmodified histone tails allowing proteins to associate with chromatin (Ali *et al*., 2012). This might suggest that dPNUTS regulates the activity of these proteins by modifying the DNA/histone binding affinity or utilises the properties of interacting partners to associate (indirectly) with DNA/chromatin. Although dTOX4 has not been reported to possess a Zinc-finger motif, analysis of the C-terminus, which is necessary for dPNUTS binding, reveals a series of separated cysteine residues (C (X4), C (X14), C (X3), C (X4), C), and has similarity to atypical zinc-finger motifs. The C-terminus is highly conserved in humans (see Chapter 5) so it would be interesting to determine if this region is capable of binding metal ions and if metal ions are required for the interaction with *dPNUTS*.

In conclusion this work has identified a number of dPNUTS-binding proteins, some confirming interactions already reported for mammalian PNUTS (TOX4 and Wdr82) and others representing novel relationships (MBD-R2 and ERR). Figure 4.17 shows where these proteins are predicted to bind to dPNUTS based on evidence from Y2H assays in this chapter and from reports in the literature.

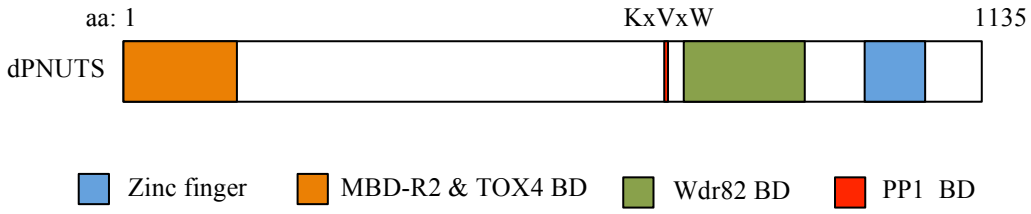

Figure 4.17. Domain map of dPNUTS showing binding sites for known and novel dPNUTS interactors. BD = binding domain.

Both dMBD-R2 and dTOX4 are predicted to interact with the N-terminus of dPNUTS, which raises the question of whether their binding is mutually exclusive or if they compete for dPNUTS binding. Results from the Y2H assay suggest dMBD-R2 and dPNUTS bind with low affinity whereas dTOX4 and dPNUTS bind with high affinity. This might suggest their association with dPNUTS is competitive but that dPNUTS predominantly associates with dTOX4. It is also possible they bind exclusively at different stages of development and therefore never have the opportunity to compete for binding. It is important to note these protein interactions were identified using a Y2H approach followed by ectopic protein expression in S2R+ cells. Therefore it will be important to confirm whether they bind *in vivo* under

normal biological conditions. Future experiments should focus on studying the endogenous proteins to establish their pattern of expression spatially and temporally and to look for functional interactions *in vivo* using the various genetic techniques available in *Drosophila*.

5. Investigating the function of dTOX4

5.1. Introduction

High Mobility Group (HMG) proteins are a superfamily of proteins that bind to DNA and facilitate various DNA-dependent nuclear activities including transcription, replication and DNA repair by inducing structural changes in the target DNA/chromatin (O'Flaherty and Kaye, 2003; Stros *et al*., 2007; Bianchi and Agresti, 2005). In mammals there are three families of HMG proteins: the HMG-nucleosome binding family (HMGN), the HMG-AT-hook family (HMGA) and the HMG-box family (HMGB) (Reeves, 2010). Each family is unique in the functional motif that binds DNA but a highly acidic C-terminal Domain is common among all families, which is thought to modulate the affinity for various DNA structures, mediate chromatin unfolding or contribute to protein-protein interactions (Hock *et al*., 2007). HMGB proteins are the most abundant family and recognise DNA through a structurally conserved 70-80 amino acid sequence, which defines the HMG-box and is composed of three α-helices that form an L-shaped configuration (Malarkey and Churchill, 2012; Bustin, 1999). This structural motif binds to the minor groove of B-form DNA, creating a severe bend and altering the local the chromatin structure to allow access of chromatin remodelling complexes and transcription factors (Reeves, 2010; Bianchi and Agresti, 2005; Malarkey and Churchill, 2012; Wilkinson *et al*., 2002). Consequently, HMGB proteins are often described as 'architectural factors' having an important role in modulating chromatin structure, replication, DNA repair, transcription regulation and proper development (Reeves, 2010).

LCP1/TOX4 belongs to the HMG-box family, which is usually divided into two groups of proteins; those that bind DNA in a sequence dependent manner and those

that bind independently of the underlying sequence. However, there are members of both groups that bind to distorted DNA structures such as four-way junctions and adducts generated by platinating agents (Ueda and Yoshida, 2010; Puch *et al*., 2011; Stros *et al*., 2007; P-ohler *et al*., 1998). TOX4 is a sequence-independent DNA-binding protein and binds to DNA adducts generated by Cisplatin, a platinum-based anticancer drug, implicating this HMGB protein in the DNA damage response (Puch *et al*., 2011).

Apart from binding to damaged DNA and being implicated in transcriptional regulation through binding in a complex with PNUTS, PP1 and Wdr82 (as discussed in Chapter 4), very little is known about TOX4. The work in this chapter aimed to characterise the TOX4 gene in *Drosophila* and provide further insight into its role in the PNUTS/PP1 complex and gene expression.

5.2. *Drosophila* gene *CG12104* is an orthologue of mammalian LCP1 (TOX4)

CG12104 was identified as the most abundant dPNUTS-interacting protein in the yeast two-hybrid screen reported in Chapter 4. Previous sequence analysis of the TOX subfamily of HMGB proteins suggested that *CG12104* encodes a protein with a partial HMG-box and has weak similarity to other proteins in the TOX family, though its C-terminus is similar to mammalian LCP1 (TOX4) (O'Flaherty and Kaye, 2003). Initial BLAST analysis using CG12104 (isoform A) revealed TOX proteins as the top hits in human, mouse, zebrafish and xenopus with TOX3 showing the highest level of similarity in humans. However further phylogenetic analysis reveals TOX4 is the closest related homologue to CG12104, to which it is also demonstrably orthologous (Figure 5.1a). Interestingly a reciprocal BLAST search using human TOX3 only identifies CG12104 in *Drosophila* whereas human TOX4, TOX2 and TOX1 identify CG12104 as the top hit as well as other less similar proteins including Dorsal Switch Protein 1 (DSP1). DSP1 is also a HMG-box protein (Lehming *et al*., 1994) and BLAST and phylogenetic analysis suggest it is related to other HMG-box proteins in humans that are not members of the TOX family including HMG-B3, HMG-B2 and HMG-B1. It is likely DSP1 was identified in the initial BLAST searches because of the highly conserved HMG-Box. This work supports the analysis of the TOX subfamily by O'Flaherty and Kaye in 2003 and given LCP1/TOX4 has been shown to bind PNUTS (Lee *et al*., 2009), a sequence alignment of CG12104 and LCP1/TOX4 was performed to determine the degree of conservation. Figure 5.1b shows there is a significant level of conservation in the C-terminus of the protein as recognised by O'Flaherty and Kaye, 2003 and 63% of the residues that make up the HMG-box in LCP1/TOX4 (red text in Figure 5.1b) are either sequence conserved (black shading, Figure 5.1b) or similar in amino acid type (grey shading,

Figure 5.1b) in CG12104. More importantly, mapping of secondary structures in both proteins revealed all three α-helices that are defining features and are essential for the function of HMG-box proteins are found in CG12104, confirming it is likely to have a functional HMG-box and may have similar roles to other HMGB proteins as discussed above. Given this analysis, CG12104 will be referred to as dTOX4 hereafter.

Figure 5.1 (next two pages). CG12104 is the *Drosophila* orthologue of human TOX4. a) Phylogenetic tree showing the relationship between *Drosophila* CG12104 and the TOX subfamily of HMG-box proteins in human, mouse, xenopus and zebrafish. TOX proteins were identified as the top hits in a BLAST search using CG12104. Other proteins identified included DSP1, which is also included in the phylogenetic analysis and is more likely related to other HMG-box proteins that are not part of the TOX subfamily. b) Multiple sequence alignment of full-length mammalian LCP1 and full-length *Drosophila* CG12104. The T-Coffee alignment tool was used in 'accurate' mode to generate the alignment. BoxShade was used to identify conserved residues. Identical residues are shaded in black and similar residues are shaded in grey. Ali2D was used to map secondary structural features. Blue lines show alpha-helices. Red text represents the amino acids that make up the HMG-box.

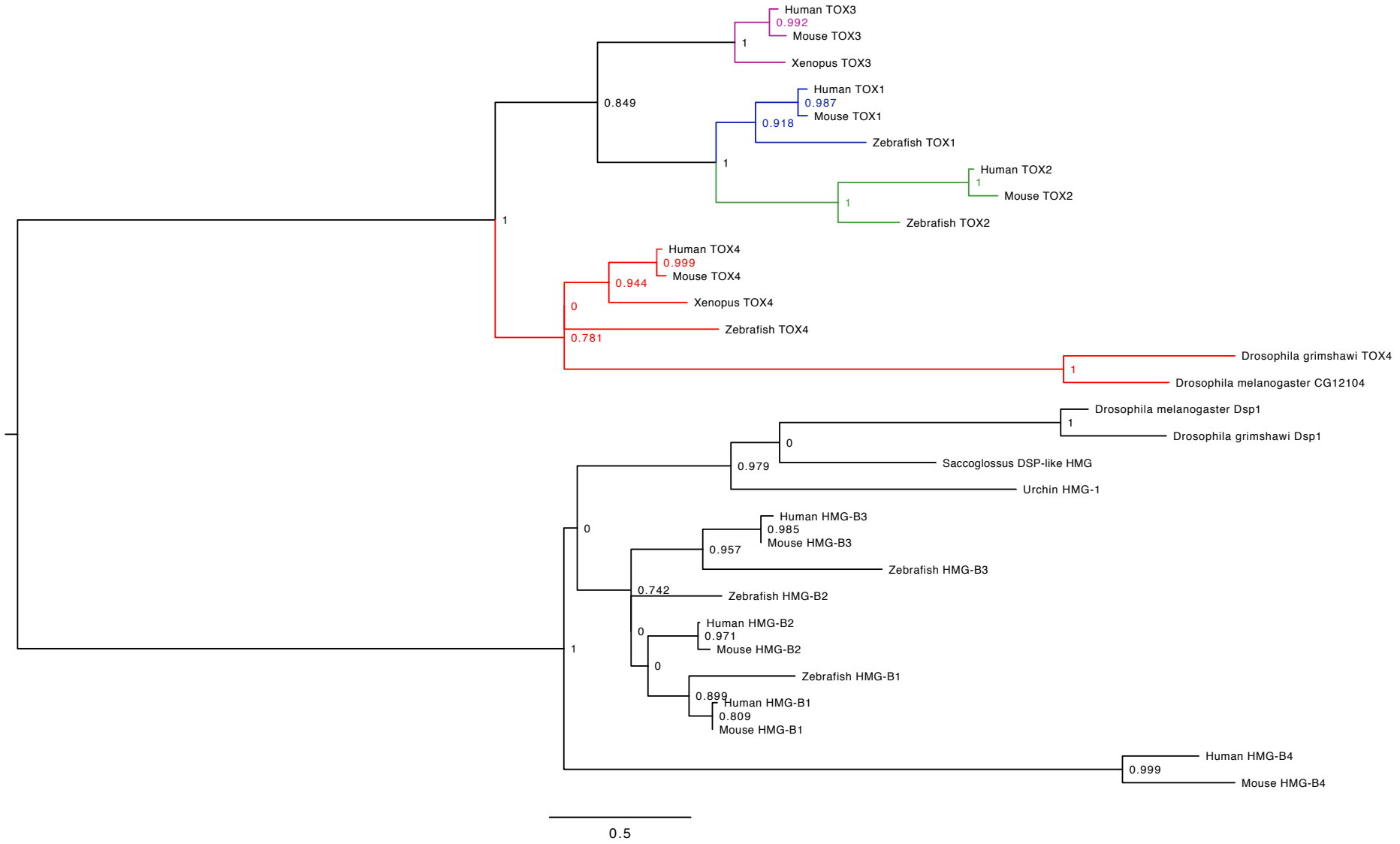
Human TOX3
0.992
Mouse TOX3
1
Xenopus TOX3
0.849
Human TOX1
0.987
Mouse TOX1
0.918
Zebrafish TOX1
1
Human TOX2
1
Mouse TOX2
1
Zebrafish TOX2
1
Human TOX4
0.999
Mouse TOX4
0.944
Xenopus TOX4
0
Zebrafish TOX4
0.781
Drosophila grimshawi TOX4
1
Drosophila melanogaster CG12104
Drosophila melanogaster Dsp1
1
Drosophila grimshawi Dsp1
0
0.979
Saccoglossus DSP-like HMG
Urchin HMG-1
0
Human HMG-B3
0.985
Mouse HMG-B3
0.957
Zebrafish HMG-B3
0.742
Zebrafish HMG-B2
0
Human HMG-B2
0.971
Mouse HMG-B2
1
0
Zebrafish HMG-B1
0.899
Human HMG-B1
0.809
Mouse HMG-B1
Human HMG-B4
0.999
Mouse HMG-B4
0.5

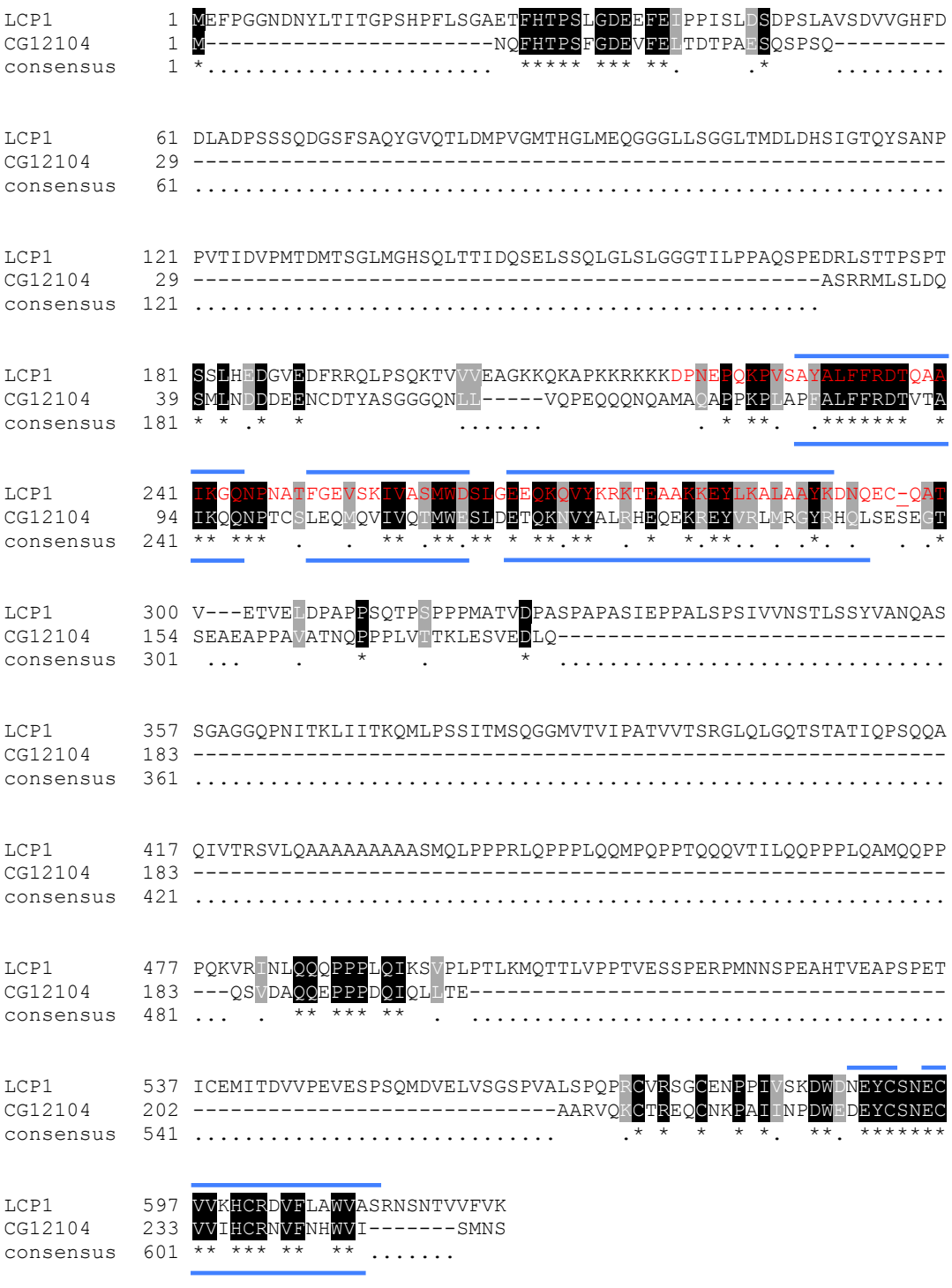
LCP1 1 MEFPGGNDNYLTITGPSHPFLSGAETFHTPSLGDEEFEIPPISLDSDPSLAVSDVVGHFD
CG12104 1 M----------NQFHTPSFGDEVFELTDTPAESQSPSQ---------
consensus 1 *..... ***** *** **. .* .....
LCP1 61 DLADPSSSQDGSFSAQYGVQTLDMPVGMTHGLMEQGGGLLSGGLTMDLDHSIGTQYSANP
CG12104 29 ----------
consensus 61 ....
LCP1 121 PVTIDVPMTDMTSGLMGHSQLTTIDQSELSSQLGLSLGGGTILPPAQSPEDRLSTTPSPT
CG12104 29 ----------ASRRMLSLDQ
consensus 121 ....
LCP1 181 SSLHEDGVEDFRRQLPSQKTVVEAGKKQKAPKKRKKKDPNEPQKPVSAYALFFRDTQAA
CG12104 39 SMLNDDDEENCDTYASGGGQNLI-----VQPEQQQNQAMAQAPPKPLAPFALFFRDTVTA
consensus 181 * * .* * ..... . * **. .******* *
LCP1 241 IKGQNPNATFGEVSKIVASMWDSLGEEQKQVYKRKTEAAKKEYLKALAAYKDNQEC-QAT
CG12104 94 IKQQNPTCSLEQMQVIVQTMWESLDETQKNVYALRHEQEKREYVRLMRGYRHQLSESEGT
consensus 241 ** *** . . ** .**.** * **.** . * *.**.. . .*. . . .*
LCP1 300 V---ETVELDPAPPSQTPSPPPMATVDPASPAPASIEPPALSPSIVVNSTLSSYVANQAS
CG12104 154 SEAEAPPAVATNQPPPLVITKLESVEDLQ----------
consensus 301 ... . * . * .....
LCP1 357 SGAGGQPNITKLIITKQMLPSSITMSQGGMVTVIPATVVTSRGLQLGQTSTATIQPSQQA
CG12104 183 ----------
consensus 361 ....
LCP1 417 QIVTRSVLQAAAAAAAAASMQLPPPRLQPPPLQQMPQPPTQQQVTILQQPPPLQAMQQPP
CG12104 183 ----------
consensus 421 ....
LCP1 477 PQKVRINLQQQPPPLQIKSVPLPTLKMQTTLVPPTVESSPERPMNNSPEAHTVEAPSPET
CG12104 183 ---QSVDAQQEPPPDQIQLITE----------
consensus 481 ... . ** *** ** . .....
LCP1 537 ICEMITDVVPEVESPSQMDVELVSGSPVALSPQPRCVRSGCENPPIVSKDWDNEYCSNEC
CG12104 202 ----------AARVQKCTREQCNKPAIINPDWEDEYCSNEC
consensus 541 ....* * * * *. **. *******
LCP1 597 VVKHCRDVFLAWVASRNSNTVVFVK
CG12104 233 VVIHCRNVFNHWVI-------SMNS
consensus 601 ** *** ** ** ....

5.3. Isolation of a null *dTOX4* mutant

To determine the *in vivo* role of *dTOX4* and understand more about its functional relationship with *dPNUTS*, a null mutant in the *dTOX4* gene was generated through imprecise *P*-element excision. Mutational analysis still remains an important approach in which to study gene function and many tools exist in the *Drosophila* community to allow the easy generation of mutant alleles. One such tool is through insertion of a *P*-transposable element, which often disrupts gene function, but can also be used to generate deletions of flanking DNA upon remobilisation (Bellen *et al*., 2011). The *Drosophila* Gene Disruption Project was created by the Berkeley *Drosophila* Genome Project (BDGP) in collaboration with a number of *Drosophila* laboratory groups and is a publicly available collection of strains containing single transposable element insertions in a single gene spanning over 40% of *Drosophila* genes (Bellen, 2004; Bellen *et al*., 2011). A strain containing a transposable *P*-element inserted in the 5' untranslated region (UTR) of *dTOX4* (P{EPgy2}CG12104^{EY02201}) was used to generate the mutant allele through imprecise excision of the *P*-element (Figure 5.3a). It was crossed to two strains, each containing a stable insertion of P{Δ2-3}, a genomic source of P-transposase that mobilises other P-elements (Robertson *et al*. ,1988). Individual males carrying the *P*-element and transposase were collected and crossed to a balancer strain. White eyed male progeny from this cross (*P*-element has been excised) were collected and crossed again against a balancer strain. Progeny carrying the excision and the balancer TM6B were inbred to generate stocks of individual excision events that were screened by PCR to look for deletions in the *dTOX4* gene using the primer strategy shown in Figure 5.2a (see Appendix 3 for crossing scheme). From this, one strain was identified (#16, Figure 5.2b, called *dTOX4*^{null} hereafter) as having an

approximately 1200bp deletion when screened with primer sets 2+3 and 1+3 (Figure 5.2a). RT- PCR confirmed the loss of *dTOX4* transcripts in $dTOX4^{null}$ flies compared to w^{1118} and a strain where the *P*-element had been precisely excised (12, Figure 5.2c). DNA sequencing analysis revealed a 1180bp portion of the *dTOX4* gene, including the translation start site and the majority of the coding sequence (CDS), is deleted in $dTOX4^{null}$ flies (Figure 5.2a).

Figure 5.2 (next page). Generating a *dTOX4* null allele. a) Genomic region of *CG12104* (*Drosophila TOX4*) showing all three transcripts and flanking genes. Grey shading represents coding regions. $CG12104^{EY02201}$ contains a *P*-element insertion in the 5' untranslated region of *dTOX4*. $dTOX4^{null}$ is the mutant allele generated through excision of the *P*-element. The map shows the extent of the deletion spanning the coding region; the genomic sequence either side of the deletion is indicated. The primer map shows the position of the primers used to detect the deletion. $dTOX4^{P216\Delta}$ is a mutant *in vitro* construct of *dTOX4* lacking the dPNUTS binding domain as a result of site-directed mutagenesis to generate a premature stop codon. The base pair changes in the $dTOX4^{P216\Delta}$ allele are shown. b) Standard PCR on DNA samples extracted from flies containing a potential deletion in the *dTOX4*. Primer sets used (as shown in (a)) are shown at the side. Numbers indicate the cross number. c) RT-PCR on the selected deletion strain (#16), a revertant strain where the *P*-element was precisely excised (#12) and w^{1118} confirmed loss of *dTOX4* transcript in the deletion strain.

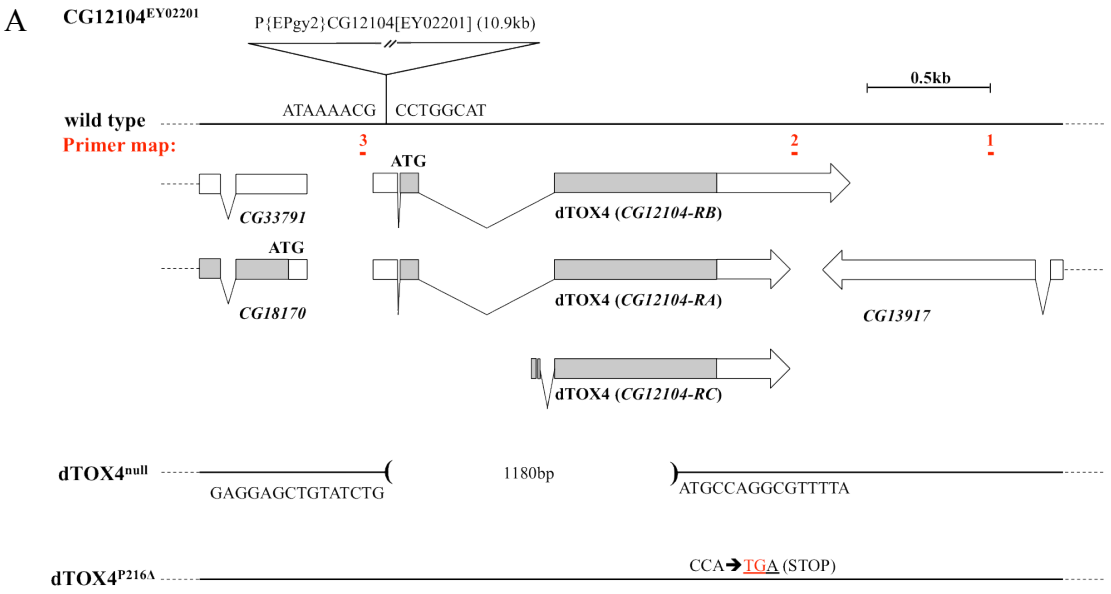
A
CG12104EY02201
P{EPgy2}CG12104[EY02201] (10.9kb)
0.5kb
wild type
ATAAAACG
CCTGGCAT
Primer map:
3
2
1
ATG
CG33791
dTOX4 (CG12104-RB)
ATG
CG18170
dTOX4 (CG12104-RA)
CG13917
dTOX4 (CG12104-RC)
dTOX4null
GAGGAGCTGTATCTG
1180bp
ATGCCAGGCGTTTTA
dTOX4P216A
CCA→TGA (STOP)

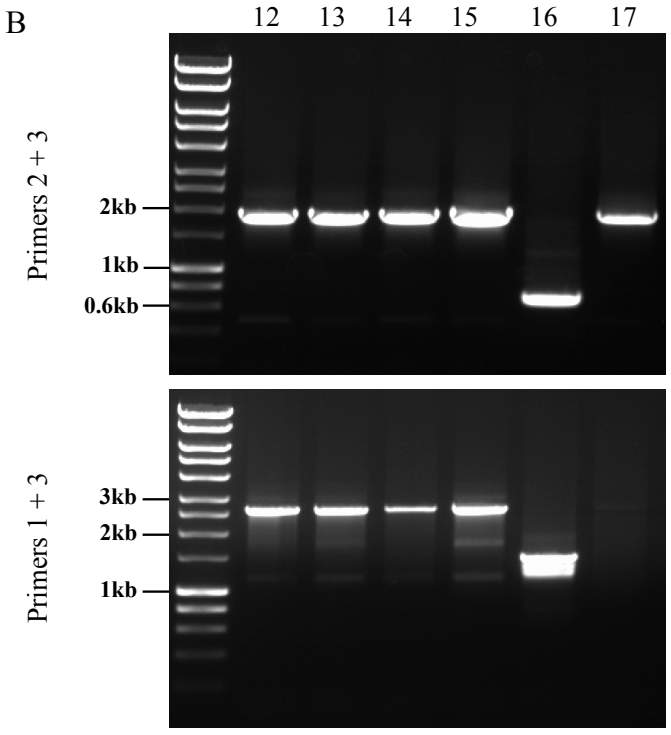
B
12
13
14
15
16
17
Primers 2 + 3
2kb
1kb
0.6kb
Primers 1 + 3
3kb
2kb
1kb

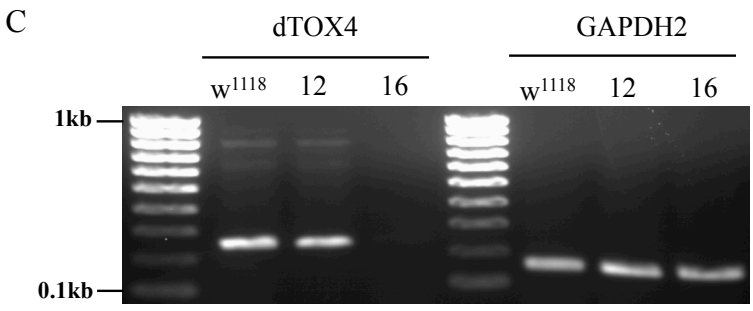
C
dTOX4
GAPDH2
w1118
12
16
w1118
12
16
1kb
0.1kb

5.4. Characterising the *dTOX4^{null}* strain

As discussed in Chapter 1, homozygous *dPNUTS^{13B}* animals die during the L1 phase of larval development. However, unlike *dPNUTS^{13B}* homozygotes, animals with two copies of the *dTOX4^{null}* allele survived to adulthood and displayed an expected 2:1 ratio of heterozygotes:homozygotes suggesting viability was not affected. Despite this, it was very clear the strain did not thrive and this led to a number of investigations to further characterise the gene function.

5.4.1 Deletion of *dTOX4* causes sterility in male and female *Drosophila*

The first avenue of investigation was to look at the effect of *dTOX4^{null}* mutation on fertility. If mutant animals are partially sterile, this could explain why the strain does not thrive and could provide a good system in which to study the role of *dTOX4* further.

Two approaches were taken; firstly, fecundity was measured by monitoring egg production in homozygous *dTOX4^{null}* female flies compared to *w^{1118}*. Egg production can be affected by various factors including the male and the seminal fluid proteins they transfer (Chapman and Davies, 2004) therefore male and female homozygous *dTOX4^{null}* animals were crossed to female and male *w^{1118}* animals respectively to determine if there was a sex related phenotype. The second approach, measured fertility by counting the number of eggs that hatched from those laid in the fecundity assay.

Egg production was significantly reduced in inbred homozygous *dTOX4^{null}* mutant animals compared to the *w^{1118}* control ($p=<0.0001$, Figure 5.3a) laying an average of

80% less during the monitored period. It was evident this was not due to factors contributed by the homozygous *dTOX4*^{null} male mutant as w^{1118} females showed no significant reduction in egg production when crossed to homozygous mutant males compared to the inbred w^{1118} control (p=0.2827, Figure 5.3a). Furthermore when crossed to w^{1118} males, homozygous mutant females still exhibited the same reduced level of egg production as when inbred (Figure 5.3a). Not only was egg production reduced in mutant animals but the embryos also failed to hatch (Figure 5.3b). No larvae emerged from eggs laid by inbred homozygous mutants, and when crossed to w^{1118} males only a few eggs hatched (approximately 90% less than the w^{1118} inbred control; p=<0.0001, Figure 5.3b). Interestingly, eggs laid by w^{1118} females mated to homozygous *dTOX4*^{null} males also fail to hatch despite egg production not being affected. A few larvae emerged and developed to adulthood, but the number of larvae was significantly lower than the inbred w^{1118} control (p=<0.0001, Figure 5.3b), suggesting that both female and male fertility is affected in *dTOX4*^{null} mutant flies.

It is clear that in both male and female mutants the chances of generating viable offspring are rare when mated to a control strain. To test whether this was a consequence of all flies being partially sterile or due to a rare adult that was semi-fertile, 20 individual homozygous *dTOX4*^{null} males were mated with virgin w^{1118} females. None of the males were able to produce viable progeny suggesting that the observed escapers are likely to be the product of an occasional semi-fertile male. Together, these results suggest *dTOX4* is essential for both male and female fertility, but the exact mechanism remains unclear. The results described could be due to a defect in germline development leading to failed fertilisation or it could be a

consequence of a defect in embryonic development whereby fertilisation does occur but progeny subsequently die.

Figure 5.3 (next page). Homozygous *dTOX4*^{null} mutants are sterile. a) The number of eggs laid per female normalised to w^{1118} to account for unavoidable changes in conditions between experimental repeats (3 repeats with 3 to 5 counts taken every 24 hours). b) The number of eggs hatched represented as a percentage of the total number of eggs laid and normalised to w^{1118}. Hatched eggs were counted 48 hours after eggs were laid. Error bars represent standard errors. (f) = female, (m) = male.

A

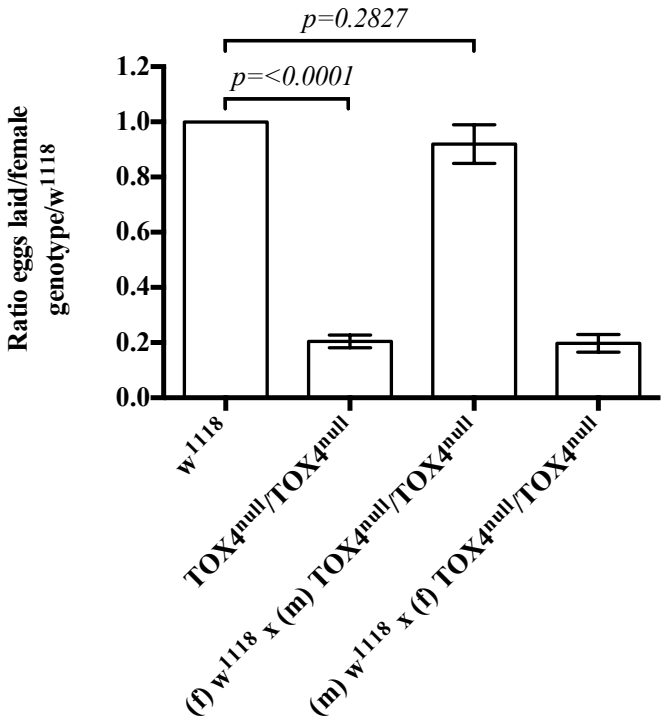
p=0.2827
p=<0.0001
Ratio eggs laid/female genotype/w1118
1.2
1.0
0.8
0.6
0.4
0.2
0.0
w1118
TOX4null/TOX4null
(f) w1118 x (m) TOX4null/TOX4null
(m) w1118 x (f) TOX4null/TOX4null

B

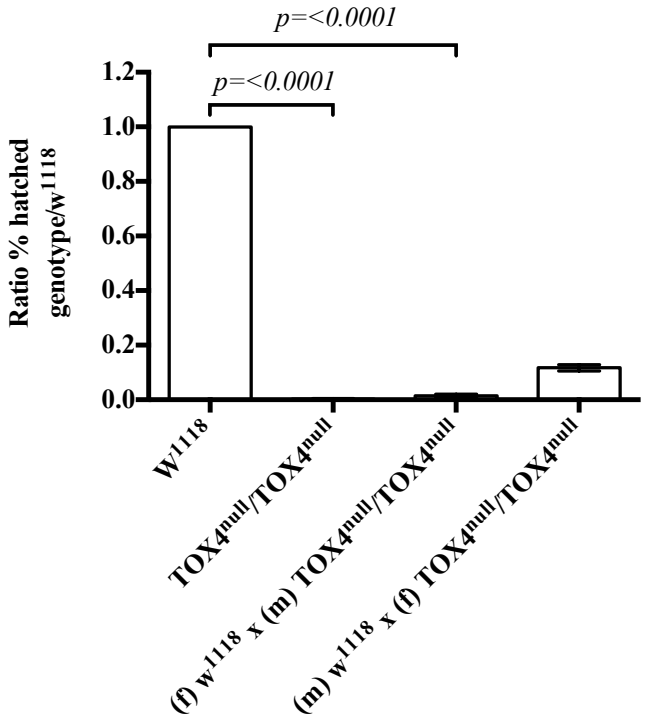
p=<0.0001
p=<0.0001
Ratio % hatched genotype/w1118
1.2
1.0
0.8
0.6
0.4
0.2
0.0
W1118
TOX4null/TOX4null
(f) w1118 x (m) TOX4null/TOX4null
(m) w1118 x (f) TOX4null/TOX4null

5.4.2 *dTOX4* mutants display defects in nurse cell chromosome dispersion and dorsoventral patterning

To understand the molecular and cellular basis for the apparent fertility defects observed in homozygous $dTOX4^{null}$ female mutants, ovaries of w^{1118} and homozygous mutant females were dissected, stained for DNA and visualised by confocal microscopy to look for defects in germline development. *Drosophila* ovaries consist of 16-20 ovarioles, each ovariole being a string of egg chambers at different developmental stages starting from the germarium (a mass of cells containing a source of germ-line and somatic stem cells) up to stage 14 when a mature egg is produced (Bate and Arias, 2009; Bastock and St Johnston, 2008; Klusza and Deng, 2010). Egg chambers consist of three cell types; 1 oocyte and 15 nurse cells (derived from germ-line stem cells) surrounded by a monolayer of follicle cells (derived from somatic stem cells) (Bate and Arias, 2009; Bastock and St Johnston, 2008). Comparing the two genotypes, there was a noticeable difference in the appearance of the nurse cell nuclei, with mutant egg chambers displaying a 'blob-like' appearance in chromosome organisation compared to controls, indicative of a defect in chromosome (de)condensation.

The role of nurse cells is to provide the developing oocyte with the majority of its nutrients and cytoplasmic content, so they have to synthesise vast amounts of mRNAs and protein to support the development of the oocyte and also provide a store of maternal products, which will be utilised during the growth and differentiation of the embryo (Bate and Arias, 2009; Klusza and Deng, 2010; Dej and Spradling, 1999; Bastock and St Johnston, 2008). This content has to be synthesised

at a very high rate to support rapid growth and is possible due to the polytene state of nurse cell chromosomes, which undergo 10-12 cycles of endoreplication to increase DNA content and support development (Dej and Spradling, 1999; Bate and Arias, 2009; Klusza and Deng, 2010). During the first five endocycles, nurse cell chromosomes are somatically paired and are visible as a 'five blob' structure up to stage 4 of oogenesis, with each blob representing one of the major polytenic chromosomal arms (X, 2L, 2R, 3L and 3R) (Klusza and Deng, 2010). At the end of the fifth cycle there is evidence to suggest a mitosis-like phase occurs as the association between somatically paired homologous chromosomes weakens and chromosome dispersal takes place resulting in a loss of the five-blob structure by stage six of oogenesis (Klusza and Deng, 2010; Dej and Spradling, 1999; Reed and Orr-Weaver, 1997).

Looking at all stages of egg chamber development in w^{1118} and homozygous $dTOX4^{null}$ egg chambers, it was clear mutant chromosomes remained in the polytene state past stage 4 of egg chamber development (Figure 5.4). Figure 5.4a shows a wild type ovariole with images of nuclei at different stages of egg chamber development taken at a higher magnification below. A "blob-like" phenotype is present up to stage 4, after which the chromosomes disperse and continue to spread further as the egg chamber progresses through oogenesis, causing the nuclei to increase in volume (Figure 5.4a). Figure 5.4b shows a homozygous mutant ovariole with nurse cell nuclei remaining in a polytene state throughout the progressive stages of egg chamber development, even up to stage 10. It is important to note that this phenotype is not fully penetrant as 37.5% of observed nuclei remained in the polytene state from stage 6 onwards with 56.9% undergoing normal dispersion (Table 5.1).

Interestingly there seemed to be a variety of dispersal phenotypes suggesting that in some nuclei chromosome dissociation does start but does so at a later stage or is not completed as shown in the bottom panel of Figure 5.4b. Nuclei like this adopted more of a ring structure and were recorded as such in Table 5.1.

Figure 5.4 (next page). *dTOX4*^{null}/*dTOX4*^{null} nurse cell chromosomes fail to disperse. a) w^{1118} ovariole with magnified images of nurse cell nuclei below showing chromosomes disperse after stage 4. b) Homozygous *dTOX4*^{null} ovariole with magnified images of nurse cell nuclei below showing chromosomes fail to disperse after stage 4. Numbers indicate the stage of egg chamber development. Ovariole scale bars = 40μm. Magnified nuclei scale bars = 2μm.

A

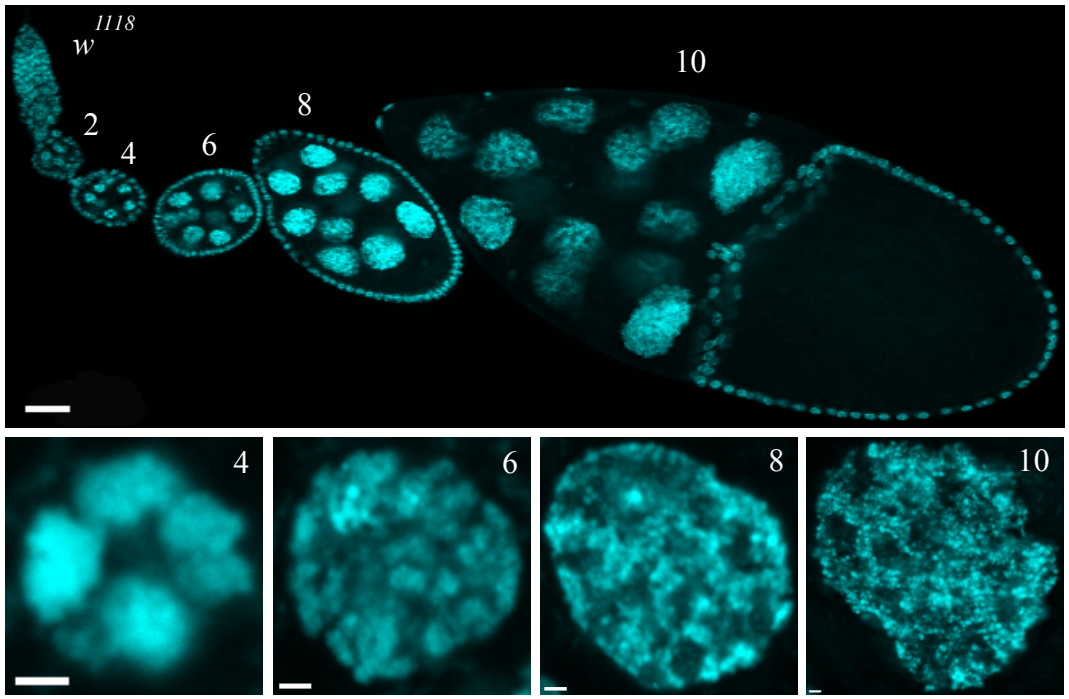

B

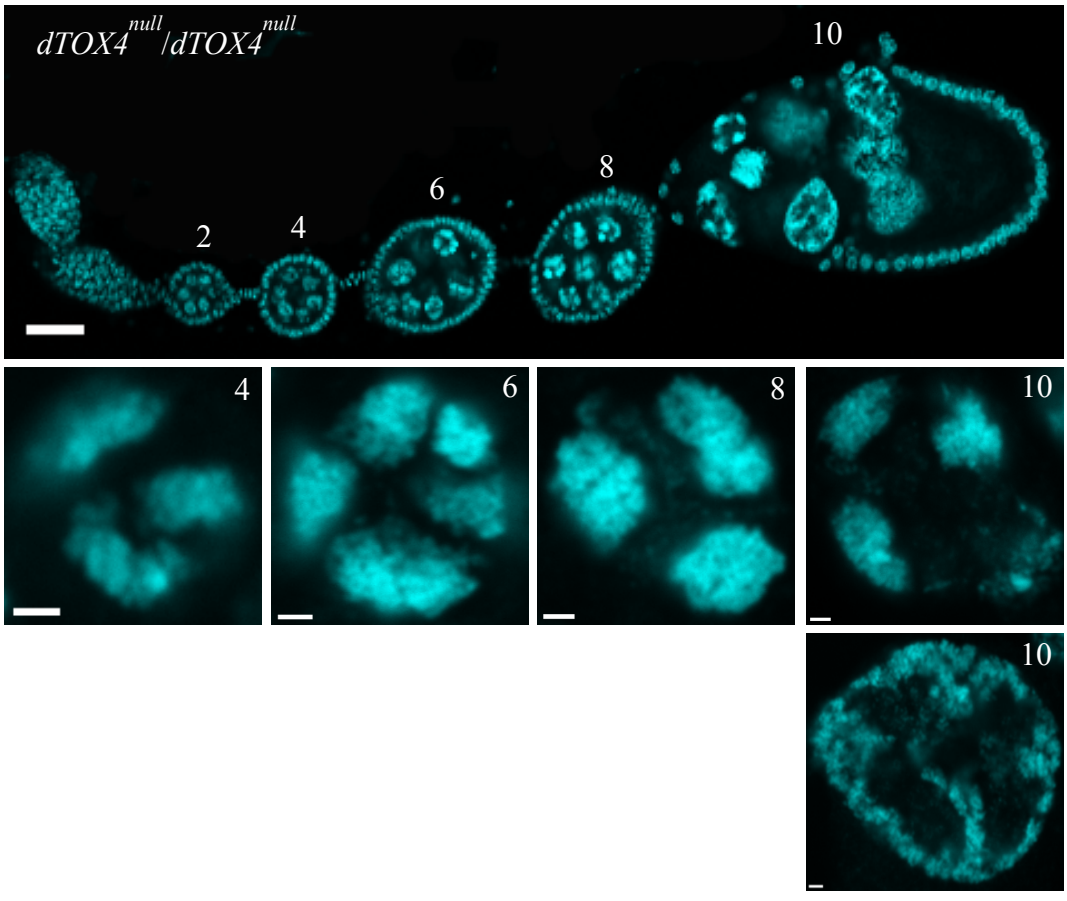

Table 5.1. The percentage of polytene nuclei (from stage 6) and appendage phenotypes observed from w^{1118} and females homozygous for $dTOX4^{null}$ including the appendage phenotypes observed when crossed to w^{1118}

	% nurse cell phenotype				% appendage phenotype				
Genotype	Wild type	Polytene	Ring	*n*	Wild type	Fused/Crown	Short/wide	Expanded operculum	*n*
w^{1118}	99.9	0.1	0.0	1343	100.0	0.0	0.0	0.0	1326
$dTOX4^{null}/dTOX4^{null}$	56.9	37.5	5.6	1436	12.6	21.6	22.1	43.7	412
(f) w^{1118} x (m) $dTOX4^{null}/dTOX4^{null}$	-	-	-	-	99.9	0.0	0.1	0.0	1564
(m) w^{1118} x (f) $dTOX4^{null}/dTOX4^{null}$	-	-	-	-	11.7	20.6	19.0	48.7	394

The *dTOX4*^{null} nurse cell nuclei phenotype has also been described in flies mutant for *squid* (*sqd*), *glorund (glo)* and *hrb27c* (also known as *hrp48*) (Goodrich *et al*., 2004; Kalifa *et al*., 2006; Kalifa *et al*., 2009), all of which encode heterogeneous nuclear ribonucleoproteins (hnRNPs). Mass spectrometry analysis carried out in a study of protein complex networks in *Drosophila*, showed dTOX4 is capable of binding to Hrp48, Squid and other hnRNPs, with the top hit being Glorund (a *Drosophila* hnRNP F/H homologue) (Guruharsha *et al*., 2011). Although hnRNP proteins were identified as binding many of the bait proteins in this study, the remarkable similarity in phenotype between *dTOX4* and *sqd*, *glo* and *hrp48* mutants suggest that the reported physical association is not simply an artefact. *Drosophila* mutant for these genes also display abnormal dorsal appendages therefore the appendages of eggs laid by homozygous *dTOX4* mutants was studied. A range of phenotypes were observed in the mutant with 21.6% of appendages exhibiting a fused/crown phenotype, 22.1% displaying short/wide appendages and the majority (43.7%) having an expanded operculum (Table 5.1). Only 12.6% of homozygous mutant eggs had narrow, well-separated appendages characteristic of wild type eggs (Table 5.1). Reassuringly, similar results were also found in homozygous mutant females that had mated with w^{1118} males, verifying the abnormal dorsal appendage phenotype is due to a maternal requirement for *dTOX4* (Table 5.1). Eggs also appeared to be much smaller than the w^{1118} control (data not shown).

5.4.3 *dTOX4* mutants display defects during spermatogenesis

To elucidate the cause of infertility in male *dTOX4* mutants, testis from w^{1118} and homozygous *dTOX4*^{null} males were dissected. An initial observation of the whole tissue revealed *dTOX4* mutant testes were, in most cases, significantly smaller than

the w^{1118} control and lacked the bundles of sperm tails that could be seen in the control. Testis were then stained for DNA, actin and phosphorylated H2AX at Serine (Ser) 139 and imaged by confocal microscopy (Figure 5.5a). Phosphorylation of histone H2A variant H2AX at Ser 139 occurs when double-stranded breaks (DSBs) are produced in DNA and is therefore a marker for DNA damage (Sharma *et al*., 2012). The rationale for looking at this was because TOX4 together with PNUTS and Wdr82 have been shown to bind DNA damaged by platinating agents (Puch *et al*., 2011) therefore could have a role in the DNA damage response.

During sperm individualisation each nuclei in a 64 spermatid cyst becomes surrounded by an actin cone, often referred to as an 'investment cone' as each spermatid is invested in its own membrane at the end of the process (Fabian and Brill, 2012). The array of investment cones make up the individualisation complex (IC), which translocates the length of the cyst, starting from the nuclear end of the developing sperm, removing excess cytoplasm and organelles from between the tails as it proceeds to the tail end (Fabrizio *et al*., 1998; Fabian and Brill, 2012). Once the individualisation process is complete the IC detaches and is known as a 'waste bag' (Fabrizio *et al*., 1998). In wild type testis the IC can be seen in the whole tissue as actin foci (Figure 5.5a, green arrow, top panel), however these were not present in *dTOX4* mutant testes (Figure 5.5a, bottom panel), suggesting individualisation does not take place and an earlier stage of spermatogenesis is affected. This was also apparent when examining squashed preparations of testicular tissue where waste bags and elongation could be seen in the control but not the *dTOX4* mutant (Figure 5.5b). Furthermore, the 64 needle shaped nuclei bundles could be visualised in the wild type tissue using confocal microscopy (Figure 5.5a, red arrow, top row) and

also in squashed preparations using phase microscopy (Figure 5.5c) but not in the *dTOX4* mutant (Figure 5.5a and 5.5c) suggesting nuclear shaping does not take place. Staining with H2AXph did not show any sites of DNA damage but in the absence of a positive control it cannot be determined whether *dTOX4* plays a role in the DNA damage response. However, the image does show the difference in the whole tissue in relation to the bundles of tails, which can easily be seen in w^{1118} but are absent in the mutant (Figure 5.5a, H2AXph).

Figure 5.5 (next page). *dTOX4*^{null}/*dTOX4*^{null} testes display defects in sperm development. a) Confocal microscopy images of w^{1118} (top panel) and *dTOX4*^{null}/*dTOX4*^{null} (bottom panel) testes stained for actin (green in merge), phosphorylated histone H2AX (magenta in merge) and DNA (TOPRO-3, Red in merge). Individualisation complexes are visible in w^{1118} testes as actin foci (green arrow). Bundles of sperm heads visible as DNA foci (red arrow) Scale bar = 40μm. b) Phase contrast micrographs of apical regions of w^{1118} (left panel) and *dTOX4*^{null}/*dTOX4*^{null} (right panel) testes. In w^{1118}, elongating spermatid tails visible as bundles of lines along the lumen of the testis (arrow). Waste bags containing excess cytoplasm and organelles removed during individualisation are found at the apical end (black arrow head). In some cases elongation can be seen in the mutant but it always starts further along the lumen (white arrow head). c) Phase contrast micrographs of squashed w^{1118} (top panel) and *dTOX4*^{null}/*dTOX4*^{null} (bottom panel) testes stained for DNA (red, Hoechst). Needle shaped sperm heads are visible in w^{1118} but not in the mutant. Phase contrast images were captured together with Helen White-Cooper (Cardiff University).

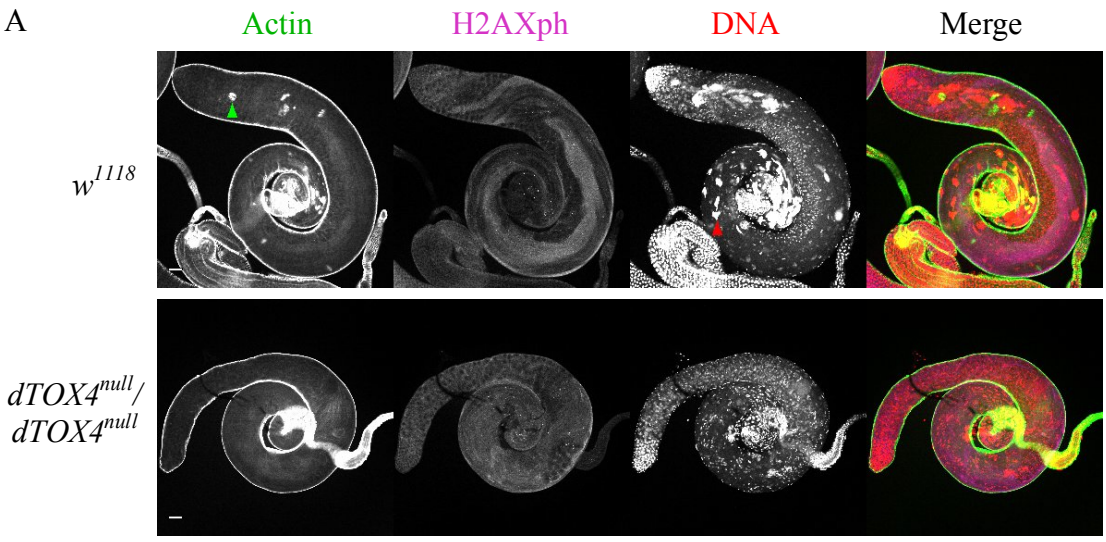
A
Actin
H2AXph
DNA
Merge
w1118
dTOX4null/
dTOX4null

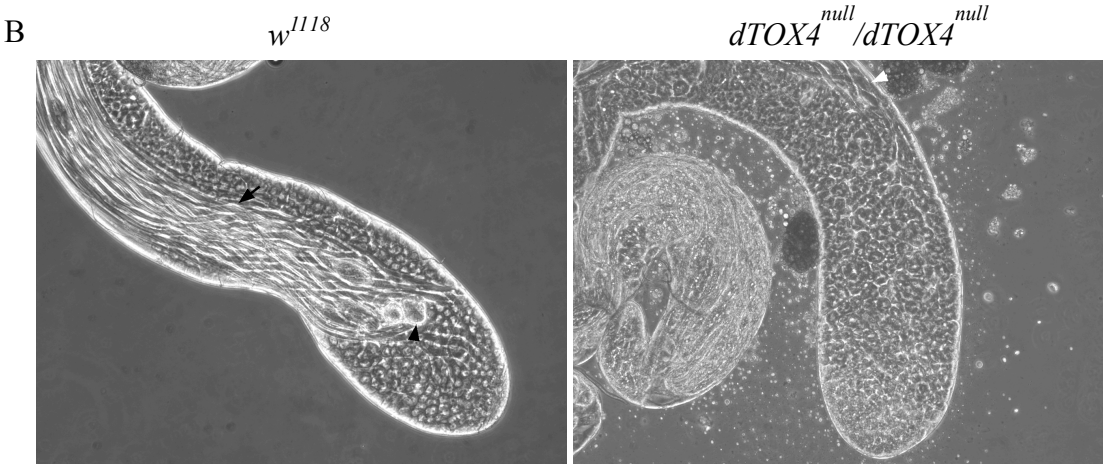
B
w1118
dTOX4null/dTOX4null

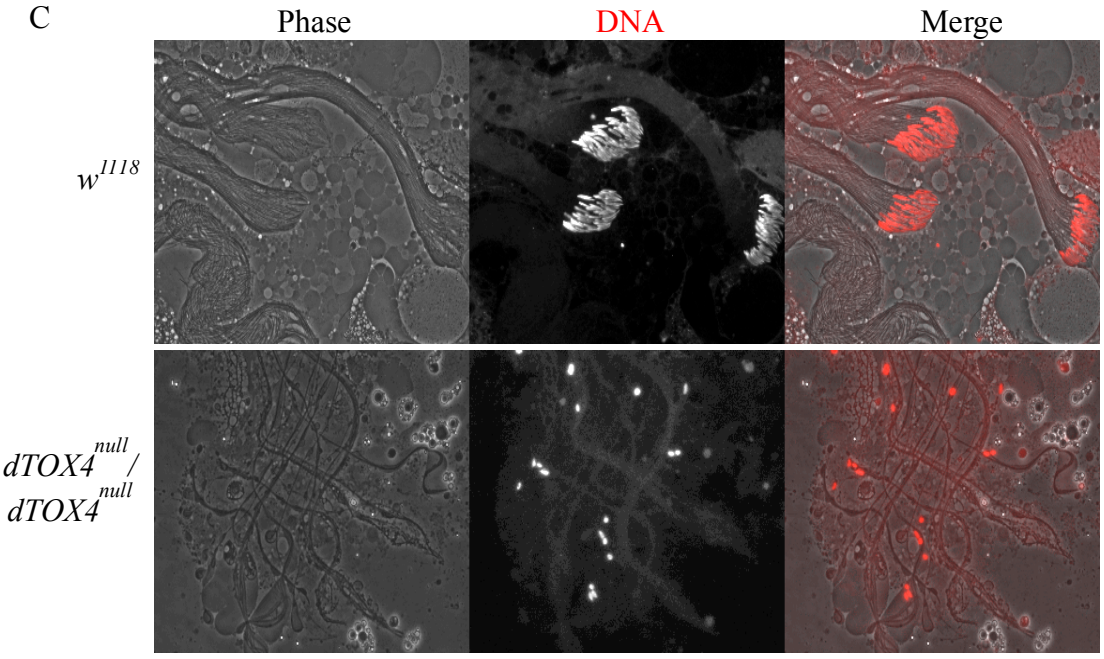
C
Phase
DNA
Merge
w1118
dTOX4null/
dTOX4null

Drosophila spermatogenesis has been well described and identification of the different stages is relatively easy as cells are large and easily visualised when squashed (White-Cooper, 2009). To gain more insight into the defects observed in *dTOX4* mutants and identify which stage of spermatogenesis is affected, squash preparations were made and examined by phase contrast microscopy (Figure 5.6). Interestingly a range of defects was observed at multiple stages of spermatogenesis. In some cases the testes were very difficult to find because they were smaller and lacked the spiral shape characteristic of wild type testes (Figure 5.6a and a'); when squashed they were found to consist only of primary spermatocytes (Figure 5.6b'). Visualisation of the DNA with Hoechst 33342 revealed a difference in chromatin occupancy when compared to w^{1118} (Figure 5.6c and c'). Immediately before the first meiotic division, the nucleus of primary spermatocytes exhibits three distinct chromatin masses, which correspond to the three major bivalents (Cenci *et al*., 1994; McKee *et al*., 2012). Once the spermatocytes have reached maturity the nucleus is fully expanded and the bivalents are far apart (Figure 5.6c) (McKee *et al*., 2012). However, the nuclei of primary spermatocytes from small mutant testes lacked the tri-lobular chromatin phenotype and instead the chromatin appeared as a 'cloudy' ring.

The most common phenotype observed is shown in Figure 5.6d' and is often referred to as the 'two wheel drive' or 'four wheel drive' phenotype due to its resemblance to mutants in the *Drosophila* gene *four wheel drive* (*fwd*), which display defects in cytokinesis (Brill *et al*., 2000). During telophase II of meiosis the mitochondria migrate to one side of the nucleus and then fuse to form two large mitochondria which become arranged as a sphere and establish a mitochondrial derivative known

as the nebenkern (Fabian and Brill, 2012; Bate and Arias, 2009). This is often referred to as the onion stage as the nebenkern contains multiple layers of wrapped mitochondrial membranes that resemble an onion (Cenci *et al*., 1994; Bate and Arias, 2009). This stage can easily be visualised using phase contrast microscopy on squash preparations as the nebenkern appears as a phase-dark circle next to the phase-light haploid nucleus (Bate and Arias, 2009) as shown in phase contrast images taken of onion stage spermatids in w^{1118} males (Figure 5.6d). In wild-type onion stage, each spermatid in a cyst has the same sized nebenkern and nucleus as represented in Figure 5.6d. In homozygous *dTOX4* mutants, the nebenkern appears abnormally large and is surrounded by two, three or four nuclei (Figure 5.6d').

Figure 5.6 (next page). Phase contrast microscopy reveals various defects in dTOX4 mutant testes. a) Wild type testes showing characteristic spiral shape and sperm development. a') Some *dTOX4* mutant testes are small and lack spiral shape and consist only of primary spermatocytes. b) Wild type primary spermatocytes with large nucleus in the centre. b') Primary spermatocytes from *dTOX4* mutant with small testes, some lacking an obvious nucleolus. c) Hoechst staining showing DNA in (b) illustrating tri-lobular configuration of chromatin. c') Hoechst staining showing DNA in (b') illustrating lack of tri-lobular chromatin and a 'cloudy' ring arrangement of chromatin. d) w^{1118} spermatids at the onion stage containing a single white nucleus (white arrowhead) associated with a single dark nebenkern (white arrow, 1Nk) d') *dTOX4* mutant spermatids at the onion stage showing a single large nebenkern associated with two (white arrow 2Nk) or four (white arrow 4Nk) nuclei. Images a and a' were taken using a 10X objective, images b to d' were taken using a

40X objective. Images were captured together with Helen White-Cooper (Cardiff University).

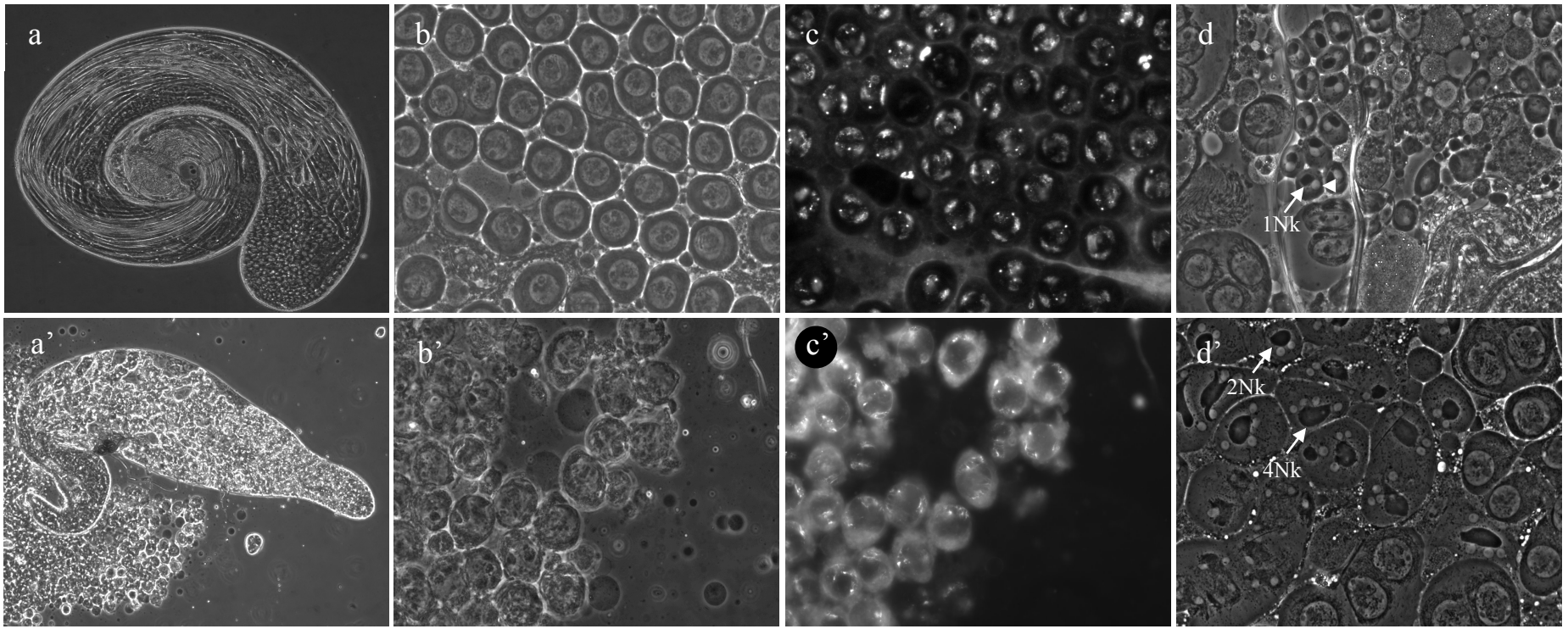

w^{1118}

dTOX4^{null}/
dTOX4^{null}

Other phenotypes were seen in the *dTOX4* mutant at a lower frequency (Figure 5.7). These included primary spermatocytes with smaller nuclei (Figure 5.7a, white arrow head, phase panel) and decondensed chromatin (Figure 5.7a, white arrow head, Hoechst panel) in a seemingly normal cyst and the appearance of needle shaped stellate crystals in otherwise normal looking *dTOX4* mutant primary spermatocytes. These phenotypes were not observed in the wild type controls (Figure 5.7b, white arrows).

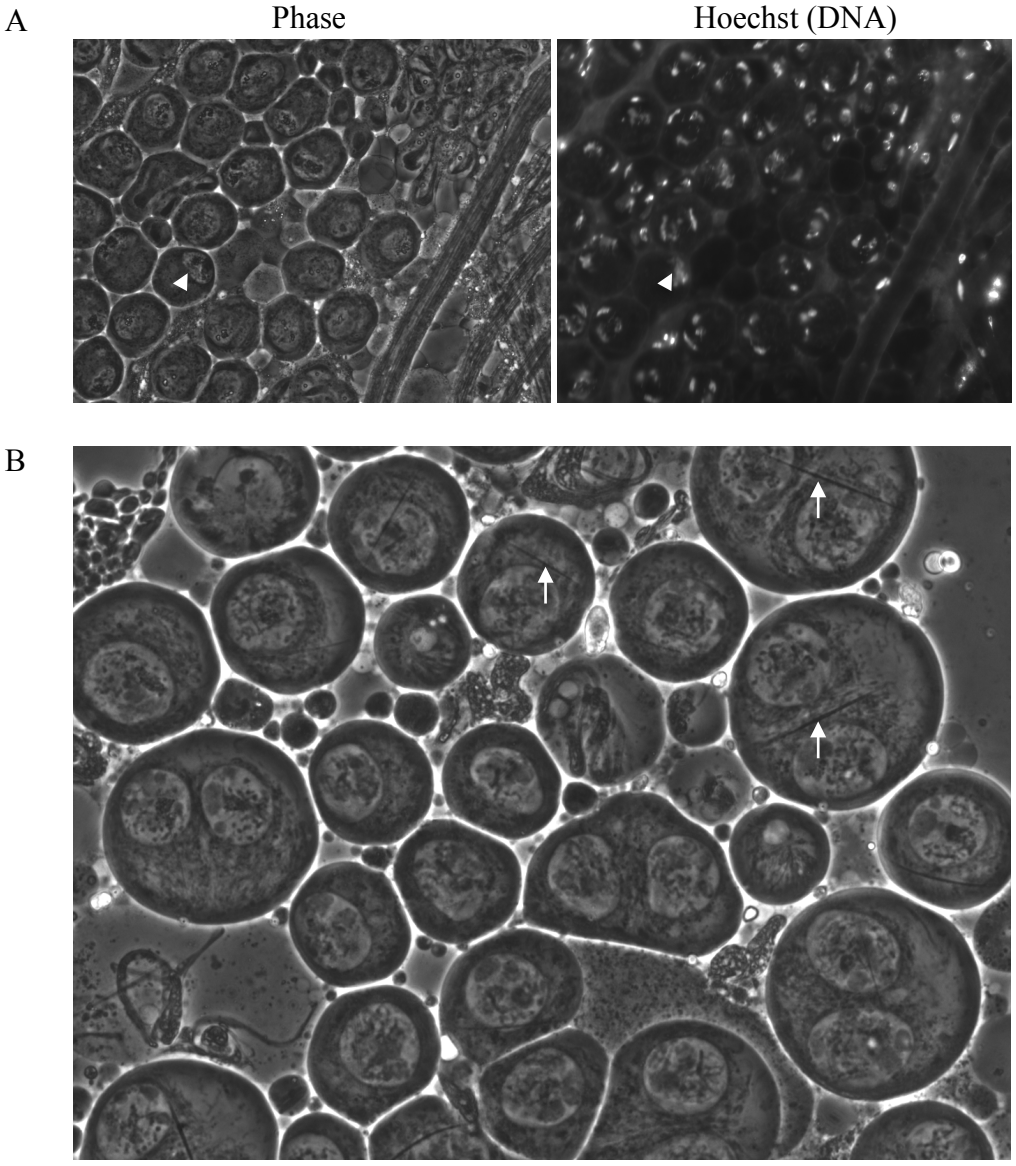

Figure 5.7. (previous page). Other phenotypes observed in squashed testes of *dTOX4* mutants. a) Some primary spermatocytes displayed smaller nuclei (Phase, white arrow head) and decondensed chromatin (Hoechst, white arrow head) in a cyst primarily consisting of normal spermatocytes. b) In some testes the appearance of stellate crystal like formations could be observed (white arrows). Images were captured together with Helen White-Cooper (Cardiff University).

5.5. *dTOX4* plays a role in *Drosophila* longevity

As mentioned in Chapter 3, loss of PNUTS expression during cardiac aging is associated with cardiomyocyte cell death and loss of cardiac function (Boon *et al*., 2013). The identity and role of PNUTS-interacting proteins that might mediate its function in healthy aging are not fully understood. Given the interaction between dPNUTS and dTOX4 and the inability of the dTOX4 mutant to thrive, the impact of the $dTOX4^{null}$ allele on *Drosophila* longevity was assessed. Survival of $dTOX4^{null}/dTOX4^{null}$ flies was significantly reduced compared to the w^{1118} control (p=<0.0001) and even loss of one copy of *dTOX4* had a significant impact on survival (p=<0.0001, Figure 5.8), suggesting *dTOX4* plays a role in healthy aging.

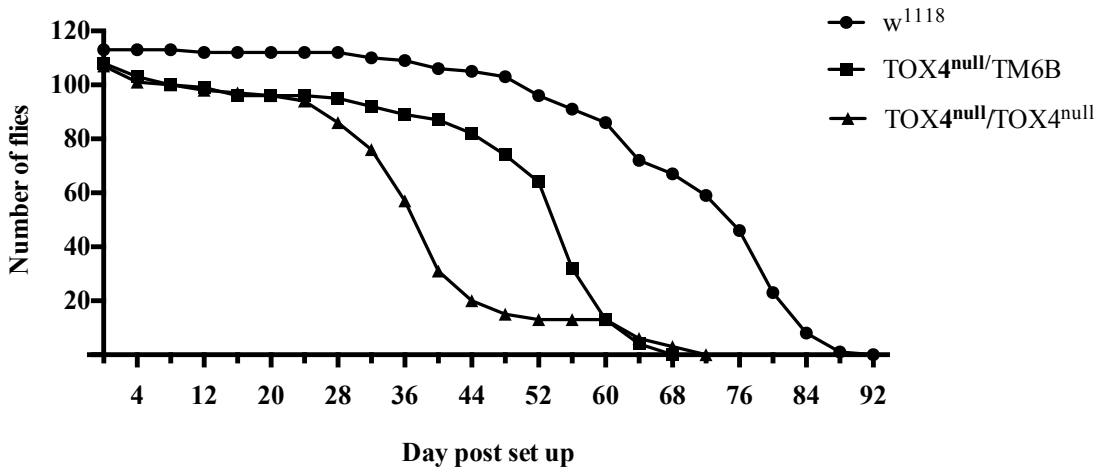

Figure 5.8. *dTOX4* has a role in *Drosophila* survival. Survival curves of *dTOX4* homozygous and heterozygous mutants and a wild type control (w^{1118}).

5.6. Generating transgenic flies overexpressing $dTOX4^{wt}$ and $dTOX4^{P216\Delta}$

The results discussed in Section 5.4 onwards assume that disruption of the *dTOX4* coding region is responsible for the phenotypes observed. Indeed, Section 5.3 provides evidence that the *dTOX4* transcript is absent in the mutant. Although generating null alleles through imprecise excision of a *P*-element is common and has proved to be very efficient, caution has to be taken as this method does have a potential caveat that could affect the validity of the results. Upon immobilisation of the *P*-element, there is the potential for it to re-insert itself in another part of the genome where it could disrupt another gene, before eventually being lost.

Therefore, to confirm that the disruption of dTOX4 is responsible for the phenotypes described, the wild type d*TOX4* gene was subcloned from the DGRC cDNA clone LP0118 into the *Drosophila* Gateway® vector pPGW (pUASP-GW) for GAL4-driven, N-terminal GFP tagged somatic and female germline ectopic overexpression of *dTOX4*. *UASP-GFP-dTOX4*^{wt} flies were made using *P*-element mediated germline

transformation into a w^{1118} strain. In parallel with this, a dTOX4 transgene with a site-directed mutation that removes the dPNUTS binding region of dTOX4 (Chapter 4) was also subcloned into pPGW and *UASP-GFP-dTOX4*$^{P216\Delta}$ flies were generated. These could be used to determine whether the *dTOX4* mutant phenotypes are dependent on the interaction between dPNUTS and dTOX4, or if they represent dPNUTS-independent functions of dTOX4.

Various transgenic lines were generated with insertion of *UASP-GFP-dTOX4*$^{wt/P216\Delta}$ on different chromosomes. To determine which lines to use for the complementation experiments, the GAL4-UAS system was used to ectopically overexpress each transgene in the fly using *daughterless* (*da*)-GAL4 for ubiquitous expression. Protein extracts were then analysed by Western blot analysis (Figure 5.9). Although not evident in Figure 5.9, the transgenic lines overexpressing *dTOX4*^{wt} expressed at a similar level to each other, and had an extremely low level of expression compared to the *dTOX4*$^{P216\Delta}$ lines. Transgenic lines overexpressing *dTOX4*$^{P216\Delta}$ varied in expression levels therefore a range of lines were selected for functional analysis (Figure 5.9.). Notably, *dTOX4*^{wt} and *dTOX4*$^{P216\Delta}$ overexpression under the control of *daughterless* had no discernable biological effect.

The selected lines were then combined with different GAL4 drivers for tissue specific expression. GAL4 driven by the *maternal-α-tubulin* promoter was combined with each transgenic line to drive overexpression in the female germline in an attempt to rescue the nurse cell nuclei and appendage phenotypes described in 5.4.2. GAL4 driven by the *bag of marbles* (*bam*) promoter was used to drive

overexpression in the male germline in an attempt to rescue the testicular phenotypes described in 5.4.3. This work is currently ongoing in the Bennett lab.

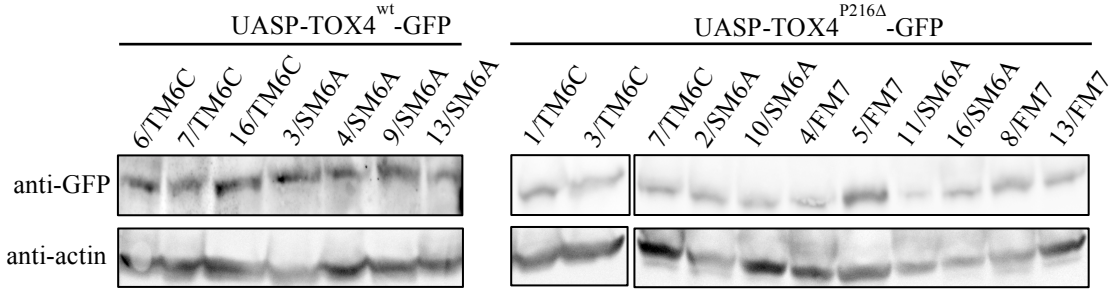

Figure 5.9. Immunoblots of UASP-dTOX4$^{wt/P216\Delta}$-GFP transgenic flies. Protein extracts from each line were analysed by Western blot anti-GFP antibody to detect the overexpressed protein. Anti-actin antibody was used as a control to determine the relative levels of protein in each extraction.

5.7. Generating transgenic dTOX4^{wt} and dTOX4$^{P216\Delta}$ genomic rescue flies

Rescuing mutant phenotypes by overexpressing wild type transgenes does have a number of limitations - in particular, efficient rescue is reliant on using a suitable GAL4 driver that drives expression in the correct spatial and temporal pattern and at the appropriate level. Rescue of mutant phenotypes using a genomic construct is often preferred since the wild type gene is under the control of its own promoter and the pattern of expression can better match that of the endogenous alleles. To do this a DNA fragment incorporating the genomic *dTOX4* sequence was chemically synthesised with a few modifications to improve its utility. Firstly, the sequence for EGFP was inserted before the transcription start site to allow visualisation of the expressed protein and determine the stage of expression in the ovaries and testes to

further understand the phenotypic changes seen in the dTOX4 mutant. An attB site was also added at the end of the sequence for ϕC31 site specific recombination (Groth *et al*., 2004) along with a *BamH1* and *Not1* enzyme restriction site at the beginning and end of the sequence respectively for sub-cloning into a suitable fly transformation vector. In parallel an identical construct was generated that carried the site-directed mutant that removes the dPNUTS-binding site through incorporation of a premature stop codon. The fragments were synthesised by GeneArt/Invitrogen, subcloned into the pCaSpeR3 fly transformation vector (pCaSpeR3 was purchased from DGRC and sent to GeneArt) and sent to the Fly Facility (University of Cambridge, Department of Genetics) for site-specific integration into the *Drosophila* genome. Analysis of these transgenes is currently ongoing in the Bennett lab.

5.8. Discussion

The work described in this chapter reports the functional analysis of *CG12104*, which is the *Drosophila* homologue of the human gene LCP1 (TOX4). In the literature LCP1 has been shown to bind PNUTS and may have a role in recruiting transcriptional complexes to chromosomes at the sites were it is bound (Lee *et al*., 2009). This study was interested in identifying the *in vivo* role of dTOX4 and exploring its potential involvement in regulating dPNUTS and dPNUTS-mediated gene expression (described in Chapter 3).

5.8.1. The role of *dTOX4* during oogenesis

dTOX4 is essential for female fertility as mutant animals fail to produce viable progeny. Tissue analysis revealed sterility in females is likely a consequence of defects in two processes during oogenesis: abnormal dorsal-ventral patterning of dorsal appendages of the eggshell and chromosome dispersal in nurse cell nuclei.

In *Drosophila*, proper establishment of the major body axes of the egg is essential for normal development of the future embryo (Clouse *et al*., 2008). Axis formation relies on the strict localisation of certain maternal mRNAs for localised protein translation (Norvell *et al*., 2005). Gurken (Grk), a TGFα-like ligand, is essential for establishing both the anterior-posterior axis during early oogenesis and the dorsal-ventral axis during mid to late oogenesis, where it activates the Epidermal Growth Factor Receptor (EGFR) in the overlying follicle cells to specify cell differentiation for proper axis formation (Johnstone and Lasko, 2001; Norvell *et al*., 2005; Neuman-Silberberg and Schüpbach, 1993; Kalifa *et al*., 2009). Spatio-temporal expression of Gurken relies on proper *grk* mRNA localisation and regulation of its translation for

localised activation of EGFR and induction of dorsal cell fates (Johnstone and Lasko, 2001; Goodrich *et al*., 2004).

Genetic and biochemical studies have identified various proteins responsible for the localisation and translational regulation of *grk* mRNA and these include the heterogeneous nuclear ribonucleoproteins (hnRNPs) Squid (Sqd), Hrp48 and Glorund (Glo) (Kalifa *et al*., 2009; Kalifa *et al*., 2006). hnRNPs are RNA binding proteins and function in a wide variety of processes including mRNA localisation/transport/stability/splicing, transcription, translation and protein stability (Dreyfuss *et al*., 2002; Goodrich *et al*., 2004). In *sqd*, *glo* and *hrp48* mutants *grk* mRNA is ectopically translated across the entire anterior region of the oocyte and the resulting phenotype is an expansion of the dorsal appendages at the anterior region of the egg (Kelley, 1993; Goodrich *et al*., 2004), as seen in *dTOX4* homozygous mutants.

Like *dTOX4* mutants, a failure in nurse cell chromosome dispersion from stage 6 is also a common phenotype in *hrp48, sqd* and *glo* mutants (Goodrich *et al*., 2004; Kalifa *et al*., 2009) . The role of chromosome dispersal in *Drosophila* oogenesis is still unknown but it has been suggested to be necessary for rapid ribosomal synthesis of proteins required for the remainder of oogenesis (Dej and Spradling, 1999; Klusza and Deng, 2010), which could explain why the eggs laid by mutants are often smaller. This phenotype has also been described for *ovarian tumour* (*otu*), *half-pint* (*hfp*) and *poly* mutants (Dej and Spradling, 1999; Van Buskirk and Schüpbach, 2002; King *et al*., 1981; King and Storto, 1988; Klusza and Deng, 2010). It has been shown that Hrp48 binds to Hfp and Glorund and it is believed, together, they participate in a

splicing complex that regulates the alternative splicing of *otu* to contribute to *grk* mRNA regulation and nurse cell chromosome dispersion (Kalifa *et al*., 2009). Moreover, the defects exhibited by *hrp48, glo* and *hfp* mutants can be rescued by the *Otu-104* isoform (Van Buskirk and Schüpbach, 2002; Kalifa *et al*., 2009; Goodrich *et al*., 2004). This suggests the defects are a consequence of disrupting *otu* regulation. Given dTOX4 may bind Hrp48 and Glorund in *Drosophila* (Guruharsha *et al*., 2011), dTOX4 could function in this RNP complex; the defects observed in the *dTOX4* mutant may therefore be a consequence of disruption of *otu* splicing. Interestingly, Hrp48 also binds to Sqd, another hnRNP shown to bind dTOX4 (Guruharsha *et al*., 2011). Goodrich *et al.*, 2004, proposed Hrp48, Sqd and Otu may also participate in a complex to regulate *grk* mRNA localisation and nurse cell chromosome dispersion through an unknown mRNA but as Sqd and Otu do not bind to Hfp and Glo respectively, it is likely Hrp48/Hfp/Glo and Hrp48/Sqd/Otu represent two distinct complexes (Goodrich *et al*., 2004; Kalifa *et al*., 2009). It is possible dTOX4 functions in both of these complexes or may act to bring both complexes together to regulate *grk* mRNA localisation and nurse cell chromosome dispersion. It would be interesting to see if *grk* mRNA localisation is affected in *dTOX4* mutants and if a wild type copy of *otu* can rescue one or both phenotypes.

One caveat to the mass spectrometry analysis showing dTOX4 binds to these hnRNP proteins is the author deemed hnRNP proteins non-specific as they were common interactors throughout their analysis (Guruharsha *et al*., 2011). However the phenotypic resemblance between hnRNP mutants and the dTOX4 mutant suggests in this case the interaction is specific and they are likely to be real interactors. This needs to be confirmed by independent co-immunoprecipitation experiments; the

molecular function of dTOX4 in these complexes would then need to be determined. As discussed in the introduction, dTOX4 is a HMGB protein; therefore it seems plausible for dTOX4 to play a structural role in these complexes by opening up secondary nucleic acid structures to allow recruitment of hnRNP complexes.

5.8.2. The role of *dTOX4* during spermatogenesis

dTOX4 is essential for male fertility as mutant animals fail to produce fertilised eggs when mated to females from a wild type strain. Whole tissue analysis revealed mutant males lack the characteristic sperm head/tail bundles and investment cones of wild type *Drosophila* suggesting spermatogenesis is impaired. Squash preparations uncovered multiple defects at the cellular level. Firstly, a number of testes appeared smaller, misshapen and consisted only of primary spermatocytes. Moreover, the chromatin of these spermatocytes appeared abnormal and lacked the tri-lobular appearance of normal spermatocytes. This phenotype is often associated with meiotic arrest mutants as primary spermatocytes fail to enter the meiotic stages (White-Cooper, 2010). However the meiotic arrest phenotype in the *dTOX4* mutant occurs less frequently than in meiotic arrest mutants reported in the literature but when it does occur, it appears more severe as testes are smaller and misshapen.

dTOX4^{null} males also displayed defects typical of mutants in genes involved in cytokinesis as spermatids had abnormally large nebenkerns surrounded by two or four nuclei. This phenotype has also previously been observed in *Drosophila* mutant for the gene *eIF4E-3*, an initiation factor which binds to the 5' cap of mRNAs and regulates their recruitment to the ribosome (Hernández *et al*., 2012). Furthermore a similar cytokinetic defect has been described in mutants for the gene Larp, which

associates with poly(A) binding protein (PABP) (Blagden *et al*., 2009). PABP was also identified as a dTOX4 binding protein in the same screen as the hnRNP proteins (Guruharsha *et al*., 2011). Interestingly PABP attaches to the 3' poly(A) tail of mRNAs and another initiation factor, eIF4G, which in turn binds to eIF4E. This brings the 3' and 5' ends of the mRNA together, forming a closed circular structure to initiate translation and maintain mRNA stability (Blagden *et al*., 2009). Given the evidence linking dTOX4 to mRNA regulation during oogenesis through its association with hnRNPs, it is conceivable that dTOX4 plays a similar role during spermatogenesis through association with PABP. eIF4E also binds to an ovarian protein called Cup, which has been shown to function together with Squid and PABP55B to regulate *gurken* translation in *Drosophila* ovaries (Clouse *et al*., 2008; Nakamura *et al*., 2004). Furthermore, work done in Dr Helen White-Cooper's lab has showed that *sqd* displays a two-wheel drive phenotype in the testes, the data for which can be found on the online resource, Flannotator (http://www.flyprot.org/) (Lowe *et al*., 2014). This suggests the cytokinetic defects observed in the testes could be due to an interaction with Squid.

Other defects included the appearance of Stellate crystalline structures, which have been associated with mutations in piRNA pathway genes (Bozzetti *et al*., 2012). *Stellate* (*ste*) is a male meiotic gene located on the X chromosome and its expression is controlled by another male meiotic gene, *Suppressor of Stellate* (*Su(ste)*), located on the Y chromosome (Stapleton *et al*., 2001). In *Su(ste)* mutants *Ste* mRNA and protein are present in abundance in primary spermatocytes, which leads to male sterility and the formation of needle-shaped crystals, as seen in the dTOX4 mutant, and other meiotic defects including chromosome fragmentation (Stapleton *et al*.,

2001). Moreover, mutants of *homeless*, a RNA helicase, which functions in collaboration with *Su(ste)* to repress *ste* in primary spermatocytes, have the same meiotic defects as *Sus(ste)* mutants (Stapleton *et al*., 2001). *homeless* is also required for the localisation of mRNAs for anteroposterior and dorsoventral axis formation during oogenesis, including *grk* and *osk*, and mutants of *homeless* cause female sterility, as well as male sterility (Gillespie and Berg, 1995; Stapleton *et al*., 2001). It is therefore conceivable that the sterility defects observed in males are a consequence of a role for *dTOX4* in *ste* mRNA regulation.

It is very clear *dTOX4* is essential for both proper oogenesis and spermatogenesis but its role at the molecular level is still unknown. It is possible dTOX4 functions in various RNP complexes and the defects observed are a consequence of misregulation of mRNA processing and defective protein translation. This is further supported by the fact that dTOX4 has also been shown to bind to various ribosomal proteins in mass spectrometry analysis as well as the hnRNPs already discussed (Guruharsha *et al*., 2011). The importance of dTOX4s identity as a HMGB protein in this remains unclear. HMGB proteins are better known for interacting with DNA, but given all that has been discussed, the results could represent an RNA binding function of dTOX4 that has not been reported elsewhere. It will also be interesting to see if dTOX4 operates in similar pathways/complexes during oogenesis and spermatogenesis, possibly through association with Squid, or if it acts in independent pathways/complexes.

5.8.3. *dTOX4* promotes longevity in *Drosophila*

dTOX4 mutant flies exhibit reduced survival compared to a wild type control suggesting it contributes to *Drosophila* longevity. Although the data is preliminary there is a rationale supporting further investigation of this function. It has already been suggested that TOX4 plays a role in DNA damage as it binds to sites of DNA damage induced by platinating agents together with PNUTS and Wdr82 (Puch *et al*., 2011). It is well known that increased levels of DNA damage are associated with aging. PNUTS has also been directly linked to cardiac aging where a decrease in PNUTS is associated with an increase in microRNA-34a as cardiac aging progresses (Boon *et al*., 2013; Garinis *et al*., 2008). MicroRNA-34a is transcriptionally regulated by *p53*, a tumour suppressor gene induced during DNA damage involved in DNA repair and apoptosis (Dorn, 2013). It is possible aging is affected by dTOX4 through association with a PNUTS/PP1/Wdr82 complex and effects on gene expression or DNA damage.

5.8.4. dTOX4 and PNUTS

Unfortunately it was not possible to verify rescue of the mutant phenotypes with either overexpressed or genomic wild type dTOX4 due to time constraints. Likewise the relevance of the interaction between dPNUTS and dTOX4 in the results described could not be determined. However, the necessary tools to test this were generated and the Bennett lab is continuing work to confirm these limitations. It is possible the phenotypes represent dPNUTS-independent roles of dTOX4, in which case investigating the association of dTOX4 and hnRNPs is a plausible avenue to follow up. If these phenotypes are dependent on dPNUTS then is PP1 also involved and what are the substrates? Given these proteins exist in a complex with Wdr82 in

mammals and humans; does this have a role in the phenotypes observed? The PNUTS-PP1/Wdr82/TOX4 complex has been shown to function in the regulation of chromatin decondensation at late telophase (Lee *et al*., 2010) so is Wdr82 also involved. It is possible the different phenotypes represent two distinct roles of dTOX4, one in mRNA regulation possibly through binding to hnRNPs and the other in chromosomes decondensation through association with dPNUTS and dWdr82.

6. Epigenetic regulation of transcription via histone phosphorylation

6.1. Introduction

One aspect that has emerged through studies on PP1 is the importance of phosphorylation in maintaining cell identity through epigenetic regulation of transcription (Rudenko *et al*., 2003). Gene expression patterns are established early during animal development to specify cell identity and are maintained throughout the multiple cell divisions necessary for proper development by epigenetic modifications such as phosphorylation, methylation and acetylation. These modifications exist on DNA and the N-terminal tail of histones and different modifications/combinations of modifications have different effects on gene expression that mainly act to modulate chromatin structure via recruitment of chromatin remodelling complexes (Farkas *et al*., 2000).

One of the major findings from studies looking at transcriptional memory in *Drosophila* is the discovery of the Polycomb group (PcG) of repressive protein complexes, which repress gene expression via association with post-translational epigenetic modifications (Martinez *et al*., 2009). They localise to many chromosomal sites and hundreds of target genes have been identified in *Drosophila* and mammals, with most functioning in major developmental pathways, suggesting PcG proteins are major regulators of transcription during development (Di Croce and Helin, 2013; Simon and Kingston, 2009; Schwartz *et al*., 2006; Nègre *et al*., 2006; Tolhuis *et al*., 2006; Boyer *et al*., 2006; Lee *et al*., 2006). PcG proteins exist as subunits in two major complexes; Polycomb Repressive Complex 1 (PRC1) and PRC2 (Chen *et al*., 2010). PRC2 has histone methyltransferase activity in its enhancer of zeste 2 (EZH2)

(E(z) in *Drosophila*) subunit, which mediates the mono- di- and tri-methylation of histone H3 on lysine 27 (H3K27me1/2/3) allowing recruitment and binding of PRC1 to target genes via its chromobox-domain subunits (Cao *et al*., 2002; Enderle *et al*., 2011). PRC1 is thought to promote gene silencing through regulation of chromatin condensation (Simon and Kingston, 2009; Margueron and Reinberg, 2011). The H3K27me3 epigenetic mark is predominantly associated with the repression of homeotic and developmental genes to maintain cell identity and prevent uncontrolled proliferation during development (Gehani *et al*., 2010).

In 2003 it was hypothesised that recruitment of regulatory proteins to methylated histone tails could be modified by phosphorylation of neighbouring residues (Fischle *et al*., 2003). In 2005 it was reported that tri-methylation of histone H3 lysine 9 (H3K9) associates with Heterochromatin Protein 1 (HP1, isoforms -α, -β, -γ), triggering a change in chromatin structure to a repressive state (heterochromatin formation), a mechanism analogous to the H3 lysine 27 (H3K27)/PcG situation (Fischle *et al*., 2005; Hirota *et al*., 2005). They showed that upon phosphorylation of the adjacent Serine 10 (S10) residue, HP1 dissociated from methylated K9 to allow expression of target genes. If phosphorylation of S10 was inhibited, the interaction between HP1 and methylated K9 was maintained (Hirota *et al*., 2005; Fischle *et al*., 2005). This led to the proposal that phosphorylation of histone H3 at serine 28 (H3S28) may inhibit the interaction between methylated K27 and PcG proteins, suggesting H3S28 is a key site for gene regulation. In 2011, Lau and Cheung described the reactivation of the PcG-silenced gene, α-globin, by inducing phosphorylation of H3S28 at its promoter using mitogen-and-stress-activated kinase 1 (MSK1). They also reported a decrease in H3K27 methylation and PcG elements

when MSK1 was present; suggesting phosphorylation of H3S28 displaced the repressive PcG complex (Lau and Cheung, 2011b; Lau and Cheung, 2011a). Other recent work has also shown that a phospho-methyl mark does exist at S28-K27 and S28 phosphorylation modifies recruitment of PcG to K27 (Gehani *et al*., 2010). However the kinases and phosphatases that control the phosphorylation state of this important regulatory site remain poorly understood.

Since the discovery of this field, many epigenetic modifications have been linked to cancer adding further complexity to cancer biology (Rodríguez-Paredes and Esteller, 2011). In 2010 a report linked drug resistant cancer cells to changes in the epigenetic landscape of those cells (Sharma *et al*., 2010). Many cancers have aberrant epigenetic states and more studies are discovering mutations that cause cancer stem from epigenetic changes (Rodríguez-Paredes and Esteller, 2011; Brower, 2011). From these studies it has become increasingly evident that epigenetic modifications could act as biomarkers for cancer detection (Rodríguez-Paredes and Esteller, 2011; Brower, 2011). Furthermore these modifications are reversible, suggesting they are good drug targets as has been shown by Squamocin, which modulates H3S10/H3S28 phosphorylation and can inhibit the proliferation of cancer cells (Lee *et al*., 2011).

A number of studies have used *Drosophila* to demonstrate the link between PcG proteins and cancer. They have revealed that mutations in core PcG proteins cause hyperproliferation of the eye imaginal disc in *Drosophila* (Classen *et al*., 2009). This was accompanied by the activation of the JAK-STAT mitogenic pathway suggesting PcG proteins act as tumour suppressors by repressing JAK-STAT signalling (Classen *et al*., 2009). The *Drosophila* eye has also been used as a model to show cells harbouring a mutation in the PcG protein, Polyhomeotic, over proliferate and fail to

differentiate (Martinez *et al*., 2009). These studies propose PcG proteins have tumour suppressor activity and highlight the need to further understand H3S28 regulation and its effect on PcG recruitment.

6.1.1. Aims

The aim of the work of this chapter was to develop assays that would permit the *Drosophila* genome to be interrogated for kinases and phosphatases that regulate H3S28 phosphorylation, PcG-chromatin interactions and transcriptional memory. Two complementary experimental approaches were attempted. The first approach was to develop probes capable of Fluorescence Resonance Energy Transfer (FRET) that could be used in an RNA interference (RNAi) based *in vitro* substrate screen to identify kinases and phosphatases that regulate H3S28 phosphorylation. In parallel with this a functional *in vivo* screen was planned to complement the substrate screen with the aim of identifying kinases/phosphatases that enhance or suppress the eye overgrowth phenotype observed upon *polyhomeotic* loss-of-function using heritable RNAi in adult *Drosophila*. Work was also done to study the role of PNUTS-PP1 in histone phosphorylation and other histone marks associated with active transcription to further understand the role of this holoenzyme in gene expression in *Drosophila*.

6.1.2. Detecting protein interactions using FRET

FRET is a method capable of detecting protein-protein interactions in living and fixed cells by fluorescently labelling proteins of interest (Snapp and Hegde, 2001; Karpova *et al*., 2003). An interaction is identified through the non-radioactive transfer of energy from one fluorescent molecule (known as the donor) to another fluorescent molecule (known as the acceptor), upon donor excitation, when the adjoining proteins interact and bring the fluorophores into close proximity (Figure

6.1) (Snapp and Hegde, 2001). Many parameters influence the probability and efficiency of FRET, but the most important to consider when designing a FRET probe is the distance separating the fluorescent pairs (this needs to be less than approximately 10nm) and the spectral overlap between donor and acceptor fluorescent proteins (Snapp and Hegde, 2001; Broussard *et al*., 2013; Ishikawa-Ankerhold *et al*., 2012). The donor should be excited at a wavelength lower than the acceptor, the emission spectrum of the donor should overlap significantly with the excitation spectrum of the acceptor and the emission spectrum of the acceptor should be reasonably separate from the donor emission spectrum to allow selective measurement of the acceptor emission (Snapp and Hegde, 2001; Ma *et al*., 2014). Other factors to consider when choosing fluorescent proteins include the 'brightness' (a protein should emit enough signal above autofluorescence to be detected and imaged), its expression in the chosen system (expression levels need to be similar) and its photostability (Shaner *et al*., 2005). Differences in expression levels often arise when using intermolecular probes (detecting an interaction between two separate proteins) and this can be circumvented by using an intramolecular FRET biosensor were the two proteins and their fluorescent proteins are expressed as part of the same molecule (Broussard *et al*., 2013). A wide variety of fluorescent proteins are available and the literature reports many optimized FRET pairs but one of the most efficient and commonly used is ECFP and EYFP (Ma *et al*., 2014; Broussard *et al*., 2013; Ishikawa-Ankerhold *et al*., 2012).

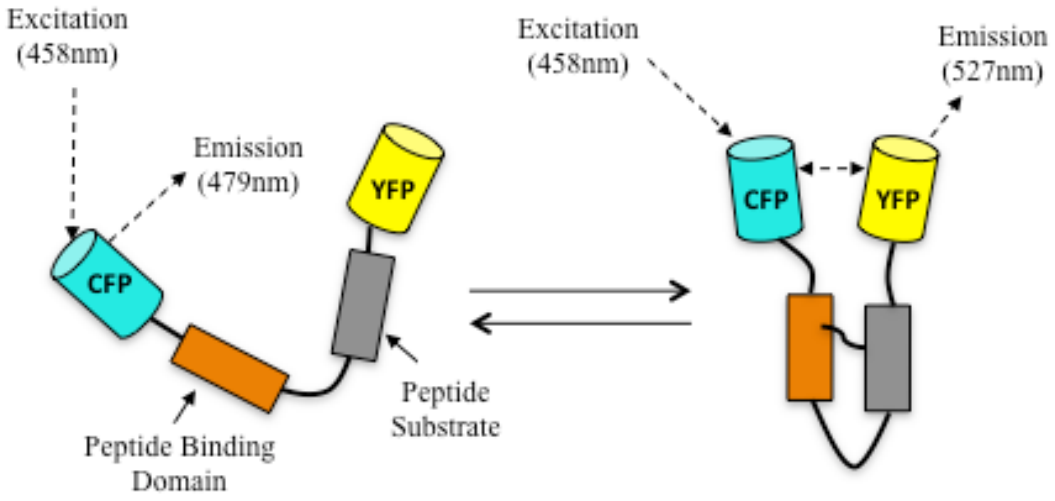

Figure 6.1. Structure and design of FRET probes. In the absence of binding, FRET cannot occur and energy from excitation of the donor (CFP) is lost. Upon interaction of the peptide substrate with the peptide-binding domain, the fluorophores are brought into close proximity and energy is transferred from CFP to YFP and an increase in acceptor (YFP) fluorescence is observed.

Numerous methods for detecting FRET in microscopy are available (Van Munster *et al*., 2005). Techniques include sensitized emission (see 6.2.4), acceptor photobleaching (see 6.2.5), spectral imaging and Fluorescence lifetime imaging microscopy (FLIM) (Broussard *et al*., 2013). FLIM-FRET measures the lifetime decay of the donor fluorophore over time, after excitation (Ma *et al*., 2014; Broussard *et al*., 2013). The time it takes to decay back to the ground state is shortened when in close proximity to an acceptor fluorophore as energy is transferred from the donor to the acceptor (quenching) (Ishikawa-Ankerhold *et al*., 2012). However measurements are sensitive to the local environment therefore pH, temperature, oxygen, ion concentration, polarity and refractive index of the medium

have to be strictly controlled (Ma *et al*., 2014). Furthermore, FLIM requires expensive and custom designed instruments, which means it is not always readily available. Spectral imaging is usually used in combination with sensitized emission and collects images spanning the entire fluorescence emission spectrum to determine what proportion of the signal is from ECFP and EYFP (FRET) and what is from autofluorescence (Broussard *et al*., 2013). This improves sensitivity and allows a more accurate calculation of true FRET signal to be made (Broussard *et al*., 2013). Sensitized emission and acceptor bleaching are more commonly used approaches in FRET experiments and require more commercially available instruments. These are discussed further in sections 6.2.4 and 6.2.5.

6.1.3. RNA interference (*in vitro* vs. heritable)

RNAi is a high throughput method for analysing gene function, which acts to silence target genes by using short (~19 nucleotides) double-stranded RNA (dsRNA) fragments. These bind to the target mRNA resulting in cleavage and degradation of the mRNA, thereby abrogating gene function. There are many different methods for introducing dsRNA fragments into a system. The FRET-based substrate screen in *Drosophila* S2R+ cells would make use of *in vitro* transcribed dsRNA, which would be introduced into cells by transfection. The phenotypic screen in *Drosophila* adults would make use of the UAS-GAL4 system to drive expression of an inverted repeat construct stably inserted into the genome. Upon expression of the inverted repeat a dsRNA hairpin structure is produced, which has homology to the target mRNA (Dietzl *et al*., 2007). Gene knock down can be specifically targeted to the eye using the *eyeless* promoter.

6.2. FRET substrate screen

6.2.1. Design of the H3S28 Phospho-FRET probe

To identify kinases and phosphatases that regulate H3S28 phosphorylation a H3S28Phospho-FRET probe was made based on a previously designed probe for detecting H3S10 and H3S28 phosphorylation consisting of ECFP, the first 30 residues of Histone H3, the phospho-binding protein 14-3-3τ and YFP (Lin *et al*., 2004). Although Lin and Ting had observed FRET, the low dynamic range of the FRET change suggested there was potential to improve the probe. In 2005, Nguyen and Daugherty described the evolutionary optimization of ECFP/YFP to CyPet/YPet, improving the dynamic range and sensitivity of FRET (Nguyen and Daugherty, 2005). However CyPet is known to fold poorly (Ouyang *et al*., 2008) therefore to avoid any complications with CyPet dynamics, the ECFP component was kept and the YFP component was altered to YPet. Moreover, there was no evidence in the literature to suggest any of the other isoforms of 14-3-3 had a higher affinity for phosphorylated H3S28 than 14-3-3τ and so this along with the linker sequence (amino acid sequence: AGGTGGSL) and first 30 amino acid residues of Histone H3 were used to construct the H3S28Ph-FRET probe (referred to as $H3^{wt}$). To further improve the construct, a KOZAK sequence was inserted before ECFP, specifying the translation start site and a nuclear localisation signal (NLS) and stop codon (TAA) were inserted after YPet. Various restriction sites were removed and created (Figure 6.2) for future manipulation of the construct and to enable making of a mutant H3 FRET probe. The probe was synthesised by GeneArt and cloned into the entry vector pDONR221. It was then subcloned into the vector pAW for expression in S2R+ cells.

6.2.2. Making a S10,28A mutant Histone H3 FRET probe

In all FRET experiments it is important to have good controls that define the limits of experimental FRET values to avoid false positive/negative results. Previous reports demonstrating FRET have often used a mutant version of the probe; therefore S10 and S28 were mutated to alanine (S10,28A) in the redesigned $H3^{wt}$-FRET probe so that it could not be phosphorylated. The *Age1* restriction site was also removed for diagnostic identification of the mutant probe (Figure 6.2). The H3S10,28A mutant FRET probe (referred to as $H3^{S10,28A}$) was synthesised by GeneArt in the pMA-T vector and then ligated into the backbone of the $H3^{wt}$ probe in pAW after restriction enzyme digestion of $H3^{S10,28A}$ in pMA-T. It was then checked by sequencing and diagnostic digest with *Age1*.

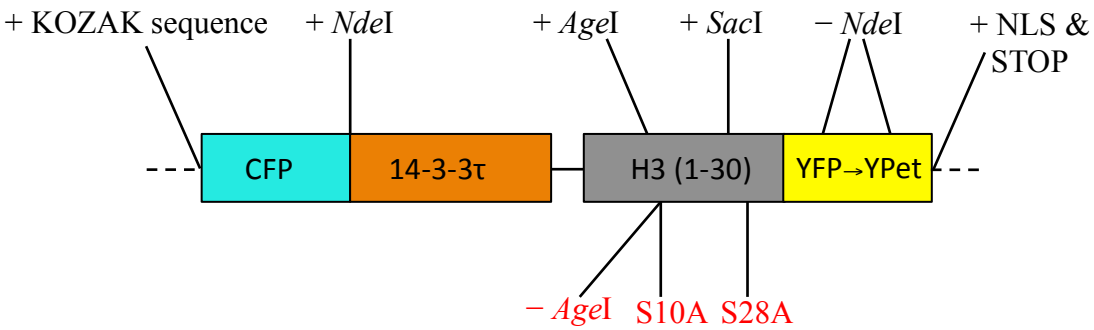

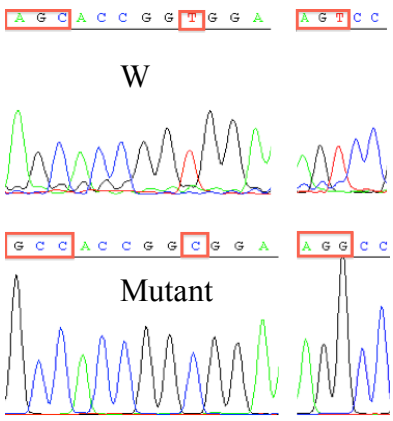

Figure 6.2. (previous page) Making the mutant H3S10,28A FRET probe. a) Structure of H3S28Ph probe highlighting the changes made to the original probe (black). The changes made to make the mutant FRET probe are shown in red. Both serine 10 and serine 28 are changed to alanine in the mutant. Removal of the *Age1* restriction site in the mutant is a diagnostic change to confirm insertion of the mutant fragment. KOZAK sequence: TCAAC. Nuclear Localisation signal: CCCAAGAAGAAGCGCAAG. Stop codon: TAA. +*Nde1*: ATGCAC→ATGCAT. +*Age1*: ACCGGC→ACCGGT. +*Sac1*: GAGCTG→GAGCTC. –*Nde1*: CATATG→CACATG. –*Age1*: ACCGGT→ACCGGC. S10A: AGC→GCC. S28A: TCC→GCC. b) The mutant probe was sequenced across the inserted mutant fragment to check the correct fragment had been inserted.

6.2.3. RNA interference in S2R+ cells

To validate the Histone $H3^{wt}$ and $H3^{S10,28A}$ FRET probes, dsRNA fragments were synthesised for RNAi-mediated knockdown of *Jil-1* and *PP187B* in S2R+ cells, which would act as negative and positive controls respectively in the FRET substrate screen. Jil-1 is a kinase known to regulate H3S10 phosphorylation (Regnard *et al*., 2011) and is a good candidate to be a H3S28 kinase. PP1 has been shown, in the context of mitosis, to dephosphorylate H3S10 and H3S28 and is also likely to be an interphase H3S28 phosphatase (Qian *et al*., 2011) (Rudenko, 2004). To test the effectiveness of the synthesised dsRNAs, the level of gene knockdown in S2R+ cells was determined by RT-PCR before co-transfection with the $H3^{wt}$ and $H3^{S10,28A}$ FRET probes (Figure 6.3). Several attempts were made at generating dsRNA fragments that significantly reduced the level of *Jil-1* and *PP187B*. Originally four dsRNAs were generated for *Jil-1* and two for *PP187B* using wild type *Drosophila* 3rd instar larvae

cDNA and primers designed to amplify sequences from previously screened amplicons for these genes. Amplicon sequences were taken from www.flyrnai.org. However only one (*PP187B* 27290) produced a noticeable reduction in gene expression (Figure 6.3). This dsRNA was selected to validate the FRET probes for the *in vitro* RNAi screen.

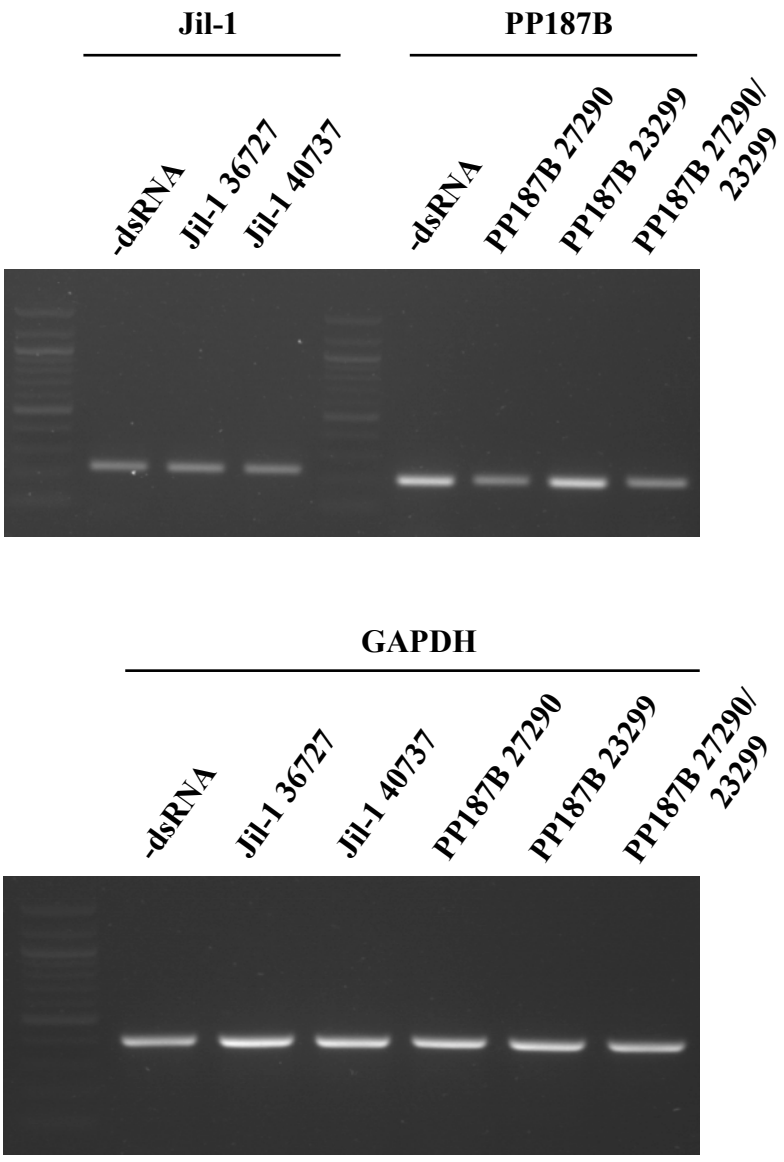

Figure 6.3. Expression levels of *Jil-1* and *PP187*B in S2R+ cells transfected with dsRNA fragments targeting each gene. *GAPDH* levels were used as an internal control.

6.2.4. Sensitised emission

One of the most widely used and simplest approaches in FRET-based experiments requires excitation of the donor molecule (CFP) and detection of the acceptor (YPet) emission (em) (Karpova *et al*., 2003). Any fluorescence from YPet should be as a result of FRET, as it cannot be excited at 458nm and the energy from ECFP is transferred to YPet, causing it to enter an excited state due to spectral overlap of ECFP and YPet (Ishikawa-Ankerhold *et al*., 2012). This allows a FRET ratio to be calculated of the mean $YPet^{emission(em)}$ (FRET):$ECFP^{em}$ intensity in cells expressing a FRET probe after excitation of ECFP (458nm) alone (Figure 6.4a). However emission cross-talk due to emission spectra overlap can occur meaning some of the signal in the FRET ($YPet^{em}$) channel upon excitation of ECFP at 458nm, will be from ECFP fluorescence bleed-through. It is therefore necessary to have controls to correct for this to give a reliable FRET measurement. Ideally controls would include cells expressing ECFP alone, YPet alone, unlinked ECFP and YPet, ECFP and YPet linked with a positive biological control and a negative biological control (Broussard *et al*., 2013). For preliminary validation of the FRET probes, the $H3^{S10,28A}$ probe was the only control available so initial experiments looked for a difference in the FRET ratio between $H3^{wt}$ and $H3^{S10,28A}$. S2R+ cells were transfected with either probe and imaged using confocal microscopy. FRET was measured by exciting ECFP at 458nm and detecting YPet emission at 527nm. The experiments were carried out in the presence or absence of *PP187B* dsRNA. In two individual experiments (Figure 6.4b) $H3^{S10,28A}$ (-dsRNA) gave a lower FRET ratio than $H3^{wt}$ (-dsRNA) as expected. However the dynamic range was very small and ideally for a screen, a greater reduction in the FRET ratio for the mutant would be needed. Importantly the difference between $H3^{wt}$ (-dsRNA) and $H3^{S10,28A}$ (-dsRNA) in the first experiment

was not significant (p=0.31) whereas it was in the second experiment (p<0.0001, Figure 6.4b). This highlights the differences between FRET experiments and the need to use controls in every repeat. It is also important to note that different transfection reagents were used for these experiments. Cellfectin II (Invitrogen) was used for experiment one but due to its poor transfection efficiency (<1%), Effectene® (Qiagen) was used for the second experiment, giving a better transfection efficiency of ~30%. This could explain the variation between experiments and highlights the need for consistent experimental conditions in each repeat.

When dsRNA for *PP187B* (phosphatase) was added, a significant reduction in FRET was observed in the second experiment (Figure 6.4b), although an increase in FRET signal would have been expected due to an increase in Histone H3 phosphorylation. One possible explanation for this is PP187B was not reduced to a significant level, which is likely given the results in Figure 6.3, or that transfection of S2R+ cells with dsRNA was not successful.

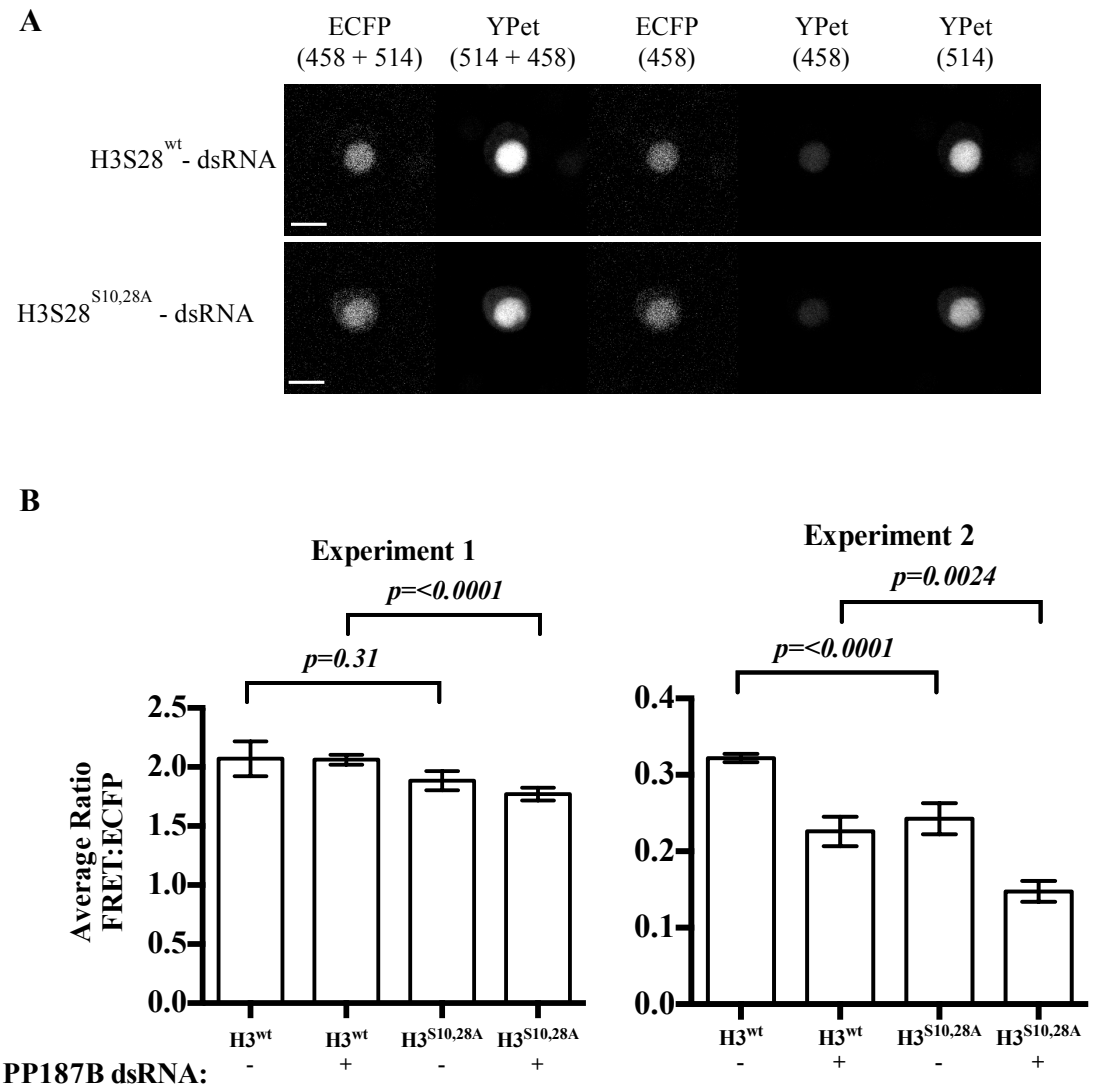

Figure 6.4. Simultaneous imaging of ECFP and YPet in S2R+ cells transfected with $H3^{wt}$ or $H3^{S10,28A}$ FRET probes. a) Representative images of cells expressing $H3^{wt}$ and $H3^{S10,28A}$ FRET probes. The excitation wavelength used for each image is shown above. Scale bars = 15μm b) average FRET:ECFP ratios upon excitation of ECFP in two individual experiments. Experiment 1: n= 27, 26, 22 and 20 (left to right). Experiment 2: n= 30 25, 19, 21 (left to right). Error bars represent the standard error for each dataset.

6.2.5. Acceptor Photobleaching

Acceptor photobleaching is a simple and quick assay for verifying FRET and detecting protein interactions and is therefore an appealing choice when designing FRET experiments (Broussard *et al*., 2013; Snapp and Hegde, 2001). The leading principle behind acceptor photobleaching is FRET should not occur in the absence of an acceptor therefore by photobleaching the acceptor an increase in donor intensity should be seen if the two fluorophores are in close proximity (Karpova *et al*., 2003; Broussard *et al*., 2013; Snapp and Hegde, 2001). If an increase in donor fluorescence is observed after bleaching, this is a reliable diagnostic readout as bleaching usually causes a decrease in fluorescence intensity (Karpova *et al*., 2003). The advantage of this approach is it is not affected by bleed-through and successful photobleaching is easily observed by a sudden decrease in acceptor fluorescence (Snapp and Hegde ,2001). Furthermore bleaching is straightforward on a confocal laser scanning microscope (CLSM) and can allow bleaching of a region of interest (ROI) (Broussard *et al*., 2013). The main disadvantage is that it destroys the biosensor so only one measurement can be taken for a particular cell (Snapp and Hegde, 2001).

Thirty images of ROIs in S2R+ cells transfected with the $H3^{wt}$ or $H3^{S10,28A}$ FRET probes were taken, with photobleaching of YPet between images 4 and 5. The nuclear intensity was measured for ECFP (channel 479nm, figure 6.5a) and YPet (channel 527, figure 6.5a) before and after bleaching and the percentage increase/decrease in intensity calculated (respectively). In all cases YPet was successfully bleached (Figure 6.5); a comparable level of bleaching was observed for cells transfected with $H3^{wt}$ and $H3^{S10,28A}$ (average % decrease = 73.9 ± 4.5 and 74.4 ± 2.4 respectively). An increase in ECFP was observed in all cells, including those

transfected with the $H3^{S10,28A}$ probe despite it lacking the phosphorylatable S10 and S28 residues (Figure 6.5a). The percentage increase in ECFP fluorescence for cells transfected with $H3^{wt}$ was greater than that observed in cells transfected with $H3^{S10,28A}$ (average % increase = 28.0 ± 7.8 and 24.0 ± 11.1) however statistical analysis (student's t-test) suggests the difference is not significant (p=0.19, figure 6.5b). Given these results the decision was made to abandon the FRET based screen.

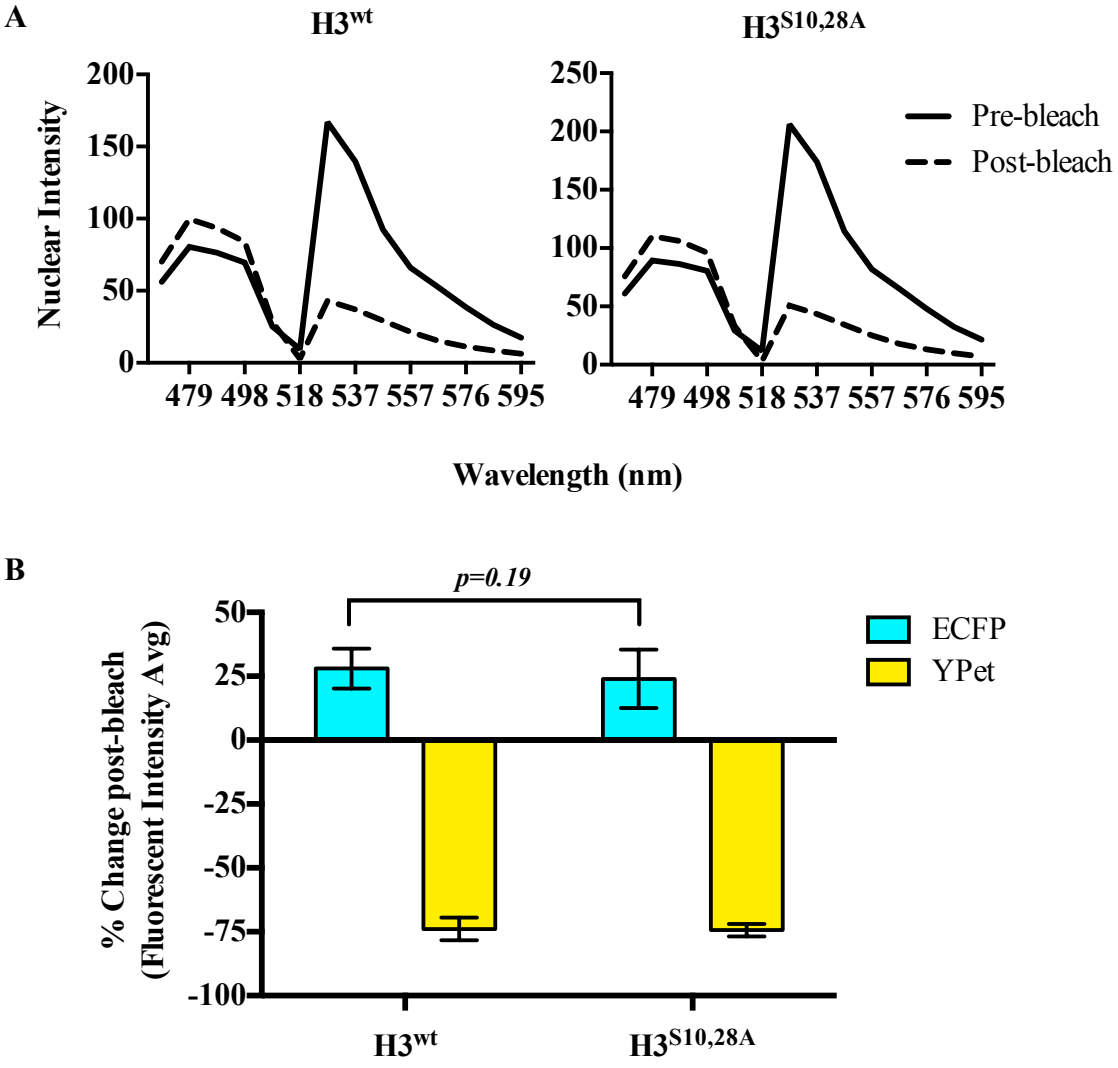

Figure 6.5. Acceptor photobleaching of S2R+ cells transfected with $H3^{wt}$ and $H3^{S10,28A}$ FRET probes. a) Nuclear intensity of representative examples of cells transfected with either $H3^{wt}$ or $H3^{S10,28A}$ FRET probes immediately before and after

bleaching of the acceptor fluorophore (YPet). Quantification shows an increase in ECFP emission (479nm) and a dramatic decrease in YPet emission (527nm). b) The average percentage increase of ECFP emission and decrease of YPet emission for cells transfected with $H3^{wt}$ (n=21) or $H3^{S10,28A}$ (n=20) FRET probes. *p* value shows there is no significant difference in ECFP emission change between the two probes. Error bars represent the standard error for each dataset.

6.3. Phenotypic screen

In 2009, Martinez *et al*. showed that loss of the PcG component *polyhomeotic* in the eye causes cells to over proliferate and in 2011, Feng *et al*. provided more evidence suggesting that mis-regulation of PcG promotes proliferation. To further understand the molecular mechanisms underlying this phenomenon and to complement the substrate screen, a phenotypic screen was designed to identify kinases and phosphatases that enhance/suppress the overgrowth phenotype observed in eyes upon *polyhomeotic* loss of function. To generate the strains needed for this screen an initial set of experiments were performed to determine which PcG element gives the strongest overgrowth phenotype when knocked down by RNAi in the eye. The three PcG elements targeted for knockdown were *polyhomeotic, polycomb* and *sex combs extra*, which have all been shown to cause hyperproliferation in loss of function mutants (Classen *et al*., 2009). 11 available RNAi lines (flies carrying an inverted repeat construct under UAS control) for these genes were crossed to flies with either a moderate (5534, see section 2.6.9) or strong (5535, see section 2.6.9) *eyeless*-GAL4 (*ey*-GAL4) promoter, to induce expression of the gene-specific inverted repeats exclusively in the eye. The number of flies in the progeny with either normal

or overgrown eyes was recorded (Table 6.1). Representative images of selected RNAi lines are shown in Figure 6.6.

Table 6.1. The number of eye phenotypes observed upon gene knockdown in the eye

			Phenotype (moderate)			Phenotype (Strong)			
Gene	**RNAi Line**	**Chromosome**	**wt**	**MOG**	**SOG**	**wt**	**MOG**	**SOG**	**Viability**
polyhomeotic	TRiP 31608	3	75	6	-	62	1	-	Viable
	TRiP 31190	3	55	5	-	83	7	-	Viable
	TRiP 33669	3	73	-	-	72	-	-	Viable
	VDRC 50028	3	-	-	-		-	-	DBE-V
	VDRC 100811	2	64	-	-	42	-	-	Viable
	NF 18414R-1	2	56	-	-		-	-	Viable*
	NF 18414R-2	X	68	-	-	51	-	6	Viable*
polycomb	NF 32443R-1	3	-	-	-	-	-	-	DBE-PL
	TRiP 33622	3	75	-	-	52	-	-	Viable
	TRiP 33964		1	-	-	-	-	-	DE
	TRiP 31110	3	42	13	-	93	7	-	Viable
sex combs extra	VDRC 106328	2	-	-	-	-	-	-	DBE-V
	NF 5595R-1	3	-	-	1	-	-	-	DE
	NF 5595R-2	3	-	-	4	-	-	-	DE
	TRiP 31612	3	37	10	6	24	4	2	Viable

wt=wild type eyes, MOG=mild overgrowth, SOG=strong overgrowth, - = no flies with this phenotype. Moderate and strong = moderate (Bloomington stock number 5534) and strong (Bloomington stock number 5535) ey-GAL4 promoters. DBE-V=die before eclosion but should be viable, Viable*=viable with ey-GAL4, DBE-PL=die before eclosion (pupal lethal), DE=delayed eclosion.

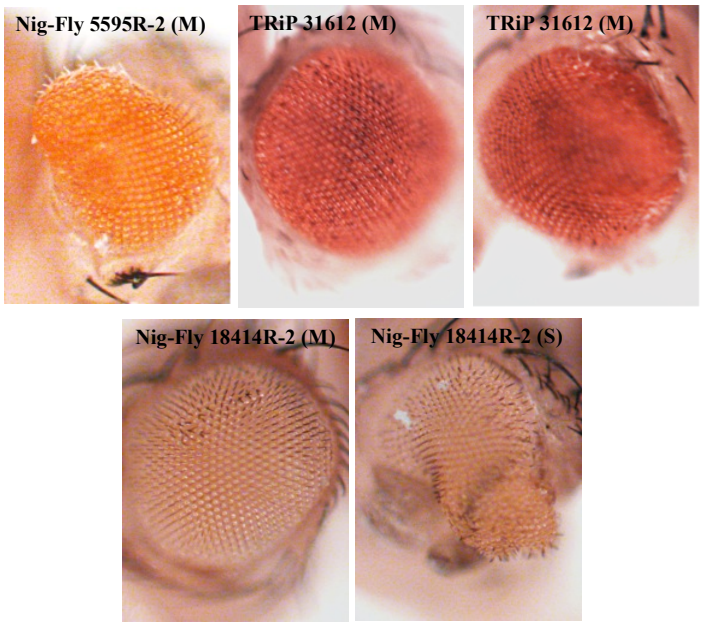

Figure 6.6. Representative images of eye phenotypes for selected RNAi lines. RNAi lines indicated were crossed to a source of either moderate (M) or strong (S) *eyeless*-GAL4.

To identify enhancers of PcG-mediated overgrowth it was necessary to select RNAi lines where the majority of flies had wild type eyes and a small number displayed over growth. On this basis the TRiP line 31612 (targets *sex combs extra*) and Nig-Fly line 1814R-2 (targets *polyhomeotic*) were selected with the moderate *ey*-GAL4 promoter (Table 6.1). The rationale behind this decision was to select RNAi lines that would identify both weak and strong enhancers of overgrowth. TRiP 31612 produced a number of flies with different eye phenotypes (Table 6.1) therefore it would be difficult to identify weak enhancers as the number of flies displaying an over growth phenotype may be similar to the results in Table 6.1. However it would be simple to identify strong enhancers, where an increase in the number of flies displaying a strong overgrowth phenotype in the eye would be expected. Nig-Fly 18414R-2 should identify weak enhancers as all flies displayed a wild type eye

phenotype with the moderate *ey*-GAL4 promoter. Any over growth would identify an enhancer and it is clear from the results with the strong *ey*-GAL4 promoter that Nig-Fly 18414R-2 can produce an overgrowth phenotype (Figure 6.6).

To identify suppressors of PcG-mediated overgrowth the Nig-Fly RNAi line 5595R-2 (targets *polyhomeotic*) was selected on the basis that only a small number of flies emerged and all had a strong over growth eye phenotype (Table 6.1 and Figure 6.6), suggesting that knockdown of *polyhomeotic* is semi-lethal. A suppressor would be easily identified by rescue of the overgrowth phenotype and an increase in the number of flies emerging.

6.3.1. Making a tester strain for the *in vivo* phenotypic screen

The inverted repeat for the selected genes was recombined with *ey*-GAL4 (moderate) and a temperature sensitive tubulin-GAL80 (*tub-GAL80^{ts}*) element (McGuire *et al*., 2003) to make a permanent strain that could be crossed to RNAi lines targeting kinases and phosphatases in the *Drosophila* genome. The *tub-GAL80^{ts}* is necessary due to the semi-lethality exhibited upon knockdown of *sex combs extra* using the RNAi line 5595R-2. GAL80 suppresses GAL4-mediated gene expression allowing a stock to be maintained at a permissive temperature and experiments to be carried out at a restrictive temperature that will relieve GAL80 suppression of GAL4. The only RNAi line that was recombined successfully with *ey*-GAL4 and tub-GAL80^{ts} was Nig-Fly 5595R-2 (targets *sex combs extra*); this will be referred to as the tester strain from hereafter.

A series of experiments to validate the tester strain were carried out to ensure it would be suitable for use in the screen. Firstly, the strain was kept at a permissive temperature of 22°C and restrictive temperature of 29°C to check it behaved as originally observed. At the permissive temperature the strain survived and no flies displayed an overgrown eye phenotype therefore it was concluded the *tub-GAL80*^{ts} element was working. However, when stored at the restrictive temperature, which should relieve repression of the *Sex combs extra* inverted repeat (*Sce*$^{IR5595R-2}$) and induce knockdown of *Sce*, all flies survived and none displayed an overgrowth phenotype. This was unexpected considering only a small number of flies survived in the original experiment with Nig-Fly 5595R-2 and those that did emerge displayed severely overgrown eyes. It was thought the inverted repeat might not be strong enough when in combination with the GAL80 element so the tester strain was crossed to a strain carrying UAS-*Dicer2*, a component of the RNAi machinery in an attempt to enhance knockdown of *Sce.* However the progeny of this cross still survived.

Another mini screen was done using a variety of *ey*-GAL4 strains of differing strengths to determine if any enhanced the overgrowth phenotype originally observed, and could consequently be used to make a new tester strain. Three *ey*-GAL4 strains (Bloomington stock numbers 8221, 8220 and 5534) caused pupal lethality when crossed to *Sce*$^{IR5595R-2}$. An advantage of this lethal phenotype is it would make the screen more stringent and easier to perform. Lethality is difficult to rescue so if knockdown of a particular kinase/phosphatase suppressed lethality it is likely to be involved in PcG regulation and the assay would simply be looking for emerging flies. The three *ey*-GAL4 elements were combined with *Sce*$^{IR5595R-2}$ and

tub-GAL80^{ts} and the same validation tests were performed. The new tester strains survived at the permissive temperature and were pupal lethal at the restrictive temperature as expected. To further test the strains they were crossed to a wild type strain (w^{1118}) to ensure that only those without the *Sce*$^{IR5595R-2}$ emerged at the restrictive temperature. Unfortunately flies with both *ey*-GAL4 and *Sce*$^{IR5595R-2}$ elements emerged although some did have an overgrowth phenotype. A final attempt to validate the tester strain involved crossing it to a line expressing GFP tagged STAT. A report in 2009 showed the JAK-STAT signalling pathway is upregulated when PcG components are knocked down (Classen *et al*., 2009). Knockdown of *Sce*$^{IR5595R-2}$ could be detected by looking for an increase in GFP in affected flies. Unfortunately no difference was seen suggesting the inverted repeat was not effective in combination with other elements tested.

6.4. The PP1/PNUTS phosphatase regulates active marks of transcription

Validation of the tools to do an unbiased screen to identify histone phosphatases that regulate H3 serine 10 and serine 28 phosphorylation and the recruitment of PcG complexes was unsuccessful. Therefore focus shifted to PP1, which has been shown to dephosphorylate histones *in vitro* during mitosis (Qian *et al*., 2011). Chapter 3 described the co-localisation of PP1-PNUTS with sites bound by RNAPII on polytene chromosomes and showed RNAPII is a substrate of PP1-PNUTS. However not all sites bound by PP1-PNUTS co-localised with RNAPII suggesting other chromatin associated substrates may be targeted by PP1-PNUTS. Given histones are targets of PP1 mediated dephosphorylation during mitosis, the histone phosphorylation status of the underlying chromatin was studied in cells lacking PP1 and PNUTS. To do this, negatively marked *dPNUTS*^{13B} or *PP187B* (the major PP1

isoform in *Drosophila*) mutant clones were generated in the salivary gland using Flp/FRT mediated recombination. Salivary glands were dissected from 3rd instar larvae, fixed, stained for histone H3S10 and H3S28 phosphorylation and imaged using confocal microscopy. The salivary glands of third instar *Drosophila* larvae offer a good system in which to study various aspects of transcription as the chromosomes in this tissue undergo many rounds of replication without cell division. This gives rise to large polytene chromosomes that contain thousands of copies of each gene and enable better visualisation of histone modification status in antibody labelling experiments. Figure 6.7 shows both H3S10 and H3S28 phosphorylation were increased in *PP187B* mutant clones. $PNUTS^{13B}$ clones also displayed an increase in H3S10 phosphorylation.

As previously discussed, serine 28 phosphorylation disrupts recruitment of PcG proteins to methylated H3K27 via epitope masking and also induces a methyl-acetylation switch on K27 to activate transcription (Lau and Cheung, 2011b). Given H3S28 phosphorylation was increased in *PP187B* mutants, the H3K27 acetylation status of *PP187B* and *dPNUTS* mutant clones was studied. Interestingly an increase in H3K27 acetylation was observed in negatively marked *PP187B* and *dPNUTS* mutant clones (Figure 6.7) suggesting PP1-PNUTS may indirectly regulate H3K27 acetylation via histone phosphorylation.

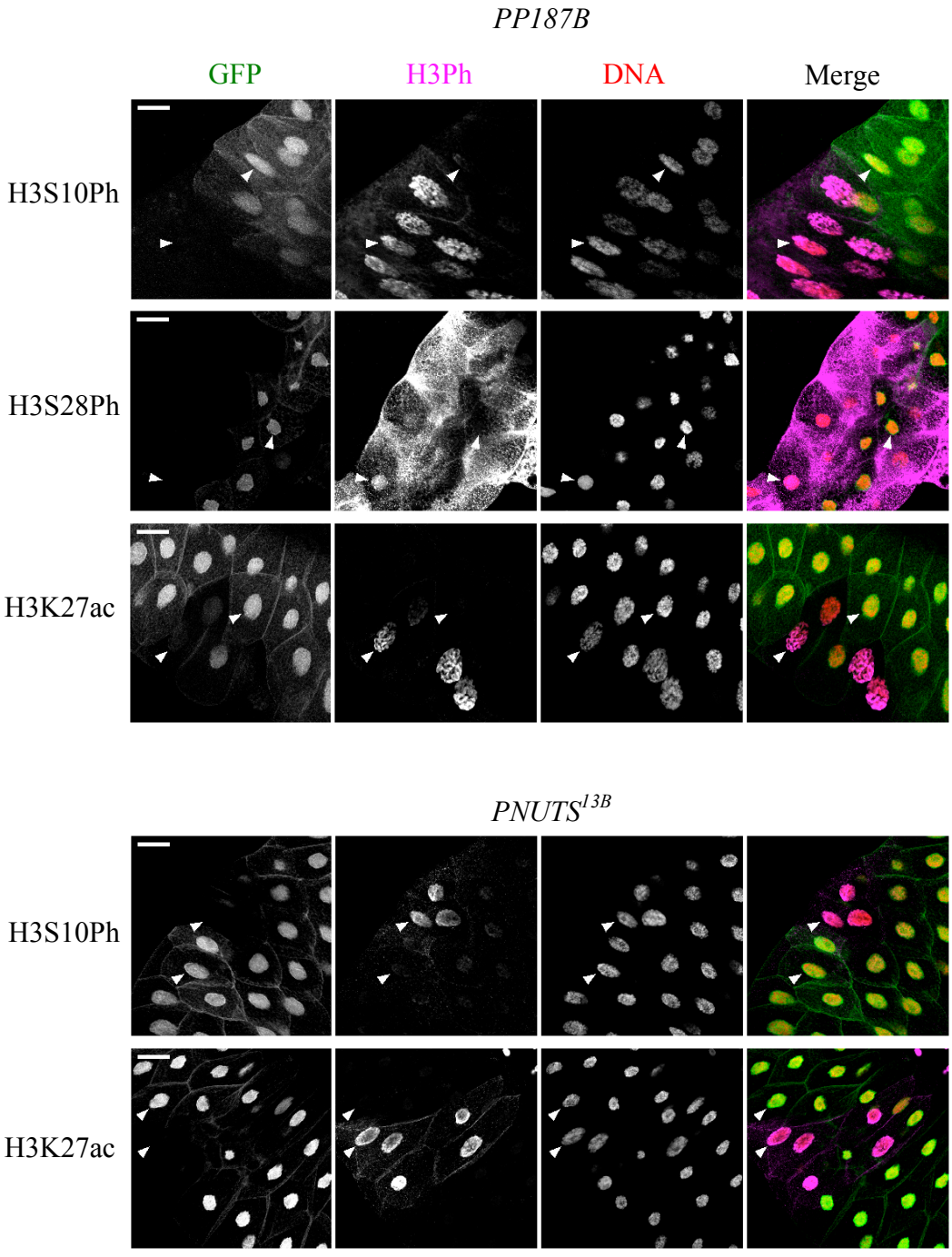

Figure 6.7. PP1-PNUTS regulates histone phosphorylation and acetylation. Negatively marked (non-GFP) PP1 mutant (top panels) and PNUTS^{13B} clones (bottom panel) generated by Flp/FRT mediated recombination in the salivary glands of 3rd instar larvae. Salivary glands stained for Histone H3 S10 phosphorylation and H3 K27 acetylation. Scale bars = 55 μM. For control see Figure 6.8.

Given PNUTS/PP1 binds to Wdr82, which associates with the COMPASS complex, responsible for the di- and tri- methylation of histone H3 lysine 4 (H3K4me2/3) (Hallson *et al*., 2012), the histone methylation status of mutant *PP187B* and *dPNUTS*^{13B} clones was examined using antibodies specific for each methylated form of H3K4. Interestingly levels of Histone H3K4me2 and H3K4me3 were markedly increased in negatively marked *dPNUTS*^{13B} nuclei and to a lesser extent in *PP187B* mutant nuclei (Figure 6.8). This suggests PP1-PNUTS regulates the di- and tri-methylation of H3K4, marks that are both associated with active transcription (Heintzman *et al*., 2007; Hallson *et al*., 2012).

Figure 6.8 (next page). H3K4me2/3 is increased in PNUTS^{13B} and PP1 mutant clones. Negatively marked (non-GFP) PP1 mutant (top panels) and PNUTS^{13B} clones (middle panels) generated by Flp/FRT mediated recombination in the salivary glands of 3rd instar larvae. Salivary glands stained for indicated histone methylation marks. Control = PNUTS^{13B} clones stained with anti-rabbit Alexa-555 secondary antibody and shows it does not have specificity for non-GFP cells. Scale bars = 55μM.

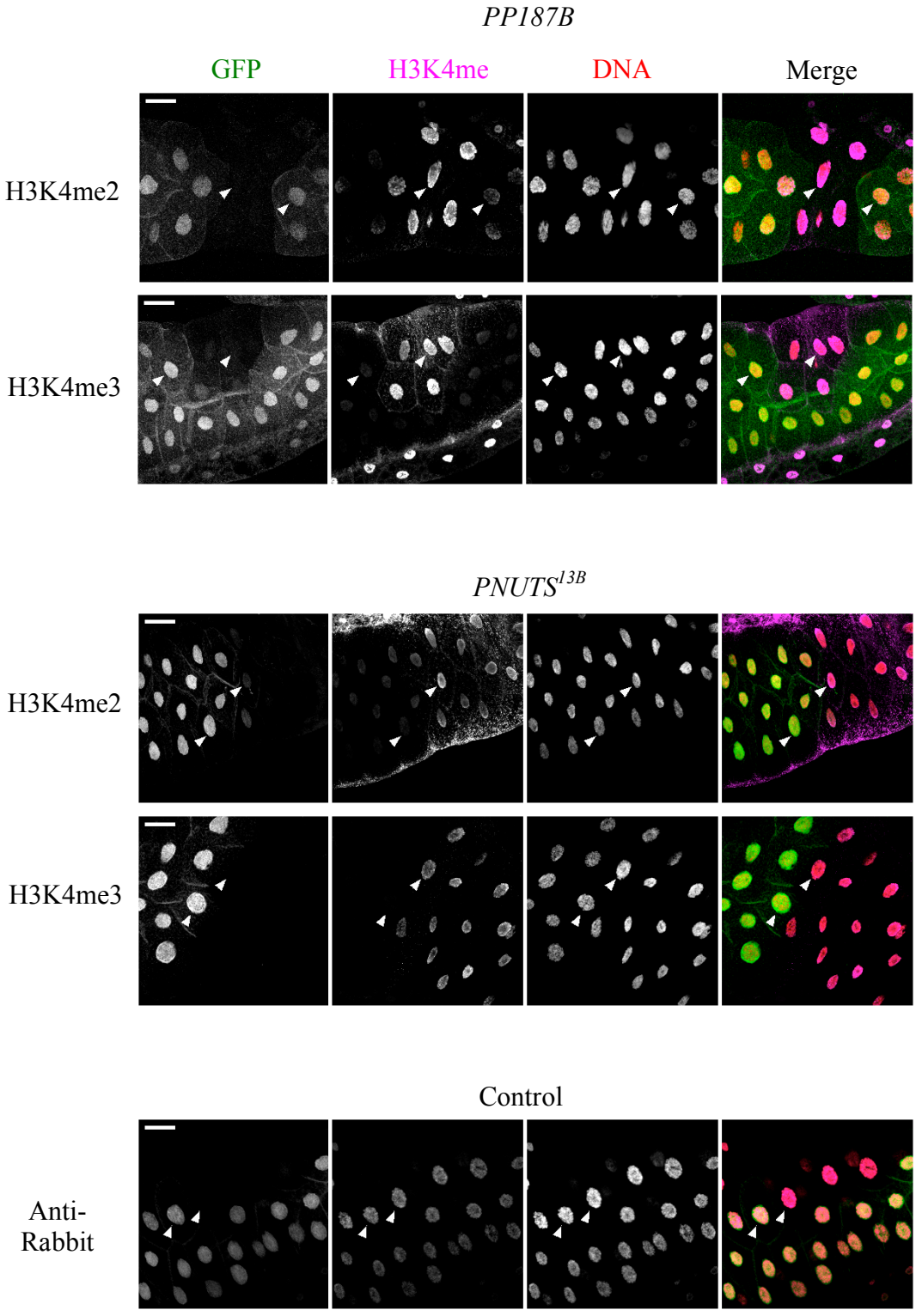
PP187B
GFP
H3K4me
DNA
Merge
H3K4me2
H3K4me3
PNUTS13B
H3K4me2
H3K4me3
Control
Anti-
Rabbit

6.5. Discussion

Epigenetic post-translational modifications on histones and DNA are essential for maintaining appropriate patterns of gene expression during development by modulating chromatin structure (Rossetto *et al*., 2014). Different modifications exist on specific histone residues that can directly or indirectly affect chromatin structure through the recruitment of chromatin-associated factors; modifications include methylation, acetylation, phosphorylation and ubiquitination. Histone phosphorylation is a key regulator of active gene expression and the outcome of many signal transduction pathways to allow changes in gene expression patterns to be made in response to external stimuli. H3S28 phosphorylation has been reported to activate transcription by preventing recruitment of repressive polycomb group proteins to neighbouring methylated lysine 27, however little is known about the kinases and phosphatases that regulate this key residue.

This chapter describes the development of tools to identify *Drosophila* kinases and phosphatases that regulate H3 serine 28 phosphorylation, recruitment of PcG to chromatin and gene expression using a FRET based *in vitro* substrate screen in S2R+ cells and an *in vivo* phenotypic screen in adult flies. An intramolecular FRET probe capable of detecting H3S28 phosphorylation was developed, consisting of the first 30 residues of histone H3 conjugated to YPet and the phosphor binding protein 14-3-3τ conjugated to ECFP linked together via a short linker sequence. A non-phosphorylatable variant was also made through substitution of S10 and S28 for alanine in the H3 component. Initial validation of these probes using acceptor photobleaching and sensitized emission to measure a FRET ratio proved unsuccessful, as measurements displayed a small dynamic range and no difference

between $H3^{wt}$ and $H3^{S10,28A}$ was observed, making them unsuitable for a large scale screen. There are many reasons why the $H3^{S10,28A}$ negative control behaves like the $H3^{wt}$ probe. Firstly high concentrations of the probe may have been present leading to the potential for intermolecular FRET to occur between fluorophores in adjacent molecules rather than within the same probe, giving a false positive signal. The small intensity changes observed with the $H3^{wt}$ probe also presented a major problem and suggested that the probe may not be efficient. This could be due to the design of the reporter, as YPet is better paired with CyPet rather than ECFP. Furthermore the linker sequence may not have been flexible enough to allow binding between the two reporter proteins, although the reporter design was taken from the original probe used in the literature.

It is important to note that the results described were preliminary and the view was to validate the FRET probe to see if any evidence of an interaction could be detected using sensitised emission and acceptor photobleaching. The view was to use the $H3^{S10,28A}$ probe as a negative control to determine the background level of fluorescence. Of course other negative controls would have been necessary to further validate the probes and undertake the *in vitro* screen. Further validation of the FRET probes using synthesised dsRNA, as a way of mimicking the conditions that would be used in the screen, also proved unsuccessful, as the dsRNA fragments did not significantly reduce the level of target gene expression.

A tester fly strain was made that could be used in an RNAi-based *in vivo* screen to identify kinases and phosphatases that enhance/suppress the eye overgrowth phenotype observed upon loss of PcG proteins. *Eyeless*-GAL4 was recombined with

an inverted repeat element targeting knockdown of *sex combs extra*, a subunit of PRC1, and a temperature sensitive tub-GAL80 element for controlled gene silencing. The strain was optimised and initial tests showed the strain survived at the permissive temperature and was semi-lethal at the experimental temperature with flies that emerged displaying an overgrowth phenotype in the eye. However further validation by crossing to a wild type strain suggested the tester strain would not be suitable for a screen as flies expressing the inverted repeat emerged in the progeny and displayed no overgrowth phenotype in the eye. This is unexpected given a wild type strain should not be able to suppress the semi-lethal phenotype of the tester strain.

Focus shifted to PP1 and its role in epigenetic regulation of gene expression via H3S28 phosphorylation. Work in Chapter 3 showed the association of PP1 and dPNUTS at many sites on *Drosophila* polytene chromosomes with some sites marked by RNAPII. Further work showed RNAPII is a target of dPNUTS-PP1 mediated dephosphorylation but what other substrates could be targeted by PP1 at sites not bound by RNAPII, and is dPNUTS necessary for dephosphorylation of these unknown substrates? Negatively marked mutant *PP187B* clones in the *Drosophila* salivary gland confirmed H3S28 and H3S10 are likely to be targets of PP1-mediated dephosphorylation as both marks were increased in mutant clones. Furthermore clonal analysis revealed *dPNUTS* is also essential for regulation of H3 phosphorylation as $dPNUTS^{l3B}$ clones exhibited an increase in H3S10 phosphorylation. Unfortunately problems with the H3S28 phospho-specific antibody meant results could not be obtained for the effect of *dPNUTS* at this site. However, phosphorylation of H3S28 has also been reported to induce a methyl-acetylation

switch on the neighbouring lysine 27 residue (Lau and Cheung, 2011b) and staining revealed H3K27 acetylation is increased in both *PP187B* and *dPNUTS* mutant clones. This is consistent with there being a role for *dPNUTS* in regulating H3S28 phosphorylation. To provide evidence of the role of dPNUTS-PP1 in a phosphor-methyl switch one could look at the H3K27 methylation status in PNUTS and PP1 mutants clones and determine if PNUTS associates with PcG-regulated promoters using a ChIP based approach.

The histone H3K4 methylation status of *PP187B* and *dPNUTS* mutant clones was studied due to the association of PNUTS-PP1 with Wdr82, a component of the methyltransferase complex, COMPASS (Hallson *et al*., 2012). Mutant clones exhibited an increase in H3K4 di- and tri-methylation, the main target of COMPASS mediated methylation (Hallson *et al*., 2012). One interpretation of these results is that Wdr82 binds competitively to COMPASS and dPNUTS and in the absence of dPNUTS there is more COMPASS-bound Wdr82, which promotes COMPASS function. Consequently, it would be interesting to test whether dPNUTS overexpression abrogates Wdr82-dependent COMPASS function, leading to a loss of H3K4 methylation.

It appears various changes in histone modification status occur in *PP187B* and *dPNUTS* mutant clones suggesting the dPNUTS-PP1 holoenzyme is essential for epigenetic control of gene expression. However, active marks of transcription are increased in mutant clones suggesting PP1 and dPNUTS negatively regulate epigenetic control of active transcription. This is contradictory to its role in active transcription (Chapter 3) but may be necessary for temporal and spatial control of

target genes in response to certain stimuli. Interestingly, genes targeted by PcG proteins are not always repressed, with reports suggesting PcG proteins associate with actively transcribed genes and with different phosphorylated forms of RNAPII (Brookes *et al*., 2012). In repressed PcG target genes, PcG proteins associate with stalled RNAPII phosphorylated at Ser5 and in expressed targets, PcG associates with elongating RNAPII marked by phosphorylated Ser5, Ser2 and Ser7 (Brookes *et al*., 2012). It is thought in actively transcribed genes, PcG acts to regulate the level of mRNA, therefore PcG may not only function to completely repress target genes but also regulate their expression through mRNA abundance (Enderle *et al*., 2011; Brookes *et al*., 2012).

It will be interesting to see if PcG proteins are also localised at sites marked by PNUTS and RNAPII on polytene chromosomes and if genes affected in *dPNUTS* mutants exhibit an altered histone modification status that matches the findings in this chapter.

7. Final Discussion and summary

This work describes the characterisation of the PP1 nuclear regulatory subunit, PNUTS, in *Drosophila* and of PNUTS-interacting proteins that are conserved in humans and mammals. Mutational analysis showed *dPNUTS* is essential for cell survival and development in *Drosophila* as null mutants die as L1 larvae and mutant cells are unable to proliferate in developing tissues. Many RNAPII-dependent genes are misregulated in loss-of-function animals. Most notably, genes involved in metabolic processes such as carbohydrate metabolism are downregulated, whereas genes involved in apoptosis are upregulated. These changes are consistent with the growth defect and lethality exhibited by *dPNUTS* mutant animals. The RNAPII CTD was found to be hyperphosphorylated at Ser5 in mutant larval extracts and on polytene chromosomes in flies overexpressing a non-PP1 binding variant of *dPNUTS*. These data suggest that dPNUTS may play a direct role in transcription, or in co-transcriptional events such as RNA processing, through regulating RNAPII CTD phosphorylation status (Hsin and Manley, 2012). The latter explanation is favoured because RNAPII occupancy across selected loci was not affected and because CTD Ser5 phosphorylation is thought to primarily regulate mRNA capping. Future work should be directed at identifying genomic loci where dPNUTS is bound, e.g. by ChIP or DamID approaches. This information could then be used to determine which genes are direct targets of dPNUTS and to reassess the effects of altered RNAPII phosphorylation on mRNA levels and processing.

Analysis of modification status at specific gene loci using native chromatin immunoprecipitation approaches (Brand *et al*., 2008) will help determine if the effects on gene expression are due to changes in histone modification status.

Alternatively, looking at the effect of loss of function of *dPNUTS* on RNA processing events such as 5' capping using cap-trapping techniques (see Chapter 6) will determine if the gene expression changes observed are a result of defects in transcription-coupled processes.

Identification of dPNUTS-binding proteins using a yeast two-hybrid approach and biochemical analyses to confirm these interactions, identified dTOX4, dWdr82, dMBD-R2 and the *Drosophila* estrogen related receptor (dERR) as dPNUTS interactors. Binding to dERR could offer some insight into the effects on metabolic genes observed as it is necessary for co-ordinating metabolic gene expression patterns during *Drosophila* development (Tennessen *et al*., 2011). There are three ERR isoforms in mammals (ERRα, β and γ) that also have roles in metabolic processes (Eichner *et al*., 2010; Charest-Marcotte *et al*., 2010; Alaynick *et al*., 2007) and have been linked to cancer progression, predominantly breast cancer, but little is known about the molecular basis of this association (Ariazi *et al*., 2002; Stein *et al*., 2008; Eichner *et al*., 2010). It is well known cancer cells exhibit the Warburg effect whereby they take on an altered metabolic programme and become dependent on aerobic glycolysis rather than mitochondrial oxidative phosphorylation to efficiently create biomass (Zhao *et al*., 2013). It has also been suggested the primary function of dERR is biomass production during larval development, which is reminiscent of the Warburg effect (Tennessen *et al*., 2011). Further characterisation of the interaction between ERR and PNUTS in *Drosophila* may have implications in cancer therapeutics as cancer drug resistance has been linked to altered metabolic pathways in cancer cells (Zhao *et al*., 2013). Targeting of proteins involved in these pathways

may therefore offer a way to overcome drug resistance for better treatment of the disease.

The identification and confirmation of dTOX4 and dWdr82 as dPNUTS-binding proteins was consistent with reports in humans and mammals that show these proteins are part of a complex with PP1. Although this work has not confirmed the *Drosophila* orthologues exist as a complex, it is likely that these interactions are conserved. This is further supported by work in yeast, which shows Swd2, a homologue of mammalian Wdr82, is part of the stable APT complex which includes Glc7, the yeast homologue of PP1 (Nedea *et al*., 2003). The exact role of the TOX4/Wdr82/PNUTS/PP1 complex and its substrates remains to be determined but it is likely it functions in transcription or related RNA processing events as all members are known to be chromatin associated (Lee *et al*., 2010). dTOX4 is a member of the high mobility group of proteins that facilitate various DNA-dependent nuclear activities including transcription and DNA repair by binding to DNA and inducing changes in local chromatin structure. LCP1, the human homologue of dTOX4, binds to PNUTS and exhibits transcriptional activity, suggesting it may have a direct role in transcription (Lee *et al*., 2009). Furthermore, Wdr82 associates with RNAPII phosphorylated at Ser5 in its CTD (Mohan *et al*., 2011). Confirmation that these proteins exist as a complex in *Drosophila* and characterisation using various genetic and biochemical approaches available in this model system will provide further insight into its chromatin-associated functions.

Mutational analysis of *dTOX4* in *Drosophila* revealed unexpected phenotypes with homozygous adults displaying defects in oogenesis and spermatogenesis resulting in

sterility. Females had defects in dorsal ventral patterning in the egg and chromosome dispersal/decondensation in nurse cell nuclei. Males displayed multiple defects in spermatogenesis, predominantly cytokinesis, and were unable to produce mature sperm. How such processes are regulated by dTOX4 and the importance of dPNUTS binding to dTOX4 remains to be determined. If dPNUTS is necessary for these functions then identifying substrates and the role of phosphorylation in these processes will be important. PNUTS is known to be necessary for proper chromosome decondensation in human cells (Landsverk *et al*., 2005); it is possible that dTOX4 mediates a similar role for *dPNUTS* in the *Drosophila* germline. However, it is possible these phenotypes represent PNUTS-independent roles of dTOX4. Notably, the phenotypes observed in the ovary are the same as in mutants in various hnRNP proteins that regulate mRNA localisation and reports in the literature suggest dTOX4 may bind to these proteins (Guruharsha *et al*., 2011). One of these hnRNP proteins, Squid, also displays defects in cytokinesis in the testes (Lowe *et al*., 2014). Confirmation of these interactions may be important in understanding the *dTOX4* mutant phenotypes observed. Expression data in FlyAtlas shows *dTOX4* (*CG12104*) is most highly expressed in the testes and ovaries (data not shown). LCP1 is also most highly expressed in the testes in humans (O'Flaherty and Kaye, 2003). Therefore characterisation of the defects in *dTOX4* mutants could have important implications in understanding male infertility. Male factor infertility is a growing concern with an increasing number of patients exhibiting reduced sperm concentration, decreased motility and a high percentage of abnormal sperm morphology (Fardilha *et al*., 2011). An understanding of the molecular basis for male factor infertility will be important in identifying targets for therapeutic intervention.

Preliminary evidence suggests *dTOX4* null mutants have a reduced lifespan and therefore may have a role in the ageing process, possibly by affecting gene expression patterns or through involvement in DNA damage pathways. TOX4 is known to bind sites of DNA damage induced by platinating agents and interestingly PNUTS and Wdr82 were also found at these sites (Puch *et al*., 2011). PNUTS has also been implicated in cardiac aging where a decrease in PNUTS expression is linked to an increase in microRNA-34a as aging progresses (Boon *et al*., 2013). Further analysis of the *dTOX4* mutant may help in our understanding of processes that promote aging.

Analysis of histone modifications in *dPNUTS* and *PP187B* mutant cells suggest that some effects on gene expression observed in *dPNUTS* mutant animals may be related to changes in epigenetic histone modifications. Various marks of active transcription were upregulated in both *dPNUTS* and *PP187B* mutants. Post-translational modifications on histones regulate transcription by recruiting chromatin-modifying complexes that affect the local chromatin structure and determine access of proteins such as transcription factors. Whether the epigenetic status of genes misregulated in *dPNUTS* mutants is altered remains to be determined. Aberrant epigenetic regulation has been strongly linked to various cancers in the literature, with many cancers exhibiting altered epigenetic landscapes (Rodríguez-Paredes and Esteller, 2011).

7.1. Future work

Due to time constraints it was not possible to determine if the phenotypes observed in the *dTOX4* mutant were a result of disruption of the *dTOX4* gene. However, the tools to investigate this were developed and are currently under investigation.

Overexpression of wild type *dTOX4* using GAL4-UAS mediated overexpression under the control of the *bam* and *mat-α-tubulin* promoters should provide some insight into this but it is not known what stage of spermatogenesis and oogenesis *dTOX4* is expressed so these may be unsuitable promoters for rescue experiments. Expression of GFP tagged genomic *dTOX4* is likely to provide better insight not only in terms of rescue but also to determine where dTOX4 is expressed in both tissues. One caveat is the GFP tag may affect the behaviour of the genomic construct, therefore an untagged version should also be used. Another possible approach is to use the GAL4-UAS system to overexpress short hairpin RNAs for RNAi mediated knockdown of dTOX4 to see if loss of expression produces the same phenotypic consequence as the $dTOX4^{null}$ allele. One potential problem with this approach is the publicly available RNAi lines are not always efficient and complete knockdown of the protein encoding mRNA is very rarely achieved. Furthermore off-target effects can be observed which complicate analysis.

In parallel with this, it will be important to determine whether binding to dPNUTS is necessary for dTOX4 function. Complementation experiments, using either UAS or genomic constructs for $dTOX4^{P216\Delta}$ in the testes and ovaries should provide further insight into this. To further understand the relationship between dPNUTS and dTOX4, it will be interesting to examine the ability of these proteins to co-localise with each other and RNAPII on chromosomes.

If dPNUTS binding is not required for the function of dTOX4 in male and female fertility or aging, then determining the relationship between dTOX4 and the various hnRNP proteins discussed in Chapter 5 may explain the phenotypes observed. Using

similar techniques described in this thesis, such as biochemical analysis of tagged expression constructs and genetic complementation experiments to see if the mutant phenotype can be rescued by expressing a wild type copy of *Otu*, will determine if dTOX4 associates with hnRNP complexes. Analysis of *gurken* mRNA distribution in *dTOX4* mutant egg chambers will provide an immediate answer as to whether *gurken* misregulation is responsible for the observed defects in dorsal-ventral patterning.

Confirming dTOX4, dWdr82 and dPNUTS exist in a complex with PP1, as in humans and mammals, is the first step towards characterising these interactions in *Drosophila*. Transfection of S2 cells with tagged dTOX4 and dWdr82 with or without tagged dPNUTS will determine if they bind as a complex. The exact role of this complex in transcription or chromatin-related processes in *Drosophila* will provide further insight into this conserved complex.

dERR and dMBD-R2 represent novel PNUTS-binding proteins and further characterisation of these interactions may provide insight into the role of *dPNUTS* in determining gene expression patterns that control metabolic state, as well as other cellular processes. In this respect, identifying sites of interaction in dPNUTS may facilitate the development of targeted mutations in dPNUTS that disrupt specific protein-protein interactions. Looking at the levels of circulating sugars in *dPNUTS* mutant larvae will determine if processes regulated by dERR are affected, suggesting a functional interaction may exist. Examining the distribution of dMBD-R2 and dPNUTS on polytene chromosomes in wild type flies and flies expressing an RNAi construct against dMBD-R2, will help to establish a possible function of dMBD-R2 in the recruitment of dPNUTS to chromatin. Mutational analysis of dMBD-R2 will

determine if loss-of-function of *dMBD-R2* has the same phenotypic effect as the *dPNUTS* mutant.

Finally, repeating the dPTEN complementation experiments with a weaker (hypomorphic) *dPNUTS* mutant allele together with further biochemical analysis using tagged expression constructs in S2R+ cells will confirm if they do interact in *Drosophila*. Further analysis using a reporter for visualising PIP3 levels at the cell membrane (a GFP-PH domain fusion protein whereby the PH domain binds to PIP3) in flies overexpressing PNUTS will determine if a functional interaction does exist in *Drosophila*.

7.2. Implications for the future

As PP1 is involved in numerous cellular processes both in the cytoplasm and nucleus, inhibiting its catalytic subunit using therapeutic compounds will probably produce unwanted side effects. It may be more desirable to target PP1 holoenzymes such as the PP1/PNUTS/Wdr82/TOX4 multiprotein complex to manipulate phosphorylation in specific disease states, including cancer. Drug specificity could be achieved through disrupting the interaction between PP1c and its regulatory subunits or by disrupting the interaction between all subunits and the substrate. Therefore further characterisation of PNUTS-associated proteins and the substrates of PNUTS-PP1 is necessary to identify possible sites for drug targeting. (McConnell and Wadzinski ,2009). As proof of concept, small molecules have been identified that can disrupt PP1 complexes (McConnell and Wadzinski, 2009). One example is the use of trichostatin A (TSA), a histone deacetylase (HDAC) inhibitor, to disrupt PP1-HDAC complexes for the potential treatment of prostate cancer and

glioblastoma (Chen *et al*., 2005). Disrupting PP1-HDAC allows PP1 to become more highly associated with Akt, leading to its dephosphorylation and inactivation of the growth promoting pathway it regulates (McConnell and Wadzinski, 2009; Chen *et al*.,2005).

8. References

Adams, M.D., Celniker, S.E., Holt, R.A., Evans, C.A., Gocayne, J.D., Amanatides, P.G., Scherer, S.E., *et al*. 2000. The genome sequence of *Drosophila* melanogaster. *Science* 287(5461), pp. 2185–2195.

Aggen, J.B., Nairn, A.C. and Chamberlin, R. 2000. Regulation of protein phosphatase-1. *Chemistry & Biology* 7(1), pp. R13–R23.

Alaynick, W.A., Kondo, R.P., Xie, W., He, W., Dufour, C.R., Downes, M., Jonker, J.W., *et al*. 2007. ERRgamma directs and maintains the transition to oxidative metabolism in the postnatal heart. *Cell metabolism* 6(1), pp. 13–24.

Ali, M., Yan, K., Lalonde, M.-E., Degerny, C., Rothbart, S.B., Strahl, B.D., Côté, J., *et al*. 2012. Tandem PHD Fingers of MORF/MOZ Acetyltransferases Display Selectivity for Acetylated Histone H3 and Are Required for the Association with Chromatin. *Journal of Molecular Biology* 424(5), pp. 328–338.

Allen, P.B., Kwon, Y.-G., Nairn, A.C. and Greengard, P. 1998. Isolation and characterization of PNUTS, a putative protein phosphatase 1 nuclear targeting subunit. *Journal of Biological Chemistry* 273(7), pp. 4089–4095.

Alonso, A., Sasin, J., Bottini, N., Friedberg, I., Friedberg, I., Osterman, A., Godzik, A., *et al*. 2004. Protein Tyrosine Phosphatases in the Human Genome. *Cell* 117(6), pp. 699–711.

Amoyel, M. and Bach, E.A. 2014. Cell competition: how to eliminate your neighbours. *Development* 141(5), pp. 988–1000.

Ariazi, E.A., Clark, G.M. and Mertz, J.E. 2002. Estrogen-related receptor alpha and estrogen-related receptor gamma associate with unfavorable and favorable biomarkers, respectively, in human breast cancer. *Cancer Research* 62(22), pp. 6510–6518.

Axton, J., Dombrádi, V., Cohen, P.T. and Glover, D.M. 1990. One of the protein phosphatase 1 isoenzymes in *Drosophila* is essential for mitosis. *Cell* 63(1), pp. 33-

46.

Ballou, L.M. and Lin, R.Z. 2008. Rapamycin and mTOR kinase inhibitors. *Journal of Chemical Biology* 1(1-4), pp. 27–36.

Barford, D. 2010. The Structure and Topology of Protein Serine/Threonine Phosphatases. *Handbook of Cell Signalling*, Three-volume Set 2nd Edition, Chapter 86.

Bastock, R. and St Johnston, D. 2008. *Drosophila* oogenesis. *Current Biology* 18(23), pp. R1082–R1087.

Bate, M. and Arias, A.M. 2009. *The Development of Drosophila Melanogaster*. Cold Spring Harbor Laboratory Press.

Bellen, H.J. 2004. The BDGP Gene Disruption Project: Single Transposon Insertions Associated With 40% of *Drosophila* Genes. *Genetics* 167(2), pp. 761–781.

Bellen, H.J., Levis, R.W., He, Y., Carlson, J.W., Evans-Holm, M., Bae, E., Kim, J., *et al*. 2011. The *Drosophila* Gene Disruption Project: Progress Using Transposons With Distinctive Site Specificities. *Genetics* 188(3), pp. 731–743.

Bennett, D. and Alphey, L. 2007. Yeast two-hybrid screens to identify *Drosophila* PP1-binding proteins. *Methods in Molecular Biology* 365, pp. 155–179.

Bennett, D., Lyulcheva, E. and Alphey, L. 2006. Towards a Comprehensive Analysis of the Protein Phosphatase 1 Interactome in *Drosophila*. *Journal of Molecular Biology* 364(2), pp. 196–212.

Bentley, D.L. 2005. Rules of engagement: co-transcriptional recruitment of pre-mRNA processing factors. *Current Opinion in Cell Biology* 17(3), pp. 251–256.

Berndt, N. and Ludlow, J.W. 2004. Interaction between the retinoblastoma protein and protein phosphatase 1 during the cell cycle. *Methods in Molecular Biology* 281, pp. 17–32.

Bianchi, M.E. and Agresti, A. 2005. HMG proteins: dynamic players in gene regulation and differentiation. *Current opinion in genetics & development* 15(5), pp.

496–506.

Blagden, S.P., Gatt, M.K., Archambault, V., Lada, K., Ichihara, K., Lilley, K.S., Inoue, Y.H., *et al*. 2009. *Drosophila* Larp associates with poly(A)-binding protein and is required for male fertility and syncytial embryo development. *Developmental Biology* 334(1), pp. 186–197.

Blair, S.S. 2003. Genetic mosaic techniques for studying *Drosophila* development. *Development* 130(21), pp. 5065–5072.

Boles, M.K., Wilkinson, B.M., Maxwell, A., Lai, L., Mills, A.A., Nishijima, I., Salinger, A.P., *et al*. 2009. A mouse chromosome 4 balancer ENU-mutagenesis screen isolates eleven lethal lines. *BMC Genetics* 10(1), p. 12.

Bollen, M. 2001. Combinatorial control of protein phosphatase-1. *Trends in biochemical sciences* 26(7), pp. 426–431.

Bollen, M. and Beullens, M. 2002. Signaling by protein phosphatases in the nucleus. *Trends in cell biology* 12(3), pp. 138–145.

Bollen, M., Peti, W., Ragusa, M.J. and Beullens, M. 2010. The extended PP1 toolkit: designed to create specificity. *Trends in biochemical sciences* 35(8), pp. 450–458.

Bononi, A., Agnoletto, C., De Marchi, E., Marchi, S., Patergnani, S., Bonora, M., Giorgi, C., *et al*. 2011. Protein Kinases and Phosphatases in the Control of Cell Fate. *Enzyme Research* 2011, pp. 1–26.

Boon, R.A., Iekushi, K., Lechner, S., Seeger, T., Fischer, A., Heydt, S., Kaluza, D., *et al*. 2013. MicroRNA-34a regulates cardiac ageing and function. *Nature* 495(7439), pp. 107–110.

Boyer, L.A., Plath, K., Zeitlinger, J., Brambrink, T., Medeiros, L.A., Lee, T.I., Levine, S.S., *et al*. 2006. Polycomb complexes repress developmental regulators in murine embryonic stem cells. *Nature* 441(7091), pp. 349–353.

Bozzetti, M.P., Fanti, L., Di Tommaso, S., Piacentini, L., Berloco, M., Tritto, P. and Specchia, V. 2012. The 'Special' crystal-Stellate System in *Drosophila* melanogaster Reveals Mechanisms Underlying piRNA Pathway-Mediated Canalization. *Genetics*

Research International 2012(5), pp. 1–5.

Böhmer, F., Szedlacsek, S., Tabernero, L., Östman, A. and Hertog, den, J. 2012. Protein tyrosine phosphatase structure-function relationships in regulation and pathogenesis. *FEBS Journal* 280(2), pp. 413–431.

Brand, A.H. and Perrimon, N. 1993. Targeted gene expression as a means of altering cell fates and generating dominant phenotypes. *Development* 118(2), pp. 401–415.

Brand, M., Rampalli, S., Chaturvedi, C.-P. and Dilworth, F.J. 2008. Analysis of epigenetic modifications of chromatin at specific gene loci by native chromatin immunoprecipitation of nucleosomes isolated using hydroxyapatite chromatography. *Nature protocols* 3(3), pp. 398–409.

Brill, J.A., Hime, G.R., Scharer-Schuksz, M. and Fuller, M.T. 2000. A phospholipid kinase regulates actin organization and intercellular bridge formation during germline cytokinesis. *Development* 127(17), pp. 3855–3864.

Brookes, E., de Santiago, I., Hebenstreit, D., Morris, K.J., Carroll, T., Xie, S.Q., Stock, J.K., *et al*. 2012. Polycomb associates genome-wide with a specific RNA polymerase II variant, and regulates metabolic genes in ESCs. *Cell stem cell* 10(2), pp. 157–170.

Broussard, J.A., Rappaz, B., Webb, D.J. and Brown, C.M. 2013. FRET methods. *Nature protocols* 8(2), pp. 265–281.

Brower, V. 2011. Epigenetics: Unravelling the cancer code. *Nature* 471(7339), pp. S12–3.

Brückner, A., Polge, C., Lentze, N., Auerbach, D. and Schlattner, U. 2009. Yeast two-hybrid, a powerful tool for systems biology. *International Journal of Molecular Sciences* 10(6), pp. 2763–2788.

Buratowski, S. 2009. Progression through the RNA Polymerase II CTD Cycle. *Molecular Cell* 36(4), pp. 541-546.

Bustin, M. 1999. Regulation of DNA-dependent activities by the functional motifs of the high-mobility-group chromosomal proteins. *Molecular and Cellular Biology*

19(8), pp. 5237–5246.

Cao, R., Wang, L., Wang, H., Xia, L., Erdjument-Bromage, H., Tempst, P., Jones, R.S., *et al*. 2002. Role of histone H3 lysine 27 methylation in Polycomb-group silencing. *Science* 298(5595), pp. 1039–1043.

Cenci, G., Bonaccorsi, S., Pisano, C., Verni, F. and Gatti, M. 1994. Chromatin and microtubule organization during premeiotic, meiotic and early postmeiotic stages of *Drosophila* melanogaster spermatogenesis. *Journal of Cell Science* 107 (Pt 12), pp. 3521–3534.

Ceulemans, H. 2004. Functional Diversity of Protein Phosphatase-1, a Cellular Economizer and Reset Button. *Physiological Reviews* 84(1), pp. 1–39.

Chapman, T. and Davies, S.J. 2004. Functions and analysis of the seminal fluid proteins of male *Drosophila* melanogaster fruit flies. *Peptides* 25(9), pp. 1477–1490.

Charest-Marcotte, A., Dufour, C.R., Wilson, B.J., Tremblay, A.M., Eichner, L.J., Arlow, D.H., Mootha, V.K., *et al*. 2010. The homeobox protein Prox1 is a negative modulator of ERR{alpha}/PGC-1{alpha} bioenergetic functions. *Genes & Development* 24(6), pp. 537–542.

Chawla, A., Repa, J.J., Evans, R.M. and Mangelsdorf, D.J. 2001. Nuclear receptors and lipid physiology: opening the X-files. *Science* 294(5548), pp. 1866–1870.

Chen, C.S., Weng, S.C., Tseng, P.H., Lin, H.P. and Chen, C.S. 2005. Histone Acetylation-independent Effect of Histone Deacetylase Inhibitors on Akt through the Reshuffling of Protein Phosphatase 1 Complexes. *Journal of Biological Chemistry* 280(46), pp. 38879–38887.

Chen, S., Bohrer, L.R., Rai, A.N., Pan, Y., Gan, L., Zhou, X., Bagchi, A., *et al*. 2010. Cyclin-dependent kinases regulate epigenetic gene silencing through phosphorylation of EZH2. *Nature cell biology* 12(11), pp. 1108–1114.

Chen, Y., Jrgensen, M., Kolde, R., Zhao, X., Parker, B., Valen, E., Wen, J., *et al*. 2011. Prediction of RNA Polymerase II recruitment, elongation and stalling from histone modification data. *BMC Genomics* 12(1), pp. 544–544.

Cheng, A., Kaldis, P. and Solomon, M.J. 2000. Dephosphorylation of Human Cyclin-dependent Kinases by Protein Phosphatase Type 2C and 2 Isoforms. *Journal of Biological Chemistry* 275(44), pp. 34744–34749.

Chien, S., Reiter, L.T., Bier, E. and Gribskov, M. 2002. Homophila: human disease gene cognates in *Drosophila*. *Nucleic Acids Research* 30(1), pp. 149–151.

Chintapalli, V.R., Wang, J. and Dow, J.A.T. 2007. Using FlyAtlas to identify better *Drosophila* melanogaster models of human disease. *Nature Genetics* 39(6), pp. 715–720.

Ciurciu, A., Duncalf, L., Jonchere, V., Lansdale, N., Vasieva, O., Glenday, P., Rudenko, A., *et al*. 2013. PNUTS/PP1 regulates RNAPII-mediated gene expression and is necessary for developmental growth. *PLoS genetics* 9(10), p. e1003885.

Classen, A.-K., Bunker, B.D., Harvey, K.F., Vaccari, T. and Bilder, D. 2009. A tumor suppressor activity of *Drosophila* Polycomb genes mediated by JAK-STAT signaling. *Nature Genetics* 41(10), pp. 1150–1155.

Clouse, K.N., Ferguson, S.B. and Schüpbach, T. 2008. Squid, Cup, and PABP55B function together to regulate gurken translation in *Drosophila*. *Developmental Biology* 313, pp. 713-724.

Clyne, P.J., Certel, S.J., de Bruyne, M., Zaslavsky, L., Johnson, W.A. and Carlson, J.R. 1999. The Odor Specificities of a Subset of Olfactory Receptor Neurons Are Governed by Acj6, a POU-Domain Transcription Factor. *Neuron* 22(2), pp. 339–347.

Cohen, P. 2002a. Protein kinases--the major drug targets of the twenty-first century? *Nature reviews. Drug discovery* 1(4), pp. 309–315.

Cohen, P. 1989. The structure and regulation of protein phosphatases. *Annual review of biochemistry* 58, pp. 453–508.

Cohen, P.T.W. 2002b. Protein phosphatase 1--targeted in many directions. *Journal of Cell Science* 115(Pt 2), pp. 241–256.

Cooley, L., Kelley, R. and Spradling, A. 1988. Insertional mutagenesis of the

Drosophila genome with single P elements. *Science* 239(4844), pp. 1121–1128.

Cooley, L., Thompson, D. and Spradling, A.C. 1990. Constructing deletions with defined endpoints in *Drosophila*. *PNAS* 87(8), pp. 3170–3173.

David, C.J., Boyne, A.R., Millhouse, S.R. and Manley, J.L. 2011. The RNA polymerase II C-terminal domain promotes splicing activation through recruitment of a U2AF65-Prp19 complex. *Genes & Development* 25(9), pp. 972-983.

Dej, K.J. and Spradling, A.C. 1999. The endocycle controls nurse cell polytene chromosome structure during *Drosophila* oogenesis. *Development* 126(2), pp. 293–303.

Dent, P., Lavoinne, A., Nakielny, S., Caudwell, F.B., Watt, P. and Cohen, P. 1990. The molecular mechanism by which insulin stimulates glycogen synthesis in mammalian skeletal muscle. *Nature* 348(6299), pp. 302–308.

Di Croce, L. and Helin, K. 2013. Transcriptional regulation by Polycomb group proteins. *Nature structural & molecular biology* 20(10), pp. 1147–1155.

Dietzl, G., Chen, D., Schnorrer, F., Su, K.-C., Barinova, Y., Fellner, M., Gasser, B., *et al*. 2007. A genome-wide transgenic RNAi library for conditional gene inactivation in *Drosophila*. *Nature* 448(7150), pp. 151–156.

Dombrádi, V., Axton, J.M., Barker, H.M. and Cohen, P.T. 1990. Protein phosphatase 1 activity in *Drosophila* mutants with abnormalities in mitosis and chromosome condensation. *FEBS Letters* 275(1-2), pp. 39–43.

Dombrádi, V., Mann, D.J., Saunders, R.D. and Cohen, P.T. 1993. Cloning of the fourth functional gene for protein phosphatase 1 in *Drosophila* melanogaster from its chromosomal location. *European Journal of Biochemistry* 212(1), pp. 177–183.

Dorn, G.W. 2013. miR-34a and the cardiomyopathy of senescence: SALT PNUTS, SALT PNUTS! *Cell metabolism* 17(5), pp. 629–630.

Dreyfuss, G., Kim, V.N. and Kataoka, N. 2002. Messenger-RNA-binding proteins and the messages they carry. *Nature Reviews Molecular Cell Biology* 3(3), pp. 195–205.

Dulucq, S.S. and Krajinovic, M.M. 2010. The pharmacogenetics of imanitib. *Genome Medicine* 2(11), pp. 85–85.

Easow, G., Teleman, A.A. and Cohen, S.M. 2007. Isolation of microRNA targets by miRNP immunopurification. *RNA* 13(8), pp. 1198–1204.

Efimov, V.A., Chakhmakhcheva, O.G., Archdeacon, J., Fernandez, J.M., Fedorkin, O.N., Dorokhov, Y.L. and Atabekov, J.G. 2001. Detection of the 5'-cap structure of messenger RNAs with the use of the cap-jumping approach. *Nucleic Acids Research* 29(22), pp. 4751–4759.

Egloff, M.P., Johnson, D.F., Moorhead, G., Cohen, P.T., Cohen, P. and Barford, D. 1997. Structural basis for the recognition of regulatory subunits by the catalytic subunit of protein phosphatase 1. *EMBO Journal* 16(8), pp. 1876–1887.

Egloff, S. and Murphy, S. 2008. Cracking the RNA polymerase II CTD code. *Trends in Genetics* 24(6), pp. 280-288.

Egloff, S., Zaborowska, J., Laitem, C., Kiss, T. and Murphy, S. 2012. Ser7 phosphorylation of the CTD recruits the RPAP2 Ser5 phosphatase to snRNA genes. *Molecular Cell* 45(1), pp. 111-122.

Eichner, L.J., Perry, M.-C., Dufour, C.R., Bertos, N., Park, M., St-Pierre, J. and Giguère, V. 2010. miR-378∗ Mediates Metabolic Shift in Breast Cancer Cells via the PGC-1β/ERRγ Transcriptional Pathway. *Cell metabolism* 12(4), pp. 352–361.

Ejsmont, R.K. and Hassan, B.A. 2014. The Little Fly that Could: Wizardry and Artistry of *Drosophila* Genomics. *Genes* 5(2), pp. 385–414.

Enderle, D., Beisel, C., Stadler, M.B., Gerstung, M., Athri, P. and Paro, R. 2011. Polycomb preferentially targets stalled promoters of coding and noncoding transcripts. *Genome Research* 21(2), pp. 216–226.

Fabian, L. and Brill, J.A. 2012. *Drosophila* spermiogenesis: Big things come from little packages. *Spermatogenesis* 2(3), pp. 197–212.

Fabrizio, J.J., Hime, G., Lemmon, S.K. and Bazinet, C. 1998. Genetic dissection of

sperm individualization in *Drosophila* melanogaster. *Development* 125, pp. 1833-1843.

Fardilha, M., Esteves, S.L.C., Korrodi-Gregório, L., Vintém, A.P., Domingues, S.C., Rebelo, S., Morrice, N., *et al*. 2011. Identification of the human testis protein phosphatase 1 interactome. *Biochemical pharmacology* 82(10), pp. 1403–1415.

Farkas, G., Leibovitch, B.A. and Elgin, S.C. 2000. Chromatin organization and transcriptional control of gene expression in *Drosophila*. *Gene* 253(2), pp. 117–136.

Faux, M.C.M. and Scott, J.D.J. 1996. More on target with protein phosphorylation: conferring specificity by location. *Trends in biochemical sciences* 21(8), pp. 312–315.

Feng, S., Huang, J. and Wang, J. 2011. Loss of the Polycomb group gene polyhomeotic induces non-autonomous cell overproliferation. *EMBO Reports* 12(2) pp. 157-163.

Fields, S. and Song, O. 1989. A novel genetic system to detect protein-protein interactions. *Nature* 340(6230), pp. 245–246.

Figueiredo, J., da Cruz E Silva, O.A.B. and Fardilha, M. 2014. Protein phosphatase 1 and its complexes in carcinogenesis. *Current cancer drug targets* 14(1), pp. 2–29.

Fischer, E.H. 2010. Phosphorylase and the origin of reversible protein phosphorylation. *Biological Chemistry* 391(2/3).

Fischer, E.H. and Krebs, E.G. 1955. Conversion of phosphorylase b to phosphorylase a in muscle extracts. *Journal of Biological Chemistry* 216(1), pp. 121–132.

Fischle, W., Tseng, B.S., Dormann, H.L., Ueberheide, B.M., Garcia, B.A., Shabanowitz, J., Hunt, D.F., *et al*. 2005. Regulation of HP1-chromatin binding by histone H3 methylation and phosphorylation. *Nature* 438(7071), pp. 1116–1122.

Fischle, W., Wang, Y. and Allis, C.D. 2003. Binary switches and modification cassettes in histone biology and beyond. *Nature* 425(6957), pp. 475–479.

Formstecher, E. 2005. Protein interaction mapping: A *Drosophila* case study.

Genome Research 15(3), pp. 376–384.

Garcia, A., Cayla, X., Guergnon, J., Dessauge, F., Hospital, V., Rebollo, M.P., Fleischer, A., *et al*. 2003. Serine/threonine protein phosphatases PP1 and PP2A are key players in apoptosis. *Biochimie* 85(8), pp. 721–726.

Garinis, G.A., van der Horst, G.T.J., Vijg, J. and Hoeijmakers, J.H.J. 2008. DNA damage and ageing: new-age ideas for an age-old problem. *Nature cell biology* 10(11), pp. 1241–1247.

Garza, D., Medhora, M., Koga, A. and Hartl, D.L. 1991. Introduction of the transposable element mariner into the germline of *Drosophila* melanogaster. *Genetics* 128(2), pp. 303–310.

Gehani, S.S., Agrawal-Singh, S., Dietrich, N., Christophersen, N.S., Helin, K. and Hansen, K. 2010. Polycomb Group Protein Displacement and Gene Activation through MSK-Dependent H3K27me3S28 Phosphorylation. *Molecular Cell* 39(6), pp. 886–900.

Gillespie, D.E. and Berg, C.A. 1995. Homeless is required for RNA localization in *Drosophila* oogenesis and encodes a new member of the DE-H family of RNA-dependent ATPases. *Genes & Development* 9(20), pp. 2495–2508.

Goberdhan, D.C., Paricio, N., Goodman, E.C., Mlodzik, M. and Wilson, C. 1999. *Drosophila* tumor suppressor PTEN controls cell size and number by antagonizing the Chico/PI3-kinase signaling pathway. *Genes & Development* 13(24), pp. 3244–3258.

Golic, K.G. and Lindquist, S. 1989. The FLP recombinase of yeast catalyzes site-specific recombination in the *Drosophila* genome. *Cell* 59(3), pp. 499–509.

Goodrich, J.S., Clouse, K.N. and Schüpbach, T. 2004. Hrb27C, Sqd and Otu cooperatively regulate gurken RNA localization and mediate nurse cell chromosome dispersion in *Drosophila* oogenesis. *Development* 131(9), pp. 1949–1958.

Greenspan, R.J. 2004. *Fly Pushing*. CSHL Press.

Greil, F., Moorman, C. and van Steensel, B. 2006. [16] DamID: Mapping of In Vivo

Protein–Genome Interactions Using Tethered DNA Adenine Methyltransferase. In: *Methods in Enzymology*. Methods in Enzymology. Elsevier, pp. 342–359.

Groth, A.C.A., Fish, M.M., Nusse, R.R. and Calos, M.P.M. 2004. Construction of transgenic *Drosophila* by using the site-specific integrase from phage phiC31. *Genetics* 166(4), pp. 1775–1782.

Guindon, S. and Gascuel, O. 2003. A simple, fast, and accurate algorithm to estimate large phylogenies by maximum likelihood. *Systematic Biology* 52(5), pp. 696-704.

Guruharsha, K.G., Rual, J.-F., Zhai, B., Mintseris, J., Vaidya, P., Vaidya, N., Beekman, C., *et al*. 2011. A Protein Complex Network of *Drosophila* melanogaster. *Cell* 147(3), pp. 690–703.

Hahn, S. 2004. Structure and mechanism of the RNA polymerase II transcription machinery. *Nature structural & molecular biology* 11(5), pp. 394–403.

Hallson, G., Hollebakken, R.E., Li, T., Syrzycka, M., Kim, I., Cotsworth, S., Fitzpatrick, K.A., *et al*. 2012. dSet1 Is the Main H3K4 Di- and Tri-Methyltransferase Throughout *Drosophila* Development. *Genetics* 190(1), pp. 91–100.

Hanada, M., Kobayashi, T., Ohnishi, M., Ikeda, S., Wang, H., Katsura, K., Yanagawa, Y., *et al*. 1998. Selective suppression of stress-activated protein kinase pathway by protein phosphatase 2C in mammalian cells. *FEBS Letters* 437(3), pp. 172–176.

Handler, A.M. and Harrell, R.A. 1999. Germline transformation of *Drosophila* melanogaster with the piggyBac transposon vector. *Insect molecular biology* 8(4), pp. 449–457.

He, R.-J., Yu, Z.-H., Zhang, R.-Y. and Zhang, Z.-Y. 2014. Protein tyrosine phosphatases as potential therapeutic targets. *Acta Pharmacologica Sinica* 35(10), pp. 1227–1246.

Heintzman, N.D., Stuart, R.K., Hon, G., Fu, Y., Ching, C.W., Hawkins, R.D., Barrera, L.O., *et al*. 2007. Distinct and predictive chromatin signatures of transcriptional promoters and enhancers in the human genome. *Nature Genetics*

39(3), pp. 311–318.

Hemmings, H.C., Greengard, P., Tung, H.Y. and Cohen, P. 1984. DARPP-32, a dopamine-regulated neuronal phosphoprotein, is a potent inhibitor of protein phosphatase-1. *Nature* 310(5977), pp. 503–505.

Hendrickx, A., Beullens, M., Ceulemans, H., Abt, Den, T., Van Eynde, A., Nicolaescu, E., Lesage, B., *et al*. 2009. Docking Motif-Guided Mapping of the Interactome of Protein Phosphatase-1. *Chemistry & Biology* 16(4), pp. 365–371.

Hentges, K.E. and Justice, M.J. 2004. Checks and balancers: balancer chromosomes to facilitate genome annotation. *Trends in Genetics* 20(6), pp. 252–259.

Hernández, G., Han, H., Gandin, V., Fabian, L., Ferreira, T., Zuberek, J., Sonenberg, N., *et al*. 2012. Eukaryotic initiation factor 4E-3 is essential for meiotic chromosome segregation, cytokinesis and male fertility in *Drosophila*. *Development* 139(17), pp. 3211–3220.

Heroes, E., Lesage, B., Görnemann, J., Beullens, M., Van Meervelt, L. and Bollen, M. 2013. The PP1 binding code: a molecular-lego strategy that governs specificity. *The FEBS journal* 280(2), pp. 584–595.

Hintermair, C., Heidemann, M., Koch, F., Descostes, N., Gut, M., Gut, I., Fenouil, R., Ferrier, P., Flatley, A., Kremmer, E., Chapman, R.D., Andrau, JC. and Eick, D. 2012. Threonine-4 of mammalian RNA polymerase II CTD is targeted by Polo-like kinase 3 and required for transcriptional elongation. *The EMBO Journal* 31(12), pp. 2784-2797.

Hirose, Y. and Ohkuma, Y. 2007. Phosphorylation of the C-terminal Domain of RNA Polymerase II Plays Central Roles in the Integrated Events of Eucaryotic Gene Expression. *Journal of biochemistry* 141(5), pp. 601–608.

Hirose, Y. and Manley, J.L. 2000. RNA polymerase II and the integration of nuclear events. *Genes & Development* 14(12), pp. 1415-1429.

Hirota, T., Lipp, J.J., Toh, B.-H. and Peters, J.-M. 2005. Histone H3 serine 10 phosphorylation by Aurora B causes HP1 dissociation from heterochromatin. *Nature*

438(7071), pp. 1176–1180.

Hock, R., Furusawa, T., Ueda, T. and Bustin, M. 2007. HMG chromosomal proteins in development and disease. *Trends in cell biology* 17(2), pp. 72–79.

Hopkins, A.L. and Groom, C.R. 2002. The druggable genome. *Nature reviews. Drug discovery* 1(9), pp. 727–730.

Hsin, J.-P. and Manley, J.L. 2012. The RNA polymerase II CTD coordinates transcription and RNA processing. *Genes & Development* 26(19), pp. 2119–2137.

Ishikawa-Ankerhold, H.C., Ankerhold, R. and Drummen, G.P.C. 2012. Advanced fluorescence microscopy techniques--FRAP, FLIP, FLAP, FRET and FLIM. *Molecules* 17(4), pp. 4047–4132.

Jagiello, I., Beullens, M., Vulsteke, V., Wera, S., Sohlberg, B., Stalmans, W., Gabain, von, A., *et al*. 1997. NIPP-1, a nuclear inhibitory subunit of protein phosphatase-1, has RNA-binding properties. *Journal of Biological Chemistry* 272(35), pp. 22067–22071.

Janssens, V. and Goris, J. 2001. Protein phosphatase 2A: a highly regulated family of serine/threonine phosphatases implicated in cell growth and signalling. *Biochemical Journal* 353(Pt 3), pp. 417–439.

Janssens, V., Longin, S. and Goris, J. 2008. PP2A holoenzyme assembly: in cauda venenum (the sting is in the tail). *Trends in biochemical sciences* 33(3), pp. 113–121.

Jennings, B.H. 2011. *Drosophila* â€“ a versatile model in biology & medicine. *Materials Today* 14(5), pp. 190–195.

Jeong, D.G., Wei, C.H., Ku, B., Jeon, T.J., Chien, P.N., Kim, J.K., Park, S.Y., *et al*. 2014. DSPs. *Acta Cryst (2014). D70, 421-435 [doi:10.1107/S1399004713029866]*, pp. 1–15.

Jerebtsova, M., Klotchenko, S.A., Artamonova, T.O., Ammosova, T., Washington, K., Egorov, V.V., Shaldzhyan, A.A., *et al*. 2011. Mass spectrometry and biochemical analysis of RNA polymerase II: targeting by protein phosphatase-1. *Molecular and cellular biochemistry* 347(1-2), pp. 79–87.

Johnstone, O. and Lasko, P. 2001. Translational Regulation and RNA Localization in D rosophila Oocytes and Embryos. *Annual review of genetics* 35(1), pp. 365–406.

Kalifa, Y., Armenti, S.T. and Gavis, E.R. 2009. Glorund interactions in the regulation ofgurkenandoskarmRNAs. *Developmental Biology* 326(1), pp. 68–74.

Kalifa, Y., Huang, T., Rosen, L.N., Chatterjee, S. and Gavis, E.R. 2006. Glorund, a *Drosophila* hnRNP F/H Homolog, Is an Ovarian Repressor of nanos Translation. *Developmental Cell* 10, pp. 291-301.

Kamenski, T., Heilmeier, S., Meinhart, A. and Cramer, P. 2004. Structure and Mechanism of RNA Polymerase II CTD Phosphatases. *Molecular Cell* 15(3), pp. 399–407.

Karpova, T.S., Baumann, C.T., He, L., Wu, X., Grammer, A., Lipsky, P., Hager, G.L., *et al*. 2003. Fluorescence resonance energy transfer from cyan to yellow fluorescent protein detected by acceptor photobleaching using confocal microscopy and a single laser. *Journal of Microscopy (Oxford)* 209(Pt 1), pp. 56–70.

Kavela, S., Shinde, S.R., Ratheesh, R., Viswakalyan, K., Bashyam, M.D., Gowrishankar, S., Vamsy, M., *et al*. 2013. PNUTS Functions as a Proto-Oncogene by Sequestering PTEN. *Cancer Research* 73(1), pp. 205–214.

Kelley, R.L. 1993. Initial organization of the *Drosophila* dorsoventral axis depends on an RNA-binding protein encoded by the squid gene. *Genes & Development* 7(6), pp. 948–960.

Kennerdell, J.R. and Carthew, R.W. 2000. Heritable gene silencing in *Drosophila* using double-stranded RNA. *Nature biotechnology* 18(8), pp. 896–898.

Kile, B.T., Hentges, K.E., Clark, A.T., Nakamura, H., Salinger, A.P., Liu, B., Box, N., *et al*. 2003. Functional genetic analysis of mouse chromosome 11. *Nature* 425(6953), pp. 81–86.

Kim, Y.-M., Watanabe, T., Allen, P.B., Kim, Y.-M., Lee, S.J., Greengard, P., Nairn, A.C., *et al*. 2003. PNUTS, a protein phosphatase 1 (PP1) nuclear targeting subunit. Characterization of its PP1- and RNA-binding domains and regulation by

phosphorylation. *Journal of Biological Chemistry* 278(16), pp. 13819–13828.

King, R.C. and Storto, P.D. 1988. The role of the otu gene in *Drosophila* oogenesis. *Bioessays* 8(1), pp. 18–24.

King, R.C., Riley, S.F., Cassidy, J.D., White, P.E. and Paik, Y.K. 1981. Giant polytene chromosomes from the ovaries of a *Drosophila* mutant. *Science* 212(4493), pp. 441–443.

Kirchner, J., Gross, S., Bennett, D. and Alphey, L. 2007. Essential, overlapping and redundant roles of the *Drosophila* protein phosphatase 1 alpha and 1 beta genes. *Genetics* 176(1), pp. 273–281.

Kirchner, J., Vissi, E., Gross, S., Szöor, B., Rudenko, A., Alphey, L. and White-Cooper, H. 2008. *Drosophila* Uri, a PP1α binding protein, is essential for viability, maintenance of DNA integrity and normal transcriptional activity. *BMC Molecular Biology* 9(1), p. 36.

Klusza, S. and Deng, W.-M. 2010. poly is required for nurse-cell chromosome dispersal and oocyte polarity in *Drosophila*. *Fly* 4(2), pp. 128–136.

Kolupaeva, V. and Janssens, V. 2012. PP1 and PP2A phosphatases - cooperating partners in modulating retinoblastoma protein activation. *FEBS Journal* 280(2), pp. 627–643.

Komarnitsky, P., Cho, E.J. and Buratowski, S. 2000. Different phosphorylated forms of RNA polymerase II and associated mRNA processing factors during transcription. *Genes & Development* 14(19), pp. 2452-2460.

Kreivi, J.P., Trinkle-Mulcahy, L., Lyon, C.E., Morrice, N.A., Cohen, P. and Lamond, A.I. 1997. Purification and characterisation of p99, a nuclear modulator of protein phosphatase 1 activity. *FEBS Letters* 420(1), pp. 57–62.

Krishnamurthy, S., He, X., Reyes-Reyes, M., Moore, C. and Hampsey, M. 2004. Ssu72 Is an RNA Polymerase II CTD Phosphatase. *Molecular Cell* 14(3), pp. 387–394.

Lam, K.C., Mühlpfordt, F., Vaquerizas, J.M., Raja, S.J., Holz, H., Luscombe, N.M.,

Manke, T., *et al*. 2012. The NSL complex regulates housekeeping genes in *Drosophila*. *PLoS genetics* 8(6), pp. e1002736–e1002736.

Lambrecht, C., Haesen, D., Sents, W., Ivanova, E. and Janssens, V. 2013. Structure, Regulation, and Pharmacological Modulation of PP2A Phosphatases. In: *Methods in Molecular Biology*. Methods in Molecular Biology. Totowa, NJ: Humana Press, pp. 283–305.

Lammers, T. and Lavi, S. 2007. Role of Type 2C Protein Phosphatases in Growth Regulation and in Cellular Stress Signaling. *Critical Reviews in Biochemistry and Molecular Biology* 42(6), pp. 437–461.

Landsverk, H.B., Kirkhus, M., Bollen, M., Küntziger, T. and Collas, P. 2005. PNUTS enhances in vitro chromosome decondensation in a PP1-dependent manner. *Biochemical Journal* 390(Pt 3), pp. 709–717.

Landsverk, H.B., Mora-Bermúdez, F., Landsverk, O.J.B., Hasvold, G., Naderi, S., Bakke, O., Ellenberg, J., *et al*. 2010. The protein phosphatase 1 regulator PNUTS is a new component of the DNA damage response. *EMBO Reports* 11(11), pp. 868–875.

Lau, P. and Cheung, P. 2011a. Unlocking polycomb silencing through histone H3 phosphorylation. *Cell Cycle* 10(10), pp. 1514–1515.

Lau, P.N.I. and Cheung, P. 2011b. Histone code pathway involving H3 S28 phosphorylation and K27 acetylation activates transcription and antagonizes polycomb silencing. *PNAS* 108(7), pp. 2801–2806.

Lee, C.-C., Lin, Y.-H., Chang, W.-H., Lin, P.-C., Wu, Y.-C. and Chang, J.-G. 2011. Squamocin modulates histone H3 phosphorylation levels and induces G1 phase arrest and apoptosis in cancer cells. *BMC Cancer* 11(1), pp. 58–58.

Lee, J.-H. and Skalnik, D.G. 2008. Wdr82 is a C-terminal domain-binding protein that recruits the Setd1A Histone H3-Lys4 methyltransferase complex to transcription start sites of transcribed human genes. *Molecular and Cellular Biology* 28(2), pp. 609–618.

Lee, J.-H.J., You, J.J., Dobrota, E.E. and Skalnik, D.G.D. 2010. Identification and

characterization of a novel human PP1 phosphatase complex. *Journal of Biological Chemistry* 285(32), pp. 24466–24476.

Lee, S.J., Lee, J.K., Maeng, Y.S., Kim, Y.M. and Kwon, Y.G. 2009. Langerhans cell protein 1 (LCP1) binds to PNUTS in the nucleus: implications for this complex in transcriptional regulation. *Experimental & Molecular Medicine* 41(3), pp. 189–200.

Lee, T.I., Jenner, R.G., Boyer, L.A., Guenther, M.G., Levine, S.S., Kumar, R.M., Chevalier, B., *et al*. 2006. Control of Developmental Regulators by Polycomb in Human Embryonic Stem Cells. *Cell* 125(2), pp. 301–313.

Lefort, V. and Gascuel, O. 2015. FastME 2.0: a comprehensive, accurate and fast distance-based phylogeny inference program. Submitted to *Molecular Biology and Evolution*.

Lehming, N., Thanos, D., Brickman, J.M., Ma, J., Maniatis, T. and Ptashne, M. 1994. An HMG-like protein that can switch a transcriptional activator to a repressor. *Nature* 371(6493), pp. 175-179.

Lin, C.-W., Jao, C.Y. and Ting, A.Y. 2004. Genetically encoded fluorescent reporters of histone methylation in living cells. *Journal of the American Chemical Society* 126(19), pp. 5982–5983.

Liu, Y., Schmidt, B. and Maskell, D.L. 2010. MSAProbs: multiple sequence alignment based on pair hidden Markov models and partition function posterior probabilities. *Bioinformatics* 26(16), pp. 1958-1964.

Loukeris, T.G., Arcà, B., Livadaras, I., Dialektaki, G. and Savakis, C. 1995. Introduction of the transposable element Minos into the germ line of *Drosophila* melanogaster. *PNAS* 92(21), pp. 9485–9489.

Lowe, N., Rees, J.S., Roote, J., Ryder, E., Armean, I.M., Johnson, G., Drummond, E., *et al*. 2014. Analysis of the expression patterns, subcellular localisations and interaction partners of *Drosophila* proteins using a pigP protein trap library. *Development* 141(20), pp. 3994–4005.

Lutas, A., Wahlmark, C.J., Acharjee, S. and Kawasaki, F. 2012. Genetic analysis in

Drosophila reveals a role for the mitochondrial protein p32 in synaptic transmission. *G3: Genes, Genomes, Genetics* 2(1), pp. 59–69.

Ma, L., Yang, F. and Zheng, J. 2014. Application of fluorescence resonance energy transfer in protein studies. *Journal of Molecular Structure* 1077(C), pp. 87–100.

Ma, T., Trinh, M.A., Wexler, A.J., Bourbon, C., Gatti, E., Pierre, P., Cavener, D.R., *et al*. 2013. Suppression of eIF2α kinases alleviates Alzheimer's disease–related plasticity and memory deficits. *Nature Neuroscience* 16(9), pp. 1299–1305.

Maehama, T. and Dixon, J.E. 1998. The tumor suppressor, PTEN/MMAC1, dephosphorylates the lipid second messenger, phosphatidylinositol 3,4,5-trisphosphate. *Journal of Biological Chemistry* 273(22), pp. 13375–13378.

Maehama, T., Kosaka, N., Okahara, F., Takeuchi, K.-I., Umeda, M., Dixon, J.E. and Kanaho, Y. 2004. Suppression of a phosphatidylinositol 3-kinase signal by a specific spliced variant of *Drosophila* PTEN. *FEBS Letters* 565(1), pp. 43–47.

Malarkey, C.S. and Churchill, M.E.A. 2012. The high mobility group box: the ultimate utility player of a cell. *Trends in biochemical sciences* 37(12), pp. 553–562.

Manders, E., Verbeek, F.J. and Aten, J.A. 1993. Measurement of co-localization of objects in dual-colour confocal images. *Journal of microscopy* 169(3), pp. 375–382.

Margueron, R. and Reinberg, D. 2011. The Polycomb complex PRC2 and its mark in life. *Nature* 469(7330), pp. 343–349.

Martinez, A.-M., Schuettengruber, B., Sakr, S., Janic, A., Gonzalez, C. and Cavalli, G. 2009. Polyhomeotic has a tumor suppressor activity mediated by repression of Notch signaling. *Nature Genetics* 41(10), pp. 1076–1082.

Marygold, S.J., Roote, J., Reuter, G., Lambertsson, A., Ashburner, M., Millburn, G.H., Harrison, P.M., *et al*. 2007. The ribosomal protein genes and Minute loci of *Drosophila* melanogaster. *Genome biol* 8(10), p. R216.

McConnell, J.L. and Wadzinski, B.E. 2009. Targeting Protein Serine/Threonine Phosphatases for Drug Development. *Molecular Pharmacology* 75(6), pp. 1249–1261.

McGuire, S.E., Le, P.T., Osborn, A.J., Matsumoto, K. and Davis, R.L. 2003. Spatiotemporal rescue of memory dysfunction in *Drosophila*. *Science* 302, pp. 1765-1768.

McKee, B.D., Yan, R. and Tsai, J.-H. 2012. Meiosis in male *Drosophila*. *Spermatogenesis* 2(3), pp. 167–184.

Meinhart, A. and Cramer, P. 2004. Recognition of RNA polymerase II carboxy-terminal domain by 3'-RNA-processing factors. *Nature* 430(6996), pp. 223-226.

Mendjan, S., Taipale, M., Kind, J., Holz, H., Gebhardt, P., Schelder, M., Vermeulen, M., *et al*. 2006. Nuclear Pore Components Are Involved in the Transcriptional Regulation of Dosage Compensation in *Drosophila*. *Molecular Cell* 21(6), pp. 811–823.

Mermoud, J.E., Cohen, P.T. and Lamond, A.I. 1994. Regulation of mammalian spliceosome assembly by a protein phosphorylation mechanism. *EMBO Journal* 13(23), pp. 5679–5688.

Metaxakis, A. 2005. Minos as a Genetic and Genomic Tool in *Drosophila* melanogaster. *Genetics* 171(2), pp. 571–581.

Mohan, M., Herz, H.-M., Smith, E.R., Zhang, Y., Jackson, J., Washburn, M.P., Florens, L., *et al*. 2011. The COMPASS family of H3K4 methylases in *Drosophila*. *Molecular and Cellular Biology* 31, pp. 4310-4318.

Moorhead, G.B.G., Trinkle-Mulcahy, L. and Ulke-Lemée, A. 2007. Emerging roles of nuclear protein phosphatases. *Nature Reviews Molecular Cell Biology* 8(3), pp. 234–244.

Morata, G. and Ripoll, P. 1975. Minutes: mutants of *drosophila* autonomously affecting cell division rate. *Developmental Biology* 42(2), pp. 211–221.

Muller, H.J. 1927. ARTIFICIAL TRANSMUTATION OF THE GENE. *Science* 66(1699), pp. 84–87.

Muller, H.J. 1918. Genetic Variability, Twin Hybrids and Constant Hybrids, in a Case of Balanced Lethal Factors. *Genetics* 3(5), pp. 422–499.

Mustelin, T. 2007. A brief introduction to the protein phosphatase families. *Methods in Molecular Biology* 365, pp. 9–22.

Myers, M.P.M., Stolarov, J.P.J., Eng, C.C., Li, J.J., Wang, S.I.S., Wigler, M.H.M., Parsons, R.R., *et al*. 1997. P-TEN, the tumor suppressor from human chromosome 10q23, is a dual-specificity phosphatase. *PNAS* 94(17), pp. 9052–9057.

Nakamura, A., Sato, K. and Hanyu-Nakamura, K. 2004. *Drosophila* cup is an eIF4E binding protein that associates with Bruno and regulates oskar mRNA translation in oogenesis. *Developmental Cell* 6(1), pp. 69–78.

Nedea, E., He, X., Kim, M., Pootoolal, J., Zhong, G., Canadien, V., Hughes, T., *et al*. 2003. Organization and Function of APT, a Subcomplex of the Yeast Cleavage and Polyadenylation Factor Involved in the Formation of mRNA and Small Nucleolar RNA 3'-Ends. *Journal of Biological Chemistry* 278(35), pp. 33000–33010.

Neuman-Silberberg, F.S. and Schüpbach, T. 1993. The *Drosophila* dorsoventral patterning gene gurken produces a dorsally localized RNA and encodes a TGF alpha-like protein. *Cell* 75(1), pp. 165–174.

Newgard, C.B., Brady, M.J., O'Doherty, R.M. and Saltiel, A.R. 2000. Organizing glucose disposal: emerging roles of the glycogen targeting subunits of protein phosphatase-1. *Diabetes* 49(12), pp. 1967–1977.

Nègre, N., Hennetin, J., Sun, L.V., Lavrov, S., Bellis, M., White, K.P. and Cavalli, G. 2006. Chromosomal distribution of PcG proteins during *Drosophila* development. *PLoS Biology* 4(6), pp. e170–e170.

Nguyen, A.W. and Daugherty, P.S. 2005. Evolutionary optimization of fluorescent proteins for intracellular FRET. *Nature biotechnology* 23(3), pp. 355–360.

Ni, J.Q., Liu, L.P., Binari, R., Hardy, R., Shim, H.S., Cavallaro, A., Booker, M., *et al*. 2009. A *Drosophila* Resource of Transgenic RNAi Lines for Neurogenetics. *Genetics* 182(4), pp. 1089–1100.

Norvell, A., Debec, A., Finch, D., Gibson, L. and Thoma, B. 2005. Squid is required for efficient posterior localization of oskar mRNA during *Drosophila* oogenesis.

Development Genes and Evolution 215(7), pp. 340–349.

O'Flaherty, E. and Kaye, J. 2003. TOX defines a conserved subfamily of HMG-box proteins. *BMC Genomics* 4(1), pp. 13–13.

Olsen, J.V., Blagoev, B., Gnad, F., Macek, B., Kumar, C., Mortensen, P. and Mann, M. 2006. Global, In Vivo, and Site-Specific Phosphorylation Dynamics in Signaling Networks. *Cell* 127(3), pp. 635–648.

Orian, A. 2006. Chromatin profiling, DamID and the emerging landscape of gene expression. *Current opinion in genetics & development* 16(2), pp. 157–164.

Osborne, M.A., Zenner, G., Lubinus, M., Zhang, X., Songyang, Z., Cantley, L.C., Majerus, P., *et al*. 1996. The Inositol 5'-Phosphatase SHIP Binds to Immunoreceptor Signaling Motifs and Responds to High Affinity IgE Receptor Aggregation. *Journal of Biological Chemistry* 271(46), pp. 29271–29278.

Ouyang, M., Sun, J., Chien, S. and Wang, Y. 2008. Determination of hierarchical relationship of Src and Rac at subcellular locations with FRET biosensors. *PNAS* 105(38), pp. 14353–14358.

P-ohler, J.R., Norman, D.G., Bramham, J., Bianchi, M.E. and Lilley, D.M. 1998. HMG box proteins bind to four-way DNA junctions in their open conformation. *EMBO Journal* 17(3), pp. 817–826.

Pandey, U.B. and Nichols, C.D. 2011. Human Disease Models in *Drosophila* melanogaster and the Role of the Fly in Therapeutic Drug Discovery. *Pharmacological Reviews* 63(2), pp. 411–436.

Phatnani, H.P. and Greenleaf, A.L. 2006. Phosphorylation and functions of the RNA polymerase II CTD. *Genes & Development* 20(21), pp. 2922–2936.

Pierre, S.E.S., Ponting, L., Stefancsik, R., McQuilton, P. and McQuilton, P. 2014. FlyBase 102--advanced approaches to interrogating FlyBase. *Nucleic Acids Research* 42(Database issue), pp. D780–D788.

Puch, du, C.B.M., Barbier, E., Kraut, A., Couté, Y., Fuchs, J., Buhot, A., Livache, T., *et al*. 2011. TOX4 and its binding partners recognize DNA adducts generated by

platinum anticancer drugs. *Archives of Biochemistry and Biophysics* 507(2), pp. 296–303.

Qian, J.J., Lesage, B.B., Beullens, M.M., Van Eynde, A.A. and Bollen, M.M. 2011. PP1/Repo-man dephosphorylates mitotic histone H3 at T3 and regulates chromosomal aurora B targeting. *Current Biology* 21(9), pp. 766–773.

Raghavan, S., Williams, I., Aslam, H., Thomas, D., Szöor, B., Morgan, G., Gross, S., *et al*. 2000. Protein phosphatase 1beta is required for the maintenance of muscle attachments. *Current Biology* 10(5), pp. 269–272.

Rain, J.C., Selig, L., De Reuse, H., Battaglia, V., Reverdy, C., Simon, S., Lenzen, G., *et al*. 2001. The protein-protein interaction map of Helicobacter pylori. *Nature* 409(6817), pp. 211–215.

Raja, S.J., Charapitsa, I., Conrad, T., Vaquerizas, J.M., Gebhardt, P., Holz, H., Kadlec, J., *et al*. 2010. The Nonspecific Lethal Complex Is a Transcriptional Regulator in*Drosophila*. *Molecular Cell* 38(6), pp. 827–841.

Reed, B.H. and Orr-Weaver, T.L. 1997. The *Drosophila* gene morula inhibits mitotic functions in the endo cell cycle and the mitotic cell cycle. *Development* 124(18), pp. 3543–3553.

Reeves, R. 2010. Nuclear functions of the HMG proteins. *Biochimica et Biophysica Acta (BBA) - Gene Regulatory Mechanisms* 1799(1-2), pp. 3–14.

Regnard, C., Straub, T., Mitterweger, A., Dahlsveen, I.K., Fabian, V. and Becker, P.B. 2011. Global analysis of the relationship between JIL-1 kinase and transcription. *PLoS genetics* 7(3), pp. e1001327–e1001327.

Reiter, L.T., Potocki, L., Chien, S., Gribskov, M. and Bier, E. 2001. A systematic analysis of human disease-associated gene sequences in *Drosophila* melanogaster. *Genome Research* 11(6), pp. 1114–1125.

Ritter, A.R. and Beckstead, R.B. 2010. Sox14 is required for transcriptional and developmental responses to 20-hydroxyecdysone at the onset of *drosophila* metamorphosis. *Developmental Dynamics* 239(10), pp. 2685–2694.

Rivers, A.M. 1996. The B56 Family of Protein Phosphatase 2A (PP2A) Regulatory Subunits Encodes Differentiation-induced Phosphoproteins That Target PP2A to Both Nucleus and Cytoplasm. *Journal of Biological Chemistry* 271(36), pp. 22081–22089.

Robertson, H.M., Preston, C.R. and Phillis, R.W. 1988. A stable genomic source of P element transposase in *Drosophila* melanogaster. *Genetics* 118, pp. 461-470.

Rodríguez-Paredes, M. and Esteller, M. 2011. Cancer epigenetics reaches mainstream oncology. *Nature Medicine*, pp. 1–10.

Rosado-Lugo, J.D. and Hampsey, M. 2014. The Ssu72 Phosphatase Mediates the RNA Polymerase II Initiation-Elongation Transition. *Journal of Biological Chemistry* 289(49), pp. 33916-33926.

Rossetto, D., Avvakumov, N. and Côté, J. 2014. Histone phosphorylation. *Epigenetics : official journal of the DNA Methylation Society* 7(10), pp. 1098–1108.

Rubin, G.M. and Lewis, E.B. 2000. A brief history of *Drosophila*'s contributions to genome research. *Science* 287(5461), pp. 2216–2218.

Rubin, G.M. and Spradling, A.C. 1982. Genetic transformation of *Drosophila* with transposable element vectors. *Science* 218(4570), pp. 348–353.

Rudenki, A. 2004. Characterisation of nuclear protein phosphatase type 1 in *Drosophila melanogaster*, PhD Thesis, University of Oxford, UK.

Rudenko, A., Bennett, D. and Alphey, L. 2003. Trithorax interacts with type 1 serine/threonine protein phosphatase in *Drosophila*. *EMBO Reports* 4(1), pp. 59–63.

Ryder, E. and Russell, S. 2003. Transposable elements as tools for genomics and genetics in *Drosophila*. *Briefings in Functional Genomics* 2(1), pp. 57–71.

Sacco, F., Perfetto, L., Castagnoli, L. and Cesareni, G. 2012. The human phosphatase interactome: An intricate family portrait. *FEBS Letters* 586(17), pp. 2732–2739.

Sambrook, J. and Russell, D.W. 2001. Molecular Cloning. CSHL Press.

Schneider, I. 1972. Cell lines derived from late embryonic stages of *Drosophila*

melanogaster. *Journal of embryology and experimental morphology* 27(2), pp. 353–365.

Schotta, G., Ebert, A., Dorn, R. and Reuter, G. 2003. Position-effect variegation and the genetic dissection of chromatin regulation in *Drosophila*. *Seminars in cell & developmental biology* 14(1), pp. 67–75.

Schroeder, S.C., Schwer, B., Shuman, S. and Bentley, D. 2000. Dynamic association of capping enzymes with transcribing RNA polymerase II. *Genes & Development* 14(19), pp. 2435-2440.

Schwartz, Y.B., Kahn, T.G., Nix, D.A., Li, X.-Y., Bourgon, R., Biggin, M. and Pirrotta, V. 2006. Genome-wide analysis of Polycomb targets in *Drosophila* melanogaster. *Nature Genetics* 38(6), pp. 700–705.

Searles, L.L., Jokerst, R.S., Bingham, P.M., Voelker, R.A. and Greenleaf, A.L. 1982. Molecular cloning of sequences from a *Drosophila* RNA polymerase II locus by P element transposon tagging. *Cell* 31(3 Pt 2), pp. 585–592.

Sents, W., Ivanova, E., Lambrecht, C., Haesen, D. and Janssens, V. 2013. The biogenesis of active protein phosphatase 2A holoenzymes: a tightly regulated process creating phosphatase specificity. *The FEBS journal* 280(2), pp. 644–661.

Seshacharyulu, P., Pandey, P., Datta, K. and Batra, S.K. 2013. Phosphatase: PP2A structural importance, regulation and its aberrant expression in cancer. *Cancer letters* 335(1), pp. 9–18.

Shaner, N.C.N., Steinbach, P.A.P. and Tsien, R.Y.R. 2005. A guide to choosing fluorescent proteins. *Nature Methods* 2(12), pp. 905–909.

Sharma, A., Singh, K. and Almasan, A. 2012. Histone H2AX Phosphorylation: A Marker for DNA Damage. In: *Methods in Molecular Biology*. Methods in Molecular Biology. Totowa, NJ: Humana Press, pp. 613–626.

Sharma, S.V., Lee, D.Y., Li, B., Quinlan, M.P., Takahashi, F., Maheswaran, S., McDermott, U., *et al*. 2010. A Chromatin-Mediated Reversible Drug-Tolerant State in Cancer Cell Subpopulations. *Cell* 141(1), pp. 69–80.

Shi, Y. 2009. Serine/Threonine Phosphatases: Mechanism through Structure. *Cell* 139(3), pp. 468–484.

Shi, Y., Di Giammartino, D.C., Taylor, D., Sarkeshik, A., Rice, W.J., Yates, J.R., Frank, J. and Manley, J.L. 2009. Molecular architecture of the human pre-mRNA 3' processing complex. *Molecular Cell* 33(3), pp. 365-376.

Simon, J.A. and Kingston, R.E. 2009. Mechanisms of Polycomb gene silencing: knowns and unknowns. *Nature Reviews Molecular Cell Biology* 10, pp. 697-708.

Smith, A., Smith, A., Alrubaie, S., Coehlo, C., Leevers, S.J. and Ashworth, A. 1999. Alternative splicing of the *Drosophila* PTEN gene. *Biochimica et biophysica acta* 1447(2-3), pp. 313–317.

Snapp, E.L. and Hegde, R.S. 2001. Rational Design and Evaluation of FRET Experiments to Measure Protein Proximities in Cells. Hoboken, NJ, USA: John Wiley & Sons, Inc.

Spradling, A.C., Stern, D., Beaton, A., Rhem, E.J., Laverty, T., Mozden, N., Misra, S., *et al*. 1999. The Berkeley *Drosophila* Genome Project gene disruption project: Single P-element insertions mutating 25% of vital *Drosophila* genes. *Genetics* 153(1), pp. 135–177.

Stapleton, W., Das, S. and McKee, B.D. 2001. A role of the *Drosophila* homeless gene in repression of Stellate in male meiosis. *Chromosoma* 110(3), pp. 228–240.

Stebbing, J., Lit, L.C., Zhang, H., Darrington, R.S., Melaiu, O., Rudraraju, B. and Giamas, G. 2014. The regulatory roles of phosphatases in cancer. *Oncogene* 33(8), pp. 939–953.

Stein, R.A., Chang, C.-Y., Kazmin, D.A., Way, J., Schroeder, T., Wergin, M., Dewhirst, M.W., *et al*. 2008. Estrogen-related receptor alpha is critical for the growth of estrogen receptor-negative breast cancer. *Cancer Research* 68(21), pp. 8805–8812.

Stowers, R.S. and Schwarz, T.L. 1999. A genetic method for generating *Drosophila* eyes composed exclusively of mitotic clones of a single genotype. *Genetics* 152(4),

pp. 1631–1639.

Strålfors, P., Hiraga, A. and Cohen, P. 1985. The protein phosphatases involved in cellular regulation. Purification and characterisation of the glycogen-bound form of protein phosphatase-1 from rabbit skeletal muscle. *European Journal of Biochemistry* 149(2), pp. 295–303.

Strimmer, K. and Von Haeseler, A. 1996. Quartet Puzzling: A Quartet Maximum-Likelihood Method for Reconstructing Tree Topologies. *Molecular Biology and Evolution* 13(7), pp. 964-969.

Stros, M., Launholt, D. and Grasser, K.D. 2007. The HMG-box: a versatile protein domain occurring in a wide variety of DNA-binding proteins. *Cellular and molecular life sciences : CMLS* 64(19-20), pp. 2590–2606.

Svejstrup, J.Q. 2012. Transcription: another mark in the tail. *The EMBO Journal* 31(12), pp. 2753-2754.

Tennessen, J.M., Baker, K.D., Lam, G., Evans, J. and Thummel, C.S. 2011. The*Drosophila*Estrogen-Related Receptor Directs a Metabolic Switch that Supports Developmental Growth. *Cell metabolism* 13(2), pp. 139–148.

Theodosiou, N.A. and Xu, T. 1998. Use of FLP/FRT system to study *Drosophila* development. *Methods* 14(4), pp. 355–365.

Thibault, S.T., Singer, M.A., Miyazaki, W.Y., Milash, B., Dompe, N.A., Singh, C.M., Buchholz, R., *et al*. 2004. A complementary transposon tool kit for *Drosophila* melanogaster using P and piggyBac. *Nature Genetics* 36(3), pp. 283–287.

Tolhuis, B., Muijrers, I., de Wit, E., Teunissen, H., Talhout, W., van Steensel, B. and van Lohuizen, M. 2006. Genome-wide profiling of PRC1 and PRC2 Polycomb chromatin binding in *Drosophila* melanogaster. *Nature Genetics* 38(6), pp. 694–699.

Tonks, N.K. and Neel, B.G. 2001. Combinatorial control of the specificity of protein tyrosine phosphatases. *Current Opinion in Cell Biology* 13(2), pp. 182–195.

Trinkle-Mulcahy, L., Andersen, J., Lam, Y.W., Moorhead, G., Mann, M. and Lamond, A.I. 2006. Repo-Man recruits PP1 gamma to chromatin and is essential for

cell viability. *The Journal of cell biology* 172(5), pp. 679–692.

Trinkle-Mulcahy, L., Andrews, P.D., Wickramasinghe, S., Sleeman, J., Prescott, A., Lam, Y.W., Lyon, C., *et al*. 2003. Time-lapse imaging reveals dynamic relocalization of PP1gamma throughout the mammalian cell cycle. *Molecular Biology of the Cell* 14(1), pp. 107–117.

Trinkle-Mulcahy, L.L., Ajuh, P.P., Prescott, A.A., Claverie-Martin, F.F., Cohen, S.S., Lamond, A.I.A. and Cohen, P.P. 1999. Nuclear organisation of NIPP1, a regulatory subunit of protein phosphatase 1 that associates with pre-mRNA splicing factors. *Journal of Cell Science* 112 (Pt 2), pp. 157–168.

Tsaytler, P., Harding, H.P., Ron, D. and Bertolotti, A. 2011. Selective inhibition of a regulatory subunit of protein phosphatase 1 restores proteostasis. *Science* 332(6025), pp. 91–94.

Ubersax, J.A. and Ferrell, J.E. 2007. Mechanisms of specificity in protein phosphorylation. *Nature Reviews Molecular Cell Biology* 8(8).

Udho, E., Tedesco, V.C., Zygmunt, A. and Krucher, N.A. 2002. PNUTS (phosphatase nuclear targeting subunit) inhibits retinoblastoma-directed PP1 activity. *Biochemical and Biophysical Research Communications* 297(3), pp. 463–467.

Ueda, T. and Yoshida, M. 2010. HMGB proteins and transcriptional regulation. *Biochimica et Biophysica Acta (BBA) - Gene Regulatory Mechanisms* 1799(1-2), pp. 114–118.

Van Buskirk, C. and Schüpbach, T. 2002. half pint Regulates Alternative Splice Site Selection in *Drosophila*. *Developmental Cell* 2, pp. 343-353.

Van Criekinge, W. and Beyaert, R. 1999. Yeast Two-Hybrid: State of the Art. *Biological procedures online* 2, pp. 1–38.

van den Heuvel, S. and Dyson, N.J. 2008. Conserved functions of the pRB and E2F families. *Nature Reviews Molecular Cell Biology* 9(9), pp. 713–724.

Van Eynde, A., Wera, S., Beullens, M., Torrekens, S., Van Leuven, F., Stalmans, W. and Bollen, M. 1995. Molecular cloning of NIPP-1, a nuclear inhibitor of protein

phosphatase-1, reveals homology with polypeptides involved in RNA processing. *Journal of Biological Chemistry* 270(47), pp. 28068–28074.

Van Munster, E.B., Kremers, G.J., Adjobo-Hermans, M.J.W. and Gadella, T.W.J. 2005. Fluorescence resonance energy transfer (FRET) measurement by gradual acceptor photobleaching. *Journal of Microscopy (Oxford)* 218(Pt 3), pp. 253–262.

Venken, K.J.T. and Bellen, H.J. 2005. Emerging technologies for gene manipulation in *Drosophila* melanogaster. *Nature Reviews: Genetics* 6(3), pp. 167–178.

Venken, K.J.T. and Bellen, H.J. 2007. Transgenesis upgrades for *Drosophila* melanogaster. *Development* 134(20), pp. 3571–3584.

Venken, K.J.T., He, Y., Hoskins, R.A. and Bellen, H.J. 2006. P[acman]: a BAC transgenic platform for targeted insertion of large DNA fragments in D. melanogaster. *Science* 314(5806), pp. 1747–1751.

Virshup, D.M. and Shenolikar, S. 2009. From Promiscuity to Precision: Protein Phosphatases Get a Makeover. *Molecular Cell* 33(5), pp. 537–545.

Wang, W., Cronmiller, C. and Brautigan, D.L. 2008. Maternal Phosphatase Inhibitor-2 Is Required for Proper Chromosome Segregation and Mitotic Synchrony During *Drosophila* Embryogenesis. *Genetics* 179(4), pp. 1823–1833.

Washington, K., Ammosova, T., Beullens, M., Jerebtsova, M., Kumar, A., Bollen, M. and Nekhai, S. 2002. Protein phosphatase-1 dephosphorylates the C-terminal domain of RNA polymerase-II. *Journal of Biological Chemistry* 277(43), pp. 40442–40448.

White-Cooper, H. 2010. Molecular mechanisms of gene regulation during *Drosophila* spermatogenesis. *Reproduction* 139(1), pp. 11–21.

White-Cooper, H. 2004. Spermatogenesis: analysis of meiosis and morphogenesis. *Methods in Molecular Biology* 247, pp. 45–75.

White-Cooper, H. 2009. Studying how flies make sperm—Investigating gene function in *Drosophila* testes. *Molecular and cellular endocrinology*.

Wilkinson, B., Chen, J.Y.-F., Han, P., Rufner, K.M., Goularte, O.D. and Kaye, J. 2002. TOX: an HMG box protein implicated in the regulation of thymocyte selection. *Nature Immunology* 3(3), pp. 272–280.

Yanagawa, S.I., Lee, J.S. and Ishimoto, A. 1998. Identification and Characterization of a Novel Line of*Drosophila* Schneider S2 Cells That Respond to Wingless Signaling. *Journal of Biological Chemistry* 273(48), pp. 32353–32359.

Yeo, M., Lin, P.S., Dahmus, M.E. and Gill, G.N. 2003. A Novel RNA Polymerase II C-terminal Domain Phosphatase That Preferentially Dephosphorylates Serine 5. *Journal of Biological Chemistry* 278(28), pp. 26078–26085.

Zhao, S. and Lee, E.Y.C. 1997. A Protein Phosphatase-1-binding Motif Identified by the Panning of a Random Peptide Display Library. *Journal of Biological Chemistry* 272(45), pp. 28368–28372.

Zhao, Y., Butler, E.B. and Tan, M. 2013. Targeting cellular metabolism to improve cancer therapeutics. *Cell Death and Disease* 4(3), pp. e532–10.

Appendix 1

Crossing scheme for induction of PNUTS^{13B} clones in wild type background (wing disc and salivary gland):

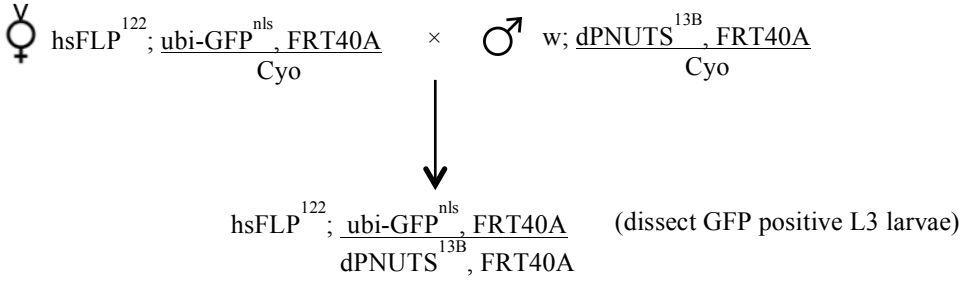

Crossing scheme for induction of PNUTS^{13B} clones in a *minute* background in the wing disc:

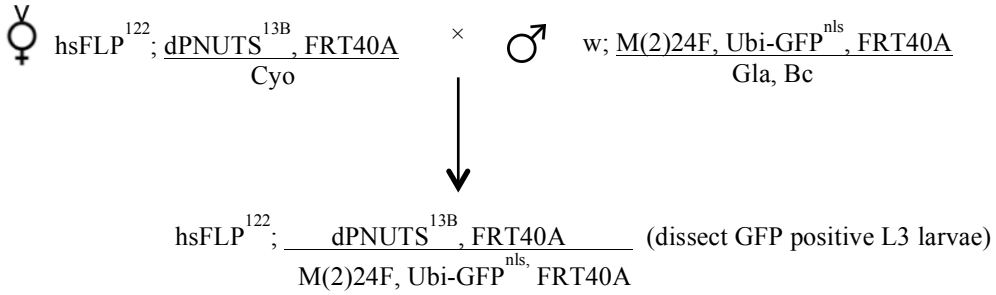

Crossing scheme to make wild type control for *minute* experiments:

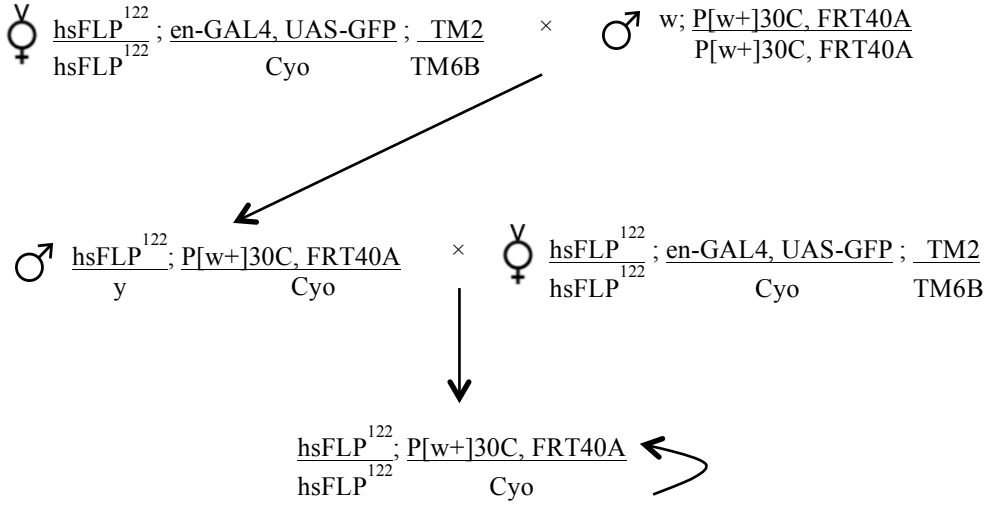

Crossing scheme for induction of wild type clones in wild type background (wing disc):

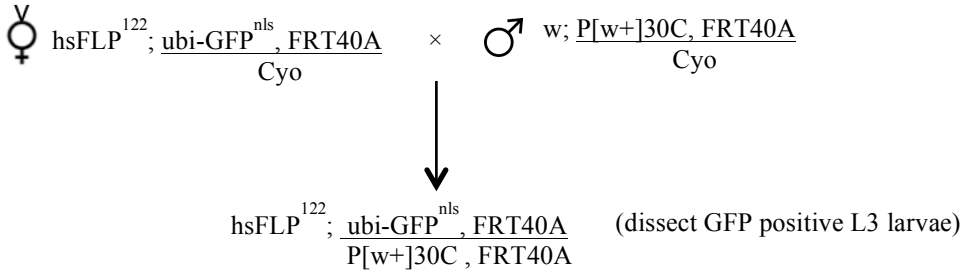

Crossing scheme for induction of wild type clones in a *minute* background (wing discs):

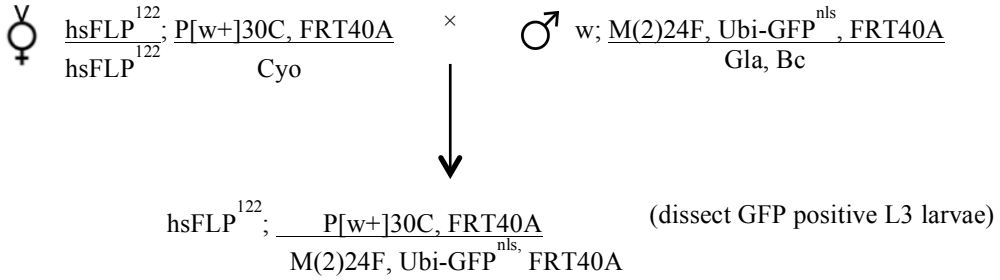

Appendix 2

Crossing scheme for induction of PP187B$^{Su(var)3\text{-}6[1]}$ clones (salivary gland):

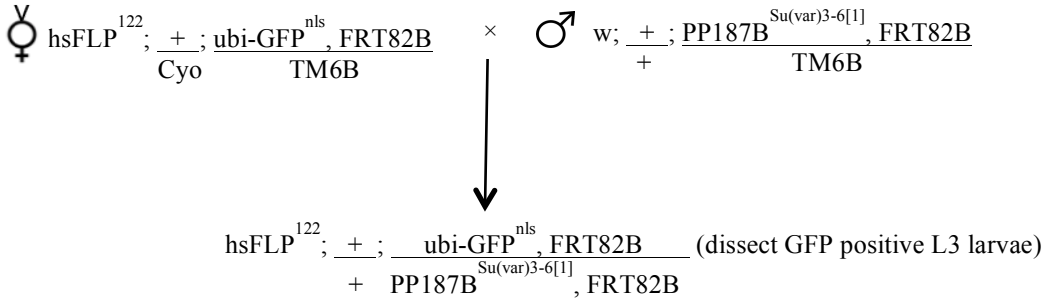

Appendix 3

Crossing scheme to make dTOX4 mutant by imprecise excision of a P-element:

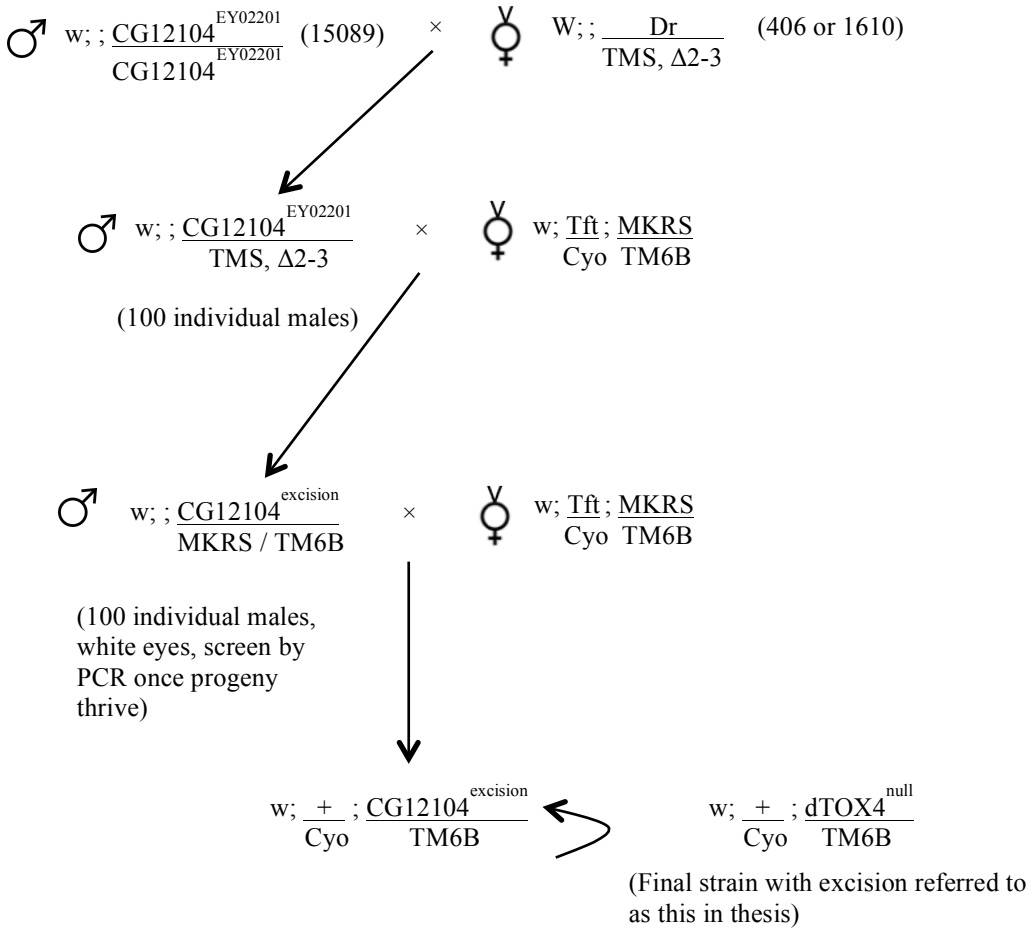

Appendix 4

Crossing schemes to make GFP-dTOX4^{wt} and GFP-dTOX4$^{P216\Delta}$ overexpression rescue strains

To recombine UAS-GFP-dTOX4^{wt} and UAS-GFP-dTOX4$^{P216\Delta}$ with maternal-α-tubulin-GAL4: (note UAS-GFP-dTOX4$^{wt\ or\ P216\Delta}$ have been shortened to UAS-dTOX4$^{wt\ or\ P216\Delta}$)

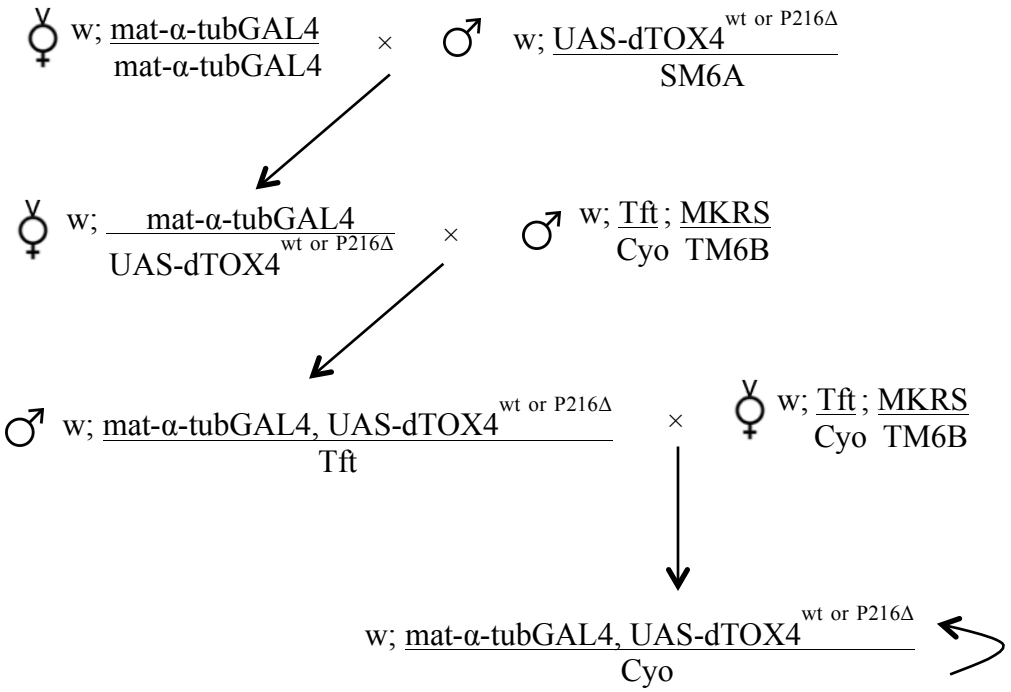

To recombine bam-GAL4 on 3rd chromosome with dTOX4null:

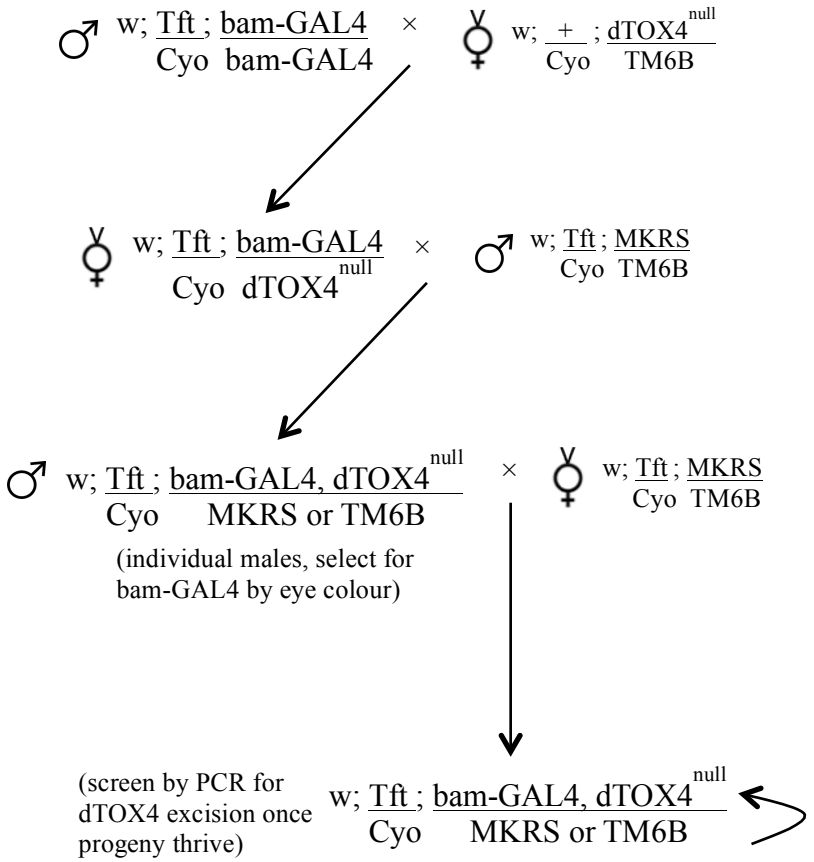

Appendix 5

Crossing scheme to recombine PNUTS^{13B} and PTEN[3] for PNUTS/PTEN complementation experiments:

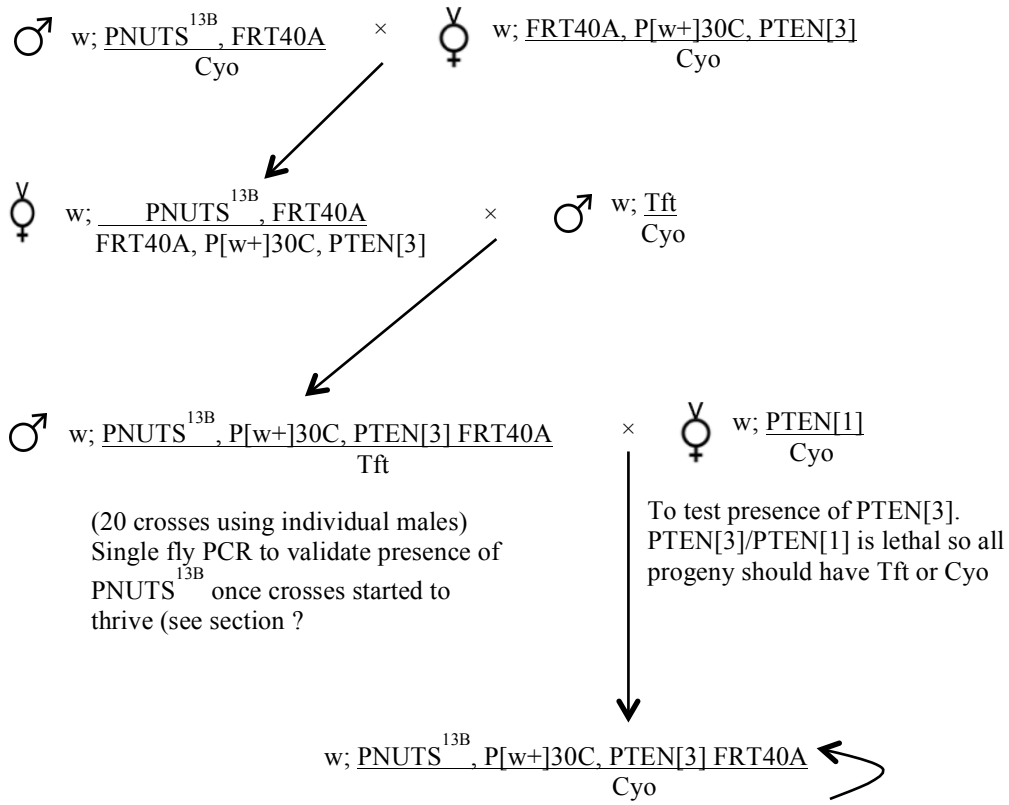

Crossing scheme for complementation analysis of PNUTS/PTEN:

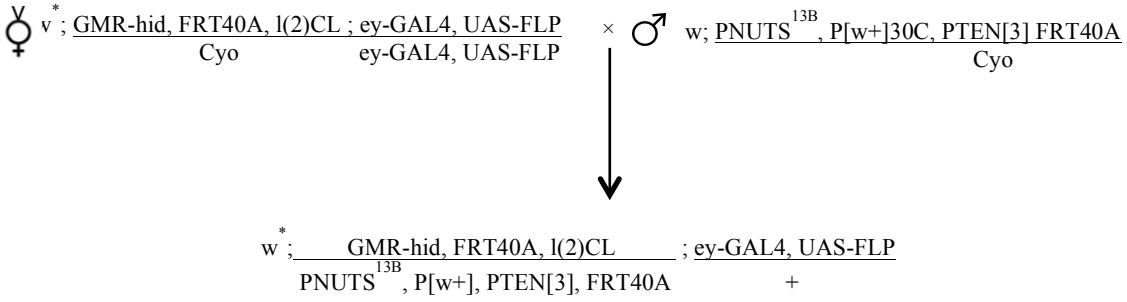

Crossing scheme for PNUTS/PTEN complementation experiments: PNUTS^{13B} control:

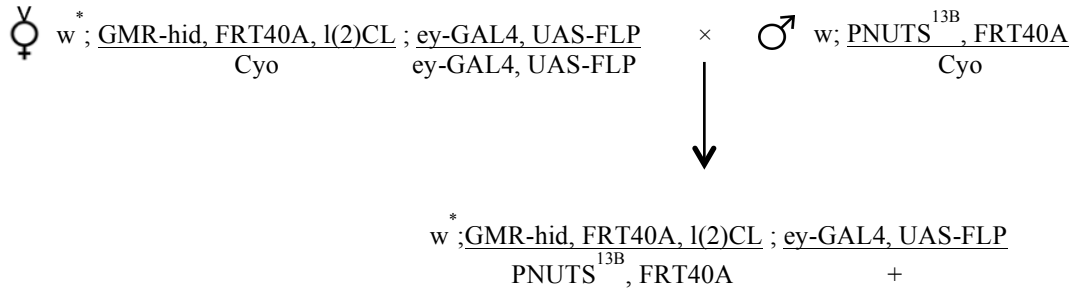

Crossing scheme for PNUTS/PTEN complementation experiments: PTEN[3] control:

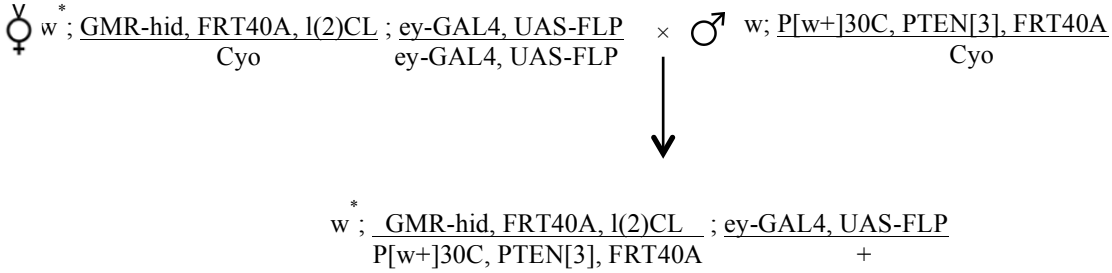

Crossing scheme for PNUTS/PTEN complementation experiments: wild type (P[w+]30C) control:

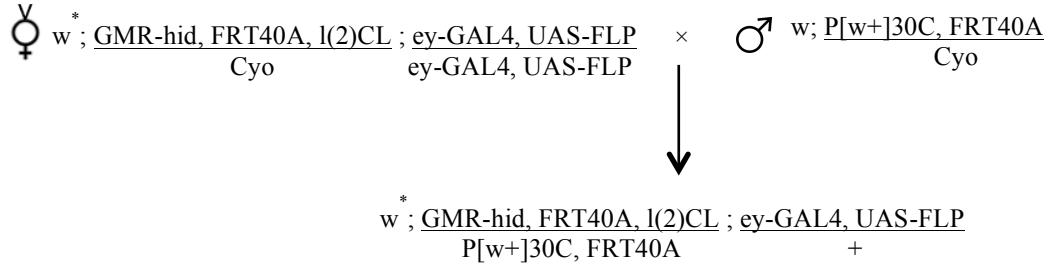

Appendix 6

Crossing scheme to make tester strain for phenotypic screen in Chapter 6:

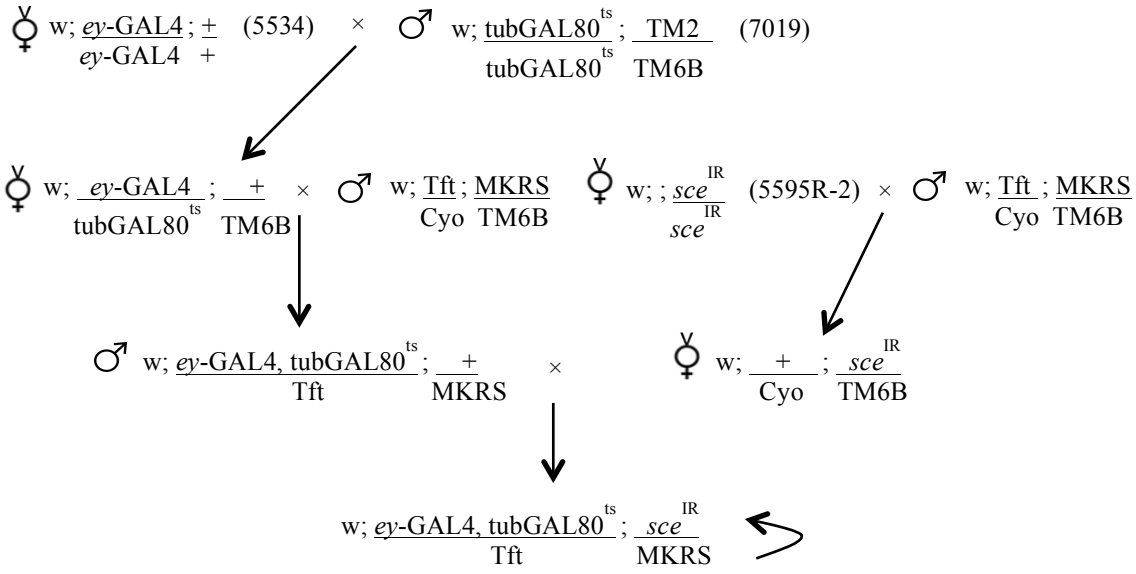

Appendix 7

Yeast two-hybrid screen results. Identified proteins together with domain analysis and the selected interaction domain are shown. Results provided by Hybrigenics.

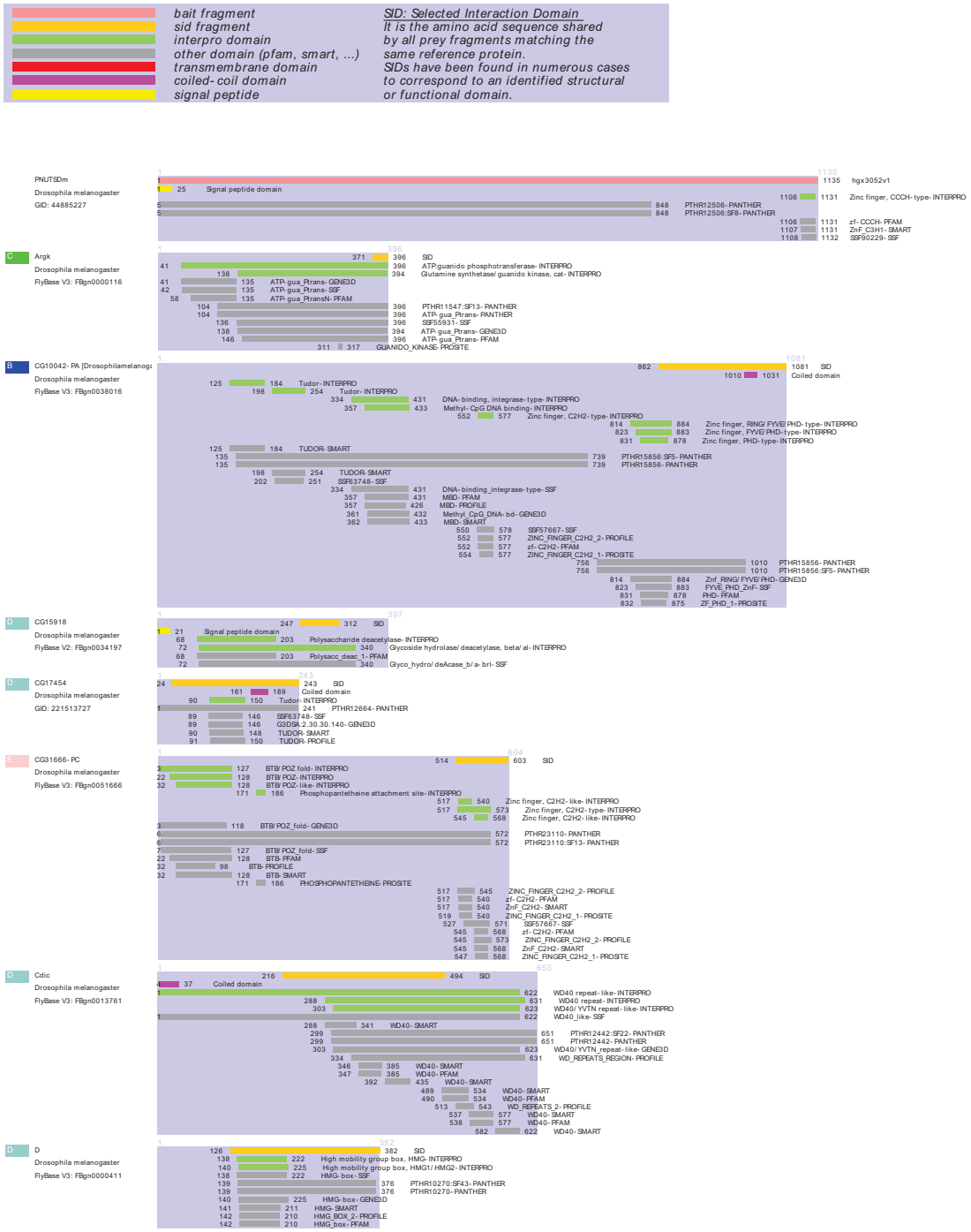

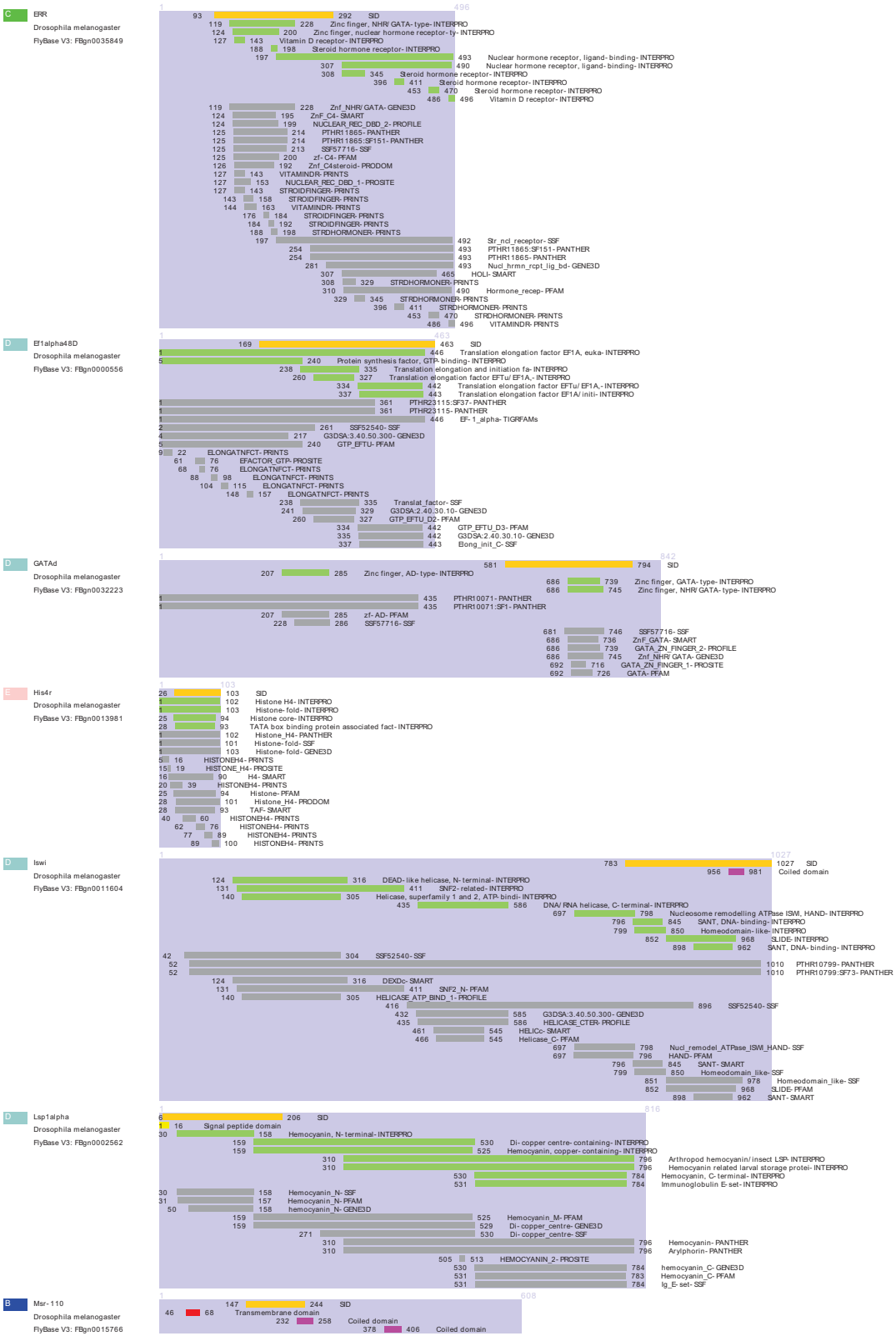
C
ERR
Drosophila melanogaster
FlyBase V3: FBgn0035849
D
Ef1alpha48D
Drosophila melanogaster
FlyBase V3: FBgn0000556
D
GATAd
Drosophila melanogaster
FlyBase V3: FBgn0032223
E
His4r
Drosophila melanogaster
FlyBase V3: FBgn0013981
D
Iswi
Drosophila melanogaster
FlyBase V3: FBgn0011604
D
Lsp1alpha
Drosophila melanogaster
FlyBase V3: FBgn0002562
B
Msr-110
Drosophila melanogaster
FlyBase V3: FBgn0015766

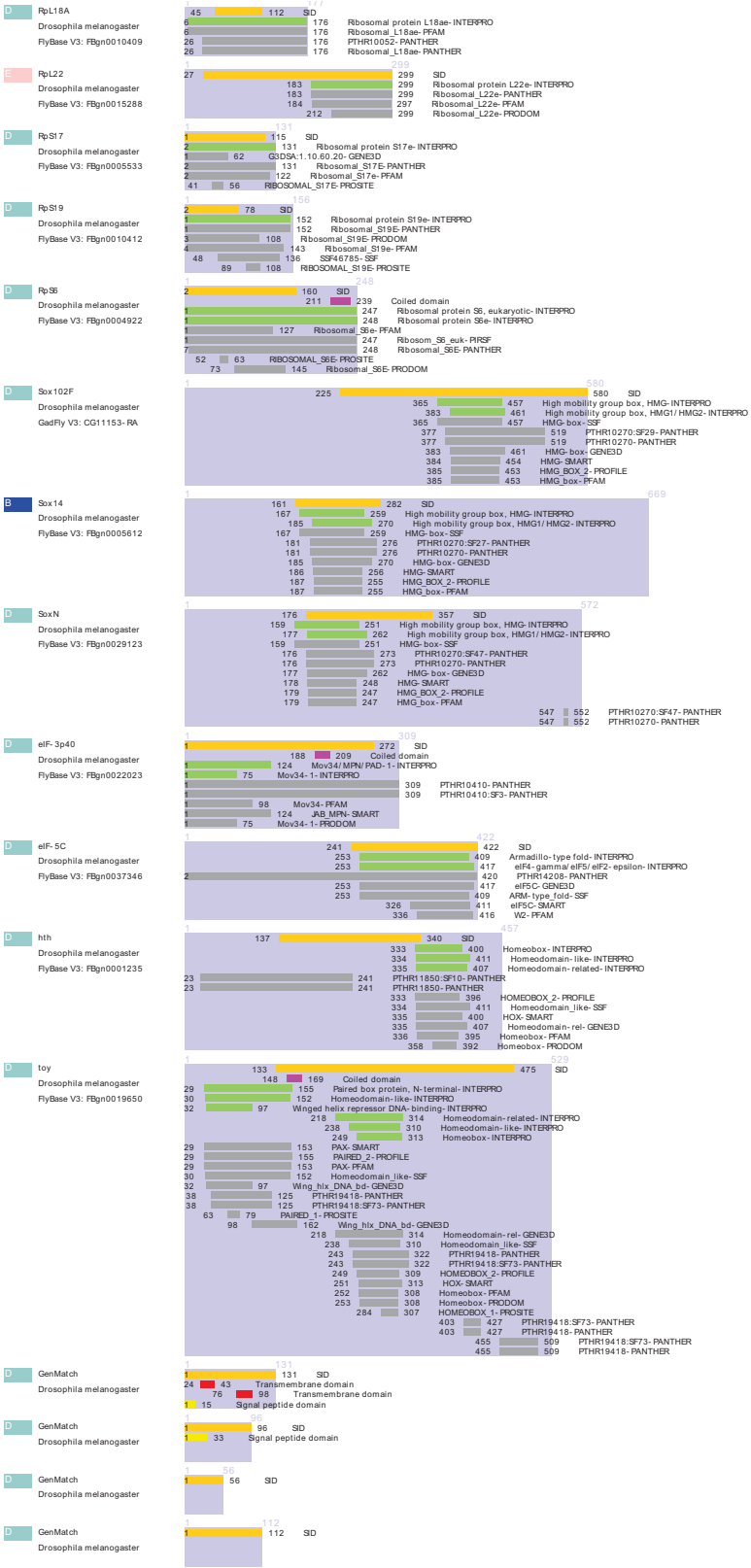
D RpL18A
Drosophila melanogaster
FlyBase V3: FBgn0010409
E RpL22
Drosophila melanogaster
FlyBase V3: FBgn0015288
D RpS17
Drosophila melanogaster
FlyBase V3: FBgn0005533
D RpS19
Drosophila melanogaster
FlyBase V3: FBgn0010412
D RpS6
Drosophila melanogaster
FlyBase V3: FBgn0004922
D Sox102F
Drosophila melanogaster
GadFly V3: CG11153-RA
B Sox14
Drosophila melanogaster
FlyBase V3: FBgn0005612
D SoxN
Drosophila melanogaster
FlyBase V3: FBgn0029123
D eIF-3p40
Drosophila melanogaster
FlyBase V3: FBgn0022023
D eIF-5C
Drosophila melanogaster
FlyBase V3: FBgn0037346
D hth
Drosophila melanogaster
FlyBase V3: FBgn0001235
D toy
Drosophila melanogaster
FlyBase V3: FBgn0019650
D GenMatch
Drosophila melanogaster
D GenMatch
Drosophila melanogaster
D GenMatch
Drosophila melanogaster
D GenMatch
Drosophila melanogaster

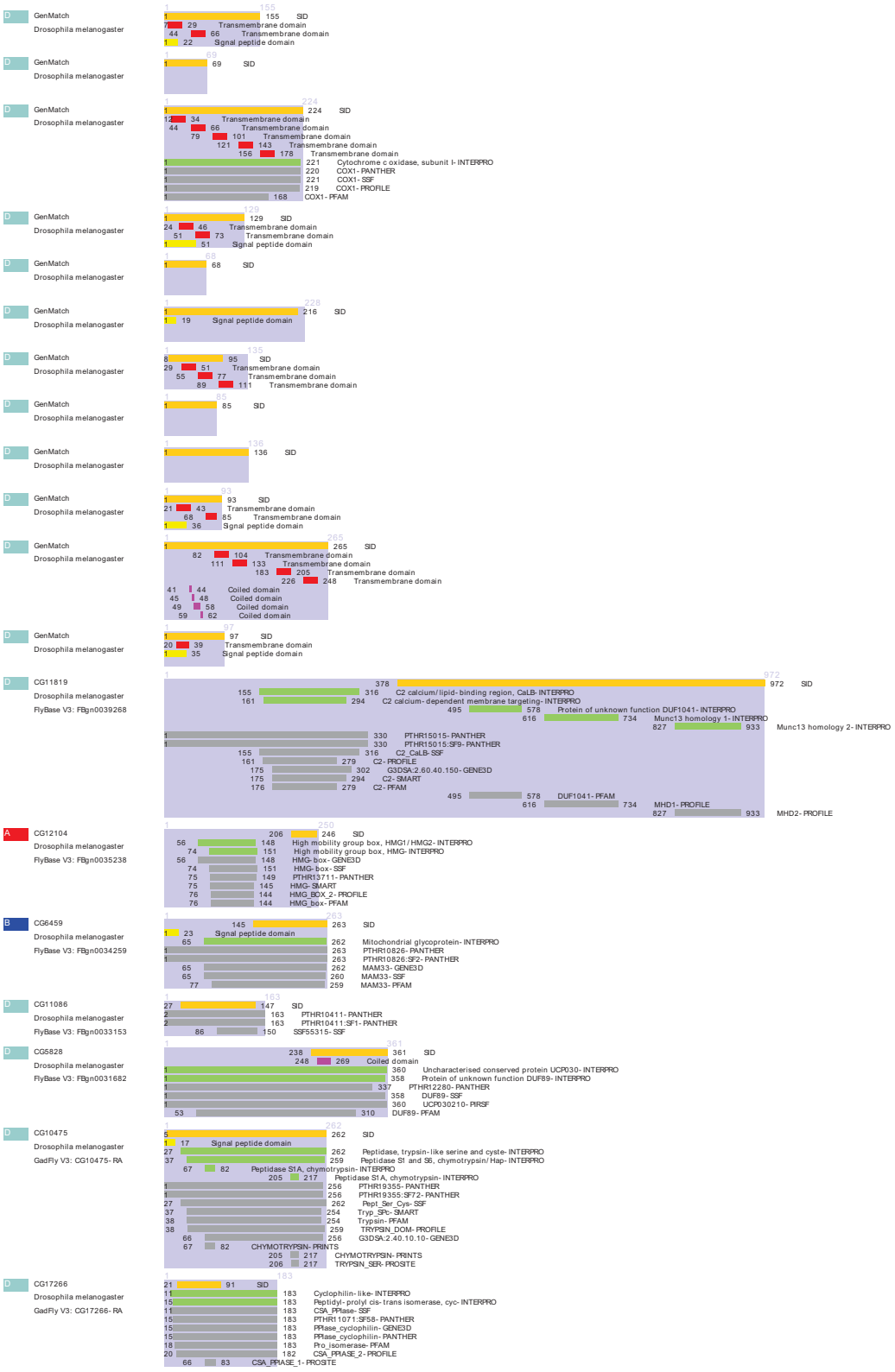
D GenMatch
Drosophila melanogaster
1 155 SID
7 29 Transmembrane domain
44 66 Transmembrane domain
1 22 Signal peptide domain
D GenMatch
Drosophila melanogaster
1 69 SID
D GenMatch
Drosophila melanogaster
1 224 SID
12 34 Transmembrane domain
44 66 Transmembrane domain
79 101 Transmembrane domain
121 143 Transmembrane domain
156 178 Transmembrane domain
1 221 Cytochrome c oxidase, subunit I- INTERPRO
1 220 COX1- PANTHER
1 221 COX1- SSF
1 219 COX1- PROFILE
1 168 COX1- PFAM
D GenMatch
Drosophila melanogaster
1 129 SID
24 46 Transmembrane domain
51 73 Transmembrane domain
1 51 Signal peptide domain
D GenMatch
Drosophila melanogaster
1 68 SID
D GenMatch
Drosophila melanogaster
1 216 SID
1 19 Signal peptide domain
D GenMatch
Drosophila melanogaster
8 95 SID
29 51 Transmembrane domain
55 77 Transmembrane domain
89 111 Transmembrane domain
D GenMatch
Drosophila melanogaster
1 85 SID
D GenMatch
Drosophila melanogaster
1 136 SID
D GenMatch
Drosophila melanogaster
1 93 SID
21 43 Transmembrane domain
68 85 Transmembrane domain
1 36 Signal peptide domain
D GenMatch
Drosophila melanogaster
1 265 SID
82 104 Transmembrane domain
111 133 Transmembrane domain
183 205 Transmembrane domain
226 248 Transmembrane domain
41 44 Coiled domain
45 48 Coiled domain
49 58 Coiled domain
59 62 Coiled domain
D GenMatch
Drosophila melanogaster
1 97 SID
20 39 Transmembrane domain
1 35 Signal peptide domain
D CG11819
Drosophila melanogaster
FlyBase V3: FBgn0039268
1 378 972 SID
155 316 C2 calcium/lipid- binding region, CaLB- INTERPRO
161 294 C2 calcium- dependent membrane targeting- INTERPRO
495 578 Protein of unknown function DUF1041- INTERPRO
616 734 Munc13 homology 1- INTERPRO
827 933 Munc13 homology 2- INTERPRO
1 330 PTHR15015- PANTHER
1 330 PTHR15015:SF9- PANTHER
155 316 C2_CaLB- SSF
161 279 C2- PROFILE
175 302 G3DSA:2.60.40.150- GENE3D
175 294 C2- SMART
176 279 C2- PFAM
495 578 DUF1041- PFAM
616 734 MHD1- PROFILE
827 933 MHD2- PROFILE
A CG12104
Drosophila melanogaster
FlyBase V3: FBgn0035238
1 206 246 250 SID
56 148 High mobility group box, HMG1/ HMG2- INTERPRO
74 151 High mobility group box, HMG- INTERPRO
56 148 HMG- box- GENE3D
74 151 HMG- box- SSF
75 149 PTHR13711- PANTHER
75 145 HMG- SMART
76 144 HMG_BOX_2- PROFILE
76 144 HMG_box- PFAM
B CG6459
Drosophila melanogaster
FlyBase V3: FBgn0034259
1 145 263 293 SID
1 23 Signal peptide domain
65 262 Mitochondrial glycoprotein- INTERPRO
1 263 PTHR10826- PANTHER
1 263 PTHR10826:SF2- PANTHER
65 262 MAM33- GENE3D
65 260 MAM33- SSF
77 259 MAM33- PFAM
D CG11086
Drosophila melanogaster
FlyBase V3: FBgn0033153
1 147 163 SID
2 163 PTHR10411- PANTHER
2 163 PTHR10411:SF1- PANTHER
86 150 SSF55315- SSF
D CG5828
Drosophila melanogaster
FlyBase V3: FBgn0031682
238 361 361 SID
248 269 Coiled domain
1 360 Uncharacterised conserved protein UCP030- INTERPRO
1 358 Protein of unknown function DUF89- INTERPRO
1 337 PTHR12280- PANTHER
1 358 DUF89- SSF
1 360 UCP030210- PIRSF
53 310 DUF89- PFAM
D CG10475
Drosophila melanogaster
GadFly V3: CG10475- RA
5 262 SID
1 17 Signal peptide domain
27 262 Peptidase, trypsin- like serine and cyste- INTERPRO
37 259 Peptidase S1 and S6, chymotrypsin/ Hap- INTERPRO
67 82 Peptidase S1A, chymotrypsin- INTERPRO
205 217 Peptidase S1A, chymotrypsin- INTERPRO
1 256 PTHR19355- PANTHER
1 256 PTHR19355:SF72- PANTHER
27 262 Pept_Ser_Cys- SSF
37 254 Tryp_SPc- SMART
38 254 Trypsin- PFAM
38 259 TRYPSIN_DOM- PROFILE
66 256 G3DSA:2.40.10.10- GENE3D
67 82 CHYMOTRYPSIN- PRINTS
205 217 CHYMOTRYPSIN- PRINTS
206 217 TRYPSIN_SER- PROSITE
D CG17266
Drosophila melanogaster
GadFly V3: CG17266- RA
21 91 183 SID
11 183 Cyclophilin- like- INTERPRO
15 183 Peptidyl- prolyl cis- trans isomerase, cyc- INTERPRO
11 183 CSA_PPIase- SSF
15 183 PTHR11071:SF58- PANTHER
15 183 PPIase_cyclophilin- GENE3D
15 183 PPIase_cyclophilin- PANTHER
18 183 Pro_isomerase- PFAM
20 182 CSA_PPIASE_2- PROFILE
66 83 CSA_PPIASE_1- PROSITE

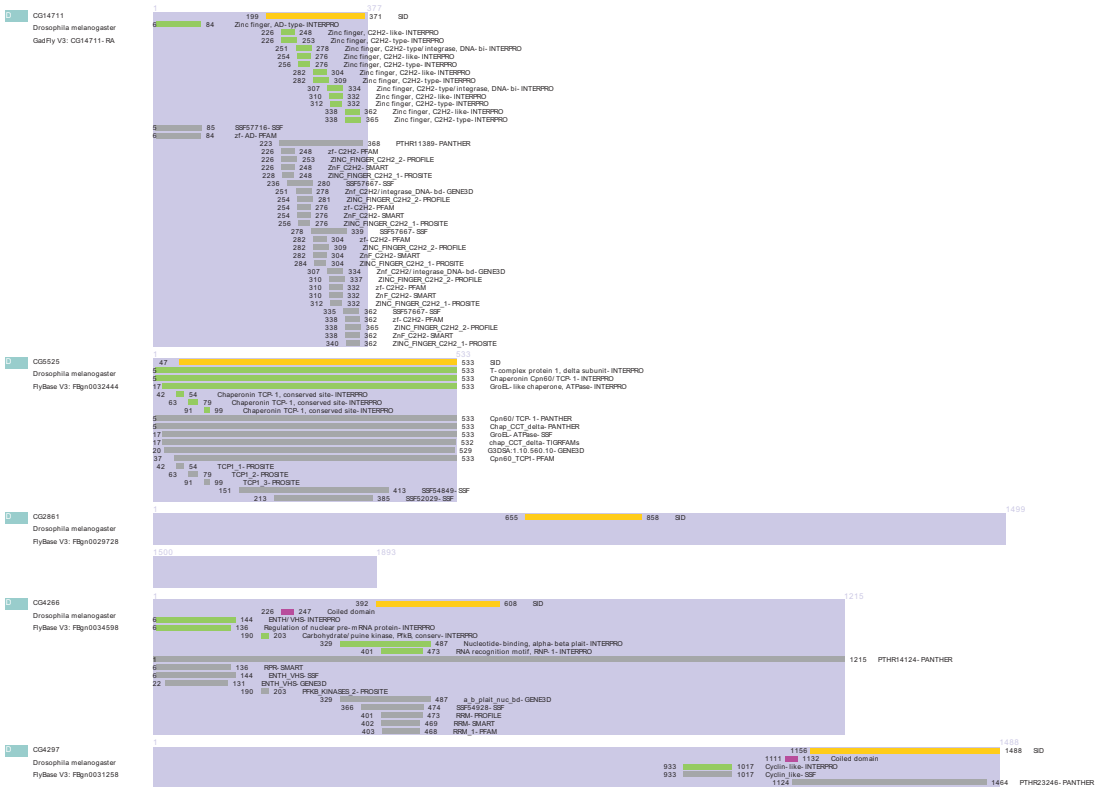
CG14711
Drosophila melanogaster
GadFly V3: CG14711- RA
CG6525
Drosophila melanogaster
FlyBase V3: FBgn0032444
CG2861
Drosophila melanogaster
FlyBase V3: FBgn0029728
CG4266
Drosophila melanogaster
FlyBase V3: FBgn0034598
CG4297
Drosophila melanogaster
FlyBase V3: FBgn0031258